ITERATIVE RECEIVERS FOR INTERFERENCE CANCELLATION AND SUPPRESSION IN WIRELESS COMMUNICATIONS

NENAD VESELINOVIC

Department of Electrical and Information Engineering,

University of Oulu

OULU 2004

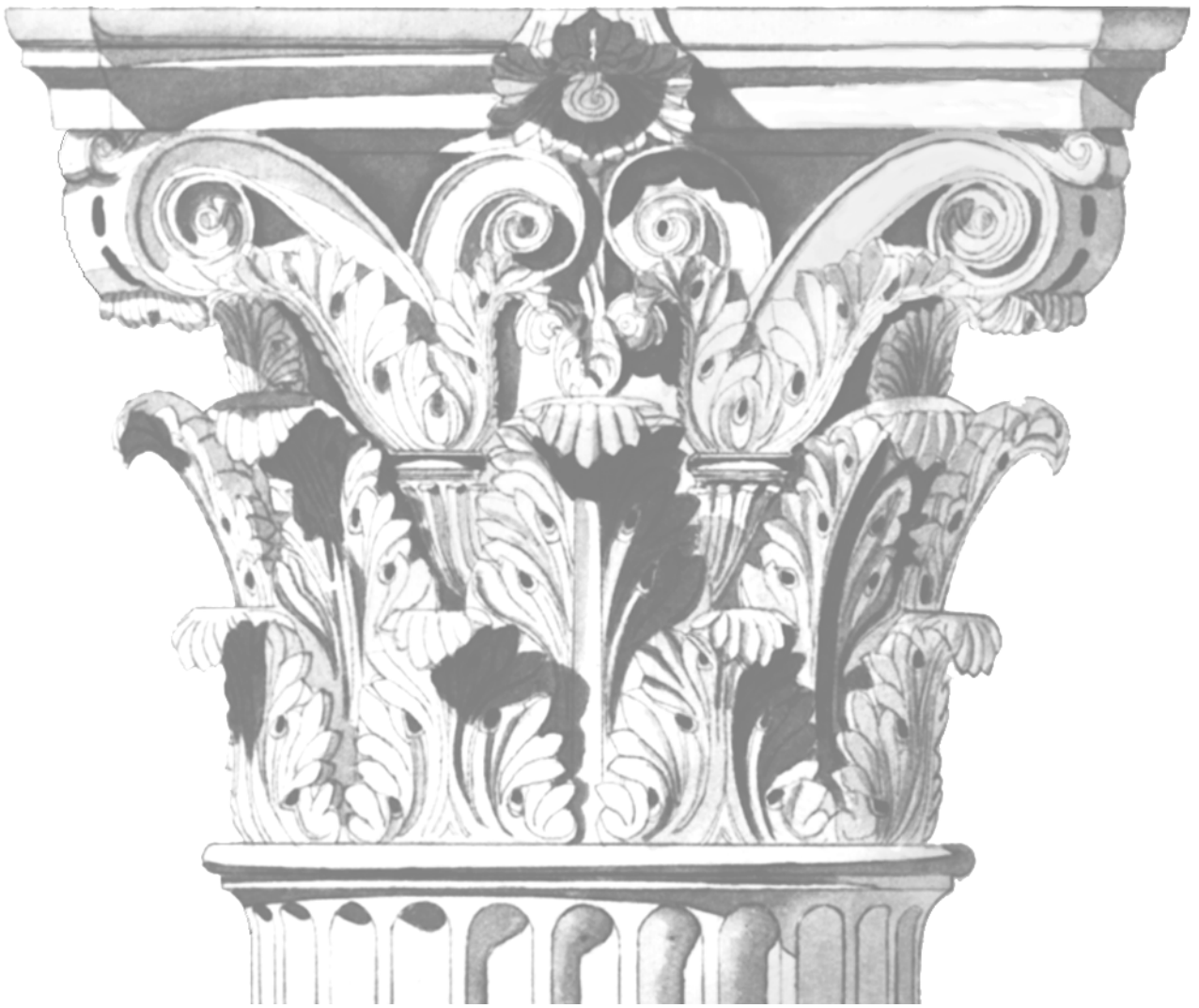

NENAD VESELINOVIC

ITERATIVE RECEIVERS FOR INTERFERENCE CANCELLATION AND SUPPRESSION IN WIRELESS COMMUNICATIONS

Academic Dissertation to be presented with the assent of the Faculty of Technology, University of Oulu, for public discussion in Raahensali (Auditorium L10), Linnanmaa, on December 9th, 2004, at 12 noon.

OULUN YLIOPISTO, OULU 2004

Supervised by
Professor Markku Juntti
Professor Tadashi Matsumoto

Reviewed by
Professor Alister Burr
Professor Lajos Hanzo

ISBN 951-42-7596-9 (nid.)
ISBN 951-42-7597-7 (PDF) http://herkules.oulu.fi/isbn9514275977/

ISSN 0355-3213 http://herkules.oulu.fi/issn03553213/

OULU UNIVERSITY PRESS
OULU 2004

Veselinovic, Nenad, Iterative receivers for interference cancellation and suppression in wireless communications
Department of Electrical and Information Engineering, University of Oulu, P.O.Box 4500, FIN-90014 University of Oulu, Finland
2004
Oulu, Finland

Abstract

The performance of conventional receivers for wireless communications may severely deteriorate in the presence of unaccounted interference. The effectiveness of methods for mitigating these effects greatly depends on the knowledge that is available about the interference and signal-of-interest (SOI), therefore making the design of robust receivers a great challenge. This thesis focuses on receiver structures for channel coded systems that exploit different levels of knowledge about the SOI and interference in an iterative fashion. This achieves both robustness and overall performance improvement compared to non-iterative receivers. Code division multiple access (CDMA) and spatial division multiple access (SDMA) systems are considered.

The overlay of a turbo coded direct-sequence spread-spectrum (DS-SS) system and strong digitally modulated tone interference is studied. An iterative receiver, which is capable of blind cancellation of both wideband and narrowband interference is proposed based on the adaptive self-reconfigurable -filter scheme. Asymptotic performance analysis of the iterative receiver shows that significant iteration gains are possible if the signal-to-interference-plus-noise-ratio (SINR) is relatively large and the processing gain (PG) of the SOI is relatively small.

Robust diversity detection in turbo-coded DS-SS system with statistically modeled interference is studied. A non-parametric type-based iterative receiver that estimates the probability density function (PDF) of interference-plus-noise is proposed. Its performance is shown to be rather robust to the number of interferers and their distances from the victim receiver and very similar to the performance of a clairvoyant receiver. Amazingly, this is achievable with no prior knowledge about the interference parameters. Furthermore, iteration gain is shown to significantly reduce the length of the pilot sequence needed for the PDF estimation.

A family of iterative minimum-mean-squared-error (MMSE) and maximum-likelihood (ML) receivers for convolutionally and space-time coded SDMA systems is proposed. Joint iterative multiuser-detection (MUD), equalization and interference suppression are proposed to jointly combat co-channel interference (CCI), inter-symbol-interference (ISI) and unknown CCI (UCCI) in broadband single-carrier systems. It is shown that both in convolutional and space-time coded systems the ISI and CCI interference can be completely eliminated if UCCI is absent. This is achievable with a number of receive antennas equal to the number of users of interest and not to the total number of transmit antennas. In case UCCI is present, the effectiveness of CCI and ISI cancellation and UCCI suppression depends on the effective degrees of freedom of the receiver. Receiver robustness can be significantly preserved by using hybrid MMSE/ML detection for the signals of interest, or by using estimation of the PDF of the UCCI-plus-noise.

A low complexity hybrid MMSE/ML iterative receiver for SDMA is proposed. It is shown that its performance is not significantly degraded compared to the optimal ML receiver. Its sensitivity to spatial correlation and a timing offset is assessed by using field measurement data. It was shown that the hybrid MMSE/ML receiver is robust against spatial correlation. The sensitivity to the timing offset is significantly reduced if the receiver performs UCCI suppression.

Keywords: equalization, interference suppression, MIMO, PDF estimation, SDMA

To my families
Veselinović and Živković

Preface

The work related to this thesis has been performed at the Centre for Wireless Communications (CWC), University of Oulu, Finland. I joined the CWC in March 2000 where I started my postgraduate studies, shortly after my graduation in the University of Belgrade, Serbia and Montenegro. I wish to thank the Director of the CWC at the time, Professor Matti Latva-aho, for giving me an opportunity to be a part of this charismatic research unit. Having Professor Markku Juntti as a supervisor of my research work was truly a privilege and I would like to thank him for that. His high research standards and technical precision will always remain my professional goals. My deepest gratitude goes to my main advisor Professor Tadashi Matsumoto with whom I had a lifetime privilege of working during the final and most important part of my thesis. His enormous experience, energy and true passion for making things different and better are something that I will remember and strive for in life. He is one of two persons without whose support this thesis would have not been completed.

Most of the work presented in this thesis was conducted in the Advanced Wireless Communication Systems (AWICS) and Future Radio Access (FUTURA) projects. I would like to thank manager of the projects, Professor Jari Iinatti, and all my colleagues that have participated them for directly or indirectly influencing my work. The help provided by Dr. Djordje Tujković in the beginning stages of the project is especially acknowledged. The fruitful discussions with Sami Siltala now with VTT Electronics and Pertti Henttu now with Elektrobit are gratefully acknowledged. I would like to thank Kari Horneman from Nokia and Jukka Nuutinen now with Elektrobit for patience in reading my papers and for many fruitful comments.

I would also like to thank other colleagues, most of which are from the "single carrier" group, Kimmo Kansanen, Kari Hooli, Yen Kai, Zhangpei Zhang, and especially Juha Karjalainen for all the lively discussions that we had. I am grateful to Mariella Saarestoniemi from CWC and Christian Schneider from Technical University of Ilmenau for the practical flavor added to the thesis through the use of field measurement data. The computer and technical support of Jari Silanpaa and Pekka Nissinaho and administrative support of Timo Aikas, Elina Kukkonen and Hanna Saarella are gratefully acknowledged.

I wish to thank the reviewers of the thesis, Professor Lajos Hanzo from the University of Southampton, UK and Professor Alister Burr from the University of York, UK, for their patience in reading the manuscript and for their insightful comments. I am grateful to Professor Tad Matsumoto, Professor Markku Juntti and Juha Karjalainen for reading and to Zach Shelby for proofreading the manuscript. Their comments have significantly improved the quality of the thesis.

During my postgraduate studies I had the privilege of being a student in the Infotech Oulu Graduate School as well as in two research projects. The financial support of Nokia, Elektrobit, the Finnish Defence Forces, Instrumentointi and TEKES, the National Technology Agency of Finland, on these projects is gratefully acknowledged. I am also thankful to Tekniikan Edistamisaatio (TES), Elisa Communications foundation and Nokia Foundation for their significant financial support.

I owe my deepest gratitude to my friends Dejan and Ljudmila Novaković with whom I shared unforgettable moments during the first year of our stay in Oulu. Being engineers themselves, they have helped me learn a lot both about our profession and life itself. I am also grateful to Anita and Dejan Danilović, Dejan Drajić, Nedeljko Cvejić, Djordje and Ilijana Tujković and Steve and Maja Dyson for all the nice moments we have shared. I wish to thank Ian and Therese Oppermann for their unforgettable open house events. My special thanks go to my friend Djordje Babić who "paved my way" to this beautiful country.

Finally, I wish to thank my parents Jelisaveta and Radiša for all the love and support they gave me throughout my life and hard years of study. I also thank my brother Predrag for always being supportive in his own way. My deep gratitude goes to Živko and Mirjana Živković whom I will always regard as my second parents.

My warmest gratitude belongs to my lovely fiancée Aleksandra Živković for all the sincere love, support and understanding she had for me throughout all these years. By sharing her moments with me she made every day of our life the most precious time I have ever had. Her capability of managing my messy mixture of work and private life makes her moral contribution to this thesis tremendous, and she is the second person without whom this thesis would not be possible to complete.

Oulu, November 1, 2004 Nenad Veselinović

List of original publications

I Veselinović N, Henttu P, Siltala S, Tujkovic D & Juntti M (2001) Wideband interference suppression, in turbo coded DS/FH spread spectrum system. Proc. IEEE International Conference on Communications (ICC), Helsinki, Finland, vol.9, p: 2789-2793.

II Veselinović N & Juntti M (2002) Turbo decoding for spread spectrum with unknown noise statistics. Proc. Conference on Information Sciences and Systems (CISS), Princeton, NJ, USA.

III Veselinović N & Juntti M (2002) Turbo coded type-based detection in man-made noise. Proc. IEEE International Symposium on Spread Spectrum Techniques and Applications (ISSSTA), Prague, Czech Republic, vol.2, p: 460-464.

IV Veselinović N & Juntti M (2003) Comparison of robust turbo decoders for diversity detection. Proc. Finnish Wireless Communications Workshop (FWCW), Oulu, Finland, vol.1, p: 71-74.

V Veselinović N & Matsumoto T (2003) Iterative signal detection in frequency selective MIMO channels with unknown cochannel interference. Proc. COST 273 Workshop (COST273), Paris, France.

VI Veselinović N, Matsumoto T & Juntti M (2004) A PDF estimation-based iterative MIMO signal detection with unknown interference. IEEE Communications Letters 7(8), p:422-424.

VII Veselinović N, Matsumoto T & Juntti M (2004) Iterative receivers for STTrC-coded MIMO turbo equalization. Proc. IEEE Vehicular Technology Conference (VTC), Milan, Italy.

VIII Veselinović N, Matsumoto T & Schneider C (2004) Interference suppression and joint detection to reduce sensitivity to timing offset and spatial correlation of STTrC-coded MIMO turbo equalization. IEICE Transactions on Communications, in press.

IX Veselinović N, Matsumoto T & Juntti M (2004) Iterative STTrC-coded multiuser detection and equalization with unknown interference. EURASIP Journal on Wireless Communications and Networking, Special Issue on Multiuser MIMO Networks, in press.

X Veselinović N, Matsumoto T & Juntti M (2004) Iterative PDF estimation based multiuser diversity detection and channel estimation with unknown interference. EURASIP Journal on Applied Signal Processing, special Issue on Turbo Processing, in press.

XI Veselinović N, & Matsumoto T (2004) Space-Time Coded Turbo Equalization and Multiuser Detection - Asymptotic Performance Analysis in the Presence of Unknown Interference. Proc. Asilomar Conference on Signals Systems and Computers (ASILOMAR), Pacific Grove, US.

For clarity, the thesis is presented as a monograph and the original publications are not reprinted.

List of symbols and abbreviations

A_A	impulsive index of the Middleton class A noise
$\mathbf{A}_k(i)$	coefficients of an equivalent channel after MMSE filter, $(N_T \times N_T)$
$b_k(i)$	modulated symbols of the kth user at the ith time instant, take values from $\mathbb{Q}$
$b_k^{(n)}(i)$	symbols transmitted from the the kth user's nth transmit antenna at the ith time instant, take values from $\mathbb{Q}$
B_k	frame length of the kth user
B	frame length of users indexed by $k = 1, ..., K$
B_I	frame length of users indexed by $k = K+1, ..., K+K_I$
$c_k(i)$	binary uncoded information symbol of kth user at the ith time instant
$d_k(i)$	binary encoded sequences of the kth user at the ith time instant
f_0	frequency offset of the users indexed by $k = K+1, ..., K+K_I$
$f_k^{(m,n)}(p)$	chip-spaced discrete time channel impulse response between the nth antenna of the kth user and mth receive antenna
$f_r(r)$	PDF of the interference distances from the receiver in a Middleton class A model interpretation
$2F+1$	length of the linear interpolating filter
$g_k^{(m,n)}$	channel impulse response between nth transmit antenna of the kth user and mth receive antenna
$g_{kl}^{(m,n)}$	complex channel gain of the lth multipath component of $g_k^{(m,n)}$
G	spreading factor of the users indexed by $k = 1, ..., K$
G_I	ratio between T_{sI} and T_s
$h_k^{(m,n)}(p)$	chip-spaced discrete convolution of $s_k(t)$ and $f_k^{(m,n)}(p)$
$\mathbf{H}$	Toeplitz channel matrix of the users indexed by $k = 1, ..., K$, $(LGN_R \times KN_T(2L-1))$
$\hat{\mathbf{H}}$	estimate of $\mathbf{H}$, $(LGN_R \times KN_T(2L-1))$
$\mathbf{H}_d$	channel matrix of desired part of CIR

$\mathbf{H}_u$	channel matrix of desired part of CIR
$\mathbf{H}(l)$	channel matrix of the users indexed by $k = 1, ..., K$ that corresponds to the lth multipath component, $(GN_R \times KN_T)$
$\mathbf{H}_k^{(m)}(l)$	channel matrix of the kth user that corresponds to the mth receive antenna and lth multipath component, $(GN_R \times KN_T)$
$\mathbf{H}_I$	Toeplitz channel matrix of the users indexed by $k = K+1, ..., K+K_I$, $(LGN_R \times KN_T(L + L_I - 1))$
$\mathbf{H}_I(l)$	channel matrix of the users indexed by $k = K+1, ..., K+K_I$ that corresponds to the lth multipath component, $(GN_R \times K_I N_T)$
$\mathbf{H}_{kI}^{(m)}(l)$	channel matrix of the kth user that corresponds to the mth receive antenna and lth multipath component, $(G \times N_T)$
$\mathbf{H}_{kjI}^{(m)}(l)$	channel matrix of the kth user, $k = K+1, ..., K+K_I$ that corresponds to the mth receive antenna, lth multipath component and jth chip interval, $(1 \times N_T)$
i	time instant index
j	time instant index
$\mathbf{J}$	WBI signal vector, $(G(T+B) \times 1)$
J_j	WBI interference sample at the jth time instant
$\hat{J}_j$	estimate of the WBI interference sample at the jth time instant, obtained by Wiener filtering
k	user index
K	number of desired users
K_{eff}	effective number of interference sources in Middleton class A model interpretation
K_I	number of undesired users (interferers)
l	multipath index
L_k	number of multipath components contained in $g_k^{(m,n)}$
L	number of consecutive symbols spanned by the maximum channel impulse response length of all users indexed by $k = 1, ..., K$
L_I	number of consecutive symbols spanned by the maximum channel impulse response length of all users indexed by $k = K+1, ..., K+K_I$
L_{eff}	length of the effective part of the CIR
m	receive antenna index
M	cardinality of the constellation set
$\mathbf{M}_k(i)$	covariance matrix of the residual interference, UCCI and noise, $(LN_R \times LN_R)$
n	transmit antenna index
$\mathbf{n}(i)$	additive white noise vector, $(LN_R \times 1)$
$\mathbf{n}_{eff}(i)$	additive white noise vector
$\mathbf{n}_e(i)$	vector of the sum of AWGN and residual WBI interference, $(G \times 1)$

N_R	number of receive antennas
N_T	number of transmit antennas for each user
$\mathbf{N}$	AWGN vector, $(G(T+B)\times 1)$
$P_k^{(n)}$	average power of the signal $b_k^{(n)}(i)$
$P_1^{ext}(\cdot)$	extrinsic probability of the argument produced by the detection block
$P_1^{app}(\cdot)$	*a posteriori* probability of the argument produced by the detection block
$P_2^{ext}(\cdot)$	extrinsic probability of the argument produced by the channel decoding block
$P_2^{app}(\cdot)$	*a posteriori* probability of the argument produced by the channel decoding block
$\hat{P}_{(\cdot)}(\mathbf{q}_l)$	multidimensional type value of the argument in the point $\mathbf{q}_l$
$\mathbb{Q}$	constellation set
$\mathbb{Q}_{ext}$	parameter of a turbo equalizer
$r^{(m)}(t)$	received signal at the mth receive antenna
$r_j^{(m)}(i)$	received signal at the jth chip interval of the ith symbol at the mth receive antenna obtained after chip-matcehd filtering and sampling
$r_k^{(m)}(t)$	received noiseless signal component at the mth receive antenna due to the kth user
$\mathbf{r}(i)$	received signal vector corresponding to N_R receive antennas and G chip intervals at the time instant i, $(GN_R\times 1)$
$\mathbf{r}(i)$	received signal vector corresponding to the mth receive antenna and G chip intervals at the time instant i, $(G\times 1)$
R	rate of channel code
$\mathbf{R}$	covariance matrix of the UCCI plus noise
$\mathbf{R}_I$	covariance matrix of the UCCI
$\mathbf{R}_{MIMO}$	spatial correlation matrix
s_k	signature waveform of the kth user
$s_k(j)$	jth chip of the kth user
$\mathbf{S}$	desired signal vector, $(G(T+B)\times 1)$
$t_k(i)$	training sequence of the kth user at the ith time instant
T	training sequence length of the users indexed by $k=1,...,K$
T_c	chip duration
T_I	training sequence length of the users indexed by $k=K+1,...,K+K_I$
T_k	training sequence length of the kth user
T_{sk}	duration of the symbols $b_k^{(n)}$ of the kth user
T_s	duration of the symbols $b_k^{(n)}$ of the users indexed by $k=1,...,K$
T_{sI}	duration of the symbols $b_k^{(n)}$ of the users indexed by $k=K+$

	$1, ..., K + K_I$
$\mathbf{u}(i)$	signal vector of users indexed by $k = 1, ..., K$, $(KN_T(2L-1) \times 1)$
$\mathbf{u}(i)$	signal vector of users indexed by $k = K+1, ..., K+K_I$, $(K_I N_T(L+L_I-1) \times 1)$
$\mathbf{W}_j$	coefficients of a Wiener filter for linear WBI interpolation at the jth time instant, $(2F \times 1)$
$\mathbf{W}_{sj}$	switching coefficients of a self reconfigurable scheme, $(2F \times 1)$
$\mathbf{W}_k(i)$	coefficients of an MMSE filter, $(LN_R \times N_T)$
$\mathbf{y}(i)$	space-time sampled received signal vector $(LGN_R \times 1)$
$\mathbf{y}_{eff}(i)$	space-time sampled received signal vector
$\hat{\mathbf{y}}(i)$	WBI-free received signal vector, $(G \times 1)$
$\mathbf{y}_l^{(m)}$	vector of received signal samples for the mth receive antenna and lth multipath component, $(G \times 1)$
$\mathbf{y}_d$	decision statistic vector for TBD, $(GN_R\lceil \frac{\tau_1 L1}{T_c} \rceil \times 1)$
$\mathbf{Y}_j$	received signal vector contained in the linear interpolating filter at the jth time instant, $(2F \times 1)$
Y_j	received signal sample at the jth time instant
$\hat{Y}_j$	WBI-free received signal sample at the jth time instant
$z^{(m)}(t)$	additive white noise
$\mathbf{z}_k(i)$	output of MMSE filter, $(N_T \times 1)$
α_q	qth element of a constellation set
$\boldsymbol{\beta}_k(i)$	vector of transmitted symbols from the N_T transmit antennas of the kth user
Γ	ratio of the Gaussian and impulsive components of the Middleton class A noise
$\mathbf{\Gamma}^{(n)}$	constraint matrix
$\delta(t)$	Dirac impulse function
$\Delta_k(i-l)$	covariance matrix of a signal obtained after soft cancellation, $(KN_T(2L-1) \times KN_T(2L-1))$
Ω_A	power of the impulsive component of the Middleton class A noise
$\mathbf{\Omega}_k(i)$	equivalent Gaussian channel coefficients, $(N_T \times N_T)$
π	interleaving
π^{-1}	de-interleaving
$\mathbf{\Psi}_k(i)$	equivalent Gaussian noise
σ^2	additive white noise variance
σ_k^2	variance of the kth mixture term in Middleton class A noise model
$\psi(t)$	chip waveform of the users indexed by $k = 1, ..., K$
$\psi_I(t)$	symbol waveform of the users indexed by $k = K+1, ..., K_I$
τ_{kl}	relative delay of the lth multipath component of $g_k^{(m,n)}(t)$
$\mathbf{\Theta}_k(i)$	covariance matrix of the equivalent Gaussian noise, $(N_T \times N_T)$

Ξ	quantizer alphabet
ACGN	additive correlated Gaussian noise
ACM	approximate conditional mean
AWGN	additive white Gaussian noise
AWN	additive white noise
BCJR	Bahl-Cocke-Jelinek-Raviv
BER	bit error rate
BLAST	Bell labs layered space-time
BPSK	binary phase shift keying
CA	collision avoidance
CC	convolutional code
CCI	co-channel interference
CD	collision detection
CDMA	code division multiple access
CIR	channel impulse response
CSI	channel state information
CSMA	carrier sense multiple access
DF	decision feedback
DFE	decision feedback equalizer
D-NLOS	dynamic non-line-of-sight
DoF	degree of freedom
DS	direct-sequence
EM	expectation-maximization
FDE	frequency domain equalization
FDMA	frequency division multiple access
FER	frame error rate
FH	frequency hopping
FIR	finite impulse response
GP	generator polynomial
HLLC	hard limited linear correlator
IIR	infinite impulse response
ISI	inter-symbol interference
KL	Kullback-Leibler
LC	linear correlator
LOBD	locally optimal Bayes detector
LOS	line-of-sight
LS	least squares
NBI	narrowband interference
MAI	multiaccess interference
MAP	maximum-*a-posteriori*

MC	multicarrier
MIMO	multiple-input multiple-output
MISE	mean-integrated-squared error
ML	maximum-likelihood
MLSE	maximum-likelihood sequence estimation
MMSE	minimum-mean-squared error
M-PSK	M-ary phase-shift-keying
MRC	maximum-ratio-combining
MUD	multiuser detection
OD	optimal detector
PEP	pairwise error probability
PDF	probability density function
PG	processing gain
QAM	quadrature-amplitude modulation
QPSK	quadrature-phase-shift-keying
RBF	radial basis function
SAGE	space alternating generalized EM
SC	soft cancellation
SDMA	space division multiple access
SER	symbol error rate
SfISfO	soft-input soft-output
SINR	signal to interference plus noise ratio
SIR	signal to interference ratio
S-NLOS	static non-line-of-sight
SNR	signal to noise ratio
SOI	signal of interest
SS	spread-spectrum
STTr	space-time-trellis
STTu	space-time-turbo
SVD	singular value decomposition
TBD	type-based detector
TDMA	time division multiple access
TH	time hopping
UCA	uniform circular array
UCCI	unknown co-channel interference
ULA	uniform linear array
WBI	wideband interference
WLAN	wireless local area network
ZFE	zero forcing equalization
$\odot$	elementwise vector product

$\lceil \cdot \rceil$	the smallest integer greater or equal to the argument
$\lfloor \cdot \rfloor$	the largest integer smaller or equal to the argument
$\|\Xi\|$	cardinality of Ξ
$\| \cdot \|$	absolute value of the argument
$\|\| \cdot \|\|$	Euclidian norm of the the argument
$(\cdot)_{\Xi}$	quantized argument
$(\cdot)^H$	Hermitian transpose of the argument
$(\cdot)^T$	transpose of the argument
$(\cdot)^{-1}$	inverse of the argument
$(\cdot)^*$	complex conjugate of the argument
$(\cdot)^{<\gamma>}$	argument related to the γth transmit antenna set
$(\cdot)_{i,j}$	element at the ith row and the jth column of the argument
$(\cdot)_{\alpha_q}$	argument related to the constellation symbol α_q
$(\cdot)_{CISI}$	argument related to the sum of CCI and ISI
$\widetilde{(\cdot)}$	soft *extrinsic* estimate of the argument
$\overline{(\cdot)}$	soft *a posteriori* estimate of the argument
$I(\cdot)$	indicator function
$\max(\cdot)$	maximum of the argument
$\min(\cdot)$	minimum of the argument
$\mathcal{M}$	bit to symbol modulation mapping function
$\mathrm{Re}(\cdot)$	real part of the argument
$\mathrm{Im}(\cdot)$	imaginary part of the argument
$D(\cdot\|\|\cdot)$	KL distance between arguments
$H(\cdot)$	entropy of the argument
$\mathrm{diag}(\cdot)$	diagonal matrix with argument vector elements on a main diagonal
$r(\cdot)$	rank of the argument

Contents

1 Introduction

By targeting the basic need for voice conversation, wireless telecommunications have become a very important part of people's everyday life. Apart from satisfying this basic need in a way that was barely imaginable only several decades ago, communication technology has amazingly changed the way people think, behave, work, entertain etc., by further extending the range of offered services. As a consequence, modern communication networks are designed to carry much more diverse contents than those imposed by traditional voice communications, and the current evidence suggests the trend to continue.

The frequency resources that enable cost efficient communications are not only limited, but their use is also strictly regulated by standardization bodies. Therefore, the requirements in terms of the bandwidth efficiency of future wireless networks are expected to be very stringent. These requirements can be fulfilled at different levels of network development. As possible examples, we mention network planing and transceiver design. Although all these approaches are in essence competing with each other, in practice their combinations are both desirable and necessary.

This thesis focuses on receiver design for the efficient use of bandwidth. From that perspective, the main factor that limits bandwidth efficiency is *interference*, which can originate from other users of the same communication system, other systems overlayed in frequency, non-linearities in the transmitter and receiver, man-made noise etc. If not appropriately treated at the receiver, it can significantly degrade the performance of the communication system. Furthermore, *interference cancellation* and *suppression* receivers are studied in this thesis in more detail. In Section 1.1 a brief introduction to signal detection in unknown interference is given. Section 1.2 briefly overviews the existing multiple access techniques. Section 1.3 presents scope and aims of the thesis, whereas its outline is presented in Section 1.4. Section 1.5 gives the overview of the author's contributions to the original publications.

1.1 Signal detection in the presence of interference

The receiver performance in the presence of interference is dominated by the knowledge it has about the interference structure. Depending on this knowledge, appropriate algorithms can be applied to use the receiver's degrees-of-freedom [1] to mitigate the degrading effects of interference. In this section, a general overview of the existing receiver techniques designed to cope with interference is given, while the more detailed literature survey is postponed to Chapter 2.

In many situations, interference can be modelled as additive white Gaussian noise (AWGN) that has structure neither in space nor in time/frequency domains. This is the extreme case which is well known to be the worst case interference both from the detection [1] and information theoretic point of view [2]. The matched filter [3] is well known to be the optimal receiver for that scenario, if the pulse shape of the signal of interest is known at the receiver.

In case that the interference possesses any kind of structure in space and/or time, the matched filter designed for AWGN noise is not capable of exploiting it. This fact has been the driving force for development of advanced algorithms that can improve the receiver's performance by exploiting this structure. Man-made signals are non-Gaussian in nature, which is a property that can be used for interference mitigation. Examples are digitally modulated signals that exhibit a finite constellation property and many other sources of man-made interference that usually occur as impulses of certain average frequency and duration [4, 5, 6]. The extreme cases of non-Gaussian interference are multiaccess interference (MAI) and intersymbol interference (ISI). The optimal receiver for MAI is known to be the multiuser detector [7], where all the interfering signals are detected jointly with the signal of interest (SOI). For ISI the optimal detector is the maximum-likelihood sequence estimator (MLSE) [8, 9]. Note that these methods require knowledge of channel state information (CSI) at the receiver side. In case that the CSI is not available but the signals are still of interest, one could resort to the rich literature on blind deconvolution [10] with blind source separation [11], blind equalization [12] and blind multiuser detection [13, 14] as special cases.

Another situation where statistical non-Gaussian interference models are more appropriate is the case where many interfering sources transmit in an uncoordinated fashion. For that case, numerous receivers that exploit this non-Gaussian nature have been proposed [15, 16, 17, 18]. Unlike the techniques that exploit the finite constellation property of the interference in this case the receiver exploits the property of discontinuous (bursty) transmission in time.

Signal correlation is another property which resulted in a variety of wide-band- and narrow-band-interference (WBI and NBI, respectively) suppression techniques that exploit interference correlation in time [19, 20], frequency [21] and spatial domains [22]. Numerous combinations of the methods described above that simultaneously make use of several signal properties and perform processing in several domains have attracted considerable attention. The examples are space-time interference suppression [23], time-frequency interference suppression [24] and joint MUD

[1] The degrees of freedom domains are space and time. The frequency domain is dual with time through the Fourier transform.

of SOI and interference for NBI and WBI interference suppression [25, 20, 26].

In channel coded systems, the complexity of an optimal receiver that jointly performs signal and interference detection with channel decoding is prohibitively complex [27]. However, the complexity can be significantly reduced by means of the suboptimal iterative receiver structures. This trend has been triggered by the discovery of turbo codes in [28] and has been applied to a wide variety of problems ever since. The underlying idea is to approximate a jointly optimal receiver with a concatenation of low complexity locally optimal receiver blocks which exchange information in an iterative fashion. In most of the cases the performance of the suboptimal iterative receivers is close to that of the globally optimal receiver due to the very reliable signal estimates obtained after channel decoding. Possible applications, the basis of which have been used in this theses, are iterative multiuser detection and decoding [29], iterative equalization and decoding [30] and iterative channel estimation, equalization and decoding [31, 32, 33][2].

1.2 Multiple-access techniques

Multiple-access refers to a technique that allows several users to share a common communications channel. The available domains for multiple access are space, time and frequency. The most traditional multiple-access techniques are based on user separation using different *signature waveforms*. The oldest multiple access technique is frequency division multiple access (FDMA) where different signature waveforms use different frequency. The user separation is then performed simply by bandpass filtering.

The introduction of digital modulations enabled the appearance of time division multiple access (TDMA) where each user's signature waveform is limited to a predetermined time interval. The user separation is then performed by synchronizing and correlating with the corresponding user's signature waveform.

The appearance of spread-spectrum techniques for anti-jamming and low probability of interception capabilities has led to the development of code division multiple access (CDMA) [35]. CDMA can be implemented using frequency hopping (FH), time hopping (TH), direct-sequence (DS) spread-spectrum (SS) as well as multicarrier (MC) techniques. In FH-CDMA users' signature waveforms are located at different center frequencies at different time intervals. The hopping from one frequency to another is controlled by user-specific hopping sequences. In DS-CDMA, different users' signature waveforms are allowed to overlap both in time and in frequency, but they are orthogonal in the *code domain*. This can be achieved by allocating each user a unique spreading sequence, whereby the signal redundancy is achieved in time domain. On the contrary, in MC-CDMA the redundancy of each user's data is achieved in frequency domain [36].

The simplest way to achieve spatial multiple access is to simply separate multi-

[2]It is worth mentioning that all these applications can be viewed as instances of the summary-product (or belief propagation) algorithm which operates by message passing between parts of a graphical model [34].

ple users far apart in order to allow for sufficient attenuation of the signals. More advanced techniques include space division multiple access (SDMA) [37], or beamforming, which is based on the use of closely spaced antennas to spatially isolate the users or spatial multiplexing [38] which relies on antennas spaced far apart and the rich scattering environment to perform user separation. Unlike in the former case, where it was necessary for different users to be placed in different spatial directions, this is not necessary for the latter one[3]. With a slight abuse of notation the term SDMA will be used throughout this thesis for the latter approach (spatial multiplexing). This can be justified by the fact that, similarly to the conventional SDMA case, it is essentially the spatial position of different users that allows for their separation at the receiver. Moreover, SDMA can be seen as an analogy to DS-CDMA where the spreading sequences in time are replaced by the unique[4] spreading sequences in space.

The use of multiple receive antennas theoretically enables multiple access using only a single carrier frequency. In wideband system, however, the frequency selectivity of the channel becomes one of the factors that dominates receiver performance. MC techniques are an effective way to mitigate this problem by converting a frequency selective channel into a set of frequency flat fading channels. Another possible way, that is the focus of the last part of this thesis, is to use a single carrier approach [39] with powerful equalization techniques. By doing so, the channel frequency selectivity can be exploited to achieve additional diversity gains.

1.3 Scope and aims of the thesis

Iterative receivers for the cancellation and suppression of unknown interference in channel-coded CDMA and SDMA systems are studied in this thesis. The main goal is to develop robust receivers that can provide reliable communications under different interference conditions. The receivers are expected to perform better than the conventional single and multiuser receivers at a cost of reasonable computational complexity increase. The main emphasis is on the interference sources that do not originate from the communication system of interest.

Linear prediction and interpolation filters for NBI and WBI suppression offer lower complexity finite impulse response (FIR) approximations of Kalman-Bucy filters that are infinite impulse response (IIR) in nature. However, due to their underlying linear nature, they do not utilize the non-Gaussian nature of the SOI. Nonlinear versions thereof exploit this information and offer significantly better performance by employing a certain nonlinearity function to the error signal that is used in minimum-mean-squared-error (MMSE) optimality criterion. The price to be paid is the increased receiver complexity, due to the used non-linearity and due to the fact that it requires online estimation of the interference parameters. Decision feedback linear interpolation and prediction filters in uncoded systems have

[3]In fact, only in the case of users being in exactly the same spatial positions it is not possible to distinguish between them.

[4]Determined by the spatial location of each user.

been shown to achieve a similar effect by cancelling the signal of interest prior to the interference estimation. Thereby the non-Gaussian nature of the SOI is taken into account implicitly, through its cancellation. In a channel coded-system, the soft feedback obtained after channel decoding can be used in a similar manner. The channel decoder is expected to provide a very reliable soft feedback estimate and the iterative (turbo) scheme is a potential low complexity alternative to the non-linear solutions. Further study is required to determine the iterative receiver performance and its limitations in practical CDMA overlay situations. This problem is a subject of the first section of Chapter 4 of the thesis.

In the case of non-Gaussian interference that originates from several uncoordinated transmissions, the problem of interference suppression becomes equivalent to that of interference probability density function (PDF) estimation. Linear receivers are not capable of exploiting the non-Gaussian nature of interference and non-linear solutions in general offer better performance and robustness against changes of interference parameters. In order to design a receiver that is robust to a variety of interference sources, the knowledge of interference statistics is required in general. Histogram estimation based receivers are an attractive solution, since they require no prior knowledge about the interference PDF. Their drawback is, however, that the number of training samples required for histogram estimation can be prohibitively large, resulting in reduced bandwidth efficiency of the system. For that purpose, iterative receivers can be particularly useful since the feedback obtained after channel decoding can be used as additional training samples for histogram estimation. Therefore, the turbo receiver can potentially provide improvement both in terms of interference PDF estimation and the overall system performance, and in terms of the bandwidth efficiency. A more detailed study is required to assess the performance, robustness, and practical realizability of the histogram estimation iterative receiver in different interference scenarios. This problem is considered in the second section of Chapter 4.

The greatest challenge that is to be faced in the design of a broadband wireless access system based on single carrier communications is receiver complexity. The iterative (turbo) soft-cancellation MMSE (SC-MMSE) based receiver for joint multiuser detection and equalization in SDMA systems offers a reasonable trade-off between complexity and performance in the presence of co-channel interference (CCI) and ISI. The results from the literature show that the CCI and ISI can be almost completely removed in the case of convolutionally coded systems. Additionally, in multipath-rich environments the SC-MMSE iterative receiver offers relatively good unknown co-channel interference (UCCI) capability due to the large number of effective degrees-of-freedom guaranteed by performing spatial and temporal sampling. However, if the channel is not multipath rich, the number of effective degrees of freedom becomes significantly smaller and the performance can be significantly degraded in the presence of UCCI. Robust receivers that are capable of preserving the effective degrees of freedom by means of interference suppression and cancellation are, therefore, highly desirable. This is especially true in high data rate scenarios in which CCI, ISI and UCCI originates from users that are all equipped with multiple transmit antennas. Robust iterative receiver design for such scenarios is the subject of Chapter 5. Estimation of the PDF of UCCI-plus-

noise can be seen as one possible way to preserve the effective degrees of freedom in channels with low frequency selectivity and a relatively small number of UCCI signals. The hybrid SC-MMSE maximum *a posteriori* (SC-MMSE-MAP) iterative receiver is another potential robust solution. Receiver complexity, performance, and sensitivity to different design and channel imperfections are to be considered in detail.

1.4 Outline of the thesis

The thesis is organized as follows. Chapter 2 presents a comprehensive literature review of previous and parallel work. Reviews of NBI and WBI interference suppression and cancellation methods for CDMA and SDMA, non-Gaussian detection and iterative processing are given in more detail.

Chapter 3 presents a generic system model for CDMA and SDMA systems. The special cases of CDMA and SDMA, which are considered in more detail throughout the thesis, are defined.

In the first part of Chapter 4, which is in part included in Paper I, an extension of the adaptive self-reconfigurable ξ-filter scheme for NBI and WBI cancellation to its iterative version is given. Using the signal-to-interference plus noise ratio (SINR) at the canceller output as a performance measure, the SINR region is determined in which the iterative interference cancellation outperforms the non-iterative one. The performance of an iterative receiver based on the ξ-filter with a turbo code is evaluated in an AWGN channel through computer simulations.

In the second part of Chapter 4, which is partly presented in Papers II-IV, the iterative receiver based on type detection is developed for mitigating statistically modelled interference with no knowledge of interference statistics. An iterative receiver is proposed to reduce the length of training overhead and to improve the interference suppression process. The soft information that is passed from the detector to the soft-input soft-output (SfISfO) channel decoder is derived in closed form. The performance of the receiver is compared to the conventional Rake and optimal receivers in static and Rayleigh fading channels with additive Gaussian and non-Gaussian noise through computer simulations.

In Chapter 5, part of which is presented in Papers V-IX and XI, a framework for joint iterative multiuser detection, equalization and unknown interference suppression in single-carrier SDMA systems is presented. Unknown interference suppression methods based on covariance matrix estimation, PDF estimation and joint detection are developed. PDF estimation and joint detection methods are developed to increase the equivalent diversity order of the covariance matrix estimation method. Their performance is evaluated in quasistatic Rayleigh fading AWGN channels through computer simulations. Results are given for convolutional and space-time coded systems. The pairwise error probability (PEP) of space-time coded systems in the asymptotic case of ideal feedback is developed in the presence of unknown interference.

In Chapter 6, which is partly presented in Paper X, the issues related to real-

istic performance evaluation and practical implementation of the turbo receiver are considered. The framework for realistic performance evaluation using field measurement data is presented. A reduced complexity time-domain hybrid SC-MMSE-MAP turbo equalizer is developed by taking into account only significant portions of the channel impulse response. Finally, the performance sensitivity of the proposed turbo equalizer to the spatial correlation and timing offset is studied.

Chapter 7 concludes the thesis. The main results are summarized and discussed. Some open questions and directions for future research work are given.

1.5 Author's contribution to the publications

The thesis is in part based on ten original publications. The author has had the main responsibility for making the analysis and writing all the Papers I-X. The author has developed MATLAB and C++ software for computer simulations in all the papers. In papers I-IV the simulation software was developed based on the existing software for turbo codes, which is due to Dr. Djordje Tujkovic.

In Paper I the author developed ideas and analysis together with the help of other authors. In Papers II-IV the idea of applying type-based detection for unknown interference is due to the second author. The first author has developed the idea, performed analysis and created examples. In Papers V-VII and IX the author has invented main ideas, produced examples and performed analysis. Other authors have provided guidance, help and criticism during the process. The ideas of applying joint detection in space and time for preserving the effective receiver's degrees of freedom in Papers VII, VIII and X are due to the second author. The first author has developed the ideas, and performed analysis. These were extended further by the author to unknown interference suppression and spatial correlation sensitivity reduction. The second author of Paper X has provided guidance for the use of filed measurement data. Other authors provided help and criticism during the process. The asymptotic performance analysis in the presence of unknown interference presented in Paper XI is due to the first author.

2 Review of earlier and parallel work

This chapter gives a literature overview of different iterative and non-iterative signal processing techniques for interference suppression and cancellation. Throughout the thesis, interference suppression stands for methods that reduce the detrimental effects of interference without prior estimation of its instantaneous value. On the other hand, interference cancellation stands for methods that first estimate the interference and then cancel it from the total received signal. The overview of the methods is given according to the interference model and, correspondingly, interference properties that are used for its cancellation or suppression. Section 2.1 reviews the rich literature of blind narrowband and wideband interference suppression methods. Section 2.2 gives an overview of the detection methods in the presence of impulsive noise. In Section 2.3 an overview of iterative (turbo) processing methods and their application in interference suppression is given.

2.1 WBI and NBI interference cancellation and suppression in uncoded systems

The progress in the area of NBI suppression and cancellation for spread-spectrum communications up until the late 1980's was reviewed in [19]. The main interference property that is used for interference mitigation is signal correlation in time. The main techniques at the time were frequency-domain techniques [40, 41, 42, 43, 44, 45], which are based on estimating and cancelling interference in frequency, and linear predictive or interpolative techniques [46, 47, 48, 49, 50, 51, 52, 53, 54, 55, 56], that are based on the linear prediction and cancellation of interference in the time-domain. Further work in this area was based on better exploitation of the properties of the signal of interest and interference in time, frequency and various transform domains. More recent overviews of these techniques can be found in [57, 20]. Improved adaptive and optimal time-domain linear predictive and interpolative techniques are proposed in [58, 59, 60, 61, 62, 63, 64]. Kalman-Bucy

filtering, which is known to be the best linear estimator[1] of the signal based on its past values, is proposed for NBI estimation and cancellation in [65]. Non-linear NBI suppression methods were proposed in [66] and [67]. These methods take into account the non-Gaussian nature of the SOI and they use the approximate conditional mean (ACM) algorithm [66] to derive non-linear versions of the Kalman-Bucy and linear prediction and interpolation algorithms. The linear adaptive version thereof [66] can be seen as a generalization of the decision-feedback (DF) based solutions proposed in [50] and [68]. The non-linear filter was shown to perform remarkably better than its linear counterpart. Moreover, improvements of the non-linear schemes have been proposed based on neural networks in [69]. A linear interpolation filter with an adjustable center weight has been proposed in [70]. It was shown to significantly outperform its counterparts that pose stringent constraints on the filter center weight. A linear code-aided MMSE technique was proposed in [71] and it was shown to outperform all the linear and non-linear prediction and interpolation approaches.

With the growing commercial interest in CDMA communications during the last decade the suppression of digitally modulated interference has attracted considerable attention. Modifications to the linear code-aided approach are proposed in [72] where the modified MMSE criterion is used to exploit the property of improperness (rotational variance [73]) of digitally modulated NBI. Although it was shown that significant performance improvement can be achieved compared to the conventional MMSE code-aided techniques, the proposed technique is restricted only to real, binary phase shift keying (BPSK), modulations. Different cyclostationarity properties of the signal and interference were exploited in [21, 74, 75], showing that the complete elimination of the NBI is possible using periodically time-variant filtering. Another important NBI suppression technique relies on multiuser detection (MUD) [76] and it has been proposed in [77] and [25]. The MUD technique is known to be the optimal way to simultaneously separate SOI from the interference, if the interferers are digitally modulated and their CSIs are known to the receiver. This NBI cancellation technique models NBI as the sum of virtual CDMA users and detects them jointly with the SOI. This technique uses essentially all the knowledge that is available about the NBI for its cancellation, thereby resulting in the best error rate performance. A performance comparison with the linear predictive techniques performed in [78] showed the superiority of the MUD-based technique. Although only a decorrelating MUD receiver [79] was considered there, essentially any of the MUD techniques can be used for this purpose. We refer to [80, 81] for a more detailed overview of conventional MUD techniques and to [82] for a recent excellent overview and performance comparison of novel MUD algorithms[2]. A further example of the application of MUD techniques for NBI suppression is the maximum-likelihood (ML) technique proposed in [90] in terms of multirate systems and in [20] for code-aided NBI suppression. There, the "onion peeling" technique is applied, where the NBI is detected first and then subtracted from the received signal prior to despreading. This method, in turn, is

[1] In the MMSE sense.

[2] These, among others, include powerful genetic algorithms [83, 84, 85], particle filter detectors [86, 87] and probabilistic data association algorithms [88, 89].

very similar to the iterative[3] MUD techniques [91, 92, 93] that are based on serial or parallel interference cancellation. Adaptive self-reconfigurable schemes robust to the change of interference bandwidth and power are proposed in [26] and [94]. They can be seen as a combination of ML estimation of interference and conventional linear interpolation techniques. A more recent overview of different NBI suppression techniques including polar suppression and consecutive mean excision algorithms can be found in [95]. These techniques have been constructed with the assumption of rapidly changing interference and they are particularly suited for DS-FH systems.

The developments of frequency-domain techniques after late 80's were mostly based on the further improvements of conventional frequency domain techniques, examples of which can be found in [96, 97, 98]. The exploitation of other transform domains has also attracted the attention of some authors, with the main examples being wavelet transforms [99, 100], lapped transforms [101], orthogonal transforms [102, 103] and convex projections [104]. A general framework for projection-based NBI suppression receivers was studied in [75] and the special cases of receivers based on the Fourier transform and singular value decomposition (SVD) are proposed and studied. It should be noted that the a similar study was done in [105], where the multiuser projection based receivers were proposed. Blind multiuser detection was proposed in [106, 107]. An order statistics-based projection receiver for NBI suppression has been proposed in [108]. Adaptive projection based receivers have been the subject of study in [109]. Hybrid solutions that combine signal processing in time and frequency domains have also drawn the attention of some authors [110, 24] showing additional improvements in terms of robustness against interference. Other research directions and algorithm improvements were based on more accurate interference modelling. The examples are techniques which are based on the hidden-Markov modelling of non-stationary NBI that were proposed in [111, 112] and [113].

Exploiting the spatial domain in wireless communications using antenna arrays has attracted enormous attention in commercial wireless communications in recent years. The assumptions that were posed by original military applications more than two decades ago were closely spaced spatially correlated antennas allowing for steering the antenna beam to a certain direction [114]. This, in turn, allows for the reception of the SOI that has a certain spatial position, and rejecting the interference coming from the other directions [37]. Modern applications have opened a large area of research by assuming largely separated and uncorrelated antennas allowing for diversity gain and CCI suppression [22]. This in turn offers higher link reliability and huge potentials both for a link [115, 116] and system capacity increase [117]. More recently the capacity benefits of multiple-input-multiple-output (MIMO) channels [116] have triggered an enormous amount of research on channel coding and signal processing techniques capable of approaching this capacity. The most significant directions are the Bell Labs layered space-time (BLAST) architecture [118] and space-time coding [119, 120]. The spatial domain in NBI suppression was exploited in CDMA overlay situations in [121, 122] where the NBI was modelled as a digitally modulated tone and in [123, 124, 125] where the autoregressive

[3]Note that these iterative techniques do not make use of a channel code.

model was used for the NBI. The appearance of the spatial domain was shown to offer additional robustness against the interference with varying power and bandwidths.

In case that the delay spread of the channel becomes greater than the symbol duration, ISI becomes another factor that limits the performance. The optimal way of mitigating ISI is the well known MLSE proposed in [8, 9]. In case that the optimality criterion is that of minimizing the symbol error rate based on the whole block of received data, a MAP equalizer becomes more appropriate [126, 127, 128]. The main drawback of the above mentioned schemes is that their complexity increases exponentially with the length of the channel impulse response. Many low complexity linear schemes have been proposed which include either zero forcing equalization (ZFE) [129], which is capable of perfectly removing ISI if the filter is infinitely long or MMSE equalization [130], which always results in some residual interference at the filter output, but it reduces to the ZFE for infinitely large signal to noise ratios. Non-linear decision feedback equalization (DFE) has been studied in [131, 132] (see [133] and [134] for a review on equalization techniques). More recently frequency domain equalization has attracted considerable attention [135, 136, 137, 39] due to its low complexity in channels with large delay spreads[4]. Zero-forcing and MMSE receivers for multiuser detection in multipath channels have been considered in [138]. The performance of equalization schemes in the presence of unknown co-channel interference has been studied in [139, 140, 141, 142]. Exploiting the spatial domain resulted in space-time equalization that was studied in [143, 144, 145]. A more detailed overview of space-time equalization can be found in [23]. In the presence of co-channel interference the detection and equalization techniques that can be applied to mitigate its effect depend on whether the CCI is not of interest, or if it is to be detected. Performance of the space-time equalization in the presence of unknown[5] dispersive interference has been studied in [146] and [147, 148, 149]. It was shown there that the length of the optimal[6] equalizers is proportional to the number of multipaths, number of co-channel interferers and signal to noise ratio. Improving the performance of space-time equalizers in the presence of interference by means of decoupled schemes was studied in [150, 151, 152]. The basic idea behind decoupled schemes was to preserve degrees of freedom of linear MMSE receivers by performing CCI suppression only in the spatial domain, while ISI was suppressed by means of optimal MLSE equalization. This receiver is based on a property of the MLSE receiver that it can achieve a maximal diversity order guaranteed by spatial and temporal sampling. Several results supporting this fact can be found in [153, 154, 155, 156, 157, 158] for single and multicarrier SDMA. Another family of powerful linear equalizers that is based on the minimum-error-rate (MER) criterion was studied in [159, 160, 161, 162]. Those receivers are based on explicitly minimizing the error probability at the filter output, instead of doing so implicitly through MMSE filtering, thereby achieving better performance in general. Non-linear equalization using multilayer perceptron neural networks,

[4]In this thesis only time domain equalization is considered.

[5]Throughout this thesis the unknown interference is considered to be of no interest to be detected.

[6]In the MMSE sense.

polynomial perceptron neural networks and radial basis function (RBF) networks have been proposed and analyzed in [163, 164, 165], showing that rather significant performance improvements are possible with neural network based equalizers when compared to conventional linear and DFE equalizers. This is due to the fact that the equalization can be viewed as a classification problem, which is inherently non-linear. In [166, 167], it was described how RBF equalization can be used for the simultaneous mitigation of ISI and unknown CCI, while in [168] adaptive Bayesian equalization in conjunction with the K-means clustering algorithm has been used for the same purpose. The support vector machine approach to non-linear equalization has been considered in [169], where it was shown that support vector machine equalizers perform as well as neural network based approaches.

Non-linear detection of CDMA signals in the presence of CCI was considered recently in [170, 171]. The actual PDF of the interference was used there to improve the performance of the conventional matched filter and soft interference cancellation based receivers. A non-parametric method for CCI suppression and equalization in a narrowband system, based on a kernel-smoothing method has been proposed in [172], showing very robust performance against CCI. If the co-channel interference is of interest and it is to be detected, different blind algorithms can be applied. The examples are blind multiuser detection and equalization [14], blind source separation [11] and algorithms that exploit finite alphabet (FA) or constant modulus (CM) properties of the SOI and CCI [23].

2.2 Signal detection with non-Gaussian noise in uncoded systems

In many situations of interest the unknown interference can be accurately modelled either as a random signal with known statistics[7] or as a white or correlated random process with a Gaussian distribution. There exist, however, many situations where this model is not appropriate. Man-made electromagnetic noise and ocean ambient noise are some of the typical examples. One of the major results in the non-Gaussian noise theory was the development of a tractable and accurate model in an impressive research effort in the 1960's and 1970's, reported in [173, 174, 4]. The Middleton class A model [4] is the widely adopted one for use in communication theory, since it was derived having in mind the real physical mechanisms that generate noise in communication receivers. The appropriateness of this model has been confirmed by many measurement campaigns [4]. An extension to multiple antenna reception was studied independently in and [175] and [176], however the lack of measurement campaigns caused these models not to be used much in practice. Different ad-hoc extensions of Middleton class A models are presented in [177], although without any physical background. The general problem of optimal and suboptimal detection in Middleton class A non-Gaussian noise has been considered in [178, 179, 180, 181, 1]. In general, the optimal detec-

[7] A digitally modulated signal, for example.

tor in non-Gaussian noise is non-linear, thereby being of higher complexity than its linear counterparts. The mitigation of such interference in general assumes the estimation of its PDF in order to find the optimal non-linearity, that in turn is to be used as a preprocessing stage for the conventional linear receiver. The performance of linear[8] and low complexity hard-limited[9] correlating receivers in CDMA with Gaussian mixture[10] impulsive noise was considered in [182, 183]. Diversity detection in non-Gaussian noise modelled as a correlated Gaussian mixture has been considered in [18] and [184]. There the optimal receiver is approximated by a receiver based on the expectation-maximization (EM) [185] and space alternating generalized EM (SAGE) algorithms [186] that are used to determine the PDF of the noise. A receiver that is based on the Huber influence functions for robust diversity detection in Gaussian mixture noise was proposed in [187] showing superior performance compared to its linear counterpart.

Among the other non-Gaussian noise models it is important to mention alpha-stable noise models [188] that have also been studied by some authors [189]. Spherically invariant random processes have more recently attracted the attention of some authors as a more generic impulsive interference model [190, 17] with alpha-stable and Gaussian mixture models as special cases. Interestingly, it was shown that the optimal receiver assuming this noise model is *canonical* and independent of the actual noise statistics.

Note that the receivers mentioned above implicitly assume knowledge of the model of the interference PDF, and that they estimate the PDF through estimation of the parameters of that model. Therefore, they can be regarded as parametric methods. In case that the knowledge about the model can not be assumed, then non-parametric PDF estimation methods are more appropriate. An example is the theory of asymptotically optimal classification using a training sequence [191], which has been applied both for single and multiuser detection in non-Gaussian noise in CDMA in [192, 193, 194, 195]. It has been shown to always mimic the performance of the optimal receiver, without any prior knowledge about the interference distribution. However, the training sequence is needed for PDF estimation. The kernel-smoothing method is another non-parametric method [196], where the PDF estimate is made based on the weighted sum of the available interference observations. A comparative overview of kernel-smoothing and several other non-parametric methods including the projection pursuit method and radial basis functions method can be found in [197][11].

[8] Optimal for Gaussian noise.

[9] This detector tries to approximate the optimum non-linearity by hard-limiting the strong interference components.

[10] It should be mentioned that the Middleton class A noise is a special case of the Gaussian mixture model.

[11] Only non-parametric methods are considered in this thesis.

2.3 Iterative interference suppression and cancellation in channel-coded systems

Iterative receiver processing has attracted significant attention since the discovery of turbo codes in [28]. It was shown there to be an effective solution for approximating the computationally intractable optimal decoding of turbo codes. After that it was realized that the principle of exchanging probabilities between different receiver blocks is more general and can be applied to reduce the complexity of a variety of global optimization problems [198, 199]. The examples are joint equalization and decoding [30], multiuser detection and decoding [29, 200], channel estimation and decoding [16, 201], NBI interference cancellation and decoding [202, 203], demodulation and decoding [204] etc.

2.3.1 Iterative suppression of NBI in channel coded CDMA systems

Multiuser MMSE detection in convolutionally coded DS-CDMA system with NBI has been considered in [202]. The iterative detection and cancellation of MAI is performed, while NBI cancellation is performed in a non–iterative fashion, and only once prior to the detection of multiple users. An interpolation filter [19] is used there for NBI estimation. Therefore, the iteration gain comes only from the MAI suppression. In [203] the iterative cancellation of NBI is performed using interpolation and frequency domain filters. It was observed there that iterative cancellation of NBI results in a performance improvement when compared to the non iterative solution. Iterative NBI suppression in a single-user hybrid DS-FH system using subspace projections has been considered in [205]. There it was demonstrated that the applied NBI interference suppression method can eliminate NBI almost completely. However, since no direct comparison between iterative and non iterative methods is made, itis not clear if the iteration gain comes only form the decoding or from the iterative NBI suppression as well.

2.3.2 Iterative mitigation of non-Gaussian interference in channel coded CDMA systems

The problem of MAP iterative decoding of turbo codes in Gaussian interference with a signal to noise ratio (SNR) mismatch has been studied in [206, 207, 208, 209] where it was shown that a turbo decoder can tolerate a certain level of SNR mismatch. The general conclusion is that the tolerance against SNR mismatch is better if the SNR value is underestimated than if it was overestimated. Different solutions for SNR estimation have also been proposed there and also in [210, 211]. Simpler implementations of the MAP decoder in the form of max-log-MAP and min-log-

MAP are shown not to depend on the SNR at all [211], at the expense of only a slight loss in performance compared to the optimal log-MAP. Iterative decoding sensitivity to the noise PDF mismatch has been studied for narrowband system in [212, 213, 214, 215]. It was shown that severe performance degradation can occur if the noise PDF mismatch is present. Another important result is that the optimal decoder in non-Gaussian noise is the conventional decoder for Gaussian noise preceded by the noise-specific non-linearity function. Different robust decoders are proposed, where in [212] it was proposed to approximate the optimal non-linearity by a step-wise linear function. In [213] it was proposed to blindly estimate the histogram of the underlying noise PDF prior to decoding. The estimation procedure, however, is ad hoc, and it requires long frames for accurate PDF estimation. A minimax decoding approach was proposed in [214], where it was assumed that the decoder has knowledge about the family of possible PDFs that can occur in the channel. Although relatively robust performance was observed, for some noise PDFs it was relatively far from the optimal case.

The robust receivers proposed above are in essence non-iterative, since they do not use decoder feedback to re-estimate the parameters of the noise. Iterative PDF estimation and decoding for a CDMA system with MAI being observed as non–Gaussian noise has been studied in [216]. It was shown there that iterative PDF estimation using the kernel-smoothing technique was capable of achieving significant iteration gains.

2.3.3 Iterative equalization, multiuser detection, and UCCI suppression in wideband single carrier systems

The most critical part of the receiver for a broadband single-carrier system is the channel equalizer. In highly dispersive environments the complexity of the MLSE equalizer is prohibitively large. This has triggered a large amount of research to reduce the complexity of classical equalization approaches. The research on iterative (turbo) equalization in channel coded systems originated from [30], where an MLSE equalizer and SfISfO channel decoder were connected in a serially concatenated scheme. Similar work was done on iterative MUD and decoding in CDMA with multipath fading channels in [217, 200]. The common finding of this research was that the iterative low complexity schemes were capable of achieving interference-free performance. Lower complexity MMSE-based turbo equalization was studied in [218, 219, 220, 221, 222, 223, 224, 225]. Similar work on MMSE multiuser detection in CDMA with multipath fading channels was done in [29] and further evaluated in [226] in the presence of unknown interference. Even with reduced complexity MMSE equalization the iterative scheme was shown to be capable of achieving ISI and CCI free performance. In the presence of UCCI the schemes were shown to remove ISI and CCI and to significantly suppress the UCCI by means of optimum combining. Optimum combining based results for OFDM transmission and non iterative receiver processing can be found in [227] and [228].

The optimum combining approach was shown there to be very sensitive to the actual channel variations of UCCI in time and frequency. Therefore it is more difficult to accurately estimate the interference covariance matrix in OFDM than in single-carrier due to the need of per subcarrier estimation if the channel is frequency selective. More recently schemes for higher-order modulation formats were proposed in [229], again with interference-free performance after a sufficient number of iterations. Further complexity reduction schemes were proposed in terms of channel shortening filters [230, 231], matched filter approximations [232], and core matrix inversion techniques [233]. Turbo equalization applying RBF networks was proposed and analyzed in [234], where it was shown that RBF equalizers can achieve very similar performance as the optimal MAP equalization with significantly reduced complexity. Turbo frequency domain equalization (FDE) schemes attracted considerable attention [220] recently, due to their low complexity in channels with large delay spreads.

Space-time trellis (STTr) codes have originally been developed for frequency flat fading channels. In order to meet the requirements for high data rate transmission their extensions to frequency selective channels is of great importance. Their performance in unequalized multipath fading channels has been studied in [235] and [236]. There it was shown that the ISI is a limiting factor on the performance, and it causes an inevitable error floor at high SNR regions. The sensitivity of STTr codes to spatial correlation has been studied in [237],[238, 239] and it was shown there that they can tolerate relatively high levels of spatial correlation. Turbo equalization for STTr codes has been considered in [230, 231] with channel shortening filters, and in [240] with decision feedback equalizers. Although significant iteration gains were demonstrated there, only single user systems were considered. Multiuser scenarios in narrowband systems with STTr codes have been considered only for flat fading channels in [241], where it was shown that the iterative receiver is capable of achieving a single user bound at the expense of the required number of receive antennas being equal to the total number of transmit antennas. A multiuser uplink with STTr codes was considered in terms of CDMA in [242]. An iterative MMSE receiver was proposed there and it was shown that it achieves a considerable capacity increase when compared to the conventional Rake receiver. Although they have not been a subject of this thesis, we mention that the iterative receivers employing BLAST architectures have been the subject of many recent studies, examples of which are convolutionally and turbo coded single user systems [243], multiuser space-time turbo (STTu) coded systems for CDMA uplink [244, 245], TDMA downlink [246] and multiuser convolutionally coded TDMA/FDMA downlink systems [247].

3 Problem and system definitions

In the first section of this chapter the detailed problem formulation is given with respect to the results previously published. In the second section of this chapter a generic system model for CDMA and SDMA uplinks is presented. In order to ease the readability, special cases of the generic model for only CDMA and SDMA are derived in the beginning of Sections 4 and 5, respectively.

3.1 Problem formulation

The decision feedback filters for NBI cancellation proposed in [50] and [68] are low complexity approximations of the nonlinear NBI cancellation filters of [66] and [67], that exploit the non-Gaussian nature of the SOI. The fact that, in general, more reliable soft feedback can be obtained in channel coded systems has been utilized in [202, 203, 205] for NBI cancellation. However, there are several important issues that have not been considered in the references mentioned above. First, only NBI cancellation was studied. Since in practice the interference can be WBI as well, a scheme that is robust to the interference bandwidth is considered in Section 4.1. Second, in [202] NBI suppression is performed only once prior to MUD. Therefore it is not clear what would be the potential benefit of iterative NBI cancellation itself. Iterative NBI cancellation was studied in [205] but no comparison with the non-iterative solution was made. The partial answer to that question is given in [203] where it was shown that in a convolutionaly coded system and for a certain value of interference power iteration gains can be substantial. However, the studies there are performed only with convolutional coding which operates in a region of relatively high SNRs[1]. Therefore it is still not clear how the iterative receiver would perform in a system employing more powerful codes[2] that operate in a region of low SNRs. Moreover, it is of particular interest to determine for which range of

[1] In high SNR region the non-Gaussian nature of the SOI has more impact than in low SNR region.

[2] Turbo coding is considered in this thesis.

interference and noise powers the iteration gain becomes significant. These issues are studied in Section 4.1 as well.

Middleton class A noise has been widely adopted as a model for man-made interference in communications receivers [248]. To perform robust CDMA single and multiuser detection in man-made noise, type based detection has been proposed in [192, 249, 193]. It was shown to mimic the performance of an optimal receiver in many different interference scenarios both in cases with and without multiantnenna and/or multipath diversity. However, its main drawback is that the length of the required training sequence can be prohibitively long, thereby reducing the bandwidth efficiency of the system. An iterative (turbo) receiver in a channel coded system appears to be a natural solution to this problem, whereby the decoded data can be used as an extension of the training sequence. Since the type based detector's performance has not been studied in channel coded systems the main design issue is the optimal transmission of soft information from the detector to a decoder. Another important issue is the amount of bandwidth efficiency that can be preserved by the iterative receiver. These are the main subjects of consideration in Section 4.2.

An interesting Middleton class A model interpretation is presented in [250] where an interference scenario is presented that results in a Middleton class A distribution. Thereby it is possible to establish correspondence between the number of interferers and their distances from the receiver on one side and the parameters of the model on the other side. This approach, in turn, allows for the evaluation of the proposed receiver's performance with respect to the number of interfering sources and their positions and distances from the receiver. This is another issue considered in Section 4.2.

There is an active debate in the research community about the advantages and disadvantages of single- and multi-carrier broadband communications [251, 252, 253]. One of the greatest drawbacks of the single–carrier broadband wireless access is the receiver (equalizer) complexity. On the other hand, by using advanced iterative techniques it can exploit the multipath diversity of the channel [254], which is not possible with multi-carrier signalling. An iterative (turbo) SC-MMSE based receiver for joint multiuser detection and equalization in CDMA systems [29] offers a reasonable tradeoff between complexity and performance in the presence of CCI and ISI. The further results presented in [218] for SISO and in [223] for the MIMO case show that the CCI and ISI can be almost completely removed in case of convolutionally coded SDMA systems. Note that with SDMA there is no requirement for orthogonality between different users, thus allowing for increased link capacity. Additionally, in multipath-rich environments the SC-MMSE iterative receiver offers relatively good CCI and UCCI suppression capability due to the large number of effective degrees of freedom guaranteed by performing spatial and temporal sampling [22, 226, 224]. It was demonstrated in [223, 255] that in a multiuser uplink scenario with each user having a single antenna the iterative receiver can achieve the single user performance bound even if the number of users is larger than the number of receive antennas. As far as single carrier is concerned the performance of an iterative receiver in the multiuser uplink scenario with each user having multiple antennas was studied only in flat fading [241] with STTrC

and STBC[3]. Moreover, most of the multiuser MIMO scenarios have considered orthogonal transmission in order to separate users [256] in the downlink or appropriate constellation design for the same purpose [257] in the uplink, to name a

at the *receiver* without additional transmitter complexity[5], it is of interest to study its performance in the multiuser MIMO scenario. That fact has been exploited in multiuser STTr and STTu coded systems for CDMA uplink [244, 245, 242], TDMA downlink [246] and multiuser convolutionally coded TDMA/FDMA downlink systems [247]. Therefore, Section 5.2.2 is devoted to the STTr coded uplink multiuser scenario[6].

A large number of degrees of freedom of the iterative SC-MMSE receiver makes it possible to efficiently suppress UCCI. However, if either the number of UCCIs or their powers are large, the degrees of freedom may not be sufficient to achieve satisfactory performance. It is known for the MLSE receiver the maximal diversity order can be achieved with the temporal and spatial sampling [153, 154, 155, 156, 157, 158]. This fact has been used in [150, 151, 152] where a two stage MMSE/MLSE receiver was proposed to increase the degrees of freedom for non-iterative receivers and improve UCCI suppression. In the first stage only a CCI is suppressed by spatial filtering while in the second stage an optimal MLSE equalizer is applied to eliminate ISI. However, the complexity of the MLSE second stage may be prohibitive in broadband channels. On the other hand, the SC-MMSE iterative receiver can make use of the soft feedback to reduce the complexity of the second stage. This fact has been the motivation for studies presented in Section 5.3.1, where a hybrid SC-MMSE-MAP iterative receiver is proposed for the multiuser MIMO uplink. The signals can be detected jointly both in space and time in order to reduce the degrees of freedom of the MMSE receiver and enhance the UCCI suppression capability of the receiver. Also, only a portion of the signals in space and time can be detected jointly, depending on the amount of UCCI. The goal is to design an iterative receiver that is robust with respect to CCI and UCCI.

In case of the channel not being sufficiently multipath rich the number of effective degrees of freedom of the SC-MMSE receiver becomes relatively small. Therefore, the UCCI may have detrimental effects on performance. However, in that case the non-Gaussian nature of the UCCI can potentially provide us with more robust performance. This fact has been used in several studies including [168] and [172] for equalization in narrowband systems and [170, 171, 216] in CDMA. In all the cases the performance was shown to be significantly improved compared to linear receivers. These results naturally motivate a study of the achievable diversity order of non-linear receivers in the presence of UCCI. That is the subject of Section 5.3.2.

[3]Note that in the space-time coding case each user is equipped with multiple antennas. This scenario is often referred to as multiuser MIMO and will be used in the sequel as well.

[4]STBC is another technique that can be used in the uplink due to its simplicity.

[5]Complexity can be introduced either by a multiple access scheme like CDMA or by the orthogonal designs mentioned above.

[6]We will focus on the STTr coded system, since unlike STBC, it involves orthogonality neither in space nor in time and relies purely on the properties of the different users' and transmit antennas' channels.

A further complexity reduction of the proposed receivers can be achieved in various ways. Some of the proposals are channel shortening filters [231], square root filtering [233] and more recently frequency domain equalization techniques [39]. Complexity reduction can also be achieved by using only a significant portion of the channel impulse response in the equalization process. This is the subject of Section 6.2. As it is also of interest to determine the proposed receiver's performance in a realistic scenario, it is necessary to investigate its performance using field measurement data, which is an approach that has attracted some attention recently [258]. Evaluating a receiver's behavior in the presence of imperfections of synchronization is of particular interest, since it can have particularly harmful effects in single carrier communications. Spatial correlation is another practical impairment that can have detrimental effects on the SC-MMSE receiver, which is inherently based on spatial separation between users. These issues have been considered in Sections 6.3 and 6.4.

3.2 Generic system model for CDMA and SDMA

Figure 3.1 describes the system model for the signal received at the mth receive antenna. Each of $K + K_I$ users indexed by $k = 1, ..., K + K_I$ encodes the binary information sequence $c_k(i)$, $k = 1, ..., K_I$, $i = 1, ..., B_k R N_T \log M$ using a rate R channel code, where M, N_T and B_k are the cardinality of constellation set $\mathbb{Q} = \{\alpha_1, \ldots, \alpha_M\}$[7], the number of transmit antennas and frame length of the kth user in modulated symbols, respectively. The users indexed by $k = 1, ..., K$ are the users of interest to be detected and the others indexed by $k = K + 1, ..., K + K_I$ are unknown users. For simplicity of notation frame durations B_k of users indexed by $k = 1, ..., K$ are assumed to be the same and equal to B. Similarly, the frame lengths of users indexed by $k = K + 1, ..., K + K_I$ are assumed to be the same and equal to B_I, where in general $B \neq B_I$. Also for simplicity of notation all $K + K_I$ users are assumed to use the same channel encoder and the same number of transmit antennas.

The binary encoded sequences $d_k(i)$, $i = 1, ..., B_k N_T \log M$ are first interleaved by the user specific bit-interleaver pattern, and then modulated resulting in sequences of symbols $b_k(i) = \mathcal{M}\{d_k((i-1) * \log M + 1), ..., d_k((i-1) * \log M + \log M)\} \in \mathbb{Q}$, $i = 1, ..., B_k N_T$ for $k = 1, ..., K + K_I$. The symbol $\mathcal{M}$ denotes the bit to symbol mapping function. The coded and modulated symbols are further interleaved according to the user-specific symbol-interleaver pattern. The interleaved sequences are then headed by user-specific training sequences $t_k(i) \in \mathbb{Q}$, $i = 1, ..., T_k N_T$ of length T_k, for $k = 1, ..., K + K_I$. Training sequence lengths T_k for $k = 1, ..., K$ are all assumed to be equal to T while those for $k = K + 1, ..., K + K_I$ are all assumed to be equal to T_I, with $T \neq T_I$. The entire frame is serial-to-parallel

[7] In this thesis only M-ary phase-shift-keying (M-PSK) is studied. However, the extension to the more general quadrature-amplitude modulation (QAM) schemes is straightforward.

converted, resulting in the sequences $b_k^{(n)}(i)$, $n = 1, .., N_T$, defined as

$$b_k^{(n)}(i) = \left\{ \begin{array}{cc} t_k(\lfloor \frac{i}{N_T} \rfloor + n) & i = 1, ..., T_k, \\ b_k(\lfloor \frac{i-T_k}{N_T} \rfloor + n) & i = T_k + 1, ..., T_k + B_k. \end{array} \right\} \quad \text{for } k = 1, ..., K + K_I, \tag{3.1}$$

which are transmitted using N_T transmit antennas. The signal transmitted from the n-th antenna of the k-th user in the time interval $t \in [(i-1)T_{sk}, iT_{sk}\}$ is given by

$$b_k^{(n)}(i)\sqrt{P_k^{(n)}}s_k(t), \tag{3.2}$$

where $P_k^{(n)}$ is the power of the signal transmitted from the n-th antenna of the k-th user, $s_k(t)$ is the k-th user's signature waveform and T_{sk} is the duration of the kth user's symbol. It is assumed that the symbol durations T_{sk} of users indexed by $k = 1, ..., K$ are the same and equal to T_s. On the other hand the symbol durations T_{sk}, for $k = K+1, ..., K+K_I$ are all equal to T_{sI}. The signature waveform for the kth user, $k = 1, ..., K$ is given as

$$s_k(t) = \sum_{j=0}^{G-1} s_k(j)\psi(t - jT_c), \tag{3.3}$$

where $s_k(j)$ is the jth chip of user k, T_c is the chip duration, $G = T_s/T_c$ is the spreading factor and $\psi(t)$ is the chip waveform with support $[0, T_c]$ and

$$\int_0^{T_c} |\psi(t)|^2 dt = 1. \tag{3.4}$$

The users indexed by $k = 1, ..., K$ are assumed to have the same spreading factor G, their chips are assumed to be binary, i.e., $s_k(j) \in \{-1, +1\}$ and the signature waveforms $s_k(t)$ are assumed to be periodic with period T_s. The signature waveforms for the users indexed by $k = K+1, ..., K+K_I$ are given by

$$s_k(t) = \psi_I(t)e^{\sqrt{-1}2\pi f_0 t}, \tag{3.5}$$

where $\psi_I(t)$ has a support $[0, T_{sI}]$ with

$$\int_0^{T_{sI}} |\psi_I(t)|^2 dt = 1, \tag{3.6}$$

and f_0 is the frequency offset with respect to the carrier frequency. For simplicity of notation we will assume that $T_{sI} = G_I T_c$, with G_I being an integer that satisfies[8] $G_I(T_I + B_I) = G(T + B)$.

[8]It is assumed that the frames of all $K + K_I$ users are of equal duration, from where the condition above follows.

The channel between the nth transmit antenna of the kth user and the mth receive antenna is assumed to appear as a FIR filter whose channel impulse response (CIR) is given by

$$g_k^{(m,n)}(t) = \sum_{l=0}^{L_k-1} g_{kl}^{(m,n)} \delta(t - \tau_{kl}), \tag{3.7}$$

where L_k is the number of multipath components for the kth user and $g_{kl}^{(m,n)}$ and τ_{kl} are the complex channel gain and relative delay for the lth multipath component. It is assumed that the values $g_{kl}^{(m,n)}$ are independent and identically Gaussian distributed and normalized so that

$$\sum_{l=0}^{L_k-1} E\{|g_{kl}^{(m,n)}|^2\} = 1. \tag{3.8}$$

The received noiseless signal component at the mth receive antenna due to the kth user is given by

$$\begin{aligned} r_k^{(m)}(t) &= \sum_{n=1}^{N_T} \sum_{i=1}^{B+T} b_k^{(n)}(i) \sqrt{P_k^{(n)}} s_k(t - iT_s) * g_k^{(m,n)}(t) && (3.9) \\ &= \sum_{n=1}^{N_T} \sum_{i=1}^{B+T} b_k^{(n)}(i) \sqrt{P_k^{(n)}} \sum_{j=1}^{G} c_k(j) \overline{g}_k^{(m,n)}(t) && (3.10) \\ &\quad \text{for } k = 1, ..., K, && (3.11) \end{aligned}$$

and

$$\begin{aligned} r_k^{(m)}(t) &= \sum_{n=1}^{N_T} \sum_{i=1}^{B_I+T_I} b_k^{(n)}(i) \sqrt{P_k^{(n)}} s_k(t - iT_I) * g_k^{(m,n)}(t) && (3.12) \\ &= \sum_{n=1}^{N_T} \sum_{i=1}^{B_I+T_I} b_k^{(n)}(i) \sqrt{P_k^{(n)}} \overline{g}_k^{(m,n)}(t) && (3.13) \\ &\quad \text{for } k = K+1, ..., K+K_I, && (3.14) \end{aligned}$$

where

$$\begin{aligned} \overline{g}_k^{(m,n)}(t) = \psi(t) * g_k^{(m,n)}(t) &= \sum_{l=0}^{L_k-1} g_{kl}^{(m,n)} \psi(t - \tau_{kl}) && (3.15) \\ &\quad \text{for } k = 1, ..., K, && (3.16) \end{aligned}$$

and

$$\begin{aligned} \overline{g}_k^{(m,n)}(t) = \psi_I(t) * g_k^{(m,n)}(t) &= \sum_{l=0}^{L_k-1} g_{kl}^{(m,n)} \psi_I(t - \tau_{kl}) e^{\sqrt{-1} 2\pi (t-\tau_{kl}) f_0} && (3.17) \\ &\quad \text{for } k = K+1, ..., K+K_I. && (3.18) \end{aligned}$$

Without loss of generality we will assume that $\tau_{k1} < \tau_{k2} < ... < \tau_{kL_k}$. Let us now denote the discrete-time channel response between the the nth antenna of the kth user and the mth receive antenna as

$$f_k^{(m,n)}(p) = \int_0^{T_c} \overline{g}_k^{(m,n)}(t + pT_c)\psi(t)dt, \tag{3.19}$$

which for $k = 1, ..., K$ becomes

$$f_k^{(m,n)}(p) = \sum_{l=1}^{L_k} \int_0^{T_c} g_{kl}^{(m,n)}\psi(t - \tau_{kl} + pT_c)\psi(t)dt, \tag{3.20}$$

which is non zero for $p = 0, ..., \lceil \frac{\tau_{kL_k}}{T_c} \rceil$. In case of $k = K + 1, ..., K + K_I$ (3.19) becomes

$$f_k^{(m,n)}(p) = \sum_{l=1}^{L_k} \int_0^{T_c} g_{kl}^{(m,n)}\psi_I(t - \tau_{kl} + pT_c)\psi(t)e^{\sqrt{-1}2\pi(t-\tau_{kl}+pT_c)f_0}dt, \tag{3.21}$$

and it has non zero values for $p = 0, ..., \lceil \frac{\tau_{kL_k}}{T_c} \rceil + G_I - 1$.

It is known that a sufficient decision statistic can be obtained by sampling the outputs of the chip-matched filter once per chip interval. Let us denote the total received signal as

$$r^{(m)}(t) = \sum_{k=1}^{K+K_I} r_k^{(m)}(t) + z^{(m)}(t), \tag{3.22}$$

where $z^{(m)}(t)$ is the additive white noise with variance σ^2. The signal corresponding to the jth chip interval of the ith symbol of the signal received at the mth receive antenna is obtained by chip-matched filtering and sampling and is given by

$$r_j^{(m)}(i) = \int_{iT_s+jT_c}^{iT_s+(j+1)T_c} r^{(m)}(t)\psi(t - iT_s - jT_c)dt, j = 0, ..., G - 1. \tag{3.23}$$

Let us also define the convolution of the spreading sequence $s_k(j)$ for $k = 1, ..., K$ with the equivalent discrete channel impulse response $f_k^{(m,n)}(p)$ as

$$h_k^{(m,n)}(p) = \sqrt{P_k^{(n)}}\{s_k(p)\} * \{f_k^{(m,n)}(p)\}, \tag{3.24}$$

which has non-zero values for $p = 0, ..., G + \lceil \frac{\tau_{kL_k}}{T_c} \rceil$. For $k = K + 1, ..., K + K_I$ we define

$$h_k^{(m,n)}(p) = \sqrt{P_k^{(n)}} f_k^{(m,n)}(p), \tag{3.25}$$

which has non zero values for $p = 0, ..., \lceil \frac{\tau_{kL_k}}{T_c} \rceil + G_I - 1$.

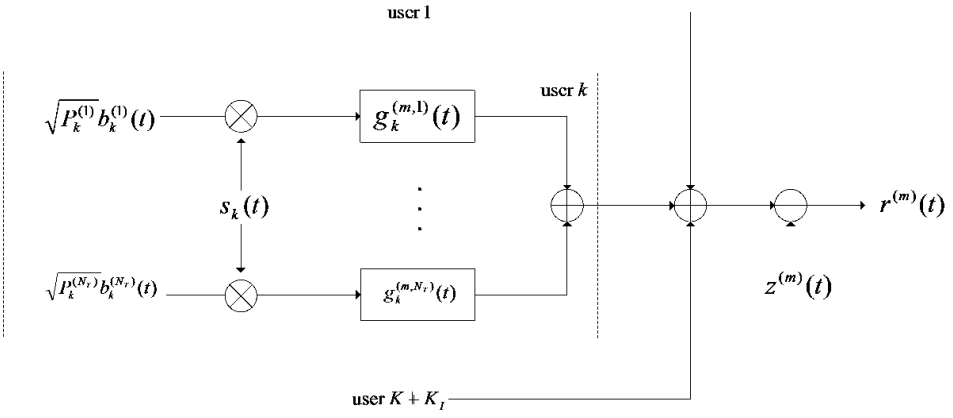

Fig. 3.1. **System model for the received signal at the mth receive antenna.**

Using (3.24), (3.22) can be expressed as

$$\begin{aligned} r_j^{(m)}(i) &= \sum_{k=1}^{K}\sum_{l=0}^{L-1}\sum_{n=1}^{N_T} h_k^{(m,n)}(lG+j)b_k^{(m,n)}(i-l) \qquad (3.26)\\ &+ e^{\sqrt{-1}2\pi f_0(iG+j)T_c}\sum_{k=K+1}^{K+K_I}\sum_{l=0}^{L_I-1}\sum_{n=1}^{N_T} h_k^{(m,n)}(lG_I+\mu_j)b_k^{(m,n)}(\lfloor\frac{iG+j}{G_I}\rfloor-l)\\ &+ z_j^{(m)}(i), \end{aligned}$$

where $\mu_j = lG+j-\lfloor\frac{lG+j}{G_I}\rfloor G_I$, $j=0,...,G-1$, $L=\max_{k=1,...,K}\{1+\lceil\lceil\tau_{kL_K}/T_c\rceil/G\rceil\}$, $L_I=\max_{k=K+1,...,K+K_I}\{1+\lceil\lceil\tau_{kL_K}/T_c\rceil/G_I\rceil\}$ and $z_j^{(m)}(i)$ is the additive noise component with variance σ^2.

Arranging the signals in vector form we make the space-time representation of the received signal at time instant i given by

$$\mathbf{y}(i) = \underbrace{\mathbf{H}\mathbf{u}(i)}_{\text{desired}} + \underbrace{\mathbf{H}_I\mathbf{u}_I(i)}_{\text{UCCI}} + \underbrace{\mathbf{n}(i)}_{\text{noise}},\ i=1,...,T+B, \qquad (3.27)$$

where $\mathbf{y}(i)$ is space-time sampled received signal vector, given by

$$\mathbf{y}(i) = [\mathbf{r}^T(i+L-1),\ldots,\mathbf{r}^T(i)]^T \in \mathbb{C}^{LGN_R\times 1} \qquad (3.28)$$

with $\mathbf{r}(i)$ being

$$\mathbf{r}(i) = [\mathbf{r}^{(1)}(i),\ldots,\mathbf{r}^{(N_R)}(i)]^T \in \mathbb{C}^{GN_R\times 1}, \qquad (3.29)$$

and

$$\mathbf{r}_m(i) = [r_1^{(m)}(i),\ldots,r_G^{(m)}(i)]^T \in \mathbb{C}^{G\times 1}. \qquad (3.30)$$

$\mathbf{H}$ is a channel matrix with the form of

$$\mathbf{H} = \begin{bmatrix} \mathbf{H}(0) & \dots & \mathbf{H}(L-1) & \dots & \mathbf{0} \\ \vdots & \ddots & & \ddots & \vdots \\ \mathbf{0} & \dots & \mathbf{H}(0) & \dots & \mathbf{H}(L-1) \end{bmatrix} \in \mathbb{C}^{LGN_R \times KN_T(2L-1)},$$

and

$$\mathbf{H}(l) = \begin{bmatrix} \mathbf{H}_1^{(1)}(l) & \dots & \mathbf{H}_K^{(1)}(l) \\ \vdots & \ddots & \vdots \\ \mathbf{H}_1^{(N_R)}(l) & \dots & \mathbf{H}_K^{(N_R)}(l) \end{bmatrix} \in \mathbb{C}^{N_R G \times KN_T},$$

with

$$\mathbf{H}_k^{(m)}(l) = \begin{bmatrix} h_k^{(m,1)}(lG) & \dots & h_k^{(m,N_T)}(lG) \\ \vdots & \ddots & \vdots \\ h_k^{(m,1)}(lG+G-1) & \dots & h_k^{(m,N_T)}(lG+G-1) \end{bmatrix} \in \mathbb{C}^{G \times N_T}.$$

The matrix $\mathbf{H}_I$ is defined as

$$\mathbf{H}_I = \begin{bmatrix} \mathbf{H}_I(0) & \dots & \mathbf{H}_I(L_I-1) & \dots & \mathbf{0} \\ \vdots & \ddots & & \ddots & \vdots \\ \mathbf{0} & \dots & \mathbf{H}_I(0) & \dots & \mathbf{H}_I(L_I-1) \end{bmatrix} \in \mathbb{C}^{LGN_R \times K_I N_T(L+L_I-1)}$$

where

$$\mathbf{H}_I(l) = \begin{bmatrix} \mathbf{H}_{K+1}^{(1)}(l) & \dots & \mathbf{H}_{K+K_I}^{(N_R)}(l) \\ \vdots & \ddots & \vdots \\ \mathbf{H}_{K+1}^{(N_R)}(l) & \dots & \mathbf{H}_{K+K_I}^{(N_R)}(l) \end{bmatrix} \in \mathbb{C}^{N_R G \times K_I N_T},$$

with

$$\mathbf{H}_k^{(m)}(l) = \begin{bmatrix} \mathbf{H}_{k1}^{(m)}(l) & \dots & \mathbf{0} \\ \vdots & \ddots & \vdots \\ \mathbf{0} & \dots & \mathbf{H}_{kG}^{(m)}(l) \end{bmatrix} \in \mathbb{C}^{GN_T \times N_T}.$$

and

$$\mathbf{H}_{kj}^{(m)}(l) = e^{\sqrt{-1}2\pi f_0(iG+j)T_c}[h_k^{(m,1)}(lG_I+\mu_j) \dots h_k^{(m,N_T)}(lG_I+\mu_j)].$$

The vectors $\mathbf{u}(i)$ and $\mathbf{u}_I(i)$ denote desired and unknown users' sequences, respectively, and they are defined as

$$\mathbf{u}(i) = [\mathbf{b}^T(i+L-1), \dots, \mathbf{b}^T(i), \dots, \mathbf{b}^T(i-L+1)]^T \in \mathbb{Q}^{KN_T(2L-1)\times 1} \quad (3.31)$$

and

$$\mathbf{u}_I(i) = [\mathbf{b}_I^T(i+L-1), \dots, \mathbf{b}_I^T(i), \dots, \mathbf{b}_I^T(i-L_I+1)]^T \in \mathbb{Q}^{K_I N_T(L+L_I-1)\times 1}, \quad (3.32)$$

with

$$\mathbf{b}(i) = [b_1^{(1)}(i), \ldots, b_1^{(N_T)}(i), \ldots, b_K^{(1)}(i), \ldots, b_K^{(N_T)}(i)]^T, \in \mathbb{Q}^{KN_T \times 1} \tag{3.33}$$

and

$$\mathbf{b}_I(i-l) = [\mathbf{b}_{I1}^T(i-l), \ldots, \mathbf{b}_{IG}^T(i-l)]^T \in \mathbb{Q}^{K_I G N_T \times 1}, \tag{3.34}$$

where

$$\begin{aligned} \mathbf{b}_{Ij}(i-l) = [&b_{K+1}^{(1)}(\lfloor \frac{iG+j}{G_I} \rfloor - l), \ldots, b_{K+1}^{(N_T)}(\lfloor \frac{iG+j}{G_I} \rfloor - l), \ldots, \\ &b_{K+K_I}^{(1)}(\lfloor \frac{iG+j}{G_I} \rfloor - l), \ldots, b_{K+K_I}^{(N_T)}(\lfloor \frac{iG+j}{G_I} \rfloor - l)]^T \in \mathbb{Q}^{K_I N_T \times 1}. \end{aligned} \tag{3.35}$$

Vector $\mathbf{n}(i) \in \mathbb{C}^{LN_R \times 1}$ contains additive white noise (AWN) with covariance $E\{\mathbf{n}(i)\mathbf{n}^H(i)\} = \sigma^2\mathbf{I}$. Note that the noise PDF is not restricted to be Gaussian, as some parts of the thesis will deal with non-Gaussian noise.

4 Iterative interference suppression and cancellation in CDMA

The common assumption made in this chapter is that of redundancy in time, introduced by spreading the signal using the DS-SS technique. Different levels of knowledge about the interference are assumed, resulting in different optimal and suboptimal ways for interference mitigation.

The chapter is organized in two sections, with the basic difference being in the interference model considered. In Section 4.1, interference is assumed to have a time correlation property, which allows for the estimation of its instantaneous value. This, in turn, allows for interference cancellation, or equivalently, for the ML detection conditioned on the *instantaneous* value of the interference. On the other hand, in Section 4.2 the interference is modelled *statistically*, using a PDF, and interference cancellation is no longer possible. Instead, either parametric or non parametric PDF estimation can be applied. The chapter is concluded in Section 4.3.

4.1 Blind iterative NBI and WBI cancellation in spread-spectrum systems

In this section the unknown interference will be assumed to posses a property that allows for its blind estimation and active cancellation. In this context, the problem of spectral overlay of NBI and the DS-SS signal of interest will be considered. Correspondingly, the property of NBI correlation in time will be used for interference cancellation. For clarity of presentation, a special case of the generic system model is given in Section 4.1.1. Linear prediction and interpolation filters are introduced in Section 4.1.2. An extended version thereof that is robust to the interference bandwidth and can cope both with NBI and WBI is described in Section 4.1.3. An iterative robust receiver is introduced in the same section. A performance analysis of the iterative receiver are presented in Section 4.1.4. The major results of Section 4.1 are summarized in Section 4.3.

4.1.1 Special case of generic model - overlay of the SS signal and WBI

Let us consider the generic model presented in Chapter 3.2 for the special case of $K = 1$, $K_I = 1$. It will be further assumed that both the SOI and WBI are experiencing a flat-fading channel, which results in $L_k = 1$, $k = 1, 2$. A further assumption will be that the SOI and WBI consume the same bandwidth, which results in $T_{sI} = T_c$ and correspondingly $G_I = 1$. The received signal given by (3.17) now reduces to

$$\mathbf{y}(i) = \underbrace{\mathbf{H}\mathbf{u}(i)}_{\text{desired}} + \underbrace{\mathbf{H}_I\mathbf{u}_I(i)}_{\text{UCCI}} + \underbrace{\mathbf{n}(i)}_{\text{noise}}, \; i = 1, ..., T + B, \tag{4.1}$$

where

$$\begin{aligned} \mathbf{y}(i) &= [r_1^{(1)}(i), \ldots, r_G^{(1)}(i)]^T \in \mathbb{C}^{G\times 1} \\ &= [r_1(i), \ldots, r_G(i)]^T, \end{aligned} \tag{4.2}$$

$$\begin{aligned} \mathbf{H} &= g_1^{(1,1)}[s_1(1), \ldots, s_1(G)]^T \in \mathbb{C}^{G\times 1} \\ &= g_1[s_1(1), \ldots, s_1(G)]^T, \end{aligned} \tag{4.3}$$

and

$$\mathbf{u}(i) = b_1^{(1)}(i) = b_1(i), \tag{4.4}$$

where dependence on m, n, and l is omitted for simplicity of notation. Furthermore

$$\begin{aligned} \mathbf{H}_I &= g_2^{(1,1)}\text{diag}(e^{\sqrt{-1}2\pi f_0(iG+1)T_c}, \ldots, e^{\sqrt{-1}2\pi f_0(iG+G)T_c})^T \in \mathbb{C}^{G\times G} \\ &= g_2\text{diag}(e^{\sqrt{-1}2\pi f_0(iG+1)T_c}, \ldots, e^{\sqrt{-1}2\pi f_0(iG+G)T_c})^T, \end{aligned} \tag{4.5}$$

and

$$\begin{aligned} \mathbf{u}(i) &= [b_2^{(1)}(iG+1), \ldots, b_2^{(1)}(iG+G)]^T \\ &= [b_2(iG+1), \ldots, b_2(iG+G)]^T, \end{aligned} \tag{4.6}$$

with $\mathbf{n}(i)$ being AWGN with covariance matrix $E\{\mathbf{n}(i)\mathbf{n}(i)^H\} = \sigma^2\mathbf{I}$. After stacking all the signal vectors into a single vector we obtain

$$\mathbf{Y} = \mathbf{S} + \mathbf{J} + \mathbf{N}, \tag{4.7}$$

where

$$\mathbf{Y} = [\mathbf{y}^T(1), \ldots, \mathbf{y}^T(T+B)]^T \in \mathbb{C}^{G(T+B)\times 1}, \tag{4.8}$$

$$\mathbf{S} = [(\mathbf{H}\mathbf{u}(1))^T, \ldots, (\mathbf{H}\mathbf{u}(T+B))^T]^T\mathbb{C}^{G(T+B)\times 1}, \tag{4.9}$$

$$\mathbf{J} = [(\mathbf{H}_I\mathbf{u}_I(1))^T, \ldots, (\mathbf{H}_I\mathbf{u}_I(T+B))^T]^T\mathbb{C}^{G(T+B)\times 1}, \tag{4.10}$$

and

$$\mathbf{N} = [\mathbf{n}^T(1), \ldots, \mathbf{n}^T(T+B)]^T\mathbb{C}^{G(T+B)\times 1}. \tag{4.11}$$

4.1.2 Linear prediction and interpolation filters for NBI cancellation

A linear interpolation filter tries to estimate the interference sample J_j based on the future and past values of the received signal relative to the time instant j. Let us denote by $\mathbf{Y}_j$ the vector containing these past and future samples as follows

$$\mathbf{Y}_j = [Y_{j-F}, \ldots, Y_{j-1}, Y_{j+1}, \ldots, Y_{j+F}]^T, \tag{4.12}$$

where F is the linear interpolator estimation window length. The optimal linear estimator in the MMSE sense produces the interference estimate as follows

$$\hat{J}_j = \mathbf{W}_j^H \mathbf{Y}_j, \tag{4.13}$$

where the tap weights of the linear estimator are obtained so as to satisfy the following optimality criterion

$$\mathbf{W}_j = \arg \min_{\mathbf{W} \in \mathbb{C}^{2F}} ||\mathbf{W}^H \mathbf{Y}_j - Y_j||^2, \tag{4.14}$$

which results in the well known Wiener solution [259]

$$\mathbf{W}_j = E\{\mathbf{Y}_j \mathbf{Y}_j^H\}^{-1} E\{\mathbf{Y}_j Y_j^*\}. \tag{4.15}$$

A linear prediction filter has a very similar form, with the only difference being that the vector $\mathbf{Y}_j$ contains either the past or future values of the received signal. In the former case the receiver is called a forward predictor while in the latter one it is a backward predictor.

The interference estimate $\hat{J}_j$ is subtracted from the received signal resulting in an interference-free signal obtained by

$$\begin{aligned} \hat{Y}_j &= Y_j - \hat{J}_j \\ &= S_j + J_j - \hat{J}_j + N_j. \end{aligned} \tag{4.16}$$

After that the signals $\hat{Y}_j$ are grouped into the vectors corresponding to the transmitted symbols $b(i)$, $i = 1, \ldots, T + B$ as follows

$$\hat{\mathbf{y}}(i) = [\hat{Y}_{iG+1}, \ldots, \hat{Y}_{iG+G}]^T = \mathbf{H} b(i) + \mathbf{n}_e(i), \tag{4.17}$$

where $\mathbf{n}_e(i)$ contains the sum of residual interference and AWGN.

4.1.3 Self-reconfigurable iterative receiver for SS signal detection and NBI and WBI cancellation

The linear prediction and interpolation schemes described above are capable of suppressing interference whose bandwidth is narrower than the bandwidth of the SOI, so that the Wiener filter output contains mainly an interference estimate. An

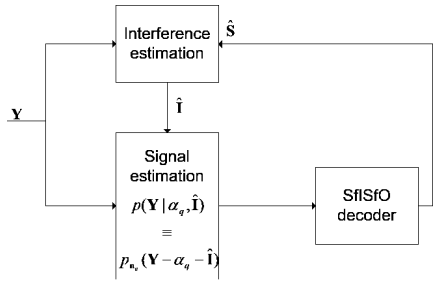

Fig. 4.1. **Principal block-diagram of the iterative self-reconfigurable receiver.**

extension thereof, called a self-reconfigurable Wiener filter is proposed in [24] and shown to be capable of suppressing interference whose bandwidth is even the same as the SOI bandwidth. Instead of only one weighting vector $\mathbf{W}_j \in \mathbb{C}^{2F\times 1}$ as in case of linear interpolation filters, the self-reconfigurable scheme uses an additional weighting vector $\mathbf{W}_{sj} \in \mathbb{Q}^{2F\times 1}$ of switching coefficients, where again F denotes the filter length. The purpose of the vector $\mathbf{W}_j$ is to adapt to the slowly time varying interference parameters, while the switching coefficients $\mathbf{W}_{sj}$ adapt to the rapidly changing interference parameters. The optimal filter coefficients are found as follows [26]

$$[\mathbf{W}_j, \mathbf{W}_{sj}] = \arg \min_{[\mathbf{W},\mathbf{W}_s]\in[\mathcal{C}^{2F\times 1},\mathcal{Q}^{2F\times 1}]} ||\mathbf{W}^H(\mathbf{W}_s^* \odot \mathbf{Y}_j) - Y_j||^2, \tag{4.18}$$

with $\odot$ denoting the element-wise vector product. This can be equivalently expressed as

$$\begin{aligned} \mathbf{W}_{sj} &= \arg \min_{\substack{\mathbf{W}_s\in\mathcal{Q}^{2F\times 1} \\ \mathbf{Y}_{sj}=\mathbf{W}_s^*\odot\mathbf{Y}_j \\ \mathbf{W}=E\{\mathbf{Y}_{sj}\mathbf{Y}_{sj}^H\}^{-1}E\{\mathbf{Y}_{sj}Y_j^*\}}} ||\mathbf{W}^H\mathbf{Y}_{sj} - Y_j||^2, \\ \mathbf{W}_j &= E\{(\mathbf{W}_{sj}^* \odot \mathbf{Y}_j)(\mathbf{W}_{sj}^* \odot \mathbf{Y}_j)^H\}^{-1}E\{(\mathbf{W}_{sj}^* \odot \mathbf{Y}_j)Y_j^*\}. \end{aligned} \tag{4.19}$$

The interference estimate is then produced as follows

$$\hat{J}_m = \mathbf{W}_m^H(\mathbf{W}_{sm}^* \odot \mathbf{Y}_m). \tag{4.20}$$

It is then subtracted from the received signal as in (4.16), again resulting in (4.17). The conditional PDF that is required for the SfISfO decoder can be given as

$$P_1^{ext}(b(i) = \alpha_q) = p(\mathbf{y}(i)|\mathbf{H}, \alpha_q) = p_{\mathbf{n}_e}(\mathbf{y}(i) - \mathbf{H}\alpha_q). \tag{4.21}$$

Assuming that the residual interference at the output of the linear interpolation filter is small, we can assume that the equivalent noise $\mathbf{n}_e$ consists only of the AWGN component with covariance matrix $E\{\mathbf{n}_e(i)\mathbf{n}_e(i)^H\} = \sigma^2\mathbf{I}$.

The procedure described above is performed in the first iteration of the iterative receiver, the general scheme of which is presented in Section 4.1. In the subsequent iterations, we make use of the soft estimate $\tilde{b}(i)$ of $b(i)$ given by

$$\tilde{b}(i) = \sum_{\alpha_q \in \mathbb{Q}} \alpha_q P_2^{app}(b(i) = \alpha_q), \tag{4.22}$$

where $P_2^{app}(b(i) = \alpha_q)$ is the *a posteriori* probability produced by the iterative decoder. The estimate of the SOI is first produced in the form of $\mathbf{H}\tilde{b}(i)$. After that, the soft cancellation of the estimate of SOI from the total received signal is performed, resulting in

$$\tilde{\mathbf{y}}(i) = \mathbf{H}(\mathbf{u}(i) - \tilde{\mathbf{u}}(i)) + \mathbf{H}_I \mathbf{u}_I(i) + \mathbf{n}(i),\ i = 1, ..., T + B. \tag{4.23}$$

The vectors $\tilde{\mathbf{y}}(i)$ are then used to make vector $\tilde{\mathbf{Y}}$ which is given as

$$\tilde{\mathbf{Y}} = \mathbf{S} - \tilde{\mathbf{S}} + \mathbf{J} + \mathbf{N}, \tag{4.24}$$

where $\mathbf{S}$, $\mathbf{J}$ and $\mathbf{N}$ are defined with (4.15), (4.16) and (4.17), respectively, and $\tilde{\mathbf{S}}$ obtained by replacing the corresponding true values $b(i)$ in $\mathbf{S}$ with their soft estimates $\tilde{b}(i)$. The interference estimate is now obtained by performing (4.18)-(4.20) with $\mathbf{Y}_j$ and Y_j being replaced by $\tilde{\mathbf{Y}}_j$ and $\tilde{Y}_j$. After obtaining the soft estimate $\hat{J}_j$ of the interference the soft cancellation is performed as in (4.16). The conditional PDF to be supplied to the SfISfO decoder is again produced as described by (4.21).

Based on the extrinsic information obtained after the detection stage the SfISfO decoder produces *a posteriori* probabilities about the symbols $b(i)$ as follows

$$P_2^{app}(b(i) = \alpha_q) = p(b(i) = \alpha_q | \mathbf{y}(i), \mathbf{H}, i = 1, ..., T + B), \tag{4.25}$$

which is used in the soft cancellation process. A detailed description of the turbo codes can be found in [28] and will not be restated here.

4.1.4 Performance analysis

The performance of the proposed iterative receivers is evaluated both analytically and by means of computer simulations. For the analytical performance evaluation SINR at the decoder input is used as the performance measure. An analytical expression for SINR at the output of the linear interpolation filter in the presence of tone interference can be found in [19] and [260] and it is expressed by

$$\gamma_{out} = \frac{P_1^{(1)}}{\frac{P_2^{(1)}}{1 + \frac{P_2^{(1)}}{2(P_1^{(1)} + \sigma^2)}[2F - 1 + \frac{\sin(2F+1)2\pi f_0 T_c}{\sin 2\pi f_0 T_c}]} + \sigma^2}, \tag{4.26}$$

in the first iteration (no feedback), and

$$\gamma_{out} = \frac{P_1^{(1)}}{\frac{P_2^{(1)}}{1+\frac{P_2^{(1)}}{2\sigma^2}[2F-1+\frac{\sin(2F+1)2\pi f_0 T_c}{\sin 2\pi f_0 T_c}]} + \sigma^2}, \tag{4.27}$$

in the case of ideal feedback. Note that for sufficiently strong interference it can be expected that the self-reconfigurable receiver will correctly adjust the switching coefficients, thereby eliminating the effect of rapidly changing interference parameters. Thereby, the performance of the self reconfigurable receiver can be expected to be similar to that of the linear interpolator with a tone jammer. Figs. 4.2 and 4.3 show the SINR at the decoder input vs. E_b/N_0 with G and the input signal to interference ratio (SIR) as parameters. It can be seen from these figures that the iterative receiver with perfect feedback significantly outperforms the non-iterative receiver if both the E_b/N_0 and input SINR are relatively large. If that is not the case, the iterative receiver does not offer performance improvement. Furthermore, the larger the processing gain the better the interference suppression capability of the non iterative receiver and the less gain from the iterative receiver that can be expected.

The results obtained from the asymptotic analysis above indicate that in typical overlay situations where the interfering signal is much stronger from the signal of interest [261] no significant improvement can be expected from the use of an iterative receiver. Moreover, since the iterative receiver makes use of the channel code, the operating E_b/N_0 point is expected to be relatively small. In Fig. 4.4 the bit error rate (BER) performance vs. E_b/N_0 is presented for the case of a spread spectrum signal overlayed with a strong interferer whose bandwidth is equal to the bandwidth of the SOI. The frequency offset of the interferer is assumed to be changed at the beginning of every frame, uniformly taking random values from the interval $[0, 1/2T_c]$. The receiver employs the iterative self reconfigurable scheme presented above. The results for non-iterative interference cancellation (type I, cancellation performed only once, iterations performed only within the decoder) and iterative interference cancellation (type II, cancellation performed at every iteration) are presented. It can be concluded from these results that the iterative receiver does not offer performance improvement in the observed SNR region, thereby justifying the speculation from above.

4.2 Iterative decoding of turbo-coded spread-spectrum signals in man-made noise

The interference model assumed in the previous section is suitable for the representation of a legacy or competing communication signal that directly overlays with the signal of interest. The interference prediction was possible thanks to the fact that the interference constellation consisted of a finite number of points and that the interference possibly remains in the same state for a long period of time. Section

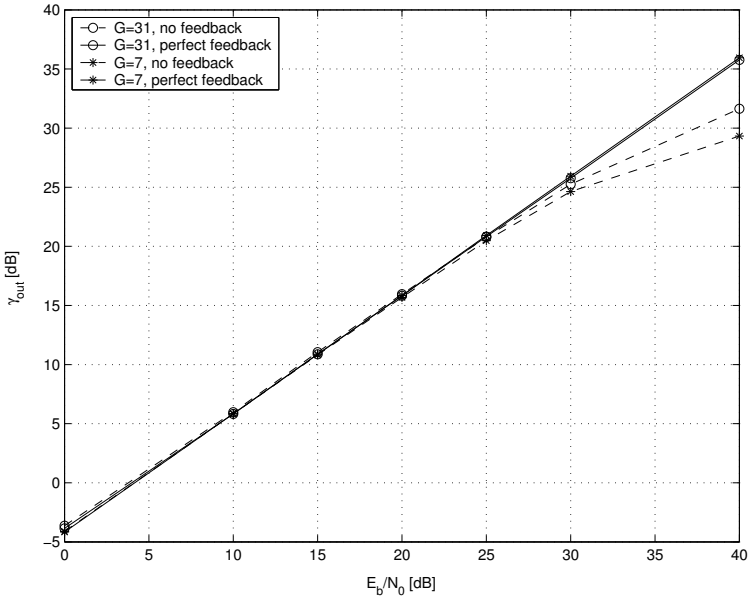

Fig. 4.2. SINR at the decoder input vs. E_b/N_0**,** $(K, K_I, N_R, N_T) = (1, 1, 1, 1)$**, channel is static both for SOI and NBI, noise is AWGN, input SIR**$= -20$**dB,** $G = 7$ **and** 31**, frequency offset** $f_0 = 1/4T_c$**.**

4.1 and Chapter 5 focus on this kind of interference model. However, there exist many situations in which the conditions for predictability of the interfering signal may not be satisfied. An example is man-made noise which is usually characterized by impulses of random occurrence and duration. The source of interference can be any electrical equipment used in everyday life (printers, microwave ovens, power lines etc.). Another example may occur in wireless local area networks (WLAN) in the case of several users contesting for the channel in an uncoordinated fashion. There, the packets are transmitted in a random fashion and collisions may occur. Although the collisions are usually handled at higher layers by means of different multiple access methods[1], that problem could also be handled at the physical layer, by means of interference suppression and cancellation. Since the interference pulses are random they impose the need for statistical modelling and the prediction of the instantaneous interference level is not possible. Among the statistical interference models the most credited and used one is the Middleton class A model [4]. The main beauty of that model is that it was developed based on the statistical and physical mechanisms that drive the interference process in communication receivers.

[1]Possible examples are carrier sense multiple access (CSMA) with or without collision detection (CD) or collision avoidance (CA) [262]

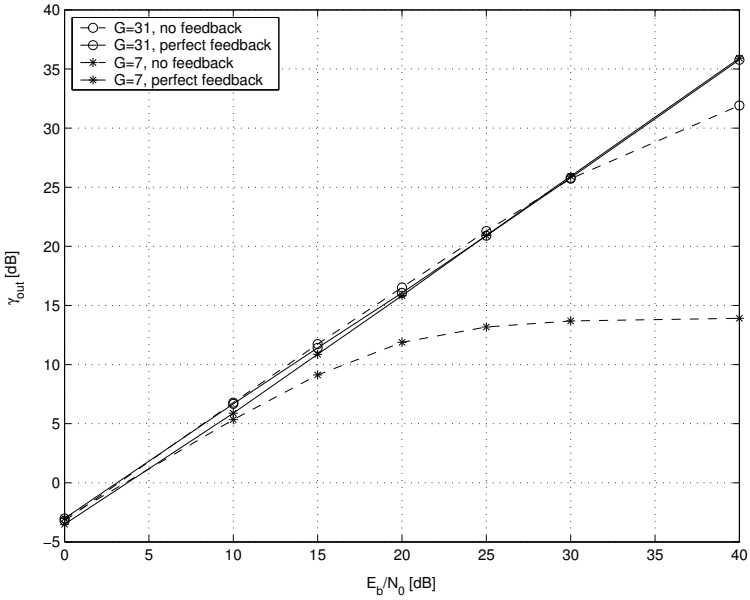

Fig. 4.3. **SINR at the decoder input vs.** E_b/N_0**,** $(K, K_I, N_R, N_T) = (1, 1, 1, 1)$**, channel is static both for SOI and NBI, noise is AWGN, input SIR**$= 0$**dB,** $G = 7$ **and** 31**, frequency offset** $f_0 = 1/4T_c$**.**

This section discusses receivers that are capable of dealing with statistically modelled interference processes. In Section 4.2.1 the special case of the generic system model is restated for the purpose of signal detection in non-Gaussian noise. The Middleton class A interference model is presented and its physical interpretation is given in the same section. Section 4.2.2 presents optimal and locally optimal receivers. Section 4.2.3 describes the principles of type-based detection and an iterative receiver based on it. Section 4.2.4 presents numerical results, and, finally, Section 4.3 concludes the whole chapter.

4.2.1 Special case of the generic model - DS-SS signal in non-Gaussian noise

$_I = 0$, $N_T = 1$ we can write the received signal at time instant i as

$$\mathbf{y}(i) = \mathbf{H}\mathbf{u}(i) + \mathbf{n}(i), \ i = 1, ..., T + B, \tag{4.28}$$

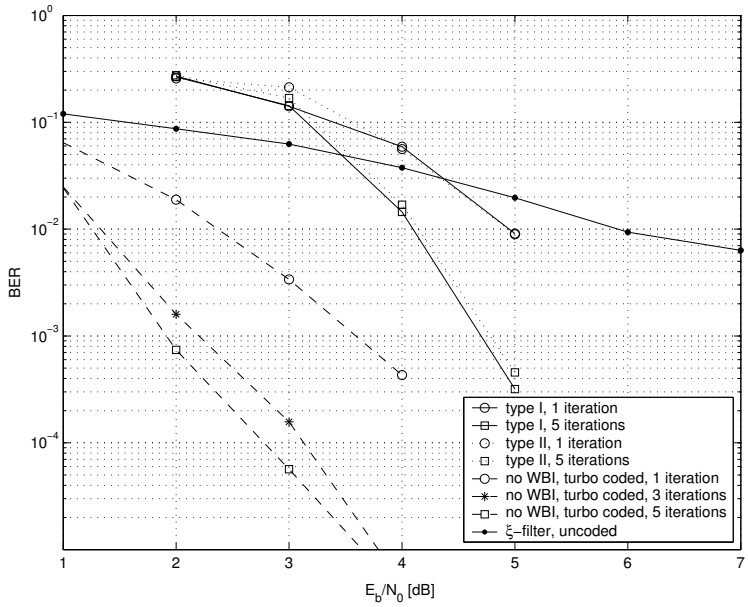

Fig. 4.4. BER performance vs. E_b/N_0**,** $(K, K_I, N_T, N_R) = (1, 1, 1, 1)$**, channel is static both for SOI and NBI, noise is AWGN, self reconfigurable iterative receiver, data-like interference with relative bandwidth** 100%**, frequency offset** f_0 **changes every frame taking values from the interval** $[0, 1/2T_c]$ **uniformly, turbo coded system.**

where vector $\mathbf{y}(i)$ is given by the Eq. (3.28) and equivalent channel matrix $\mathbf{H}$ has the form of

$$\mathbf{H} = \begin{bmatrix} \mathbf{H}(0) & \dots & \mathbf{H}(L-1) & \dots & \mathbf{0} \\ \vdots & \ddots & & \ddots & \vdots \\ \mathbf{0} & \dots & \mathbf{H}(0) & \dots & \mathbf{H}(L-1) \end{bmatrix} \in \mathbb{C}^{LGN_R \times (2L-1)},$$

and

$$\mathbf{H}(l) = \begin{bmatrix} \mathbf{H}^{(1)}(l) \\ \vdots \\ \mathbf{H}^{(N_R)}(l) \end{bmatrix} \in \mathbb{C}^{N_R G \times 1},$$

with

$$\mathbf{H}^{(m)}(l) = \begin{bmatrix} h^{(m)}(lG) \\ \vdots \\ h^{(m)}(lG+G-1) \end{bmatrix} \in \mathbb{C}^{G \times 1}.$$

Note that the dependence of $h_k^{(m,n)}(lG)$ and $\mathbf{H}_k^{(m)}(l)$ on k and n is omitted for the simplicity of notation. Vector $\mathbf{u}(i)$ that denotes the desired signal is described in (3.31) and the noise is assumed to be additive white, possibly non-Gaussian, with covariance matrix $\sigma^2\mathbf{I}$. In order to capture the lth multipath component at the mth receive antenna of the signal transmitted at the time instant i, where $l = 1, ..., \lceil \tau_{1L_1}/T_c \rceil$, we form the vectors $\mathbf{y}_l^{(m)}$, $l = 1, ..., \lceil \tau_{1L_1}/T_c \rceil$ in the following way

$$\mathbf{y}_l^{(m)} = [\mathbf{y}_{\lfloor \frac{\tau_{1l}}{GT_c} \rfloor GN_R+(m-1)G+\lceil \frac{\tau_{1l}}{T_c} \rceil - G\lfloor \frac{\tau_{1l}}{GT_c} \rfloor}, ..., \mathbf{y}_{\lfloor \frac{\tau_{1l}}{GT_c} \rfloor GN_R+(m-1)G+G-1}, \tag{4.29}$$
$$\mathbf{y}_{(\lfloor \frac{\tau_{1l}}{GT_c} \rfloor+1)GN_R+(m-1)G}, ..., \mathbf{y}_{(\lfloor \frac{\tau_{1l}}{GT_c} \rfloor+1)GN_R+(m-1)G-\lceil \frac{\tau_{1l}}{T_c} \rceil+G(1+\lfloor \frac{\tau_{1l}}{GT_c} \rfloor)}]^T \in \mathbb{C}^{G\times 1}.$$

Let us denote with $\mathbf{c}_1$ the vector containing the first user's spreading sequence. After multiplying all $\mathbf{y}_l^{(m)}$, $l = 1, ..., \lceil \frac{\tau_{1L_1}}{T_c} \rceil$, $m = 1, ..., N_R$ elementwise with $\mathbf{c}_1$ and stacking them into a vector, we obtain a decision statistic

$$\mathbf{y}_d = [\mathbf{y}_1^{(1)} \odot \mathbf{c}_1{}^T, ..., \mathbf{y}_1^{(N_R)} \odot \mathbf{c}_1{}^T, ..., \mathbf{y}_{\lceil \frac{\tau_{1L_1}}{T_c} \rceil}^{(1)} \odot \mathbf{c}_1{}^T, ..., \mathbf{y}_{\lceil \frac{\tau_{1L_1}}{T_c} \rceil}^{(N_R)} \odot \mathbf{c}_1{}^T]. \tag{4.30}$$

Assuming that the autocorrelation of the user's spreading sequence is zero for non-zero tags, the decision statistic can be rewritten as

$$\mathbf{y}_d(i) = \mathbf{h}_d b(i) + \mathbf{n}_d(i) \in \mathbb{C}^{GN_R\lceil \frac{\tau_{1L_1}}{T_c} \rceil \times 1}, \tag{4.31}$$

where

$$\mathbf{h}_d = [\mathbf{h}_1^{(1)^T}, ..., \mathbf{h}_1^{(N_R)^T}, ..., \mathbf{h}_{\lceil \frac{\tau_{1L_1}}{T_c} \rceil}^{(1)}{}^T, ..., \mathbf{h}_{\lceil \frac{\tau_{1L_1}}{T_c} \rceil}^{(N_R)}{}^T], \tag{4.32}$$

and $\mathbf{n}_d(i)$ is additive noise, which is assumed to be Middleton class A in this case.

The PDF of the instantaneous amplitude of the multivariate class A noise, with the assumption of statistically independent noise samples between multipaths and receive antennas[2], is given by [4, 177]

$$p_{\mathbf{n}_d}(\mathbf{n}_d(i)) \cong e^{-A_A} \prod_{j=1}^{LN_RG} \sum_{k=0}^{\infty} \frac{A_A^k}{k!} \frac{1}{\sqrt{2\pi\sigma_k^2}} e^{-\frac{n_{dj}^*(i)n_{dj}(i)}{2\sigma_k^2}}, \tag{4.33}$$

where A_A is the impulsive index, defined as the product of the average number of radiation events per second and the mean duration of the typical interference source emission. The larger the value of A_A, the closer the noise to the Gaussian. The variance σ_k is defined as

$$\sigma_k^2 = \frac{\frac{k}{A_A} + \Gamma}{1 + \Gamma}, \tag{4.34}$$

[2]Although the independency assumption cannot be justified in some situations [177] since interference can in practice be correlated in space and time, it provides the limiting case of the worst case scenario for the performance evaluation. This is due to the fact that the dependency and correlation between noise samples can be used to suppress or cancel the interference, resulting in better performance.

Table 4.1. $p(k\ on)$ vs. k and A_A, $p_{min} = 10^{-8}$.

A_A	$p(0\ \text{on})$	$p(1\ \text{on})$	$p(2\ \text{on})$	K_{eff}
0.1	$9.048 \cdot 10^{-1}$	$9.05 \cdot 10^{-2}$	$4.5 \cdot 10^{-3}$	6
0.001	$9.99 \cdot 10^{-1}$	$9.99 \cdot 10^{-4}$	$4.995 \cdot 10^{-7}$	2

Table 4.2. r_{mp} vs. Γ, $A_A = 0.1$, $\gamma = 1.5$, $P_0 = 0.125mW$.

Γ	$\Gamma 10^{-1}$	10^{-2}	10^{-3}	10^{-4}	10^{-5}
r_{mp}[meters]	269	127	58	27	12

with $\Gamma = \frac{\sigma_0^2}{\Omega_A}$ being the ratio of the average power of the Gaussian component of the noise σ_0^2 to that of the impulsive component (Ω_A^2). Note that the total noise power $\sigma_0^2 + \Omega_A^2$ is equal to σ^2.

An interesting physical interpretation of the model presented above is given in [250]. The scenario can be summarized as follows:

- There are infinitely many potential interfering sources with the same effective radiated power and isotropic radiation antenna. Interference power at the receiver site is proportional to the ratio $P(r) = \frac{P_0}{r^{2\gamma}}$, where P_0 is the interference power, r is the distance between interfering source and the victim receiver and γ is the propagation exponent.

- Interfering sources are randomly located in space, and the PDF of their distances from the victim receiver is given by

$$f_r(r) = 2\gamma P_0 \theta \frac{e^{-\frac{P_0\theta}{r^{2\gamma}}}}{r^{2\gamma+1}}, \theta = \left(\frac{\Omega_A}{A_A} + \sigma_G^2\right)^{-1}. \tag{4.35}$$

- Interferer emission times are Poisson distributed. $A_A \ll 1$, in practice A_A can be as large as 0.25 for the model to be valid. When two or more interferers are turned on simultaneously, the total noise-plus-interference is Gaussian distributed. The background instantaneous noise amplitude is Gaussian distributed.

The probability that exactly k interferers are turned on is now given by

$$p(k\ \text{on}) = e^{-A_A} \frac{A_A^k}{k!}. \tag{4.36}$$

Table 4.1 shows $p(k \text{ on})$ vs. k for two different parameters A_A. The smaller A_A the faster $P(k \text{ on})$ decreases with respect to k. We can define the maximum effective number of interference sources as a function of A_A, as

$$K_{eff} = \max \arg_k \{P(k \text{ on}) > p_{min}\}, \tag{4.37}$$

where we assume that all events $\{k \text{ on} | p(k \text{ on}) < p_{min}\}$ are not likely to happen.

Table 4.2 shows the most probable distance r_{mp} between interference sources and the victim receiver, based on (4.35) for fixed parameters A_A and γ, and parameter Γ variable. We can see that the smaller the Γ (that corresponds to increasing the power of the impulsive noise relative to the Gaussian) the smaller the distance r_{mp}.

4.2.2 Optimal, locally optimal and hard limited correlating iterative detectors

The optimal detector (OD) in a minimum error rate sense is the ML detector [1], regardless of the PDF of the noise. The ML receiver defined over the finite set $\mathbb{Q}$ can now be defined as follows

$$\hat{b}(i) = \arg \max_{\alpha_q \in \mathbb{Q}} p(\mathbf{y}_d | \mathbf{h}_d, \alpha_q) \tag{4.38}$$

$$= \arg \max_{\alpha_q \in \mathbb{Q}} p_{\mathbf{n}_d}(\mathbf{y}_d - \mathbf{h}_d \alpha_q), \tag{4.39}$$

and it will result in the decision about the transmitted bit. However, the SfISfO iterative decoder requires soft channel information that can be produced directly as

$$P_1^{ext}(\alpha_q) = P_1^{ext}(b(i) = \alpha_q) = p_{\mathbf{n}_d}(\mathbf{y}_d - \mathbf{h}_d \alpha_q), \alpha_q \in \mathbb{Q}. \tag{4.40}$$

The locally optimal Bayes detector (LOBD) is proposed and analyzed in [15]. Based on a small-signal assumption the likelihood function given in (4.40) can be developed in a Taylor series in the vicinity of $\alpha_q = 0$ as follows [15]

$$p_{\mathbf{n}_d}(\mathbf{y}_d - \mathbf{h}_d \alpha_q) \approx p_{\mathbf{n}_d}(\mathbf{y}_d) - \frac{dp_{\mathbf{n}_d}(\mathbf{y}_d)}{d\mathbf{y}_d} \alpha_q, \alpha_q \in \mathbb{Q}, \tag{4.41}$$

where all the terms after the second one in the Taylor series are neglected.

A hard limited linear correlator (HLLC) is a modification of the linear correlating (LC) receiver. The linear correlating receiver is a base for the vast majority of spread-spectrum receivers used so far, due to its simplicity and optimality in AWGN. However, its performance is degraded significantly in a non-Gaussian, impulsive environment. To combat the deteriorating effects of impulsive interference, a simple, non-linear modification of the linear correlator can be applied, using hard limiting after chip-matched filtering and sampling, and before correlating with the spreading sequence. Its detailed description and performance analysis can be found in [183].

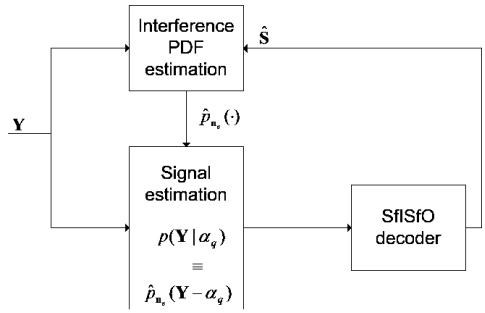

Fig. 4.5. Principal block-diagram of the iterative type-based receiver.

4.2.3 Type-based iterative detector

A type-based detector (TBD) for spread-spectrum is proposed in [194]. Its principal block diagram is presented in Fig. 4.5. A more detailed illustration of the receiver is given in Fig. 4.6. The received signal $\mathbf{y}_d(i)$, $i = T+1, ..., T+B$ is first quantized resulting in the sequence $\mathbf{y}_\Xi(i)$ and is used to form the multidimensional type (i.e., an estimate of the underlying discrete PDF) of the received symbol, defined by

$$\hat{P}_{\mathbf{y}_\Xi(i)}(\mathbf{q}) = \frac{1}{G}\sum_{j=0}^{G-1} I(\mathbf{x}_j(i) = \mathbf{q}), \mathbf{q} \in \Xi^{L_c N_R}, \tag{4.42}$$

where $L_c = \lceil \frac{\tau_1 L_1}{T_c} \rceil$ and $\mathbf{x}_j$ is defined as

$$\mathbf{x}_j(i) = [\mathbf{y}_{\Xi,j}(i), \mathbf{y}_{\Xi,G+j}(i), ..., \mathbf{y}_{\Xi,(LN_R-1)G+j}(i)]^T \in \Xi^{L_c N_R}, \tag{4.43}$$

and $I(\cdot)$ is an indicator function which has a value of 1 if its argument is true and 0 otherwise.

Prior to the detection of the signals, a training sequence is used to determine the types corresponding to all the signal constellation points. To make the type for constellation point α_q the vectors $\mathbf{y}_d(i)$, $i = 1, ..., T$ are multiplied by $e^{-\sqrt{-1}(\angle b^*(i) + \angle \alpha_q)}$ in order to remove the known phase of the desired signal. The signal obtained in such a way is then quantized, resulting in $\mathbf{y}_{\alpha_q \Xi}(i)$, $i = 1, ..., T$. The type corresponding to the constellation point α_q is now obtained by

$$\hat{P}_{\alpha_q}(\mathbf{q}) = \frac{1}{TG}\sum_{i=0}^{T}\sum_{j=0}^{G-1} \mathbf{I}(\mathbf{x}_{\alpha_q j}(i) = \mathbf{q}), \mathbf{q} \in \Xi^{L_c N_R}, \tag{4.44}$$

where $\mathbf{x}_{\alpha_q j}(i)$ is defined as

$$\mathbf{x}_{\alpha_q j}(i) = [\mathbf{y}_{\alpha_q \Xi,j}(i), \mathbf{y}_{\alpha_q \Xi,G+j}(i), ..., \mathbf{y}_{\alpha_q \Xi,(LN_R-1)G+j}(i)]^T \in \Xi^{L_c N_R}. \tag{4.45}$$

Let us also define

$$\hat{P}_{\alpha_q \mathbf{y}_\Xi(i)}(\mathbf{q}) = \frac{TG\hat{P}_{\alpha_q}(\mathbf{q}) + G\hat{P}_{\mathbf{y}_\Xi(i)}(\mathbf{q})}{TG+G}, \mathbf{q} \in \Xi^{L_c N_R}. \tag{4.46}$$

The type-based detector now forms the decision statistics given by [191]

$$S_{\alpha_q}(i) = D(\hat{P}_{\mathbf{y}_\Xi(i)} || \hat{P}_{\alpha_q \mathbf{y}_\Xi(i)}) - TD(\hat{P}_{\alpha_q} || \hat{P}_{\alpha_q \mathbf{y}_\Xi(i)}), \tag{4.47}$$

where $D(\hat{P}||\hat{Q})$ is the Kulback-Leibler distance (the relative entropy [2]) between types $\hat{P}$ and $\hat{Q}$, defined as $D(\hat{P}||\hat{Q}) = \sum_{\mathbf{q} \in \Xi^{L_c N_R}} \hat{P}(\mathbf{q}) \log \frac{\hat{P}(\mathbf{q})}{\hat{Q}(\mathbf{q})}$. In the uncoded case, a hard decision is made in favor of constellation point α_q for which the statistic $S_{\alpha_q}(i)$ is smallest, i.e.

$$\hat{b}(i) = \arg \min_{\alpha_q \in \mathbb{Q}} S_{\alpha_q}(i), \tag{4.48}$$

where $\hat{b}(i)$ denotes an estimate of the originally transmitted symbol $b(i)$. In case of a coded system, an estimate of conditional probability $p_{\mathbf{n}_d}(\mathbf{y}_d - \mathbf{h}_d \alpha_q)$ is needed for $\alpha_q \in \mathbb{Q}$. The discrete approximation of this probability can be obtained as follows

$$p_{\mathbf{n}_d}(\mathbf{y}_d(i) - \mathbf{h}_d \alpha_q) \approx \hat{P}_{\alpha_q \mathbf{n}_d}(\Phi\{\mathbf{y}_d(i)\}), \tag{4.49}$$

where $\Phi(\cdot)$ denotes a quantization function and $\hat{P}_{\alpha_q \mathbf{n}_d}(\mathbf{q})$ denotes a discrete approximation of the continuous conditional PDF $p(\mathbf{y}_d(i)|\mathbf{h}_d, \alpha_q) = p_{\mathbf{n}_d}(\mathbf{y}_d(i) - \mathbf{h}_d \alpha_q)$ which is defined by

$$\hat{P}_{\alpha_q \mathbf{n}_d}(\mathbf{q}) = \int_{\Phi^{-1}(\mathbf{q})} p_{\mathbf{n}_d}(\mathbf{y} - \mathbf{h}_d \alpha_q) d\mathbf{y}, \tag{4.50}$$

with $\mathbf{y}$ being a dummy variable. It is shown in Appendix 1 that the righthand side of (4.49) can be approximated using types by

$$\hat{P}_{\alpha_q \mathbf{n}_d}(\Phi\{\mathbf{y}_d(i)\}) \approx G(H(\hat{P}_{\mathbf{y}_\Xi(i)}) - S_{\alpha_q}(i)). \tag{4.51}$$

The iterative decoder of a turbo code based on the LogMap algorithm uses the lefthand side of (4.48) in calculating extrinsic information and appropriate metrics [212, 28]. We use the righthand side of (4.48) in the decoder as an estimate of the conditional PDF to achieve asymptotically optimal performance regardless of the noise environment.

The receiver above represents the first iteration of the iterative receiver. In second and subsequent iterations we make use of the soft feedback $\tilde{b}(i)$ produced by the SfISfO channel decoder as described by (4.22). The enlarged set of training samples is used to produce the types for different constellation points α_q. The vector made by the concatenation of $\mathbf{y}_d(i)e^{-\sqrt{-1}(\angle b^*(i) + \angle \alpha_q)}$, $i = 1, ..., T$ and $\mathbf{y}_d(i)e^{-\sqrt{-1}(\angle \tilde{b}^*(i) + \angle \alpha_q)}$, $i = T+1, ..., T+B$ is quantized, resulting in $\mathbf{y}_{\alpha_q \Xi}(i)$,

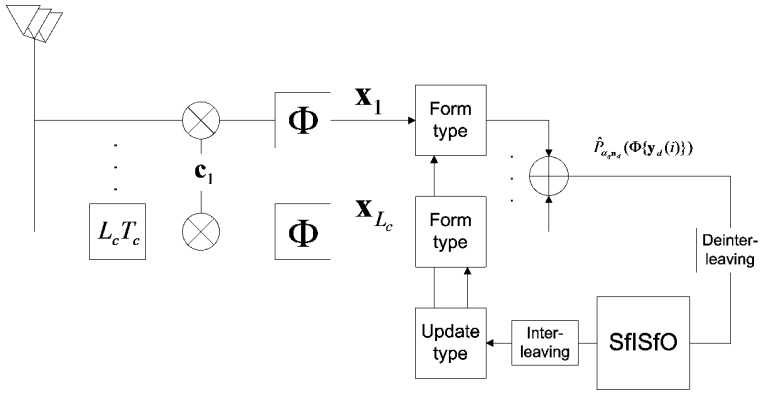

Fig. 4.6. **Type-based detector with iterative decoding.**

$i = 1, ..., T + B$. The type corresponding to the constellation point α_q is now obtained by

$$\hat{P}_{\alpha_q}(\mathbf{q}) = \frac{1}{(T+B)G} \sum_{i=1}^{T+B} \sum_{j=0}^{G-1} I(\mathbf{x}_j(i) = \mathbf{q}), \mathbf{q} \in \Xi^{L_c N_R}, \tag{4.52}$$

where $\mathbf{x}_{\alpha_q j}(i)$ is defined as in 4.43. Eqs. (4.46) and (4.47) now become

$$\hat{P}_{\alpha_q \mathbf{y}_\Xi(i)} = \frac{(T+B)G\hat{P}_{\alpha_q} + G\hat{P}_{\mathbf{y}_\Xi(i)}}{(T+B)G + G}, \tag{4.53}$$

$$S_{\alpha_q}(i) = D(\hat{P}_{\mathbf{y}_\Xi(i)} || \hat{P}_{\alpha_q \mathbf{y}_\Xi(i)}) - (T+B) D(\hat{P}_{\alpha_q} || \hat{P}_{\alpha_q \mathbf{y}_\Xi(i)}), \tag{4.54}$$

and (4.51) is used to pass the information to the SfISfO decoder.

4.2.4 Performance analysis

The performance of the receivers was studied by means of computer simulations. Simulation parameters are summarized in Table 4.3.

In Figs. 4.7 and 4.8, the bit error rate performance vs. E_b/N_0 is presented for AWGN and Middleton class A interference, respectively. Channel is assumed to be static over the whole simulation time. The scenario with $(K, K_I, N_R, L) = (1, 0, 1, 1)$ is considered. The performance of LC, HLLC, LOBD, and TBD are compared. The training sequence length for TBD is 100 symbols (6400 samples). In Gaussian noise the TBD can be seen to mimic the performance of the optimal one, which is the LC. Similar behavior can be observed in both uncoded and coded

Table 4.3. Simulation parameters.

Turbo Encoder	two RSC $(7,5)_8$ encoders, first trellis terminated, second open, pseudorandom interleaver of length 100 symbols, code rate R=1/3
Turbo Decoder	two LogMap SfISfO decoders, 5 iterations
Modulation	BPSK
Processing gain G	64
Type detector	uniform quantizer, 8 levels, 1-dimensional quantizer optimization [193]
Channel	static or Rayleigh i.i.d. between taps and antennas

cases. A simple HLLC suffers from a performance loss due to the fact that it is not optimal for Gaussian interference[3]. In Middleton class A interference the TBD again performs very close to the LOBD. On the other hand, both LC and HLLC perform significantly worse, due to the fact that they are optimal only in Gaussian and Laplacian noise, respectively.

In Figs. 4.9 and 4.10, the bit error rate performance vs. E_b/N_0 is presented for AWGN and Middleton class A interference, respectively. The channel gains are assumed to be Rayleigh distributed, independent between paths and receive antennas. In addition, the fading is assumed to be fully interleaved so that the channels at consecutive symbol intervals are also independent. Cases $(K, K_I, N_R, L) = (1,0,1,1)$, $(K, K_I, N_R, L) = (1,0,2,1)$ and $(K, K_I, N_R, L) = (1,0,1,2)$ are compared. The training sequence length for TBD is 100 symbols (6400 samples). Again, it can be seen that in case of both AWGN and Middleton class A interferences, the TBD mimics the performance of the LC and LOBD detectors, respectively. However, due to the fact that the TBD now estimates the joint effect of fast fading and interference, a performance loss of approximately 2dB compared to the optimal receivers can be observed. Note that in our simulations it was assumed that the optimal receivers have ideal knowledge about the interference PDFs and about the instantaneous channel state information.

Fig. 4.11 presents a comparison of the BER performance of iterative and non-iterative TBD receivers. Performance is plotted vs. the iteration index for $E_b/N_0 =$ 5dB and T as a parameter. Interference is assumed to be AWGN. The assumed

[3]In fact, the HLLC is an optimal detector only for Laplacian noise.

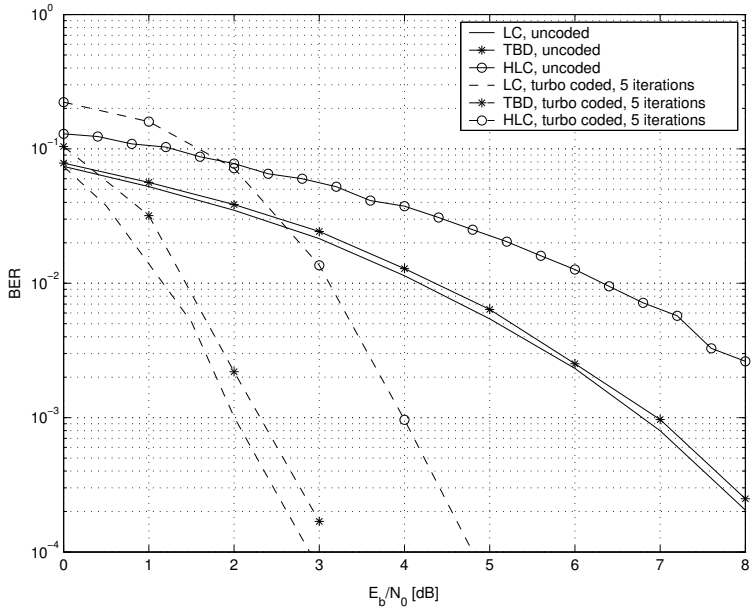

Fig. 4.7. **BER performance vs.** E_b/N_0**,** $(K, K_I, N_R, N_T, L) = (1, 0, 1, 1, 1)$**,** $(B, T) = (300, 100)$**, channel is static for SOI, interference and noise jointly modelled as AWGN, LC, HLLC and TBD receivers, turbo coded system, 5 iterations of turbo decoder, no diversity.**

scenario is $(K, K_I, N_R, L) = (1, 0, 1, 1)$. Since a training sequence of finite length can, in general, give different estimates of the type, we show the BER curves for the best, worst and mean performance for 10 independent simulation runs, for both $T = 20$ and $T = 70$. As expected, the performance is less robust to different noise realizations if T is larger. Furthermore, it can be seen that the TBD performance significantly improves as the number of iterations increases. This is especially the case for smaller values of T.

Figs. 4.12 and 4.13 show the BER performance dependence on the parameters A_A and Γ of the Middleton class A interference. The channel is assumed to be static over the whole simulation time. The training sequence length is assumed to be $T = 100$ symbols. The assumed scenario is $(K, K_I, N_R, L) = (1, 0, 1, 1)$. An uncoded system and correspondingly, non iterative receivers are considered. From Fig. 4.12 it can be seen that the performance of LOBD, TBD and HLLC is relatively independent of the parameter A_A, if $A_A < 0.1$. As an example, taking into account the parameters from Tables 4.1 and 4.2 it can be concluded that the above three detectors can provide relatively good performance if the effective number of interferers is smaller then or equal to 6. LOBD performs the best, but TBD does not suffer from large performance degradation either. From Fig.

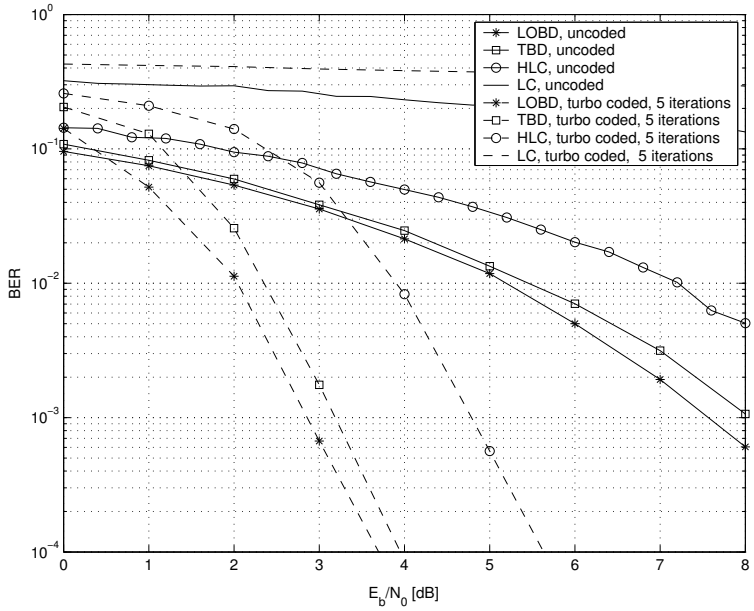

Fig. 4.8. **BER performance vs.** E_b/N_0**,** $(K, K_I, N_R, N_T, L) = (1, 0, 1, 1, 1)$**,** $(B, T) = (300, 100)$**, channel is static for SOI, interference and noise jointly modelled as Middleton class A noise with** $A_A = \Gamma = 0.1$**, LC, HLLC, LOBD and TBD receivers, turbo coded system, 5 iterations of turbo decoder, no diversity.**

4.13 it can be seen that for a given A_A, which is for the given number of effective interferers, the BER performance is relatively insensitive to the parameter Γ, which is the distance of the interferers and the victim receiver.

4.3 Summary and conclusions

This chapter focused on blind interference cancellation and suppression in channel coded spread-spectrum system. The chapter is organized according to the considered interference models.

In Section 4.1 interference was assumed to be a digitally modulated tone that can originate from the same or a competing communication system. The worst case scenario of interference bandwidth being the same as that of the SOI was considered. An iterative interference cancelling receiver based on the combination of a turbo decoder and a self-reconfigurable filter was proposed. The main novelty of the proposed scheme lies in the fact that it is robust to the interference bandwidth. Thereby, in contrast to the previous results of [202, 203, 205], the proposed

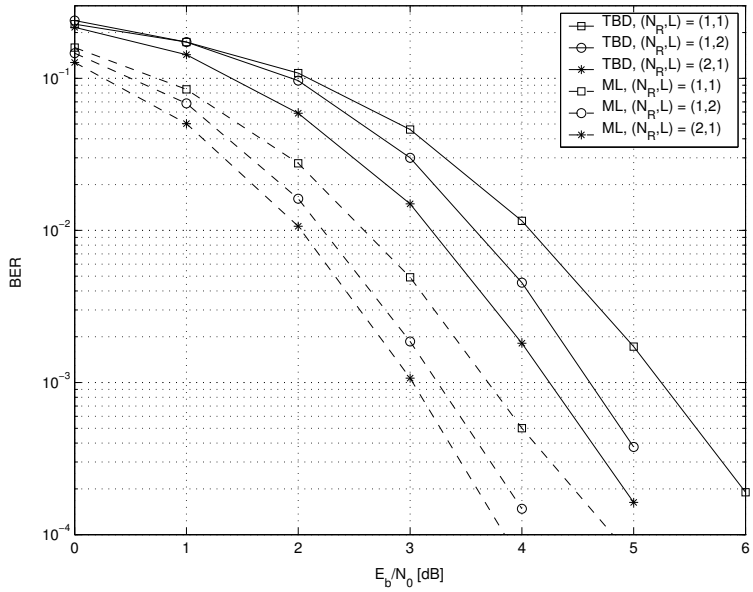

Fig. 4.9. **BER performance vs.** E_b/N_0**,** $(K, K_I, N_R, N_T, L) = (1, 0, 1, 1, 2)$ **and** $(1, 0, 2, 1, 1)$**,** $(B, T) = (300, 100)$**, channel is fast Rayleigh fading for SOI, interference and noise jointly modelled as AWGN, LC and TBD receivers, turbo coded system, 5 iterations of turbo decoder, second order diversity.**

scheme is capable of cancelling WBI as well as NBI. At the same time by using an iterative receiver structure the performance of the receiver can be potentially significantly improved.

Based on the simple asymptotic analysis performed in Section 4.1 it can be concluded that the proposed iterative receiver can provide significant performance improvement in the large SINR and E_b/N_0 regions and for relatively small processing gains. This is illustrated in Figs. 4.2 and 4.3. However, in channel coded systems with an overlay situation, these conditions are usually not fulfilled, since channel codes operate in the small E_b/N_0 regions and the interference is usually much stronger than the signal of interest. This speculation was verified by computer simulations, the results of which are presented in Fig. 4.4. This result complements those of [202, 203, 205] where only NBI is considered, and it was not explicitly shown in which SINR regions the iterative receiver can offer a performance improvement. Moreover, from the conclusions above it can be predicted that the iterative receiver can provide considerable gains if the number of signals of interest is relatively large. This is due to the their subtraction prior to the estimation of WBI having larger impact than in the single SOI case. Furthermore, by the results presented in Fig. 4.4 it was verified that the proposed scheme is capable of cancelling WBI that is of the same bandwidth as the SOI.

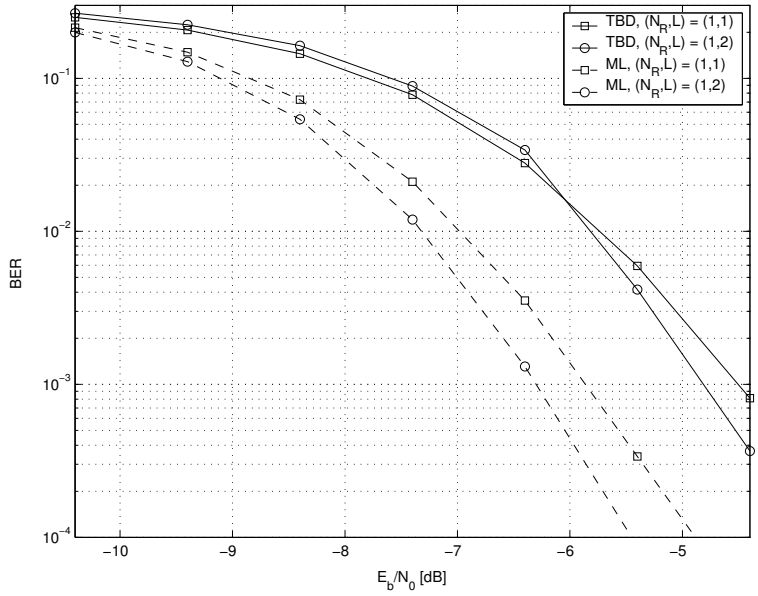

Fig. 4.10. **BER performance vs.** E_b/N_0**,** $(K, K_I, N_R, N_T, L) = (1, 0, 1, 1, 2)$ **and** $(1, 0, 2, 1, 1)$**,** $(B, T) = (300, 100)$**, channel is fast Rayleigh fading for SOI, interference and noise jointly modelled as Middleton class A noise with** $A_A = \Gamma = 0.1$**, LOBD and TBD receivers, turbo coded system, 5 iterations of turbo decoder, second order diversity.**

In Section 4.2, the interference is modelled statistically by using Middleton class A noise. A new iterative interference mitigation scheme was proposed. The scheme is an extension of the work from [191, 194] to the channel coded case, where soft information is transmitted between the detection and decoding stage in an iterative (turbo) manner. An analytical expression for the soft information at the output of the type based detector was derived in this section, which has not been considered before, up to the author's best knowledge. The main novelty when compared to the iterative and non iterative schemes of [216, 213] and [212, 215] is that the proposed scheme requires neither the knowledge of the noise distribution nor SNR estimation prior to decoding. Unlike the blind PDF estimation scheme of [213], the proposed scheme uses a training sequence and is expected to achieve accurate PDF estimation with shorter frames than its blind counterpart.

A comparative simulation study of LC, HLLC, LOBD and TBD receivers was done for a turbo-coded DS-SS system with AWGN and Middleton class A noise models. Close to optimal performance of the type-based detector was obtained in various interference scenarios both in static and i.i.d Rayleigh fading channels, with and without multiple receive antennas or multipath diversity. The performance loss

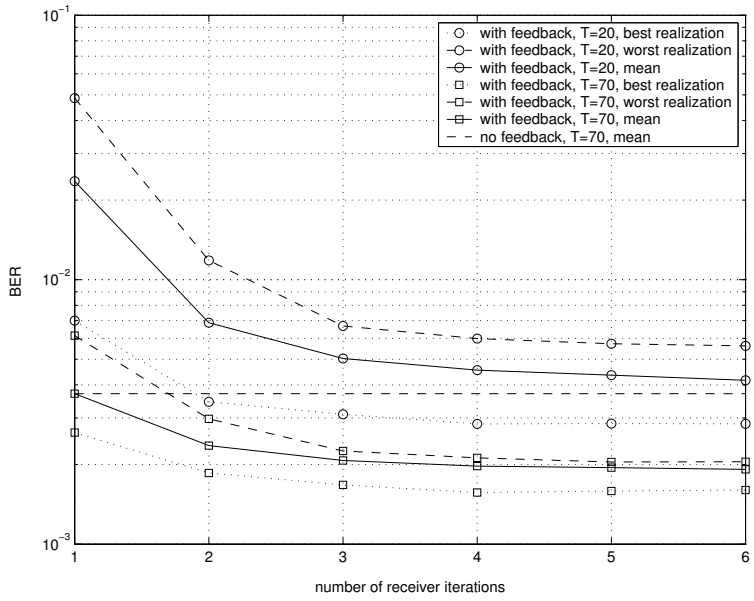

Fig. 4.11. **BER performance of iterative TBD receiver vs. number of iterations,** $(K, K_I, N_R, N_T, L) = (1, 0, 1, 1, 1)$**,** $(B, T) = (300, 100), (300, 70)$ **and** $(300, 20)$**, static channel for SOI, interference and noise jointly modelled as AWGN,** $E_b/N_0 = 2$**dB, turbo coded system, 5 iterations of turbo decoder, no diversity.**

comparing to the optimal case is within the span of 0.5 dB in a static channel and 2 dB in a Rayleigh fading channel as can be verified from Figs. 4.7-4.10. This result is consistent with the results obtained in [212, 215] for ML detectors with iterative decoding.

The iterative receiver that uses the decoder outputs to improve the interference PDF estimation is shown to outperform the non iterative one, especially for short training sequences, thereby improving the bandwidth efficiency of the system. As can be seen from Fig. 4.11 a relative improvement in bandwidth efficiency of 15% can be obtained with only a modest degradation in performance.

A particularly interesting result can be observed from Figs. 4.12 and 4.13 where the performance of different detectors was evaluated by using a suitable physical interpretation of the Middleton class A noise model. It is used there to model multiple interferers that transmit in an uncoordinated fashion. It was shown that the TBD scheme is very robust both to the number of interference sources and to the distances from the interferers to the receiver of interest. While the results in Figs. 4.12 and 4.13 were shown for the uncoded case, a similar trend is expected in the coded case. It should be noted that this behavior is not specific to the TBD alone, but seems to be the property of the optimal receiver in this kind of

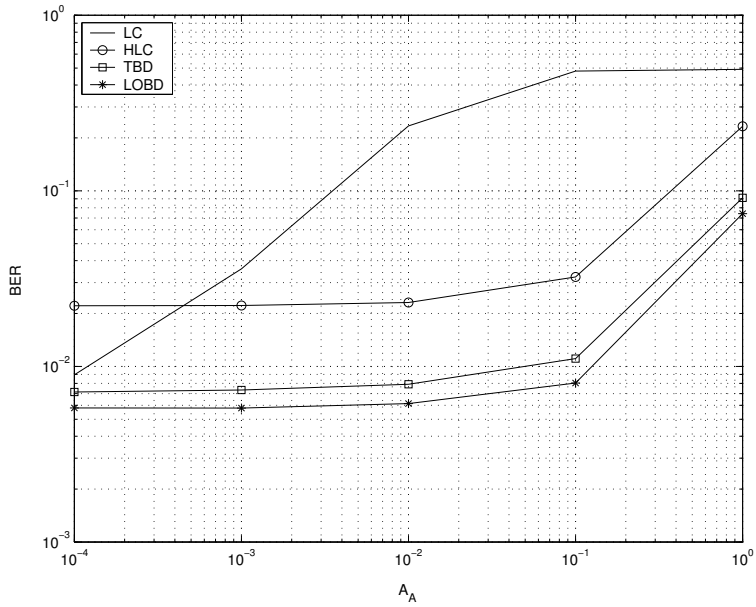

Fig. 4.12. **BER performance vs.** A_A **(number of effective interferers),** $(K, K_I, N_R, N_T, L) = (1, 0, 1, 1, 1)$**,** $(B, T) = (300, 100)$**, static channel for SOI, interference and noise jointly modelled as Middleton class A noise with** $\Gamma = 0.0001$**,** $E_b/N_0 = 5$**dB, TBD receiver, uncoded system.**

interference. To the author's best knowledge, no similar result is available in the literature so far.

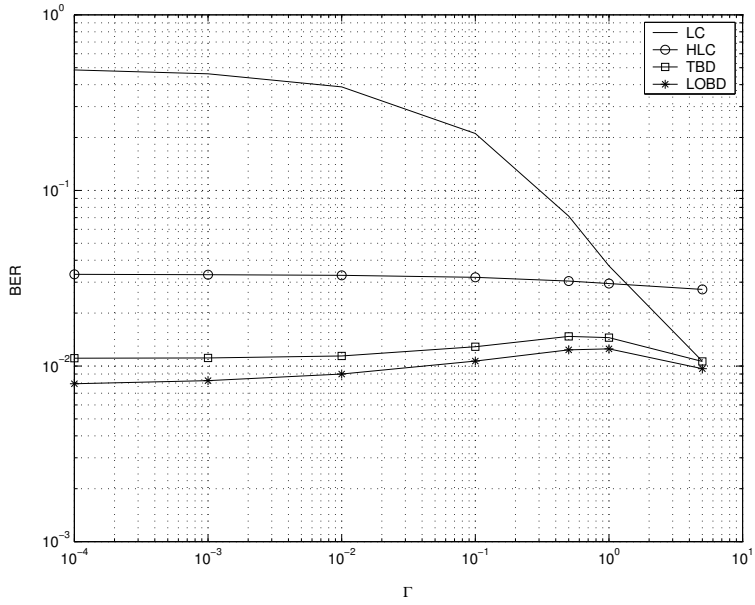

Fig. 4.13. **BER performance vs. Γ (distance from the interferers and victim receiver), $(K, K_I, N_R, N_T, L) = (1, 0, 1, 1, 1)$, $(B, T) = (300, 100)$, static channel for SOI, interference and noise jointly modelled as Middleton class A noise with $A_A = 0.1$ ($K_{eff} = 6$), $E_b/N_0 = 5$dB, TBD receiver, uncoded system.**

5 Iterative interference suppression and cancellation in SDMA

The common assumption made in the previous chapter was that the redundancy in time is introduced by spreading the signal using the DS-SS technique. This redundancy is introduced in a controlled way, to allow for orthogonality between different users and to obtain resistance against narrowband interference. In this chapter, this assumption will be relaxed and no time redundancy will be assumed in terms of spectrum spreading. Instead, the signals of different users will be separated based on their different spatial signatures, which are obtained by employing multiple transmit and receive antennas. In analogy to time-domain redundancy, the receiver will provide inherent resistance against interference that has small angular spread, by averaging interference over receive antennas.

Similarly to Chapter 4, different levels of knowledge about the interference are assumed. Only data-like interference is assumed, originating from either the same or a competing communication system. Several robust optimal and suboptimal iterative receiver schemes are studied.

This chapter is organized as follows. First, the special case of the generic system model is restated in Section 5.1, for simplicity of notation. Section 5.2 gives an overview of optimal and low complexity turbo receivers for equalization and multiuser detection, both for convolutional and space-time codes. Therefore, the focus of that section is *known* interference, i.e., CCI or the interference coming from other users that are also of interest. On the other hand, in Section 5.3 the focus is on *unknown* interference, i.e., UCCI or interference originating from undetected users. In Section 5.3.1, the interference is modelled as correlated Gaussian noise, and hybrid MMSE-MAP receivers are presented to cope with it. In Section 5.3.2, a more detailed structure of the interference is used by modelling it as a random process having a multimodal Gaussian PDF. A PDF estimation receiver is therefore presented in that section. Section 5.3.3 presents numerical results and Section 5.3.4 concludes this chapter.

5.1 Special case of the generic system model - SDMA

In this section, a special case of the generic model is presented for use in single-carrier broadband systems. We will assume that $G = 1$ and $G_I = G$ which results in $T_c = T_s = T_{sI}$, $B = B_I$ and $T = T_I$. For simplicity of notation we will also assume that the channels for all users have similar delays so that $L = L_I$. We will also make an assumption that the unknown users $k = K + 1, ..., K_I$ operate at the same carrier frequency as the users of interest, which results in the frequency offset $f_0 = 0$. Therefore, the generic model presented in Section 3.2 reduces to

$$\mathbf{y}(i) = \underbrace{\mathbf{H}\mathbf{u}(i)}_{\text{desired}} + \underbrace{\mathbf{H}_I\mathbf{u}_I(i)}_{\text{UCCI}} + \underbrace{\mathbf{n}(i)}_{\text{noise}}, \; i = 1, ..., T + B, \tag{5.1}$$

where $\mathbf{y}(i)$ is given by

$$\mathbf{y}(i) = [\mathbf{r}^T(i + L - 1), \ldots, \mathbf{r}^T(i)]^T \in \mathbb{C}^{LN_R \times 1} \tag{5.2}$$

with $\mathbf{r}(i)$ being

$$\mathbf{r}(i) = [\mathbf{r}^{(1)}(i), \ldots, \mathbf{r}^{(N_R)}(i)]^T \in \mathbb{C}^{N_R \times 1}, \tag{5.3}$$

and

$$\mathbf{r}^{(m)}(i) = r_1^{(m)}(i). \tag{5.4}$$

$\mathbf{H}$ is the equivalent channel matrix of the form

$$\mathbf{H} = \begin{bmatrix} \mathbf{H}(0) & \ldots & \mathbf{H}(L-1) & \ldots & \mathbf{0} \\ \vdots & \ddots & & \ddots & \vdots \\ \mathbf{0} & \ldots & \mathbf{H}(0) & \ldots & \mathbf{H}(L-1) \end{bmatrix} \in \mathbb{C}^{LN_R \times KN_T(2L-1)},$$

and

$$\mathbf{H}(l) = \begin{bmatrix} \mathbf{H}_1^{(1)}(l) & \ldots & \mathbf{H}_K^{(1)}(l) \\ \vdots & \ddots & \vdots \\ \mathbf{H}_1^{(N_R)}(l) & \ldots & \mathbf{H}_K^{(N_R)}(l) \end{bmatrix} \in \mathbb{C}^{N_R \times KN_T},$$

with

$$\mathbf{H}_k^{(m,n)}(l) = [h_k^{(m,1)}(l) ... h_k^{(m,N_T)}(l)] \in \mathbb{C}^{1 \times N_T}.$$

Similarly, matrix $\mathbf{H}_I$ becomes

$$\mathbf{H}_I = \begin{bmatrix} \mathbf{H}_I(0) & \ldots & \mathbf{H}_I(L-1) & \ldots & \mathbf{0} \\ \vdots & \ddots & & \ddots & \vdots \\ \mathbf{0} & \ldots & \mathbf{H}_I(0) & \ldots & \mathbf{H}_I(L-1) \end{bmatrix} \in \mathbb{C}^{LN_R \times K_I N_T(2L-1)}$$

where

$$\mathbf{H}_I(l) = \begin{bmatrix} \mathbf{H}_{K+1}^{(1)}(l) & \ldots & \mathbf{H}_{K+K_I}^{(1)}(l) \\ \vdots & \ddots & \vdots \\ \mathbf{H}_{K+1}^{(N_R)}(l) & \ldots & \mathbf{H}_{K+K_I}^{(N_R)}(l) \end{bmatrix} \in \mathbb{C}^{N_R \times K_I N_T},$$

with

$$\mathbf{H}_k^{(m,n)}(l) = [h_k^{(m,1)}(l)...h_k^{(m,N_T)}(l)] \in \mathbb{C}^{1\times N_T}.$$

Entries $h_k^{(m,n)}$ are assumed to be mutually independent complex Gaussian random variables with zero means and equal variances. It is also assumed that the variances for each transmit-receive antenna pair are normalized so that

$$\sum_{l=0}^{L-1} E\{|h_k^{(m,n)}(l)|^2\} = P_k^{(m,n)}.$$

The vectors $\mathbf{u}(i)$ and $\mathbf{u}_I(i)$ become

$$\mathbf{u}(i) = [\mathbf{b}^T(i+L-1), \ldots, \mathbf{b}^T(i), \ldots, \mathbf{b}^T(i-L+1)]^T \in \mathbb{Q}^{KN_T(2L-1)\times 1} \quad (5.5)$$

and

$$\mathbf{u}_I(i) = [\mathbf{b}_I^T(i+L-1), \ldots, \mathbf{b}_I^T(i), \ldots, \mathbf{b}_I^T(i-L_I+1)]^T \in \mathbb{Q}^{K_I N_T(L+L_I-1)\times 1}, \quad (5.6)$$

with

$$\mathbf{b}(i) = [b_1^{(1)}(i), \ldots, b_1^{(N_T)}(i), \ldots, b_K^{(1)}(i), \ldots, b_K^{(N_T)}(i)]^T, \in \mathbb{Q}^{KN_T\times 1} \quad (5.7)$$

and

$$\begin{aligned}\mathbf{b}_I(i-l) = [&b_{K+1}^{(1)}(i-l), \ldots, b_{K+1}^{(N_T)}(i-l), \ldots, \\ &b_{K+K_I}^{(1)}(i-l), \ldots, b_{K+K_I}^{(N_T)}(i-l)]^T \in \mathbb{Q}^{K_I N_T\times 1}.\end{aligned} \quad (5.8)$$

In this special case we will assume that the vector $\mathbf{n}(i) \in \mathbb{C}^{LN_R\times 1}$ contains additive white Gaussian noise (AWGN) with covariance $E\{\mathbf{n}(i)\mathbf{n}^H(i)\} = \sigma^2\mathbf{I}$.

5.2 Known interference suppression/cancellation

In situations in which the interference originates from the same communications system, its channel coding, modulation and signalling format can be assumed to be known in the receiver. That, in turn, makes it possible to perform multiuser detection [263] which is the optimal technique (in the minimum error probability sense) to detect the desired signal buried in interference. In other words, the probability that is required by the channel decoder part of the iterative scheme can be conditioned on the *instantaneous* value of the interference. Section 5.2.1 presents an iterative (turbo) receiver based on optimal (in the minimum probability of error sense) MUD and equalization techniques. The receiver principal block diagram is presented in Fig. 5.1. In Section 5.2.2 a low complexity turbo receiver is presented, which is based on soft interference cancellation followed by MMSE filtering. Sf-ISfO bit-level and symbol-level channel decoders are presented in Sections 5.2.3 and 5.2.4, respectively.

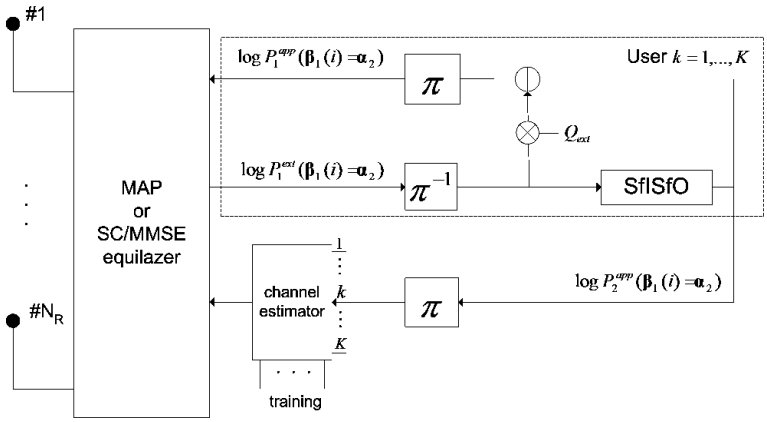

Fig. 5.1. Principal block diagram of a receiver for turbo MUD and equalization.

5.2.1 MAP-based turbo equalization and multiuser detection

The turbo equalization and multiuser detection receiver based on MAP equalization is presented in Fig. 5.1. It consists of two stages, a multiuser detector and equalizer that are followed by SfISfO decoding. Let us denote the vector of signals transmitted from N_T antennas of the kth user as

$$\boldsymbol{\beta}_k(i) = [b_k^{(1)}(i), ..., b_k^{(N_T)}]^T \in \mathbb{Q}^{N_T}. \tag{5.9}$$

The first stage produces *a posteriori* estimates of the transmitted vector $\boldsymbol{\beta}_k(i)$ as

$$\begin{aligned} P_1^{app}(\boldsymbol{\beta}_k(i) = \boldsymbol{\alpha}_q) &= P(\boldsymbol{\beta}_k(i) = \boldsymbol{\alpha}_q | \mathbf{y}(i), i = T+1, ..., T+B) \\ &= \underbrace{P(\mathbf{y}(i), i = T+1, ..., T+B | \boldsymbol{\beta}_k(i) = \boldsymbol{\alpha}_q)}_{P_1^{ext}(\boldsymbol{\beta}_k = \boldsymbol{\alpha}_q)} \cdot \\ &\quad \cdot \underbrace{P(\boldsymbol{\beta}_k(i) = \boldsymbol{\alpha}_q)}_{P_2^{ext}(\boldsymbol{\beta}_k(i) = \boldsymbol{\alpha}_q)} \\ &\quad \text{for } \boldsymbol{\alpha}_q \in \mathbb{Q}^{N_T}. \end{aligned} \tag{5.10}$$

The quantity $P_1^{app}(\boldsymbol{\beta}_k(i) = \boldsymbol{\alpha}_q)$ can be obtained by the MAP algorithm, proposed in [128, 264]. It should be noted that the operation of the MAP receiver is based on construction of a joint trellis diagram for all users and their multipath channels. Therefore, its complexity grows exponentially with the product KN_TLM. This becomes prohibitively complex even for a moderately large number of users and their channel impulse response lengths. However, the MAP receiver serves as a

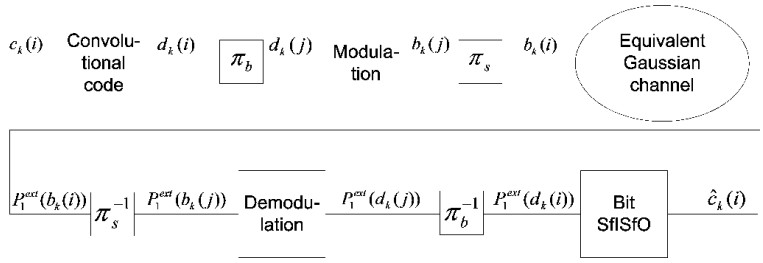

Fig. 5.2. **Block diagram of a convolutionally coded system.**

lower bound on the BER performance for lower complexity solutions that will be proposed in the subsequent sections.

The extrinsic information $P_2^{ext}(\boldsymbol{\beta}_k(i) = \boldsymbol{\alpha}_q)$ is provided by the channel decoder in the previous iteration step, as described in Sections 5.2.3 and 5.2.4. The detector extrinsic information

$$P_1^{ext}(\boldsymbol{\beta}_k(i) = \boldsymbol{\alpha}_q) = \frac{P_1^{app}(\boldsymbol{\beta}_k(i) = \boldsymbol{\alpha}_q)}{P_2^{ext}(\boldsymbol{\beta}_k(i) = \boldsymbol{\alpha}_q)}, \tag{5.11}$$

is passed to the SfISfO decoder for the next iteration. The calculation of the extrinsic information in general depends on the channel coding schemes used and it will be described for the cases of convolutional and STTr codes in the sequel.

Convolutional code. Throughout this thesis it is assumed that when convolutional coding is used each user has a single transmit antenna, resulting in $N_T = 1$. The extension to the case where each user employs several transmit antennas is straightforward. The system block diagram for that special case is presented in Fig. 5.2 where convolutional coding is performed first, followed by bit-interleaving and modulation mapping. In order to produce extrinsic information to be used in the SfISfO decoder a conversion from symbol to bit probability has to be performed after the equalization stage. For $N_T = 1$ the extrinsic information $P_1^{ext}(\boldsymbol{\beta}_k(i) = \boldsymbol{\alpha}_q)$ becomes

$$P_1^{ext}(\boldsymbol{\beta}_k(i) = \boldsymbol{\alpha}_q) = P_1^{ext}(b_k(i) = \alpha_q), \alpha_q \in \mathbb{Q}, \tag{5.12}$$

where the dependency of $b_k(i)$ on the transmit antenna is omitted for simplicity of notation. Denoting by $b_k(i) = \mathcal{M}\{d_k(j), j = j_1, ..., j_{\log M}\}$ the mapping from $\log M$ binary symbols $d_k(j)$ to symbol $b_k(i)$, the conversion from symbol to bit extrinsic probability is performed according to

$$P_1^{ext}(d_k(j_l) = +1) = \sum_{\alpha_q \in \boldsymbol{\Gamma}_{j_l}^{+1}} P_1^{ext}(b_k(i) = \alpha_q), \tag{5.13}$$

where $\boldsymbol{\Gamma}_{j_l}^{+1}$ is a subset of $\mathbb{Q}$ containing $2^{\log M - 1}$ symbols that are obtained by mapping all the binary symbol sequences $d_k(j), j = j_1, ..., j_{\log M}$ for which $j_l = +1$.

Fig. 5.3. Block diagram of an STTr coded system.

A similar procedure is performed to obtain $P_1^{ext}(d_k(j_l) = -1)$. These probabilities are then used in the bit-level SfISfO decoder described in Section 5.2.3.

STTr code. In case of an STTr code the whole vector $\boldsymbol{\beta}_k(i)$ is treated as one virtual symbol, and neither the conversion from virtual symbol $\boldsymbol{\beta}_k(i)$ to the symbols $b_k^{(n)}$, $n = 1, ..., N_T$, nor the conversion from each of the symbols $b_k^{(n)}$ to their corresponding bits is needed. The system block diagram for an STTr coded system is presented in Fig. 5.3. Therefore, the extrinsic probability (5.11) is used directly in the symbol-level SfISfO decoder described in Section 5.2.4.

5.2.2 SC-MMSE-based turbo equalization and multiuser detection

As mentioned previously, the MAP receiver requires prohibitive computational complexity. In this section a low complexity receiver will be derived. It is based on soft interference cancellation used to cancel CCI and ISI, which is followed by MMSE filtering that is used to suppress the interference which results from the inaccurate soft cancellation. Fig. 5.1 shows the principal block diagram of the low complexity iterative receiver block diagram. Let us assume at this stage that no UCCI is present, resulting in $K_I = 0$. Without loss of generality we will assume that the kth user is the user of interest.

Let us denote

$$\mathbf{u}_k(i) = \tilde{\mathbf{u}}(i) - \tilde{\mathbf{u}}(i) \odot \mathbf{e}_k, \tag{5.14}$$

where

$$\mathbf{e}_k = [\ \underbrace{0, ..., 0}_{[(L-1)K+k-1]N_T}, \underbrace{1, ..., 1}_{N_T}, \underbrace{0, ..., 0}_{(LK-k+1)N_T}\ ]^T, \tag{5.15}$$

and $\odot$ denotes the elementwise vector product. The vectors $\tilde{\mathbf{u}}(i)$ are obtained by replacing the elements of $\mathbf{u}(i)$ by their soft estimates. The soft estimates corresponding to the signals of N_T transmit antennas of the kth user are defined as

$$\tilde{\boldsymbol{\beta}}_k(i) = \sum_{\boldsymbol{\alpha}_q \in \mathcal{Q}^{N_T}} \boldsymbol{\alpha}_q P_2^{ext}(\boldsymbol{\beta}_k(i) = \boldsymbol{\alpha}_q). \tag{5.16}$$

P_2^{ext} denotes the extrinsic information obtained after SfISfO decoding (to be defined in (5.33) of Section 5.2.4). Soft cancellation of the kth user's ISI and its CCI components that originate from the remaining $K-1$ users and their ISI components is performed by

$$\mathbf{y}_k(i) = \mathbf{y}(i) - \hat{\mathbf{H}}\mathbf{u}_k(i), i = T+1, ..., B+T. \tag{5.17}$$

The signals $b_k^{(n)}(i), n = 1, ..., N_T$, are then jointly detected by filtering the signal $\mathbf{y}_k(i)$ using a linear MMSE filter whose weighting matrix $\mathbf{W}_k(i)$ satisfies the following criterion

$$[\mathbf{W}_k(i), \mathbf{A}_k(i)] = \arg\min_{\mathbf{W},\mathbf{A}} ||\mathbf{W}^H\mathbf{y}_k(i) - \mathbf{A}^H\boldsymbol{\beta}_k(i)||^2, \tag{5.18}$$

where matrices $\mathbf{W}_k(i)$ and $\mathbf{A}_k(i)$ are subject to different constraints in order to avoid the trivial solution $[\mathbf{W}_k(i), \mathbf{A}_k(i)] = [\mathbf{0}, \mathbf{0}]$. The constraints can be imposed depending on their physical meaning. For example, the constraints imposed on the elements of the matrix $\mathbf{A}_k(i)$ mean that the parameters of the equivalent Gaussian channel obtained after MMSE filtering are shaped in a desirable way.

For the receiver derived in this section the constraint will be imposed on the part of the equivalent channel obtained after MMSE filtering. It is shown in Appendix 3 (norm constraint, special case of $(n_0, l_0) = (N_T, 1)$) that the matrix $\mathbf{W}_k(i) \in \mathbb{C}^{LN_R \times N_T}$ under the constraint $a_{kjj}(i) = 1, j = 1, ..., N_T$ can be derived as

$$\mathbf{W}_k(i) = \left[\frac{\mathbf{M}_k(i)^{-1}\mathbf{h}_k^{(1)}}{1 + \mathbf{h}_k^{(1)H}\mathbf{M}_k(i)^{-1}\mathbf{h}_k^{(1)}} ... \frac{\mathbf{M}_k(i)^{-1}\mathbf{h}_k^{(N_T)}}{1 + \mathbf{h}_k^{(N_T)H}\mathbf{M}_k(i)^{-1}\mathbf{h}_k^{(N_T)}} \right], \tag{5.19}$$

where

$$\mathbf{M}_k(i) = \underbrace{\hat{\mathbf{H}}\boldsymbol{\Lambda}_k(i)\hat{\mathbf{H}}^H + \sigma^2\mathbf{I}}_{\mathbf{R}_{cov}} - \sum_{n=1}^{N_T} \mathbf{h}_k^{(n)}\mathbf{h}_k^{(n)H}, \tag{5.20}$$

and $\mathbf{h}_k^{(n)}$ is the $[(L-1)KN_T + kN_T + n]$th column of matrix $\hat{\mathbf{H}}$. Matrix $\boldsymbol{\Lambda}_k(i)$ is defined as

$$\begin{aligned} \boldsymbol{\Lambda}_k(i) &= E\{[\mathbf{u}_k(i) - \tilde{\mathbf{u}}_k(i)][\mathbf{u}_k(i) - \tilde{\mathbf{u}}_k(i)]^H\} \\ &= E\{\mathbf{u}_k(i)\mathbf{u}_k(i)^H\} - E\{\tilde{\mathbf{u}}_k(i)\tilde{\mathbf{u}}_k(i)\} \\ &= \text{diag}\{\boldsymbol{\Delta}_1(i+L-1), ..., \boldsymbol{\Delta}_K(i+L-1), \\ &\quad ..., \\ &\quad \boldsymbol{\Delta}_1(i-L+1), ..., \boldsymbol{\Delta}_K(i-L+1), \}, \end{aligned} \tag{5.21}$$

where

$$\boldsymbol{\Delta}_k(i-l) = E\{\boldsymbol{\beta}_k(i-l)\boldsymbol{\beta}_k(i-l)^H\} - \tilde{\boldsymbol{\beta}}_k(i-l)\tilde{\boldsymbol{\beta}}_k(i-l)^H, \tag{5.22}$$

and $E\{\boldsymbol{\beta}_k(i-l)\boldsymbol{\beta}_k(i-l)^H\}$ is defined as

$$E\{\beta_{k-j}(i-l)\beta_{k-j}(i-l)^H\} = \sum_{\boldsymbol{\alpha}_q \in \mathcal{Q}^{N_T}} \boldsymbol{\alpha}_q\boldsymbol{\alpha}_q^H P_2^{ext}(\boldsymbol{\beta}_{k-j}(i-l) = \boldsymbol{\alpha}_q), \tag{5.23}$$

for $j \neq k$ and all $l = 0, ..., L-1$, with

$$E\{\beta_k(i)\beta_k(i)^H\} = \sum_{\boldsymbol{\alpha}_q \in \mathcal{Q}^{N_T}} \boldsymbol{\alpha}_q \boldsymbol{\alpha}_q^H \tag{5.24}$$

for $j = 0, l = 0$.

A detailed derivation of the optimal solution for a pair of matrices $[\mathbf{W}_k(i), \mathbf{A}_k(i)]$ for other constraints is given in Appendix 4. Assuming that the MMSE filter output $\mathbf{z}_k(i) \in \mathbb{C}^{N_T \times 1}$ can be viewed as the output of the equivalent Gaussian channel [265] we can write

$$\begin{aligned} \mathbf{z}_k(i) &= \mathbf{W}_k{}^H(i)\mathbf{y}_k(i) \\ &= \boldsymbol{\Omega}_k(i)\boldsymbol{\beta}_k(i) + \boldsymbol{\Psi}_k(i), \end{aligned} \tag{5.25}$$

where matrix $\boldsymbol{\Omega}_k(i) \in \mathbb{C}^{N_T \times N_T}$ contains the gains of the equivalent channel defined as

$$\boldsymbol{\Omega}_k(i) = E\{\mathbf{z}_k(i)\boldsymbol{\beta}_k{}^H(i)\} = \mathbf{W}_k{}^H(i)\boldsymbol{\Pi}_k \tag{5.26}$$

with $\boldsymbol{\Pi}_k(i) = [\mathbf{h}_k^{(1)} \dots \mathbf{h}_k^{(N_T)}]$. The vector $\boldsymbol{\Psi}_k(i) \in \mathbb{C}^{N_T \times 1}$ is the equivalent additive Gaussian noise with covariance matrix

$$\begin{aligned} \boldsymbol{\Theta}_k(i) &= E\{\boldsymbol{\Psi}_k(i)\boldsymbol{\Psi}_k{}^H(i)\} \\ &= \mathbf{W}_k{}^H(i)\mathbf{R}_{cov}\mathbf{W}_k(i) - \boldsymbol{\Omega}_k(i)\boldsymbol{\Omega}_k{}^H(i). \end{aligned} \tag{5.27}$$

The output of the equivalent channel $\mathbf{z}_k(i)$ and its parameters $\boldsymbol{\Omega}_k(i)$ and $\boldsymbol{\Theta}_k(i)$ are used to calculate the extrinsic information

$$\begin{aligned} P_1^{ext}(\boldsymbol{\beta}_k(i) = \boldsymbol{\alpha}_q) &= p(\mathbf{z}_k(i)|\boldsymbol{\alpha}_q) \\ &= e^{-(\mathbf{z}_k(i) - \boldsymbol{\Omega}_k(i)\boldsymbol{\alpha}_q)^H \boldsymbol{\Theta}_k{}^{-1}(i)(\mathbf{z}_k(i) - \boldsymbol{\Omega}_k(i)\boldsymbol{\alpha}_q)}, \end{aligned} \tag{5.28}$$

which is to be used in the SfISfO decoding. If a convolutional code is used, further conversion from symbol to bit probability is needed, as described in 5.2.1.

5.2.3 Bit-level SfISfO decoding for convolutional codes

For decoding of the convolutional code a bit-level MAP algorithm from [28, 264] is used. For the sake of simplicity we omit the full derivation of the MAP algorithm and we refer to [28, 264] for more explanation. Given the *a priori*[1] information about the binary symbols $d_k(i)$ for $i = 1, ..., B \log M$ and $k = 1, ..., K$ the decoder of the kth user calculates the *a posteriori* probability of the binary symbol $d_k(i)$ as follows

$$\begin{aligned} P_2^{app}(d_k(i) = +1) &= p(d_k(i) = +1 | P_1^{ext}(d_k(j)), j = 1, ..., B \log M) \\ &= \underbrace{p(P_1^{ext}(d_k(j)), j = 1, ..., B \log M | d_k(i) = +1)}_{P_2^{ext}(d_k(i)=+1)} \underbrace{p(d_k(i) = +1)}_{P_1^{ext}(d_k(i)=+1)}, \end{aligned} \tag{5.29}$$

[1] *A priori* information is obtained as the extrinsic information produced by the detection block.

where $P_1^{ext}(d_k(j))$ denotes a pair $P_1^{ext}(d_k(j)=+1), P_1^{ext}(d_k(j)=-1)$. The decoder *a posteriori* probabilities are calculated by using the Bahl-Cocke-Jelinek-Raviv (BCJR) algorithm [128, 266]. After performing the BCJR algorithm the decoder extrinsic probability to be used in the detector stage[2] is calculated as

$$P_2^{ext}(d_k(i)=+1) = \frac{P_2^{app}(d_k(i)=+1))}{P_1^{ext}(d_k(i)=+1)}. \tag{5.30}$$

The calculation for $P_2^{ext}(d_k(i)=-1)$ is performed in a similar way. In order to produce the extrinsic probability of a symbol $b_k(i)$ to be used in the next receiver iteration a bit to symbol conversion is performed as follows

$$P_2^{ext}(b_k(i)=\alpha_q) = \prod_{\substack{d_k(j_l)\in\mathcal{M}^{-1}\{b_k(i)\} \\ \alpha_{qj_l}\in\mathcal{M}^{-1}\{\alpha_q\}}} P_2^{ext}(d_k(j_l)=\alpha_{qj_l}). \tag{5.31}$$

5.2.4 Symbol-level SfISfO decoding for STTr codes

The single user SfISfO channel decoding algorithm used in this thesis is a symbol-level MAP algorithm from [264]. For the sake of simplicity we omit the full derivation of the MAP algorithm and we refer to [264] and [267] for more explanation. Given the *a priori* information about the vectors $\boldsymbol{\beta}_k(i)$ for all symbol intervals $i = T+1, ..., T+B$ and all users $k = 1, ..., K$ the decoder of the kth user calculates the *a posteriori* probability of the vector $\boldsymbol{\beta}_k(i)$ as follows

$$\begin{aligned} P_2^{app}(\boldsymbol{\beta}_k(i)=\boldsymbol{\alpha}_q) &= p(\boldsymbol{\beta}_k(i)=\boldsymbol{\alpha}_q | P_1^{ext}(\boldsymbol{\beta}_k(i)=\boldsymbol{\alpha}_q), i=T+1,...,T+B) \quad (5.32) \\ &= \underbrace{p(P_1^{ext}(\boldsymbol{\beta}_k(i)=\boldsymbol{\alpha}_q), i=T+1,...,T+B|\boldsymbol{\alpha}_q)}_{P_2^{ext}(\boldsymbol{\beta}_k(i)=\boldsymbol{\alpha}_q)} \underbrace{p(\boldsymbol{\beta}_k(i)=\boldsymbol{\alpha}_q)}_{P_1^{ext}(\boldsymbol{\beta}_k(i)=\boldsymbol{\alpha}_q)}. \end{aligned}$$

The decoder *a posteriori* probabilities are calculated by using the BCJR algorithm [128, 266]. After performing the BCJR algorithm the decoder extrinsic probability to be used in the detector stage is calculated as

$$P_2^{ext}(\boldsymbol{\beta}_k(i)=\boldsymbol{\alpha}_q) = \frac{P_2^{app}(\boldsymbol{\beta}_k(i)=\boldsymbol{\alpha}_q))}{[P_1^{ext}(\boldsymbol{\beta}_k(i)=\boldsymbol{\alpha}_q)]^{Q_{ext}}}, \tag{5.33}$$

where Q_{ext} is an *ad hoc* parameter that was first introduced in [30] and further used in [267], where it was shown that the parameter Q_{ext} significantly improves the iterative receiver performance. Choosing the value of Q_{ext} to be within the interval $[0, 1]$ will result in slower convergence of the receiver. However, the effect of inaccurate extrinsic information, especially for low SNR values and low iteration indexes, can be significantly reduced. In some cases the convergence of the iterative receiver will be possible only by using the appropriate value of the Q_{ext} parameter.

[2]For MAP detection or for soft cancellation.

Table 5.1. Simulation parameters for Section 5.2.5.

Encoder	CC with generator polynomial (GP) $(7,5)_8$, code rate 1/3, trellis terminated; STTrC with $N_T = 2$, 2bps/Hz, $B = 150$ symbols, trellis terminated
Decoder	LogMap SfISfO bit-level decoder for CC; LogMap SfISfO symbol-level decoder for STTrC
Modulation	BPSK if CC used, and quadrature-phase-shift-keying (QPSK) if STTr code used
Bit interleaver	for CC random, user-specific; for STTrC not used;
Symbol interleaver	for CC not used; for STTrC random, user-specific
(B,T)	CC coded system (1000,100); STTrC coded system (15,150)
Channel	quasi-static, Rayleigh i.i.d. between taps and antennas, L=2 or 5, depending on the simulation scenario
Channel Estimation	ideal or least squares (LS) with re-estimation after each iteration (see Appendix 2)

5.2.5 Numerical examples

The performance of the proposed low complexity iterative SC-MMSE receiver is evaluated using computer simulations. Simulation parameters that are common to all numerical examples are given in Table 5.1. Parameters that are specific to the particular simulation scenario are explicitly pointed out in the text that follows.

Fig. 5.4 presents BER performance vs. per antenna E_b/N_0 for the convolutionally coded system with $(K, K_I, N_R) = (3, 0, 3)$. Perfect channel estimation is assumed. Each user has $N_T = 1$ transmit antennas, and the number of assumed multipath components is $L = 5$. For comparison, the single user performance with $(K, K_I, N_R) = (1, 0, 3)$ and the performance of the maximum-ratio-combining (MRC) lower bound for $LN_R = 15$ independent diversity branches in a convolutionally coded system are presented as well. It can be seen from Fig. 5.4 that

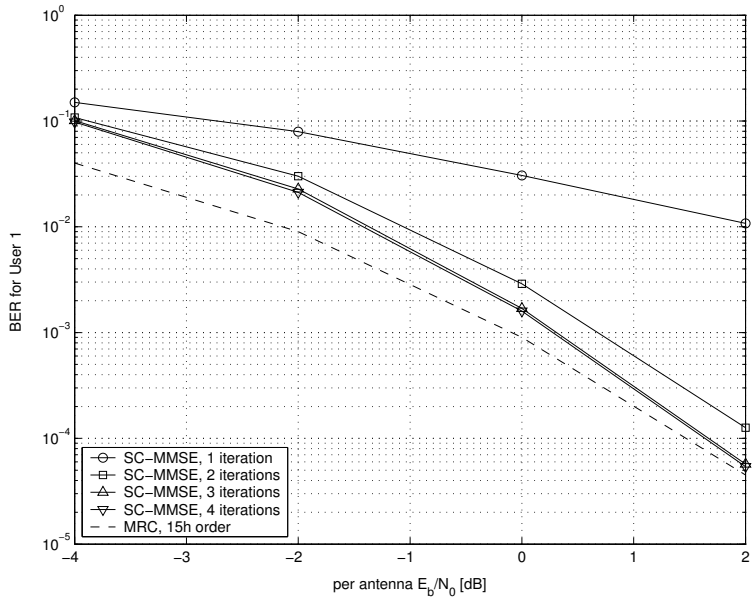

Fig. 5.4. BER vs. received per antenna E_b/N_0, convolutionally coded system with SC-MMSE iterative receiver, $(K, K_I, N_R) = (3, 0, 3)$, $(B, T) = (900, 100)$, $N_T = 1$, frequency selective channel with $L = 5$ Rayleigh distributed paths, i.i.d. between paths and antennas. All paths are of equal average power.

the iterative MMSE receiver in the multiuser scenario can achieve the single user bound. Moreover, the single user performance is very close to the MRC lower bound on performance.

It is mentioned in Section 5.2.4 that the performance of an iterative receiver can be significantly improved if the parameter Q_{ext} is used in calculation of the decoder's extrinsic information. In Fig. 5.5, the symbol error rate (SER) performance of the iterative SC-MMSE receiver vs. the factor Q_{ext} is presented for $(K, K_I, N_R) = (1, 0, 1)$ and $L = 5$. It can be seen that the value $Q_{ext} = 0.5$ gives the minimum SER performance of the iterative receiver. This comes at the expense of a larger number of iterations required to achieve convergence. This is due to the fact that if the values of extrinsic information $P_1^{ext}(\boldsymbol{\beta}_k(i) = \boldsymbol{\alpha}_q)$ for $\boldsymbol{\alpha}_q \in \mathbb{Q}^{N_T}$ are all similar to each other[3] the parameter Q_{ext} will have a tendency to make them even more similar, by increasing small and decreasing large values of $P_1^{ext}(\boldsymbol{\beta}_k(i) = \boldsymbol{\alpha}_q)$. The soft estimates of the transmitted bits will, in turn, be closer to zero, and they will have a less harmful effect on the soft cancellation process. Thereby the receiver convergence will be slowed down. The value $Q_{ext} = 0.5$

[3]This, in turn, means that the soft decisions corresponding to different constellation symbols are not reliable.

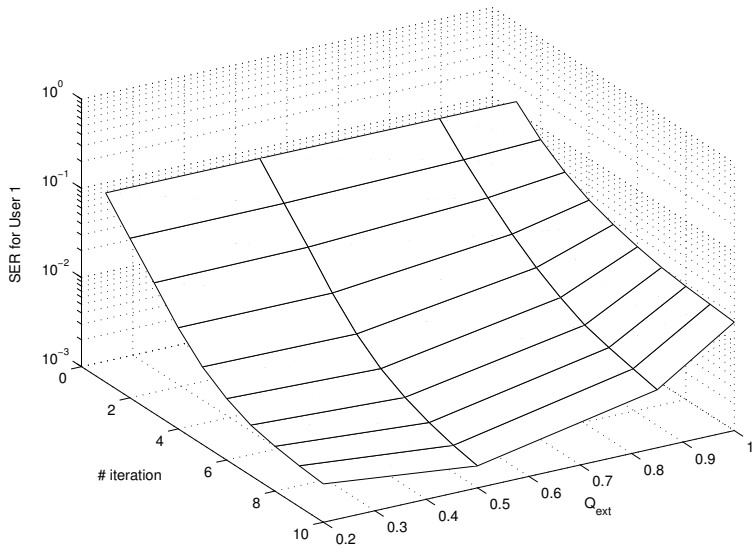

Fig. 5.5. **Dependence of the iterative SC-MMSE receivers' performance on the parameter Q_{ext}, STTr coded system, $(K, K_I, N_R) = (1, 0, 1)$, $(B, T) = (150, 15)$, $N_T = 2$,frequency selective channel with $L = 5$ Rayleigh distributed paths, i.i.d. between paths and antennas. All paths are of equal average power.**

is used as a parameter for all the simulation scenarios that involve STTr codes.

In Fig. 5.6 the SER and frame error rate (FER) performances are compared for different simulation scenarios. The number of multipath components is $L = 2$. The simulation scenarios $(K, K_I, N_R) = (1, 0, 1)$, $(K, K_I, N_R) = (3, 0, 3)$ and $(K, K_I, N_R) = (5, 0, 5)$ are compared. The performance of the receiver obtained with assumption of perfect feedback, resulting in ideal ISI and CCI removal prior to decoding, is presented for comparison. It can clearly be seen that the simultaneous increase in the number of users and the number of receive antennas yields almost the same performance of the iterative receiver and the corresponding ML lower bound. Note that the required number of receive antennas is thereby equal to the number of *users* and not to the *total number* of transmit antennas.

Fig. 5.7 shows the SER and FER performance of the joint antenna detection based receiver in different overloaded scenarios[4]. The scenarios with $(N_R, L) = (3, 5)$ and K as a parameter are considered. It can be seen that the receiver with $N_R = 3$ receive antennas can properly separate up to 4 users without severe performance degradation. However, as the number of users K increases to 5 the performance significantly degrades, and the receiver is not capable of separating different users' signals.

[4]The term overloaded stands for scenarios in which $K > N_R$.

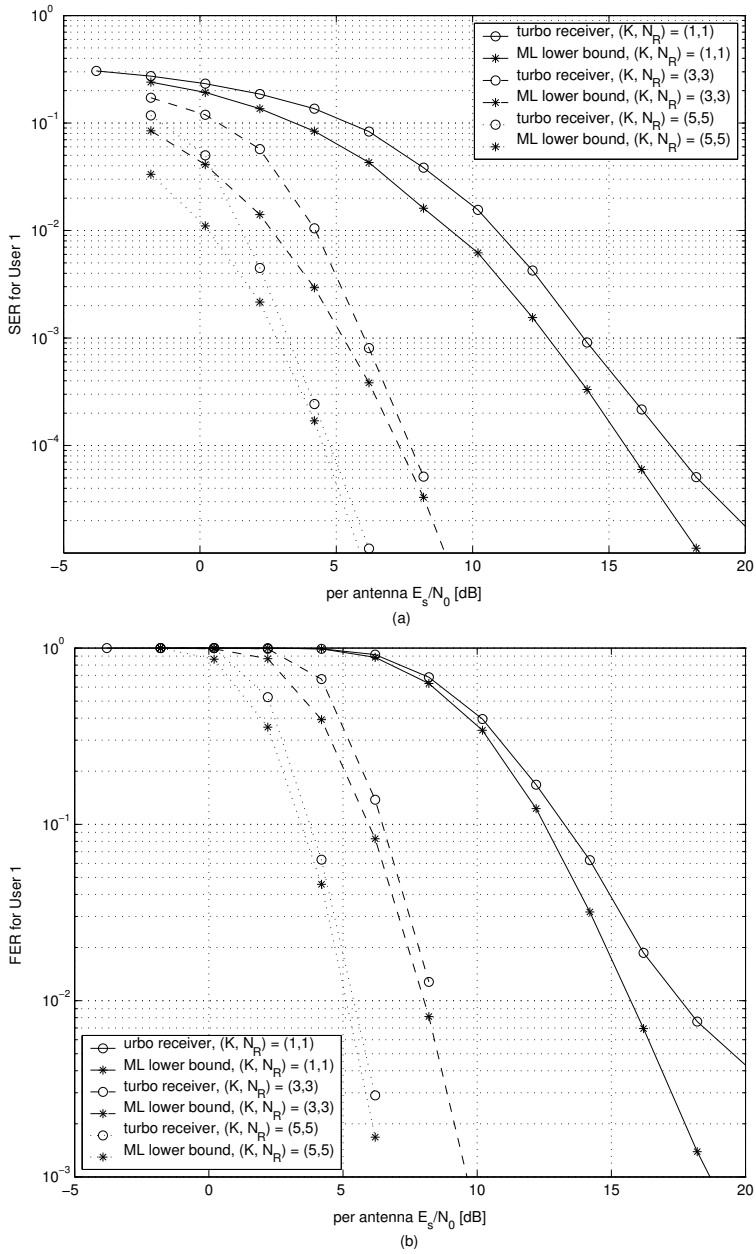

Fig. 5.6. Performance of the iterative SC-MMSE receiver in an STTr coded system, $K_I = 0$, $(K, N_R) = (1,1)$, $(3,3)$ and $(5,5)$, $(B,T) = (150,15)$, $N_T = 2$, frequency selective channel with $L = 2$ Rayleigh distributed paths, i.i.d. between paths and antennas, all paths are of equal average powers: (a) SER performance vs. per antenna E_s/N_0, (b) FER performance vs. per antenna E_s/N_0.

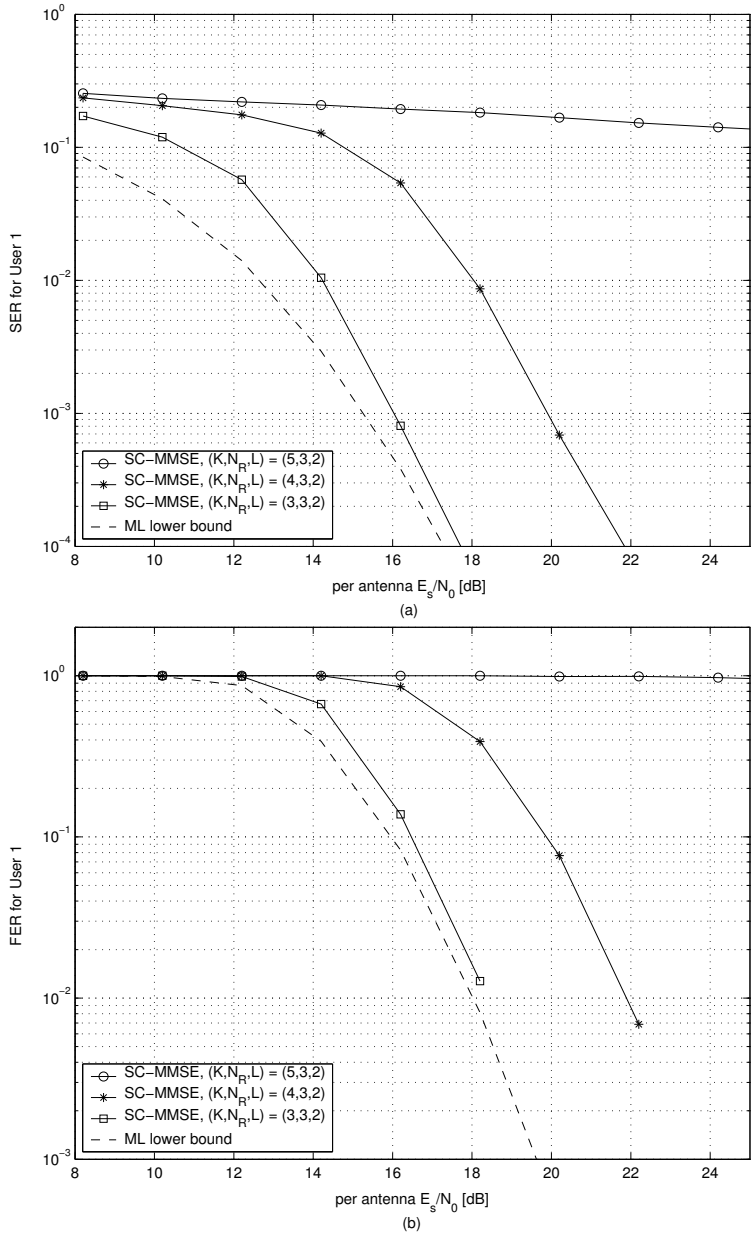

Fig. 5.7. **Performance of the iterative SC-MMSE receiver in an STTr coded system, $K_I = 0$, $N_R = 3$, $K = 3$, 4 and 5, $(B, T) = (150, 15)$, $N_T = 2$, frequency selective channel with $L = 2$ Rayleigh distributed paths, i.i.d. between paths and antennas, all paths are of equal average powers: (a) SER performance vs. per antenna E_s/N_0, (b) FER performance vs. per antenna E_s/N_0.**

5.3 Unknown interference suppression/cancellation

Unlike in the previous section where the unknown interference was assumed to be absent, in this section this assumption will be relaxed. The unknown interference is assumed to originate either form the undetected users of the same system, or from other communication systems. The section is organized according to the level of knowledge that is used about the interference structure at the receiver. Correspondingly, the receivers that appropriately exploit that structure are introduced. First, the worst case scenario will be considered, where the interference is modelled as additive correlated Gaussian noise (ACGN). A family of low complexity MMSE and hybrid MMSE-MAP turbo receivers will be introduced in Section 5.3.1. Second, interference is modelled as multimodal Gaussian, and the ML receiver that can capitalize on this structure is presented in Section 5.3.2.

5.3.1 A family of hybrid SC-MMSE-MAP iterative receivers for interference suppression

In this section an MMSE receiver that makes use of the ACGN model of interference is derived. The receiver is based on the extensions and generalizations of the receiver proposed in Section 5.2.2. The extensions are based on:

- incorporation of the available knowledge about the unknown interference into the receiver of Section 5.2.2,
- generalization of the receiver so that it detects an arbitrary number of transmit antennas jointly, regardless of the used channel coding scheme, and
- generalization of the receiver so that it detects the symbol of interest together with part of its ISI.

The interference suppression capability of SC-MMSE filtering depends on the reliability of the soft feedback and on the effective degrees of freedom. Only in case of perfect feedback can the receiver make use of all effective degrees of freedom for UCCI suppression. However, this is seldom achievable in real systems. The purpose of joint detection of several transmit antennas and/or signals together with its ISI is to preserve the effective degrees of freedom of the receiver. Since the interference suppression capability of the SC-MMSE receiver depends on the reliability of the soft cancellation, the basic idea is to cancel only a part of the total known interference (ISI and CCI) at the receiver using soft cancellation. The remaining part of the interference is detected jointly with the desired signal. Separation of the jointly detected signals is then performed in an optimal manner, using MAP detection. Joint detection only in time and only in space will be addressed as a special case of the general receiver in more detail in the sequel. In general, the number of preserved degrees of freedom is equal to the number of jointly detected transmit antennas' signals multiplied by the number of jointly detected multipath

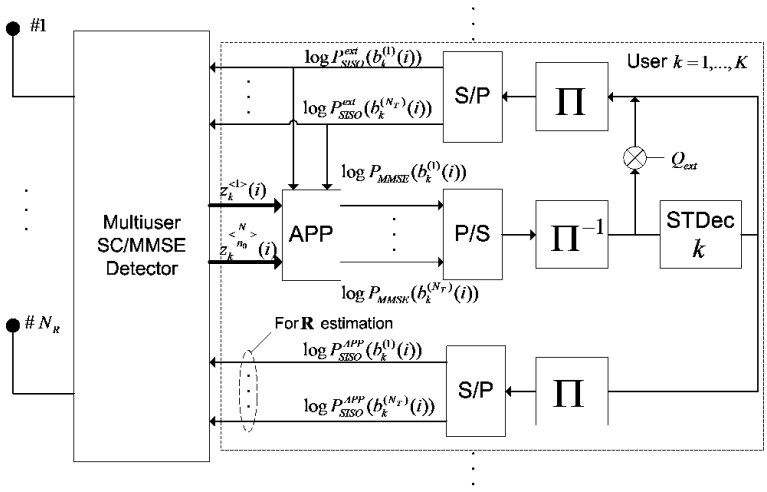

Fig. 5.8. Principal block diagram of a hybrid receiver for turbo MUD, equalization and UCCI suppression.

components. These degrees of freedom can, in turn, be used for suppression of UCCI signals.

A general block diagram of the hybrid iterative receiver is presented in Fig. 5.8. The receiver first associates the signals from transmit antennas of the kth user to the N_T/n_0 sets of size n_0, so that antennas indexed by $n = 1, ..., n_0$ belong to the first set, those indexed by $n = n_0 + 1, ..., 2n_0$ belong to the second set etc. Thereby the number of transmit antennas N_T is assumed to be an integer multiple of n_0. The receiver derivation for the more general cases of users having different numbers of transmit antennas and/or different sets of transmit antennas having different sizes is straightforward. Without loss of generality the receiver derivation is presented for the first set of transmit antennas of the kth user. The derivation is exactly the same for the rest of the transmit antenna groups and the rest of users, with a difference only in indexing. It is assumed that l_0 out of L symbols creating ISI are detected jointly.

Soft cancellation of the part of ISI and CCI. Let us denote $\tilde{\mathbf{u}}(i)$ as the vectors which are obtained by replacing the elements of $\mathbf{u}(i)$ by their soft estimates. The soft estimates are, in general, obtained groupwise. For example the soft estimates corresponding to the first antenna set are defined as

$$\tilde{\boldsymbol{\beta}}_k^{<1>}(i) = \sum_{\boldsymbol{\alpha}_q^{<1>} \in \mathcal{Q}^{n_0}} \boldsymbol{\alpha}_q^{<1>} P_2^{ext}(\boldsymbol{\beta}_k^{<1>}(i) = \boldsymbol{\alpha}_q^{<1>}), \tag{5.34}$$

where $\boldsymbol{\beta}_k^{<1>}(i) \in \mathbb{C}^{n_0 \times 1}$ is defined by

$$\boldsymbol{\beta}_k^{<1>}(i) = [b_k^{(1)}(i), ..., b_k^{(n_0)}(i)]^T. \tag{5.35}$$

As before, $P_2^{ext}(\boldsymbol{\beta}_k^{<1>}(i) = \boldsymbol{\alpha}_q)$ denotes the extrinsic information obtained after SfISfO decoding.

Let us denote with $\mathbf{u}_k^{<1>}(i)$ the vector which contains soft estimates of the signals that correspond to the n_0 transmit antennas of the first antenna set and to the first l_0-1 out of $L-1$ symbols that create ISI to the symbols $b_k^{(1)}(i), ..., b_k^{(n_0)}(i)$. The vector $\mathbf{u}_k^{<1>}(i)$ can be represented by

$$\mathbf{u}_k^{<1>}(i) = \tilde{\mathbf{u}}(i) - \tilde{\mathbf{u}}(i) \odot \mathbf{e}_k^{<1>}, \tag{5.36}$$

where

$$\mathbf{e}_k^{<1>} = [\ \underbrace{0, ..., 0}_{(L-1)KN_T}\ , \underbrace{\mathbf{e}_{k1}^{<1>}, ..., \mathbf{e}_{k1}^{<1>}}_{l_0 \text{times}}\ \underbrace{0, ..., 0}_{(L-l_0)KN_T}\ ]^T, \tag{5.37}$$

and

$$\mathbf{e}_{k1}^{<1>} = [\ \underbrace{\underbrace{0, ..., 0}_{(k-1)N_T}\ , \underbrace{1, ..., 1}_{n_0},\ \underbrace{0, ..., 0}_{\substack{N_T-n_0+\\(K-k+1)N_T}}}_{KN_T}\ ]^T, \tag{5.38}$$

with $(\cdot)^{<\gamma>}$ denoting dependency on the γth antenna set index.

After performing soft cancellation one obtains

$$\mathbf{y}_k^{<1>}(i) = \mathbf{y}(i) - \hat{\mathbf{H}}\mathbf{u}_k^{<1>}(i), i = T+1, ..., B+T, \tag{5.39}$$

where $\hat{\mathbf{H}}$ denotes the channel estimate obtained by using either only the pilot sequence $\mathbf{u}(i), i = 1, ..., T$ (non-iterative channel estimation) or both the pilot and soft estimates (iterative channel estimation). For more details about iterative channel estimation see Appendix 3.

MMSE filtering to suppress UCCI and residual interference. The signals contained in $\boldsymbol{\beta}_k^{<1>}(i-l), l = 0, ..., l_0-1$, are jointly detected by filtering the signal $\mathbf{y}_k^{<1>}(i)$ using a linear MMSE filter whose weighting matrix $\mathbf{W}_k^{<1>}(i)$ satisfies the following criterion

$$[\mathbf{W}_k^{<1>}(i), \mathbf{A}_k^{<1>}(i)] = \arg \min_{\substack{\mathbf{W} \in \mathbb{C}^{LN_R \times n_0},\\ \mathbf{A} \in \mathbb{C}^{l_0 n_0 \times n_0}}} ||\mathbf{W}^H \mathbf{y}_k^{<1>}(i) - \mathbf{A}^H \mathbf{B}_k^{<1>}(i)||^2, \tag{5.40}$$

where $\mathbf{B}_k^{<1>}(i)$ is defined as

$$\mathbf{B}_k^{<1>}(i) = [\boldsymbol{\beta}_k^{<1>T}(i), ..., \boldsymbol{\beta}_k^{<1>T}(i-l_0+1)]^T, \tag{5.41}$$

and different constraints can be imposed on $\mathbf{W}_k^{<1>}(i), \mathbf{A}_k^{<1>}(i)$ in order to avoid the trivial solution $[\mathbf{W}_k^{<1>}(i), \mathbf{A}_k^{<1>}(i)] = [\mathbf{0}, \mathbf{0}]$.

Basically any of the constraints from Appendix 4 can be used. As an illustration we will restate the optimal filter weight for the second constraint of Appendix 4. Let us denote with $\mathbf{m}_k^{(n)}$ the nth row of the matrix $[\mathbf{W}_k^{<1>}(i), \mathbf{A}_k^{<1>}(i)]$. A solution for

a matrix $[\mathbf{W}_k^{<1>}(i), \mathbf{A}_k^{<1>}(i)]$ under the family of constraints $\mathbf{m}_k^{(n)H}\mathbf{\Gamma}^{(n)}\mathbf{m}_k^{(n)} = 1$, for $n = 1, ..., n_0$ is shown in Appendix 4 to be

$$[\mathbf{W}_k^{<1>H}(i), \mathbf{A}_k^{<1>H}(i)] = [\mathbf{g}_{max,1}, ..., \mathbf{g}_{max,n_0}]^H, \tag{5.42}$$

where $\mathbf{g}_{max,n}$ is the eigenvector corresponding to the maximum eigenvalue of the matrix $\mathbf{R}_{gg}^{-1}\mathbf{\Gamma}^{(n)}$, with $\mathbf{\Gamma}^{(n)}$ being the nth constraint matrix and

$$\mathbf{R}_{gg} = \begin{bmatrix} \hat{\mathbf{H}}\mathbf{\Lambda}_k^{<1>}(i)\hat{\mathbf{H}}^H + \hat{\mathbf{R}} & \mathbf{\Pi}_k^{<1>} \\ \mathbf{\Pi}_k^{<1>H} & \sigma^2\mathbf{I} \end{bmatrix} \in \mathbb{C}^{(LN_R+l_0n_0)\times(LN_R+l_0n_0)},$$

with $\hat{\mathbf{R}}$ denoting an estimate of the covariance matrix of the interference-plus-noise defined as

$$\mathbf{R} = E\{\mathbf{H}_I\mathbf{u}_I(i)\mathbf{u}_I^H(i)\mathbf{H}_I^H + \mathbf{n}(i)\mathbf{n}^H(i)\} = \mathbf{H}_I\mathbf{H}_I^H + \sigma^2\mathbf{I}, \tag{5.43}$$

and

$$\mathbf{\Pi}_k^{<1>} = [\mathbf{h}_k^{(1)}(0), \ldots, \mathbf{h}_k^{(1)}(l_0-1), \ldots, \mathbf{h}_k^{(n_0)}(0), \ldots, \mathbf{h}_k^{(n_0)}(l_0-1)] \tag{5.44}$$

where $\mathbf{h}_k^{(n)}(l)$ is the $[(L-1)KN_T + kN_T + lKN_T + n]$th column of the matrix $\hat{\mathbf{H}}$. The matrix $\mathbf{\Lambda}_k^{<1>}(i)$ is defined as

$$\begin{aligned} \mathbf{\Lambda}_k^{<1>}(i) &= E\{[\mathbf{u}_k^{<1>}(i) - \tilde{\mathbf{u}}_k^{<1>}(i)][\mathbf{u}_k^{<1>}(i) - \tilde{\mathbf{u}}_k^{<1>}(i)]^H\} \\ &= E\{\mathbf{u}_k^{<1>}(i)\mathbf{u}_k^{<1>}(i)^H\} - E\{\tilde{\mathbf{u}}_k^{<1>}(i)\tilde{\mathbf{u}}_k^{<1>}(i)\} \\ &= \text{diag}\{\mathbf{\Delta}_1^{<1>}(i+L-1), ..., \mathbf{\Delta}_1^{<N_T/n_0>}(i+L-1), \\ &... \quad \mathbf{\Delta}_K^{<1>}(i+L-1), ..., \mathbf{\Delta}_K^{<N_T/n_0>}(i+L-1), \\ &... \quad \mathbf{\Delta}_1^{<1>}(i-L+1), ..., \mathbf{\Delta}_1^{<N_T/n_0>}(i-L+1), \\ &... \quad \mathbf{\Delta}_K^{<1>}(i-L+1), ..., \mathbf{\Delta}_K^{<N_T/n_0>}(i-L+1)\}, \end{aligned} \tag{5.45}$$

where

$$\mathbf{\Delta}_j^{<1>}(i-l) = E\{\boldsymbol{\beta}_j^{<1>}(i-l)\boldsymbol{\beta}_j^{<1>}(i-l)^H\} - \tilde{\boldsymbol{\beta}}_j^{<1>}(i-l)\tilde{\boldsymbol{\beta}}_j^{<1>}(i-l)^H, \tag{5.46}$$

with

$$E\{\beta_j^{<1>}(i-l)\beta_j^{<1>}(i-l)^H\} = \sum_{\boldsymbol{\alpha}_q^{<1>}\in\mathcal{Q}^{n_0}} \boldsymbol{\alpha}_q^{<1>}\boldsymbol{\alpha}_q^{<1>H} P_2^{ext}(\beta_j^{<1>}(i-l) = \boldsymbol{\alpha}_q^{<1>}), \tag{5.47}$$

for $j \neq k$ and $l = 1, ..., L-1$, $l = -L+1, ..., -l_0$ and

$$\mathbf{\Delta}_k^{<1>}(i-l) = E\{\boldsymbol{\beta}_k^{<1>}(i-l)\boldsymbol{\beta}_k^{<1>}(i-l)^H\}, \tag{5.48}$$

with

$$E\{\beta_k^{<1>}(i)\beta_k^{<1>}(i)^H\} = \sum_{\boldsymbol{\alpha}_q^{<1>}\in\mathcal{Q}^{n_0}} \boldsymbol{\alpha}_q^{<1>}\boldsymbol{\alpha}_q^{<1>H}. \tag{5.49}$$

for $l = -l_0 + 1, ..., 0$.

Estimation of the covariance matrix of the UCCI plus noise. One possible way to estimate the covariance matrix is to use a sample estimate by using a training sequence, as follows

$$\hat{\mathbf{R}} = \frac{1}{T}\sum_{i=1}^{T}(\mathbf{y}(i) - \hat{\mathbf{H}}\mathbf{u}(i))(\mathbf{y}(i) - \hat{\mathbf{H}}\mathbf{u}(i))^H. \tag{5.50}$$

In the second and subsequent iterations soft feedback can be used for estimation together with the training sequence, as follows

$$\begin{aligned}\hat{\mathbf{R}} &= \frac{1}{T}\sum_{i=1}^{T}(\mathbf{y}(i) - \hat{\mathbf{H}}\mathbf{u}(i))(\mathbf{y}(i) - \hat{\mathbf{H}}\mathbf{u}(i))^H \\ &+ \frac{1}{B}\sum_{i=T+1}^{T+B}(\mathbf{y}(i) - \hat{\mathbf{H}}\overline{\mathbf{u}}(i))(\mathbf{y}(i) - \hat{\mathbf{H}}\overline{\mathbf{u}}(i))^H,\end{aligned} \tag{5.51}$$

where $\overline{\mathbf{u}}(i)$ denotes the soft feedback vector. Its elements are obtained by replacing the corresponding elements of $\mathbf{u}(i)$ by their soft estimates, which in general are obtained groupwise. More precisely, the soft estimates corresponding to the first group and time instant i are defined as

$$\tilde{\boldsymbol{\beta}}_k^{<1>}(i) = \sum_{\boldsymbol{\alpha}_q^{<1>} \in \mathcal{Q}^{n_0}} \boldsymbol{\alpha}_q^{<1>} P_2^{app}(\boldsymbol{\beta}_k^{<1>}(i) = \boldsymbol{\alpha}_q^{<1>}), \tag{5.52}$$

where P_2^{app} denotes *a posteriori* information obtained after SfISfO decoding. These estimates are used in (5.42) to obtain the MMSE filter weights.

Derivation of the equivalent Gaussian channel. Assuming that the MMSE filter output $\mathbf{z}_k^{<1>}(i) \in \mathbb{C}^{n_0 \times 1}$ can be viewed as the output of the equivalent Gaussian channel [265] we can write

$$\begin{aligned}\mathbf{z}_k^{<1>}(i) &= \mathbf{W}_k^{<1>H}(i)\mathbf{y}_k^{<1>}(i) \\ &= \sum_{l=0}^{l_0-1}\boldsymbol{\Omega}_{k,l}^{<1>}(i)\boldsymbol{\beta}_k^{<1>}(i+l) + \boldsymbol{\Psi}_k^{<1>}(i),\end{aligned} \tag{5.53}$$

where matrix $\boldsymbol{\Omega}_{k,l}^{<1>}(i) \in \mathbb{C}^{n_0 \times n_0}$ contains the gains of the equivalent channel defined as

$$\boldsymbol{\Omega}_{k,l}^{<1>}(i) = E\{\mathbf{z}_k^{<1>}(i)\boldsymbol{\beta}_k^{<1>H}(i-l)\} = \mathbf{W}_k^{<1>H}(i)\boldsymbol{\Pi}_{k,l}^{<1>} \tag{5.54}$$

with $\boldsymbol{\Pi}_{k,l}^{<1>} = [\mathbf{h}_k^{(1)}(l) \dots \mathbf{h}_k^{(n_0)}(l)]$. The vector $\boldsymbol{\Psi}_k^{<1>}(i) \in \mathbb{C}^{n_0 \times 1}$ is the equivalent additive Gaussian noise with covariance matrix

$$\begin{aligned}\boldsymbol{\Theta}_k^{<1>}(i) &= E\{\boldsymbol{\Psi}_k^{<1>}(i)\boldsymbol{\Psi}_k^{<1>H}(i)\} \\ &= \mathbf{W}_k^{<1>H}(i)\mathbf{R}_{cov}\mathbf{W}_k^{<1>}(i) - \sum_{l=0}^{l_0-1}\boldsymbol{\Omega}_{k,l}^{<1>}(i)\boldsymbol{\Omega}_{k,l}^{<1>H}(i).\end{aligned} \tag{5.55}$$

The outputs of the equivalent channels $\mathbf{z}_k^{<\gamma>}(i)$ and their parameters $\mathbf{\Omega}_{k,l}^{<\gamma>}(i)$ and $\mathbf{\Theta}_k^{<\gamma>}(i)$ for $\gamma = 1, ..., N_T/n_0$ are passed to the MAP block that produces extrinsic information necessary for SfISfO decoding.

MAP equalization and joint detection. The MAP block now performs equalization and joint detection of transmit antennas within the first antenna set of the kth user in a similar manner as described in Section 5.2.1. In addition to the parameters of the equivalent Gaussian channels, the extrinsic information about all vectors $\boldsymbol{\beta}_k^{<1>}(i-l)$, for $k = 1, ..., K$ and $l = 0, ..., l_0 - 1$ are used in the MAP equalization and detection processes. The *a posteriori* estimates of the transmitted vector $\boldsymbol{\beta}_k^{<1>}(i)$ are produced as follows

$$\begin{aligned} P_1^{app}(\boldsymbol{\beta}_k^{<1>}(i) = \boldsymbol{\alpha}_q^{<1>}) &= p(\boldsymbol{\beta}_k^{<1>} = \boldsymbol{\alpha}_q^{<1>} | \mathbf{z}_k^{<\gamma>}(i), \mathbf{\Omega}_{k,l}^{<\gamma>}(i), \mathbf{\Theta}_k^{<\gamma>}(i), \\ & \quad i = T+1, ..., T+B, \gamma = 1, ..., N_T/n_0, \\ & \quad P_2^{ext}(\boldsymbol{\beta}_k^{<1>}(j-l)), k = 1, ..., K, l = 0, ..., l_0 - 1), \end{aligned} \tag{5.56}$$

where $P_2^{ext}(\boldsymbol{\beta}_k^{<1>}(j-l))$ stands for $P_2^{ext}(\boldsymbol{\beta}_k^{<1>}(j-l) = \boldsymbol{\alpha}_q^{<1>})$, $\boldsymbol{\alpha}_q^{<1>} \in \mathbb{Q}^{n_0}$, which are provided by the channel decoder in the previous iteration step. The final extrinsic information to be delivered to the channel decoder is formed by

$$\begin{aligned} P_1^{ext}(\boldsymbol{\beta}_k(i) = \boldsymbol{\alpha}_q) &= \prod_{\gamma=1}^{N_T/n_0} P_1^{ext}(\boldsymbol{\beta}_k^{<\gamma>}(i) = \boldsymbol{\alpha}_q^{<\gamma>}), \boldsymbol{\alpha}_q^{<\gamma>} \in \mathbb{Q}^{n_0}, \\ & \quad \boldsymbol{\alpha}_q = [\boldsymbol{\alpha}_q^{<1>T}, ..., \boldsymbol{\alpha}_q^{<N_T/n_0>T}]. \end{aligned} \tag{5.57}$$

In case that symbols within each group are assumed to be independent, the MAP block can perform calculation of extrinsic information for each symbol based on the extrinsic information produced for the whole group. Thereby the transmit antennas' signals are actually separated in the MAP block itself, and not in the decoder. This special case is described in more detail in Section 5.3.1.1.

SfISfO channel decoding. The *a posteriori* information $P_2^{app}(\boldsymbol{\beta}_k(i) = \boldsymbol{\alpha}_q)$ is obtained as described in Section 5.2.4. After that the *a posteriori* information $P_2^{app}(\boldsymbol{\beta}_k^{<1>}(i) = \boldsymbol{\alpha}_q^{<1>})$ is obtained for every $\boldsymbol{\alpha}_q^{<\gamma>} \in \mathbb{Q}^{n_0}$ as

$$P_2^{app}(\boldsymbol{\beta}_k^{<1>}(i) = \boldsymbol{\alpha}_q^{<1>}) = \sum_{\substack{\boldsymbol{\alpha}_q = [\boldsymbol{\alpha}_q^{<1>T}, ..., \boldsymbol{\alpha}_q^{<N_T/n_0>T}] \\ \boldsymbol{\alpha}_q^{<\gamma>} \in \mathbb{Q}^{n_0}, \gamma \neq 1}} P_2^{ext}(\boldsymbol{\beta}_k(i) = \boldsymbol{\alpha}_q), \tag{5.58}$$

and finally the extrinsic information $P_2^{app}(\boldsymbol{\beta}_k^{<1>}(i) = \boldsymbol{\alpha}_q^{<1>})$ is obtained as

$$P_2^{ext}(\boldsymbol{\beta}_k^{<1>}(i) = \boldsymbol{\alpha}_q^{<1>}) = \frac{P_2^{app}(\boldsymbol{\beta}_k^{<1>}(i) = \boldsymbol{\alpha}_q^{<1>}))}{\left[P_1^{ext}(\boldsymbol{\beta}_k^{<1>}(i) = \boldsymbol{\alpha}_q^{<1>})\right]^{Q_{ext}}}. \tag{5.59}$$

Computational complexity. Note that the complexity of the MMSE part of the receiver remains constant and equal to $O(L^3M^3)$ regardless of the used constraint. The complexity of the MAP part of the receiver is $O(M^{n_0 l_0})$. The overall computational complexity is, therefore, $O(\max\{L^3M^3, M^{n_0 l_0}\})$.

5.3.1.1 Special case - joint detection in space

The case that the receiver performs joint detection only within the set of n_0 antennas, but without joint detection of vector $\boldsymbol{\beta}_k^{<1>}(i)$ and its ISI $\boldsymbol{\beta}_k^{<1>}(i-1), ..., \boldsymbol{\beta}_k^{<1>}(i-l_0+1)$ is considered in this section. The receiver reduces to the case of $l_0 = 1$. The first constraint from Appendix 4 is used. Since all the ISI is cancelled by the soft cancellation, the MAP part becomes essentially a one shot MAP detector. Its complexity reduces to $O(M^{n_0})$. Note that the number of preserved effective degrees of freedom is equal to $n_0 - 1$. This solution is preferable from the point of view of receiver complexity, especially in channels with a large number of multipath components L. However,the number of preserved effective degrees of freedom is limited by the number of transmit antennas. In the case of $n_0 = 1$ the receiver has lower complexity, but the performance is expected to be worse than with $n_0 = 2$. However, the complexity of the latter case is higher.

In case that the symbols belonging to the same antenna set are assumed to be independent, the MAP block can calculate extrinsic information for each symbol. In this special case and for $l_0 = 1$ the calculation of the extrinsic information for symbols $b_k^{(n)}$ belonging to the first antenna set is performed for every $\alpha_q \in \mathbb{Q}$ as follows

$$P_1^{ext}(b_k^{(n)}(i) = \alpha_q) = \sum_{\mathcal{B}_n^{(\alpha_q)}} \frac{P_2^{ext}(\boldsymbol{\beta}_k^{<1>}(i) = \boldsymbol{\alpha}_q^{<1>})}{P_2^{ext}(b_k^{(n)}(i) = \alpha_q)} p(\mathbf{z}_k^{<1>}(i) | \boldsymbol{\Omega}_k^{<1>}(i), \boldsymbol{\Theta}_k^{<1>}(i)), \quad (5.60)$$

where $\mathcal{B}_n^{(\alpha_q)}$ denotes the set of all vectors $\boldsymbol{\alpha}_q^{<1>} \in \mathbb{Q}^{n_0}$ whose nth element is equal to α_q. The extrinsic information for the first antenna set that is to be directed into the channel decoder is now produced by

$$P_1^{ext}(\boldsymbol{\beta}_k^{<1>}(i) = \boldsymbol{\alpha}_q^{<1>}) = \prod_{n=1}^{n_0} P_1^{ext}(b_k^{(n)}(i) = \boldsymbol{\alpha}_{qn}^{<1>}). \quad (5.61)$$

For the convolutionally coded system a special case of $n_0 = N_T = 1$ is used. The complexity of the MAP part grows only linearly with the number of constellation symbols.

5.3.1.2 Special case - joint detection in time

In this special case the vector $\boldsymbol{\beta}_k^{<1>}(i)$ and its ISI $\boldsymbol{\beta}_k^{<1>}(i-1), ..., \boldsymbol{\beta}_k^{<1>}(i-l_0+1)$ components are detected jointly. The number of antennas within each antenna set is equal to $n_0 = 1$. The second constraint with the constraint matrix $\boldsymbol{\Gamma} = \mathbf{I}$ is used for this special case. The number of preserved degrees of freedom is now $l_0 - 1$. The complexity of the MAP part of the receiver now becomes $O(M^{l_0})$. This solution is preferable from the performance point of view, especially in channels with a large number of multipaths L. However, the complexity of this receiver is prohibitively large for most of the applications.

5.3.2 ML interference suppression

The ACGN model for interference is effective in a wide variety of situations. However, in some situations this model is no longer valid. By using the discrete alphabet property of the interference, it can be modelled as multimodal Gaussian. The linear receivers can no longer make use of its non-Gaussian nature.

The key part of the receiver based on non-Gaussian modelling is PDF estimation, which can be either parametric or non-parametric. Parametric methods are sensitive to the error in the parameter estimation. On the other hand, non-parametric methods are not subject to such an impairment. In the sequel, we will describe a kernel-smoothing based PDF estimation method and its application in an ML receiver to cope with UCCI.

The receiver described in Section 5.3.1 uses linear MMSE detection after soft cancellation. As such, it inherently makes the Gaussian assumption about the interference and it can not make use of its actual non-Gaussian nature. On the other hand, the ML receiver can make use of the non-Gaussian interference by estimating its PDF.

The ML receiver is derived for the special case of a convolutionally coded system. The extension to the STTr coded system is straightforward. The corresponding MMSE hybrid receiver is the one with $n_0 = N_T = 1$ and $l_0 = 1$, i.e., all the ISI and CCI is cancelled by soft cancellation, and joint detection neither in space nor in time is performed.

First iteration. Assuming that each user employs a single transmit antenna and convolutional code and that the 1st user is of interest, let us rewrite (5.1) as

$$\begin{aligned} \mathbf{y}(i) &= \underbrace{\mathbf{h}_1 b_1(i)}_{\text{desired}} + \underbrace{\mathbf{H}_{\text{CISI},1}\mathbf{u}_{\text{CISI},1}(i)}_{\text{CCI+ISI}} + \underbrace{\mathbf{H}_I \mathbf{u}_I(i)}_{\text{UCCI}} + \underbrace{\mathbf{n}(i)}_{\text{noise}} \\ &= \mathbf{h}_1 b_1(k) + \mathbf{x}_1, \end{aligned} \tag{5.62}$$

where $\mathbf{H}_{\text{CISI},1} = \mathbf{H} - [\mathbf{0}_{LN_R\times(L-1)K}\mathbf{h}_1\mathbf{0}_{LN_R\times LK-1}]$, $\mathbf{u}_{CISI,1}(i) = \mathbf{u}(i) - b_1(i)\mathbf{e}_1$ and $\mathbf{x}_1(i)$ denotes the total sum of the desired user's ISI, known CCI, UCCI and noise. Note that the dependence on the transmit antenna is omitted, for simplicity of notation. Since the soft feedback is not available in the first iteration, the ISI and CCI components cannot be cancelled. ML processing requires the PDF of the signal $\mathbf{x}_1(i)$, which is multimodal Gaussian, given by

$$p_{\mathbf{x}_1}(\mathbf{x}_1(i)) = \frac{1}{2^{D_{tot}}} \sum_{p=1}^{2^{D_{tot}}} \frac{1}{(\pi\sigma^2)^{LM}} e^{\frac{-(\mathbf{x}_1(i)-\mathbf{t}_{p,1})^H(\mathbf{x}_1(i)-\mathbf{t}_{p,1})}{\sigma^2}}, \tag{5.63}$$

where $D_{tot} = \log M[(2L-1)(N+N_I) - N]$, and $\mathbf{t}_{p,1}$ depends on the entries of $\mathbf{H}_I$ and $\mathbf{H}_{\text{CISI},1}$, and the signal constellation of the UCCI. The number of summation terms in (5.63) increases exponentially with the number of users K which may be large in a practical system. In that case, the samples $\mathbf{x}_1(i)$ will become less structured and their PDF will become more Gaussian-like. To justify the Gaussian approximation we calculate the Kullback-Leibler (KL) distance (relative entropy) [2] between the true PDF given by (5.63) and the corresponding Gaussian approx-

Table 5.2. KL distance between the true PDF of Eq. (5.63) and the Gaussian

$K+K_I$	1	3	5
KL distance	60	25	22.5

imation given by

$$p_{Gapp,\mathbf{x}_1}(\mathbf{x}_1(i)) = \frac{1}{\pi^{LN_R}\det(\mathbf{R}_{\mathbf{x}_1\mathbf{x}_1})} e^{-\mathbf{x}_1(i)^H \mathbf{R}^{-1}_{\mathbf{x}_1\mathbf{x}_1}\mathbf{x}_1(i)}, \tag{5.64}$$

with

$$\mathbf{R}_{\mathbf{x}_1\mathbf{x}_1} = E\{\mathbf{x}_1(i)\mathbf{x}_1(i)^H\} = \mathbf{H}_{\text{CISI},1}\mathbf{H}^H_{\text{CISI},1} + \mathbf{R}_{\mathbf{xx}}, \tag{5.65}$$

for several values of $K+K_I$. It can be seen from Table 5.2 that the KL distance decreases as $K+K_I$ increases, which means that the true PDF approaches Gaussian. Therefore, by adopting the Gaussian assumption for $\mathbf{x}_1(i)$, the extrinsic probability to be passed to the first user's SfISfO decoder can be calculated as

$$P_1^{ext}(b_1(i)=\alpha_q) = C_{ML} e^{-(\mathbf{y}(i)-\mathbf{h}_1\alpha_j)^H \mathbf{R}^{-1}_{\mathbf{x}_1\mathbf{x}_1}(\mathbf{y}(i)-\mathbf{h}_1\alpha_j)}, \alpha_q \in \mathbb{Q}, \tag{5.66}$$

where $C_{ML} = \frac{1}{\pi^{LN_R}\det(\mathbf{R}_{\mathbf{x}_1\mathbf{x}_1})}$. It can be easily shown that the MMSE filter from Section 5.3.1 for the case of $n_0 = N_T = 1$ and $l_0 = 1$ under the path constraint (see Appendix 4) becomes equal to

$$\mathbf{w}_1(i) = \frac{\mathbf{R}^{-1}_{\mathbf{x}_1\mathbf{x}_1}\mathbf{h}_1}{1+\mathbf{h}_1^H\mathbf{R}^{-1}_{\mathbf{x}_1\mathbf{x}_1}\mathbf{h}_1}. \tag{5.67}$$

After incorporating (5.67) into (5.54) and (5.55), the extrinsic probability at the output of MMSE filter, given by (5.57), can be represented as

$$P_1^{ext}(b_1(i)=\alpha_q) = C_{MMSE} e^{-(\mathbf{y}(i)-\mathbf{h}_1\alpha_j)^H \mathbf{R}^{-1}_{\mathbf{x}_1\mathbf{x}_1}(\mathbf{y}(i)-\mathbf{h}_1\alpha_j)}, \alpha_q \in \mathbb{Q}, \tag{5.68}$$

where $C_{MMSE} = \frac{(1+\mathbf{h}_1^H\mathbf{R}^{-1}_{\mathbf{x}_1\mathbf{x}_1}\mathbf{h}_1)^2}{\pi\mathbf{h}_1^H\mathbf{R}^{-1}_{\mathbf{x}_1\mathbf{x}_1}\mathbf{h}_1}$. This, however, is just the scaled extrinsic information of (5.67) obtained by using the ML detector. Since the constants C_{ML} and C_{MMSE} have no impact on the receiver performance[5], in the first iteration the proposed ML receiver is exactly the same as the first iteration of the conventional MMSE receiver presented in Section 5.3.1.

Following iterations. Starting from the second iteration we make use of the soft feedback. Soft cancellation is performed in the same way as described by (5.36)-(5.39). Assuming that the soft cancellation is perfect, the ISI components of the

[5]It is known that the MMSE and ML criterion assuming ACGN interference result in filters that differ only in the constant factor [268]

desired user and the known CCI components are assumed to be perfectly cancelled, the signal $\mathbf{x}_1(i)$ reduces to

$$\mathbf{x}_1(i) = \mathbf{x}(i) = \underbrace{\mathbf{H}_I \mathbf{u}_I(i)}_{\text{UCCI}} + \underbrace{\mathbf{n}(i)}_{\text{noise}}, \tag{5.69}$$

and the PDF of the signal $\mathbf{x}(i)$ can be given as

$$p_{\mathbf{x}}(\mathbf{x}(i)) \approx \frac{1}{2^D} \sum_{p=0}^{2^D-1} \frac{1}{(\pi\sigma^2)^{LN_R}} e^{\frac{-(\mathbf{x}(i)-\mathbf{t}_p)^H(\mathbf{x}(i)-\mathbf{t}_p)}{\sigma^2}}, \tag{5.70}$$

where $D = (2L-1)K_I \log M$, and $\mathbf{t}_p$ depends on the matrices $\mathbf{H}_I$ and the signal constellation of the UCCI. Assuming that the number K_I of UCCIs is relatively small, the structure of the UCCI can be exploited by estimating the PDF of UCCI-plus-noise given by (5.70) and applying ML filtering. After the estimate $\hat{p}_{\mathbf{x}}(\mathbf{x}(i))$ of $p_{\mathbf{x}}(\mathbf{x}(i))$ is obtained, the extrinsic probability to be passed to the first user's SfISfO decoder can be calculated as the output of the single user ML detector, as

$$P_1^{ext}(b_1(i) = \alpha_q) = \hat{p}_{\mathbf{x}}(\hat{\mathbf{y}}(i) - \alpha_q \mathbf{h}_1), i = T+1, ..., T+B, \alpha_q \in \mathbb{Q}. \tag{5.71}$$

The PDF estimation procedure is described in the sequel. First, the channel is re-estimated based on $\overline{\mathbf{u}}_1(i), i = 1, ..., B+T$ as in Section 5.3.1 and Appendix 3. Then, the estimates of $\mathbf{x}(i)$ are obtained as follows

$$\begin{aligned} \hat{\mathbf{x}}(i) &= \mathbf{y}(i) - \mathbf{H}\mathbf{u}(i), \text{for } i = 1, ..., T, \text{and} \\ \hat{\mathbf{x}}(i) &= \mathbf{y}(i) - \mathbf{H}\overline{\mathbf{u}}(i), \text{for } i = T+1, ..., T+B \end{aligned} \tag{5.72}$$

where $\overline{\mathbf{u}}(i)$ is the *a posteriori* soft feedback defined in Section 5.3.1. The estimates are used to make the estimate of the UCCI-plus-noise PDF. Note that by using the samples indexed by $i = 1, ..., B+T$ we perform iterative PDF estimation. In non-iterative PDF estimation only the first T samples, $\hat{\mathbf{x}}(i), i = 1, ..., T$, corresponding to the training sequence, would be used. In order to perform the PDF estimation, either parametric [168] or non-parametric [196] approaches can be used. The former one estimates the parameters D and $\mathbf{t}_p$ based on the samples $\hat{\mathbf{x}}(i)$. These estimates are then used in (5.70). On the other hand, the non-parametric approach estimates the PDF *directly*, where each sample $\hat{\mathbf{x}}(i)$ contributes to the total estimate through a weighting function. For example, for an arbitrary $\mathbf{a} = [a_1, ..., a_{LN_R}]^T \in \mathbb{C}^{LN_R \times 1}$ the non-parametric multidimensional kernel-based PDF estimator [196], estimates the $p_{\hat{\mathbf{x}}}(\mathbf{a})$ as

$$\hat{p}_{\mathbf{x}}(\mathbf{a}) = \frac{1}{T+B} \sum_{i=1}^{T+B} \frac{K_1\left(\frac{\hat{\mathbf{x}}(i)-\mathbf{a}}{\sigma_0}\right)}{\sigma_0^{2LN_R}}, \tag{5.73}$$

where $K_1(\mathbf{a}) = \frac{1}{(2\pi)^{LN_R}} e^{\frac{-\mathbf{a}^H\mathbf{a}}{2}}$ is a Gaussian kernel weighting function and σ_0 is a smoothing parameter. Although other kernel functions can be used [196], it will be shown that this choice gives an asymptotically unbiased and consistent PDF

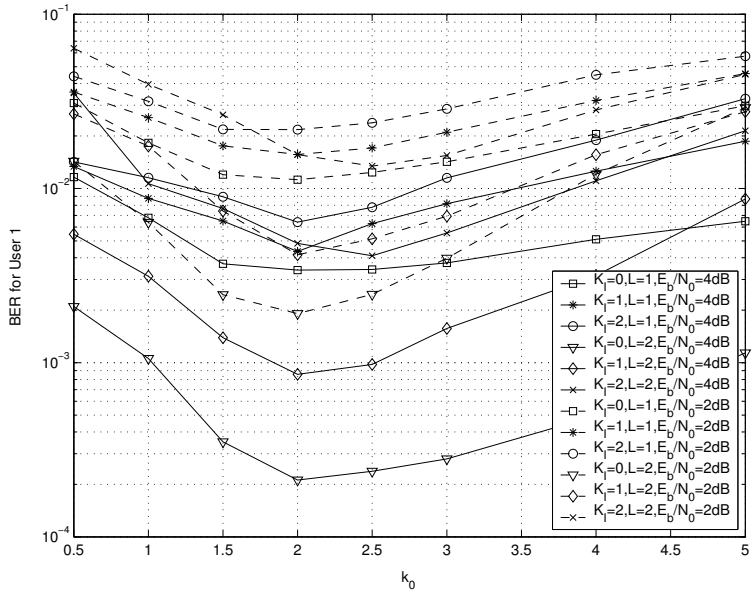

Fig. 5.9. **BER vs.** k_0 **performance of the ML receiver, non-iterative PDF estimation, convolutionally coded system,** $(K, K_I, N_R) = (3, 0, 3)$**,** $(2, 1, 3)$ **and** $(1, 2, 3)$**,** $(B, T) = (900, 100)$**,** $N_T = 1$**,** $L = 1$ **and** 2**,** $E_b/N_0 = 2$ **and** 4**dB,** 4 **iterations.**

estimator. The estimation accuracy is controlled by the smoothing parameter σ_0. A larger value of σ_0 results in a smoother but less accurate PDF estimate, and vice versa. In order to find the optimal value for σ_0 one approach is to minimize the mean-integrated squared error (MISE) [196] between the true PDF and its estimate, as defined by

$$\mathrm{MISE}(\hat{p}_{\mathbf{x}}) = \int_{\mathbb{R}^{2LN_R}} \{p_{\mathbf{x}}(\mathbf{a}) - \hat{p}_{\mathbf{x}}(\mathbf{a})\}^2 d\mathbf{a}, \tag{5.74}$$

where $d\mathbf{a} = d\mathrm{Re}a_1 d\mathrm{Im}a_1 \cdots d\mathrm{Re}a_{LN_R} d\mathrm{Im}a_{LN_R}$. It is shown in Appendix 3 that the optimal smoothing parameter $\sigma_{0,opt}$ can be lower bounded as follows

$$\sigma_{0,opt} \geq \left(\frac{2}{(T+B)(LN_R+1)}\right)^{\frac{1}{2LN_R+4}} \sigma = \gamma(LN_R). \tag{5.75}$$

A similar result was obtained in [172] for the univariate case. It is a special case of (5.75) for $LN_R = 1$. Furthermore, the estimate

$$\hat{\sigma}_0 = k_0 \gamma(LN_R), \tag{5.76}$$

of $\sigma_{0,opt}$ satisfies the sufficient conditions for consistency and asymptotic unbiasedness. These conditions are given as $\lim_{(T+B)\to\infty} \hat{\sigma}_0 = 0$ and $\lim_{(T+B)\to\infty}(T+B)\hat{\sigma}_0 = \infty$ and they are satisfied if the parameter $k_0 \in \mathbb{R}$ is chosen to be $k_0 \geq 1$ [172]. Thereby, the estimator dependence on D and $\mathbf{t}_i$ reflects only through the constant k_0 since $\gamma(LN_R)$ is independent of these parameters. The bit-error-rate performance versus the parameter k_0 with different numbers of users and different numbers of multipaths as parameters is shown in Fig. 5.9. Interestingly, the optimal value of k_0 that minimizes BER is shown to be rather *insensitive* to the change of these parameters. Moreover, it is shown in [172] and Fig. 5.9 that for $LN_R = 1$ the optimal parameter k_0 does not depend on the signal-to-noise ratio. From Fig. 5.9 it can be seen that $k_0 \approx 2$ is a good choice for a wide range of situations. This indicates that, in practice, the knowledge about the parameters K_I, L and, correspondingly, D is *not needed*. If these parameters are known in the receiver, they could be used to access a look-up-table in which the optimal values of k_0 for different combinations of parameters can be stored *a priori*. The same procedure is performed for the rest of the desired users to obtain the soft estimates $\tilde{b}_k(i)$ and $\bar{b}_k(i)$ for the next iteration.

Bit to symbol and symbol to bit conversions. The conversions are performed as described in Sections 5.2 and 5.2.3 for the case of a convolutionally coded system.

Symmetrizing. If the UCCI signal constellation is known in the receiver, the symmetry of the constellation set can be utilized to increase the number of samples that can be used for PDF estimation. In the case of M-PSK modulation, an M-fold increase of the number of samples can be achieved by using the fact that $p(\mathbf{a}) = p(\mathbf{a}e^{\frac{-\sqrt{-1}2\pi k}{\mathrm{M}}})$, $k = 0, \ldots, \mathrm{M}-1$.

Computational complexity. Since (5.71) contains the sums of exponentials, it can be approximated using the Jacobian algorithm [269]. The complexity per symbol of the proposed method is roughly $O\{(T+B)LN_R\}$ or $O\{TLN_R\}$, depending on whether we use soft feedback for PDF estimation or not, respectively. The conventional SC-MMSE receiver's complexity is $O\{L^3N_R^3\}$.

Table 5.3. Simulation parameters for Section 5.3.3.

Encoder	CC with GP $(7,5)_8$, code rate 1/3, trellis terminated; STTrC with $N_T = 2$, 2bps/Hz, trellis terminated
Decoder	LogMap SfISfO bit-level decoder for CC; LogMap SfISfO symbol-level decoder for STTrC
Modulation	BPSK if CC used, and QPSK if STTr code used
Bit interleaver	for CC random, user-specific; for STTrC not used
Symbol interleaver	for CC not used; for STTrC random, user-specific
(B,T)	CC coded system $(900, 100)$; STTrC coded system $(150, 15)$ and $(300, 30)$
Channel	exponentially decaying power delay profile, decay factor τ quasi-static, Rayleigh i.i.d. between taps and antennas, L=1,2 or 5, depending on the simulation scenario
Channel Estimation	ideal or LS with re-estimation after each iteration (see Appendix 2)

5.3.3 Numerical examples

The performance of the proposed hybrid SC-MMSE-MAP and ML receivers was evaluated by means of computer simulations. The set of common parameters used in simulations is given in Table. 5.3.

In Fig. 5.10 the BER performance vs. received per antenna E_b/N_0 is presented for the convolutionally coded system with $(K, K_I, N_R) = (2, 1, 3)$. The hybrid SC-MMSE-MAP receiver is considered for $n_0 = N_T = 1$ and $l_0 = 1$. The BER performance of the hybrid SC-MMSE-MAP receiver for $(n_0, l_0) = (1, 1)$ is compared with the SC-MMSE receiver of Section 5.2.2, which ignores the existence of the UCCI[6] ("UCCI ignored, 1 and 4 it."). It can be seen that the receiver that estimates the covariance matrix $\mathbf{R}$ performs significantly better than the receiver that

[6]Note that the SC-MMSE receiver of Section 5.2.2 for $N_T = 1$ is a special case of the hybrid SC-MMSE-MAP receiver for $(n_0, n_0) = (1, 1)$ and $\mathbf{R} = \sigma^2\mathbf{I}$.

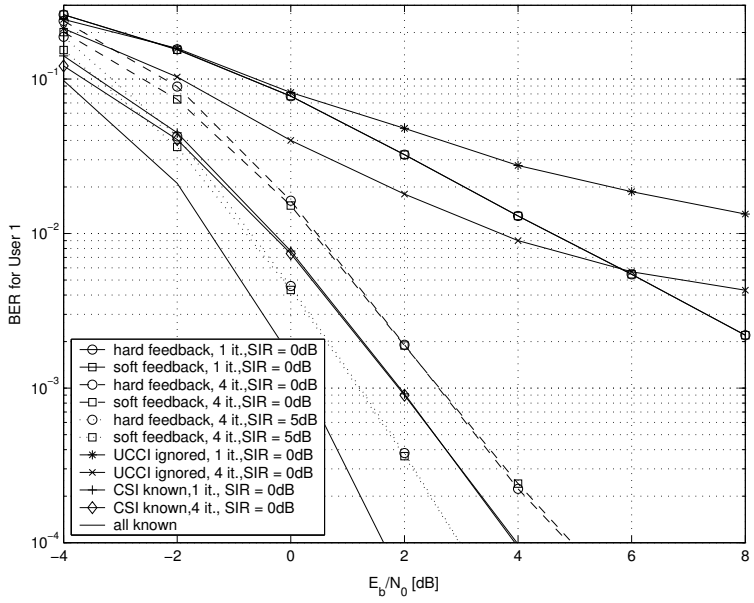

Fig. 5.10. **BER vs. received per antenna E_b/N_0, comparison of hard and soft feedback-based hybrid SC-MMSE-MAP receivers in a convolutionally coded system, $(K, K_I, N_R) = (2, 1, 3)$ and $(3, 0, 3)$, $(B, T) = (900, 100)$, $N_T = n_0 = 1$, $l_0 = 1$, $L = 5$, $\tau = 0$, channel estimation either ideal or estimated using iterative LS channel estimation, SIR=0 and 5dB, matrix R iteratively estimated, 4 iterations, threshold for hard feedback is 0.5.**

ignores the interference. The performance of the latter one plateaus at a certain BER level, while this is not observed with the former one.

The performance of the hybrid receiver that performs both iterative channel and covariance matrix estimation using soft feedback is compared to the receiver from [224] that uses hard feedback instead. In case of the receiver from [224] the soft feedback estimate of the symbol $b_k(i)$ is compared with a threshold to determine its reliability. If the soft estimate exceeds the threshold then the soft value is replaced by the constellation point that is closest to it. Otherwise, the soft value is set to zero. It can be seen that the soft feedback perform slightly better that the hard feedback at relatively low E_b/N_0 values. This is due to the fact that in the former case the feedback estimates are not discarded, resulting in more samples that are used to estimate both the channel and the interference covariance matrix. On the other hand the performance is practically the same as with hard feedback for moderate and high E_b/N_0 values, due to the increased reliability of the *a posteriori* estimates of the decoders.

The performance for $(K, K_I, N_R) = (2, 1, 3)$ with perfect channel estimation ("CSI known") is also presented in Fig. 5.10 for comparison. The performance of the receiver with iterative channel estimation is about 1dB worse than the known channel case. It can also be noted that the gain from soft feedback is smaller when the channel is perfectly known than when LS channel estimation is used. This indicates that the total gain from the soft feedback comes both from gains in channel estimation [270] and covariance matrix estimation. It should be noted that although the soft feedback gain is not very large, the complexity of the receiver using soft feedback is lower than with hard feedback. This is due to the fact that all the symbols in the frame are considered to be reliable when soft feedback is applied and no search for reliable symbols is required as in the case of hard feedback.

Also presented in Fig. 5.10 is the curve for the case $(K, K_I, N_R) = (3, 0, 3)$ when the interference is known ("All known"), i.e., belonging to the signals of interest. In that case the explicit cancellation of the interfering signal is possible and the performance is obviously improved. Perfect channel estimate for all users is assumed for that scenario. The improvement is approximately 1dB from the perfect channel information case with unknown interference at a BER of 10^{-2}.

In Figs. 5.11 and 5.12, the BER of the PDF estimation based receiver vs. per-antenna E_b/N_0 is presented for $L = 1$ and $L = 2$ cases, respectively. The non-iterative PDF estimation is used in these examples, since a long overhead ($T = 100$) was used. For comparison, the performance of the SC-MMSE-MAP receiver for $(n_0, l_0) = (1, 1)$ and iterative channel and covariance matrix estimation is presented. In both cases, the proposed receiver significantly outperforms the conventional one in $(K, K_I, N_R) = (1, 2, 3)$ and $(K, K_I, N_R) = (2, 1, 3)$ scenarios. This is the consequence of the linear processing of the conventional SC-MMSE-MAP receiver that does not take into account the actual structure of the UCCI. The performance curve for the $(K, K_I, N_R) = (3, 0, 3)$ scenario, when all the users are to be detected is shown for comparison (indicated by "all known").

The performance is closer to the "all known" case for $L = 1$ (frequency flat fading) than for $L = 2$, and for $K_I = 1$ than $K_I = 2$. This is because the PDF of (5.70) becomes more scattered in the LN_R dimensional space with increased L and

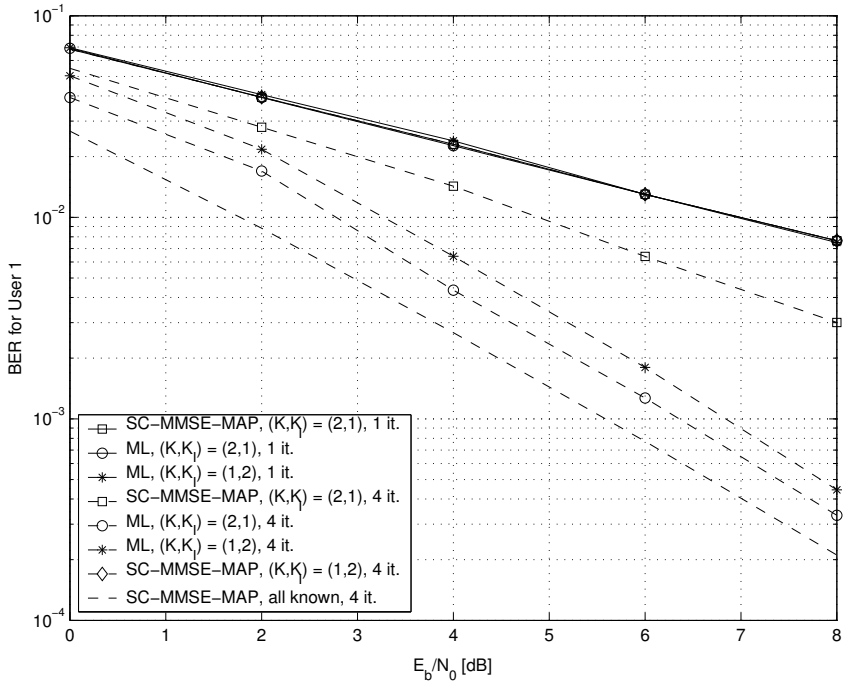

Fig. 5.11. **BER vs.** E_b/N_0 **performance of the ML iterative receiver, non-iterative PDF estimation,** $(K, K_I, N_R) = (1, 2, 3)$ **and** $(2, 1, 3)$**,** $(B, T) = (900, 100)$**,** $N_T = 1$**,** $L = 1$**, iterative LS channel estimation, SIR=**0**dB,** 4 **iterations.**

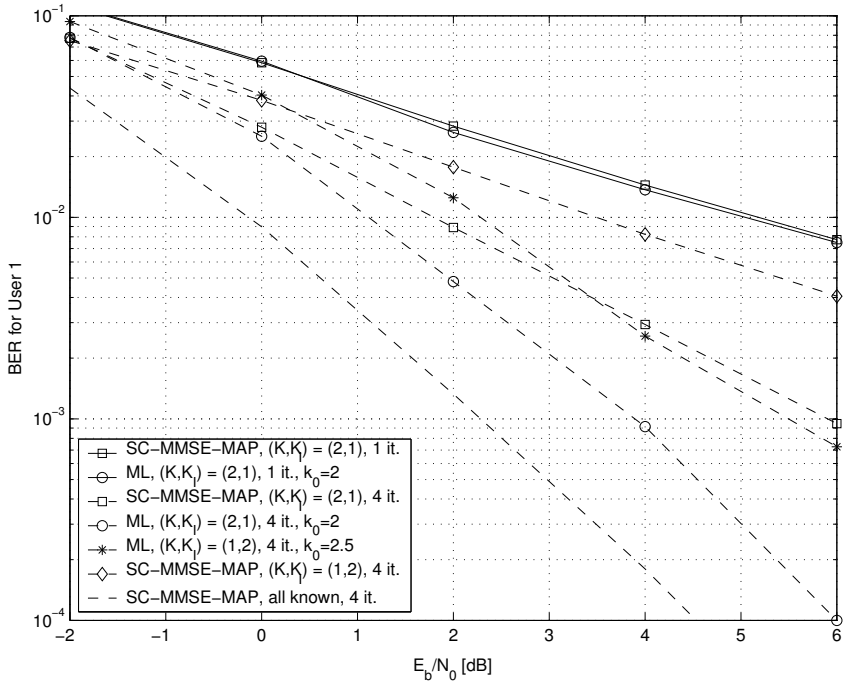

Fig. 5.12. **BER vs.** E_b/N_0 **performance of the ML iterative receiver, non-iterative PDF estimation,** $(K, K_I, N_R) = (1, 2, 3)$ **and** $(2, 1, 3)$**,** $(B, T) = (900, 100)$**,** $N_T = 1$**,** $L = 2$**, iterative LS channel estimation, SIR=**0**dB,** 4 **iterations.**

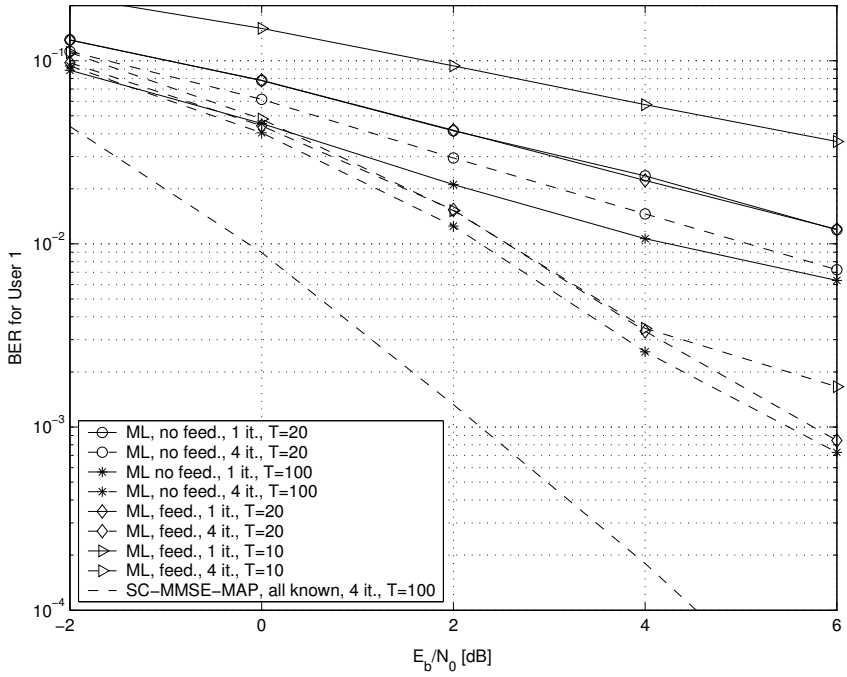

Fig. 5.13. **BER vs.** E_b/N_0 **performance of the ML iterative receiver, iterative (feed.) and non-iterative (no feed.) PDF estimation,** $(K, K_I, N_R) = (1, 2, 3)$**,** $(B, T) = (900, 100)$**,** $(900, 20)$ **and** $(900, 10)$**,** $N_T = 1$**,** $L = 2$**, iterative LS channel estimation, SIR=**0**dB,** 4 **iterations. Parameters for SC-MMSE-MAP are** $(K, K_I) = (3, 3)$ **and** $(n_0, l_0) = (1, 1)$**.**

K_I. It means that fewer samples $\hat{\mathbf{x}}$ (out of $T+B$ available) effectively contribute to the estimate $\hat{p}_{\mathbf{x}}(\mathbf{a})$ of $p_{\mathbf{x}}(\mathbf{a})$ in (5.71), which decreases the PDF estimation accuracy. The increased N_R with fixed T and B also reduces the estimation inaccuracy due to the increased dimensionality of $\mathbf{x}$ [196]. Its impact can, however, be compensated for in part by (5.75) with an appropriate choice of optimal k_0.

iterative PDF estimation is presented vs. per antenna E_b/N_0. The considered scenarios are $(K, K_I, N_R) = (1, 2, 3)$ and $(K, K_I, N_R) = (2, 1, 3)$ with $L = 2$. It can be found from Fig. 5.13 that the iterative PDF estimation-based receiver with a short ($T = 10$ and 20) training sequence can achieve almost the same performance as the non-iterative receiver with a long ($T = 100$) training sequence. It should be emphasized that the reduction in overhead due to training by iterative PDF estimation is rather significant.

Fig. 5.14 presents the SER and FER performance of the hybrid SC-MMSE-MAP iterative receiver in an STTr coded system vs. per antenna E_s/N_0. Each

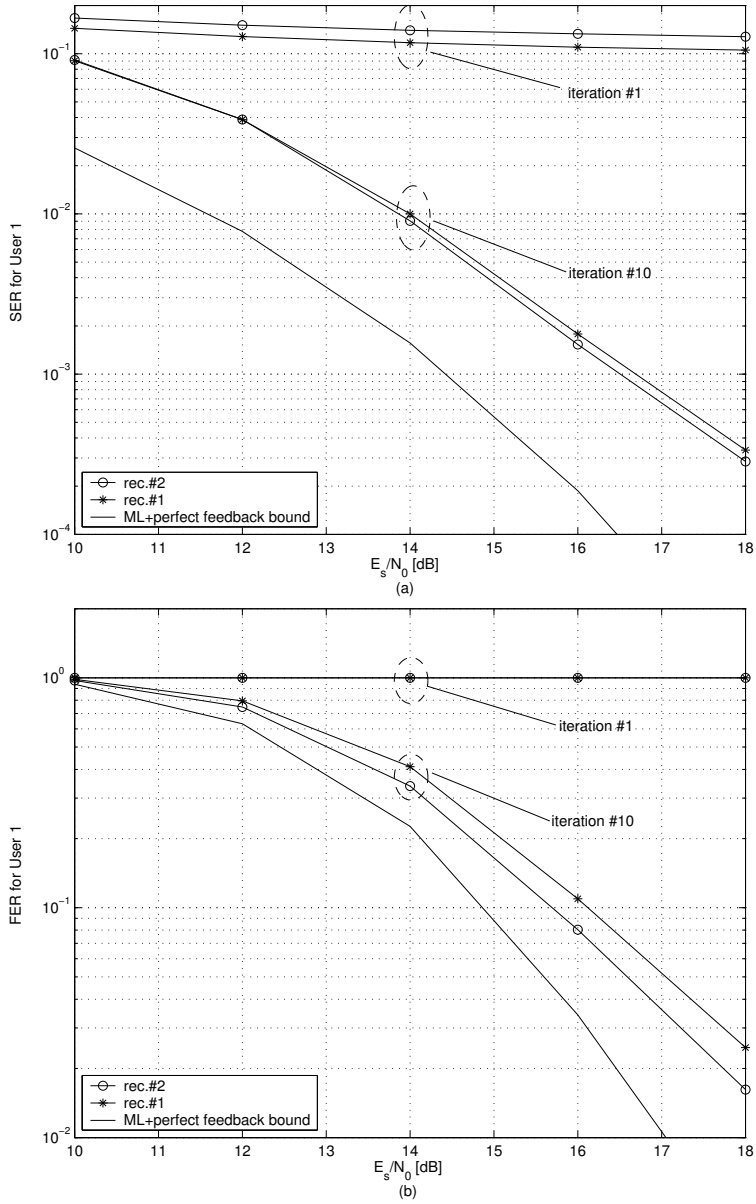

Fig. 5.14. **Performance of receiver #1 and #2 vs. per antenna E_s/N_0, $(K, K_I, N_R) = (1, 0, 1)$, $(B, T) = (150, 15)$, $N_T = 2$, $(n_0, l_0) = (1, 1)$ and $(2, 1)$, $\tau = 0$: (a) SER performance, (b) FER performance.**

user is equipped with $N_T = 2$ transmit antennas and only joint detection in space is considered. That results in receivers with either $(n_0, l_0) = (1, 1)$, denoted as rec. #1 or $(n_0, l_0) = (2, 1)$, denoted as rec. #2, that correspond to the special case described in Section 5.3.1.1. The assumed simulation scenario is $(K, K_I, K) = (1, 0, 1)$ with $L = 5$. It can be seen from Fig. 5.14 that the latter receiver performs better than the former one, due to the preserved effective degrees of freedom. The performance of both receivers is within 1.5dB of the ML bound.

In Figs. 5.15 and 5.16 the SER and FER performance of receivers #1 and #2 vs. per antenna E_s/N_0 is shown for $(K, K_I, N_R) = (3, 0, 3)$ with $L = 5$, respectively. By comparing the results of Figs. 5.15 and 5.16 it can be seen that a simultaneous increase in the number of users and number of receiver antennas results in an even smaller performance difference between the performance of receiver #1 and #2. This is due to the increased number of DoF caused by the larger number of receive antennas. The performance in a multiuser scenario is the same as the corresponding single user bound for sufficiently large E_s/N_0 values. Due to the increased number of degrees of freedom the single user bound itself is only within 0.5 dB of the ML receiver's performance.

Fig. 5.17 shows SER and FER performances of receiver #1 and #2 vs. per-antenna E_s/N_0 for $(K, K_I, N_R) = (2, 1, 3)$. It was assumed in this scenario that the UCCI uses only a single antenna. The simulation results for two values of SIR[7] are presented. In the cases of SIR equal to 3dB and 0dB the power of the signal transmitted from the UCCI's antenna was assumed to be the same as the power of the signal from the single and two antennas of any of the desired users, respectively. For comparison, the single-user bound described by $(K, K_I, N_R) = (1, 0, 3)$ is presented. It can be seen that both receivers are rather robust against the presence of unknown interference in a wide range of E_s/N_0 values, for both SIR values. Moreover, with SIR= 3dB the receivers can *perfectly* suppress the UCCI if the E_s/N_0 value becomes large. This is due to the fact that after convergence the receivers have enough *effective* degrees of freedom to separate and detect two desired users' signals and suppress one UCCI. It can also be seen from Fig. 5.17 that receivers #1 and #2 show very similar performance. This is due to the fact that the soft feedback is relatively reliable and preserving one additional DoF is of less significance.

In Fig. 5.18, SER and FER performances of both receivers (#1 and #2) are presented vs. per-antenna E_s/N_0 for $(K, K_I, N_R) = (2, 1, 3)$. In this scenario the UCCI uses two antennas in the same way as the desired users. The curves are plotted with SIR, frame length B, and channel decay exponent τ as parameters. For comparison the single-user bound described by $(K, K_I, N_R) = (1, 0, 3)$ is also presented. It can be seen again that both receivers are robust against interference over a wide range of E_s/N_0 values. However, due to the lack of *effective* degrees of freedom the performance curves tend to saturate to an error floor with high E_s/N_0 values. This can be solved in a straightforward manner by adding more receive antennas. However, it should be noted from Fig. 5.18 that the error floor can be reduced by increasing frame length while keeping the ratio T/B constant. This behavior can be explained by two reasons: first, increasing the frame length

[7]The definition of SIR is based on the signal-to-UCCI ratio.

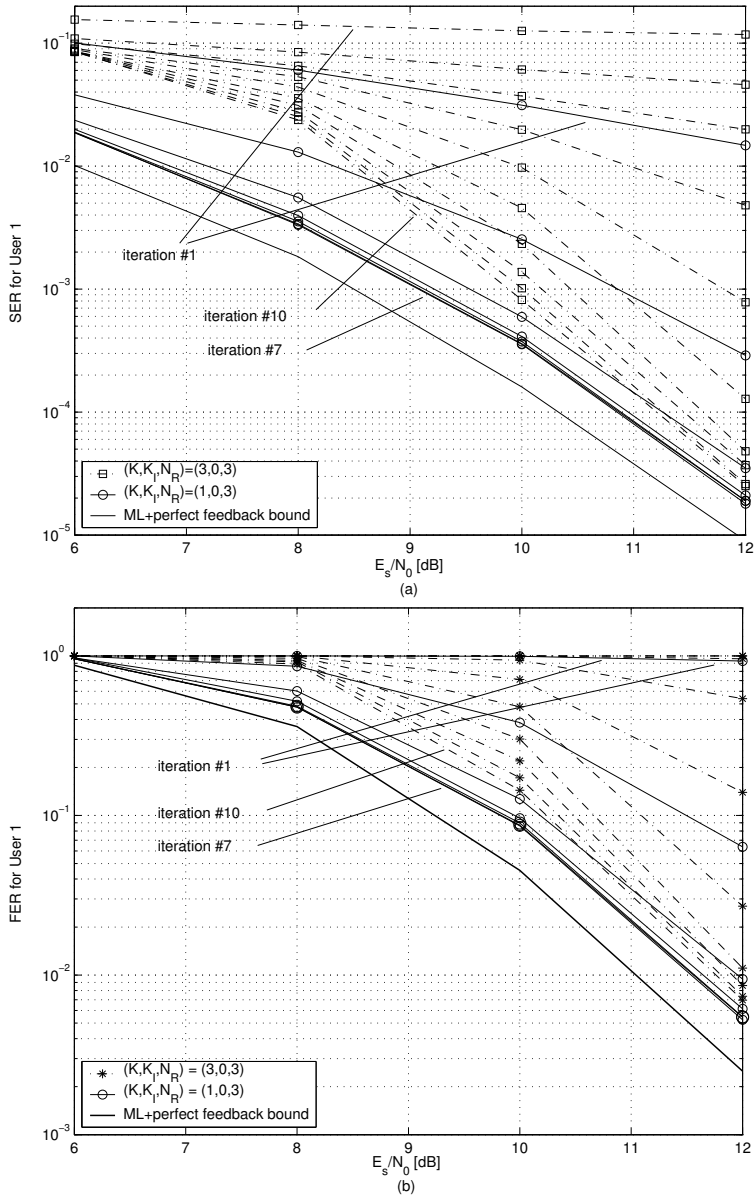

Fig. 5.15. **Performance of receiver #1 vs. per antenna E_s/N_0, $(K, K_I, N_R) = (3, 0, 3)$ and $(1, 0, 3)$, $(B, T) = (150, 15)$, $N_T = 2$, $(n_0, l_0) = (1, 1)$, $\tau = 0$: (a) SER performance, (b) FER performance.**

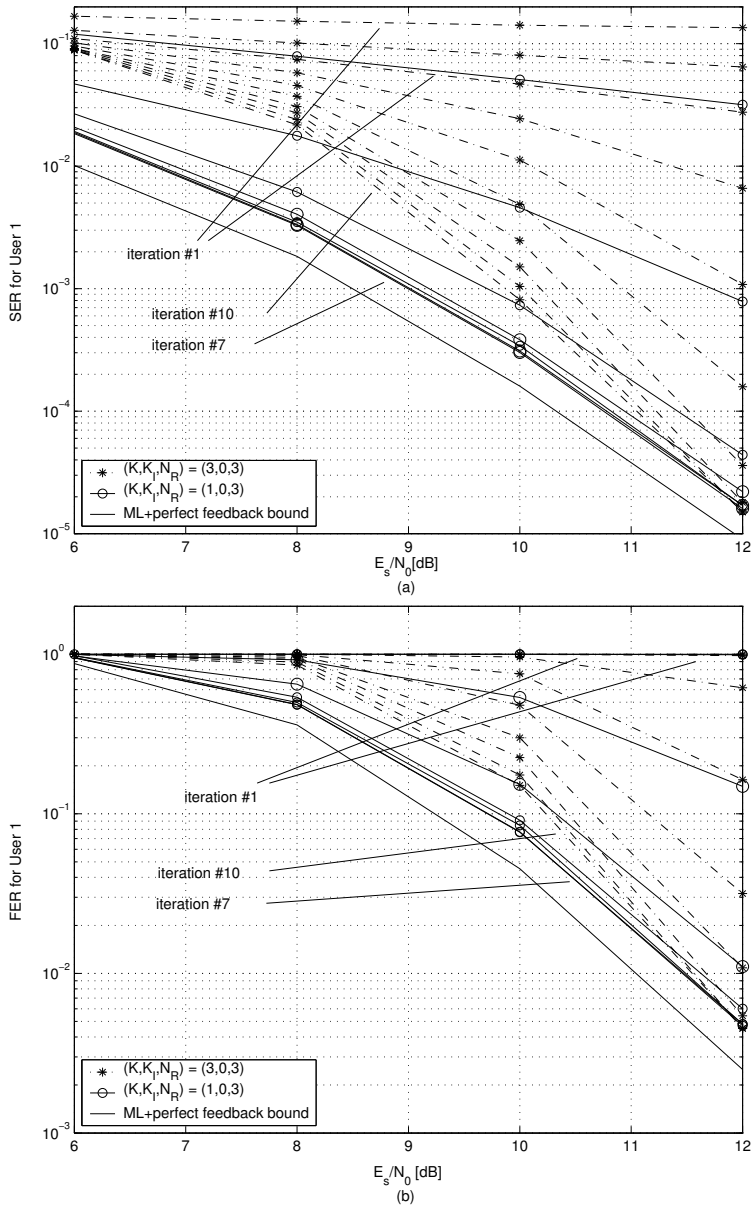

Fig. 5.16. **Performance of receiver #2 vs. per antenna E_s/N_0, $(K, K_I, N_R) = (3, 0, 3)$ and $(1, 0, 3)$, $(B, T) = (150, 15)$, $N_T = 2$, $(n_0, l_0) = (2, 1)$, $\tau = 0$: (a) SER performance, (b) FER performance.**

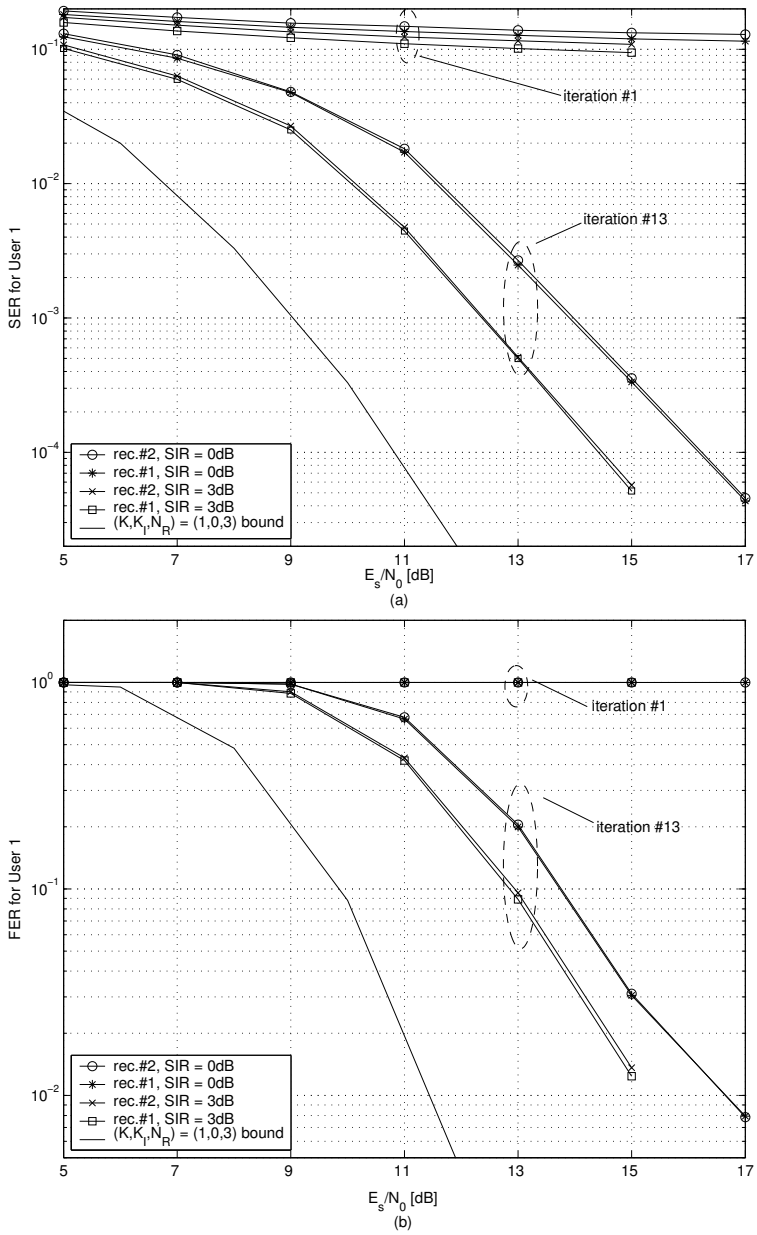

Fig. 5.17. **Performance of receiver #1 and #2 vs. per antenna E_s/N_0, $(K, K_I, N_R) = (2, 1, 3)$, $(B, T) = (150, 15)$, $N_T = 2$, $(n_0, l_0) = (1, 1)$ and $(2, 1)$, SIR=0 and 3dB (single antenna used by UCCI), $\tau = 0$: (a) SER performance, (b) FER performance.**

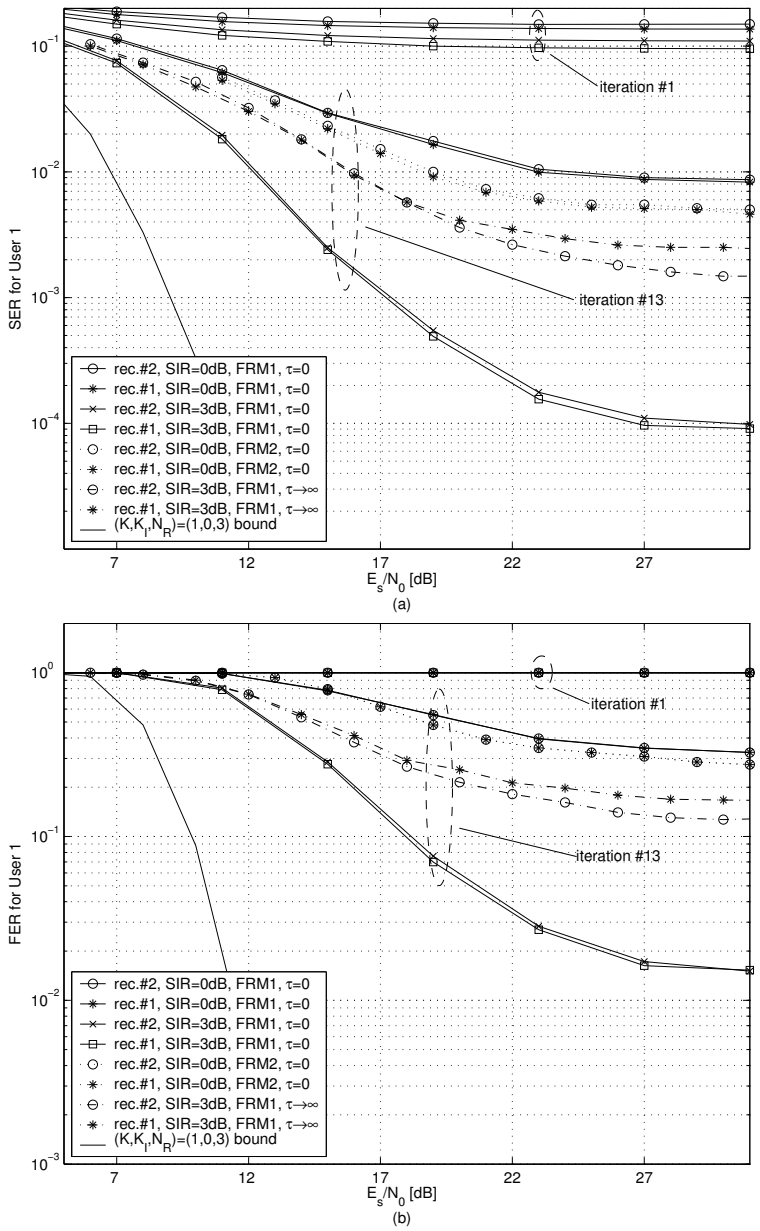

Fig. 5.18. **Performance of receiver #1 and #2 vs. per antenna E_s/N_0, $(K, K_I, N_R) = (2, 1, 3)$, $(B, T) = (150, 15)$(FRM1) and $(300, 30)$(FRM2), $N_T = 2$, $(n_0, l_0) = (1, 1)$ and $(2, 1)$, SIR=0 and 3dB (two antennas used by UCCI), $\tau = 0$ and ∞ : (a) SER performance, (b) FER performance.**

results in more samples for $\mathbf{R}$ estimation; second, the feedback becomes more accurate with the increased frame length.

It can also be seen by comparing the results for $\tau \to 0$ and $\tau \to \infty$ from Fig. 5.18 that the gain from using receiver #2 is larger if the number of significant multipath components is smaller. This is due to the fact that in the rich multipath environment ($\tau \to 0$) the number of *effective* degrees of freedom is much smaller than the number needed to perfectly suppress the UCCI. Therefore, preserving one DoF with receiver #2 does not have any significant impact on its performance. On the other hand, in flat-fading ($\tau \to \infty$) the number of *effective* degrees of freedom is comparable to the number needed to suppress the UCCI, and preserving one DoF improves performance. The performance of both receivers improves with increased SIR and in the absence of UCCI they are expected to approach the corresponding single user bounds.

It is well known that the correlation between transmit and receive antennas in a MIMO configuration is not desirable both from the transmit antenna signal separation and from the channel capacity point of view [115]. In order to separate the signals the channels between each transmit antenna are required to be sufficiently different from each other. This is in practice achievable with sufficiently spaced antennas and a rich scattering environment at both the transmitter and receiver side. The signal separation capability of the MMSE space-time equalizer described in this chapter directly depends on the spatial correlation. The results of performance evaluation with spatial correlation as a parameter is presented in Fig. 5.19, where the SER and FER performance of both receivers (#1 and #2) is presented vs. per-antenna E_s/N_0 for $(K, K_I, N_R) = (2, 1, 3)$. The UCCI again uses two antennas in the same way as the desired users. Two extreme values of correlation between transmit antenna elements of each user have been considered. In the first case, the transmit antennas are assumed to be totally uncorrelated, while in the second case they are assumed to be fully correlated[8]. It can be seen that in the totaly uncorrelated case both receivers perform almost the same. However, in case of fully correlated transmit antennas receiver #2 significantly outperforms receiver #1. This is due to the fact that receiver #1 separates different transmit antennas using MMSE filtering. On the other hand, receiver #2 separates transmit antennas in the MAP block in an optimal manner. That, in turn, results in much more robust performance of receiver #2 with respect to the fading correlation between different transmit antennas. It should be mentioned that the correlated transmit antennas of the UCCI are beneficial for the receiver performance, since the rank of the matrix $\mathbf{R}$ becomes smaller.

In Fig. 5.20 the performance of the hybrid SC-MMSE-MAP receiver that performs joint detection in time is shown in the presence of UCCI for $(K, K_I, N_R) = (2, 1, 3)$ and $L = 2$. In Fig. 5.20 the result is presented when UCCI transmits using only one antenna corresponding to the SIR=3dB. The performance of the receivers with $(n_0, l_0) = (1, 1)$, (no joint detection), denoted as rec. #1 and $(n_0, l_0) = (1, 2)$ (joint detection in time), denoted as rec. #2 are compared. It can be seen that the hybrid receiver that performs joint detection in time has significantly better

[8]It means that $\mathbf{h}_k^{(1)} = ... = \mathbf{h}_k^{(N_T)}$. Such a scenario is equivalent to a hypothetical case of infinitely small distance between transmit antenna elements.

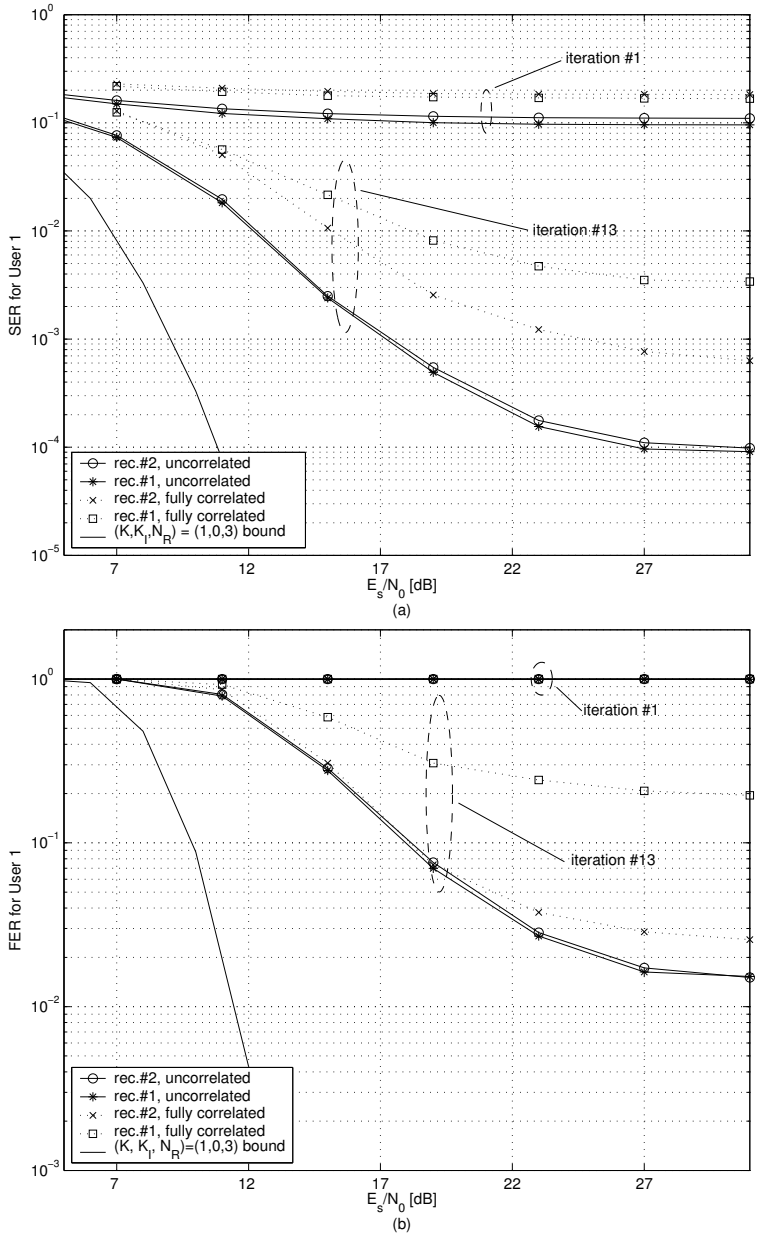

Fig. 5.19. **Performance of receiver #1 and #2 vs. per antenna E_s/N_0, $(K, K_I, N_R) = (2, 1, 3)$, $(B, T) = (150, 15)$, $N_T = 2$, SIR=0dB (two antennas used by UCCI), $\tau = 0$, transmit antennas either uncorrelated or fully correlated, channels totally uncorrelated between different taps : (a) SER performance, (b) FER performance.**

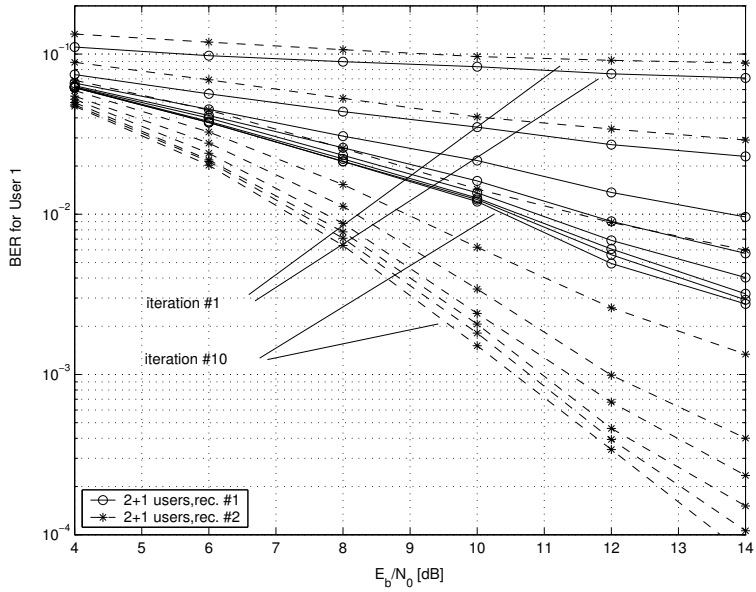

Fig. 5.20. **BER performance of a hybrid SC-MMSE-MAP receiver vs.** E_s/N_0**,** $(K, K_I, N_R) = (2, 1, 3)$**,** $(B, T) = (150, 15)$**, SIR=3dB (single antenna used by UCCI),** $N_T = 2$**,** $(n_0, l_0) = (1, 1)$ **and** $(1, 2)$ **(joint detection in time),** $L = 2$**,** $\tau = 0$**,** $Q_{ext} = 1$**.**

interference suppression capability, due to the preserved degrees of freedom.

5.3.4 Asymptotic performance analysis for an STTr coded system

In the asymptotic case of ideal feedback (5.17) becomes

$$\mathbf{y}_k(i) = \mathbf{\Pi}_k \beta_k(i) + \mathbf{H}_I \mathbf{u}_I(i) + \mathbf{n}(i), i = T+1, ..., B+T, \tag{5.77}$$

since all the ISI and known CCI are removed by the soft-cancellation. The matrix $\mathbf{\Pi}_k$ is defined as

$$\mathbf{\Pi}_k = [\mathbf{h}_k^{(1)}, ..., \mathbf{h}_k^{(N_T)}]. \tag{5.78}$$

We will assume that the signal $\mathbf{y}_k(i)$ is filtered using the MMSE filter defined in (5.40) for the special case of $(n_0, l_0) = (N_T, 1)$. We will also assume that the first constraint from Appendix 4 is used in MMSE optimization. With these assumptions the weighting matrix $\mathbf{W}_k$ becomes

$$\mathbf{W}_k = \mathbf{R}_{cov}^{-1} \mathbf{\Pi}_k^{MMSE}, \tag{5.79}$$

where

$$\mathbf{\Pi}_k^{MMSE} = \left[\frac{\mathbf{h}_k^{(1)}}{1 + {\mathbf{h}_k^{(1)}}^H \mathbf{R}_{cov}^{-1} \mathbf{h}_k^{(1)}}, ..., \frac{\mathbf{h}_k^{(N_T)}}{1 + {\mathbf{h}_k^{(N_T)}}^H \mathbf{R}_{cov}^{-1} \mathbf{h}_k^{(N_T)}} \right], \tag{5.80}$$

and $\mathbf{R}_{cov} = \mathbf{R}_I + \sigma^2 \mathbf{I}$. Note that dependency on i is omitted from (5.79) and (5.80). The equivalent Gaussian channel obtained after filtering is given as

$$\begin{aligned} \mathbf{z}_k(i) &= {\mathbf{W}_k}^H \mathbf{y}_k(i) \\ &= \mathbf{\Omega}_k \boldsymbol{\beta}_k(i) + \mathbf{\Psi}_k(i), \end{aligned} \tag{5.81}$$

where

$$\mathbf{\Omega}_k = {\mathbf{W}_k}^H \mathbf{\Pi}_k \tag{5.82}$$

and

$$\mathbf{\Theta}_k = E\{\mathbf{\Psi}_k(i) {\mathbf{\Psi}_k}^H(i)\} = {\mathbf{W}_k}^H \mathbf{R}_{cov} \mathbf{W}_k. \tag{5.83}$$

The equivalent channel output defined by (5.81) and its parameters defined by (5.82) and (5.83) are supplied to the SfISfO decoder. Let $\mathbf{C}$ and $\mathbf{E}$ be two different codeword matrices of size $N_T \times B$ and let us assume that $\mathbf{C}$ is transmitted. For the given channel realization $\mathbf{\Pi}_k$ the probability of erroneously deciding in favor of $\mathbf{E}$ can be upper bounded by

$$P(\mathbf{C} \mapsto \mathbf{E} | \mathbf{\Omega}_k, \mathbf{\Theta}_k) \leq e^{-\frac{P_k}{4\sigma^2} d^2(\mathbf{C}, \mathbf{E} | \mathbf{\Omega}_k, \mathbf{\Theta}_k)}, \tag{5.84}$$

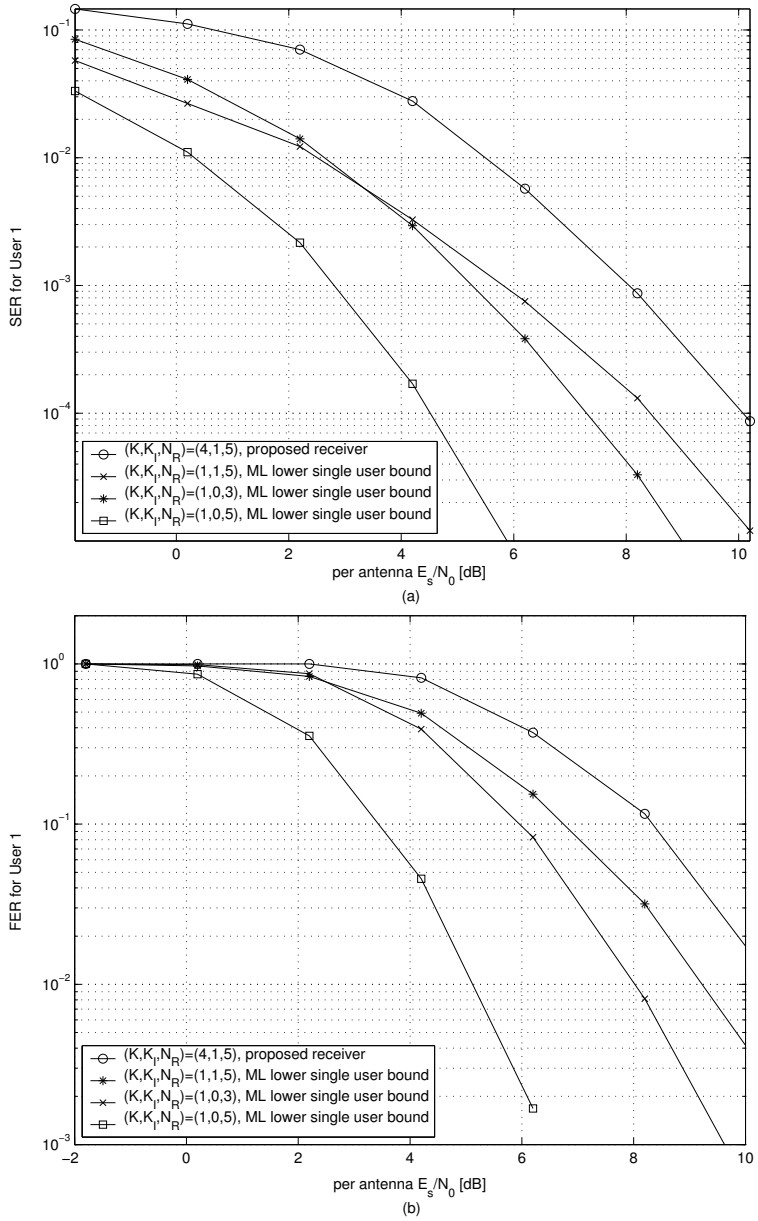

Fig. 5.21. **(a) SER performance, (b) FER performance, of a hybrid SC-MMSE-MAP receiver with** $(n_0, l_0) = (2, 1)$**,** $B = 150$**, ideal knowledge of covariance matrix** R**,** $L = 2$**,** $\tau = 0$**.**

where

$$d^2(\mathbf{C},\mathbf{E}|\mathbf{\Omega}_k,\mathbf{\Theta}_k)=\sum_{i=T+1}^{T+B}(\mathbf{c}_i-\mathbf{e}_i)^H\mathbf{\Omega}_k^H\mathbf{\Theta}_k^{-1}\mathbf{\Omega}_k(\mathbf{c}_i-\mathbf{e}_i), \tag{5.85}$$

with $\mathbf{c}_i$ and $\mathbf{e}_i$ being ith columns of $\mathbf{C}$ and $\mathbf{E}$, respectively. It can be shown that

$$\mathbf{\Omega}_k^H\mathbf{\Theta}_k^{-1}\mathbf{\Omega}_k=\mathbf{\Pi}_k^H\mathbf{R}_{cov}^{-1}\mathbf{\Pi}_k, \tag{5.86}$$

which means that

$$d^2(\mathbf{C},\mathbf{E}|\mathbf{\Omega}_k,\mathbf{\Theta}_k)=d^2(\mathbf{C},\mathbf{E}|\mathbf{\Pi}_k,\mathbf{R}_I). \tag{5.87}$$

After incorporating (5.88) and (5.86) in (5.85) we obtain

$$d^2(\mathbf{C},\mathbf{E}|\mathbf{\Pi}_k,\mathbf{R})=\sum_{i=T+1}^{T+B}(\mathbf{c}_i-\mathbf{e}_i)^H\mathbf{\Pi}_k^H(\frac{\mathbf{R}_I}{\sigma^2}+\mathbf{I})^{-1}\mathbf{\Pi}_k(\mathbf{c}_i-\mathbf{e}_i), \tag{5.88}$$

By adopting a similar approach as in [237] we can examine the properties of the vector

$$(\frac{\mathbf{R}_I}{\sigma^2}+\mathbf{I})^{-\frac{1}{2}}\mathbf{\Pi}_k(\mathbf{c}_i-\mathbf{e}_i). \tag{5.89}$$

Since it is assumed that the entries of matrix $\mathbf{H}$ (and thereby of $\mathbf{\Pi}_k$ as well) are i.i.d. it can be concluded from (5.89) that the matrix $(\frac{\mathbf{R}_I}{\sigma^2}+\mathbf{I})^{-1}$ has a similar effect as a matrix defining a spatial correlation at the receiver side, which was considered in [237]. Therefore, using the result of [237] and by performing a similar analysis, it can be concluded that the upper bound of the pairwise error probability, obtained after averaging over realizations of $\mathbf{\Pi}_k$ equals

$$\begin{aligned}P(\mathbf{C}\mapsto\mathbf{E}|\mathbf{R}_I) \quad\leq\quad & (\frac{P_k}{4\sigma^2})^{-sr((\frac{\mathbf{R}_I}{\sigma^2}+\mathbf{I})^{-1})}\prod_{i=0}^{s-1}\lambda_i^{-r((\frac{\mathbf{R}_I}{\sigma^2}+\mathbf{I})^{-1})}(\mathbf{C},\mathbf{E}) \\ & \prod_{j=0}^{r((\frac{\mathbf{R}_I}{\sigma^2}+\mathbf{I})^{-1})-1}\lambda_j^{-s}((\frac{\mathbf{R}_I}{\sigma^2}+\mathbf{I})^{-1}),\end{aligned} \tag{5.90}$$

where s is the transmit diversity order of STTrC, λ_i is the ith eigenvalue of the error matrix $\mathbf{C}-\mathbf{E}$, λ_j is the jth eigenvalue of the matrix $(\frac{\mathbf{R}_I}{\sigma^2}+\mathbf{I})^{-1}$ and $r(\cdot)$ denotes the rank of a matrix. Let us now determine the rank and eigenvalues of the matrix $(\frac{\mathbf{R}_I}{\sigma^2}+\mathbf{I})^{-1}$. If $\lambda_{\mathbf{R}_I,i}$ denotes the ith eigenvalue of the matrix $\mathbf{R}_I$ then the ith eigenvalue of the matrix $(\frac{\mathbf{R}_I}{\sigma^2}+\mathbf{I})^{-1}$ is equal to $\frac{\sigma^2}{\sigma^2-\lambda_{\mathbf{R}_I,i}}$. In the asymptotic case of large SNR[9] these eigenvalues can be either 0 (for $\lambda_{\mathbf{R}_I,i}\neq 0$) or 1 (for $\lambda_{\mathbf{R}_I,i}=0$). This, in turn, means that

$$r((\frac{\mathbf{R}_I}{\sigma^2}+\mathbf{I})^{-1})=LN_R-r(\mathbf{R}_I), \tag{5.91}$$

[9]Note that in the high SNR region the assumption of perfect SC is also more likely to be valid than in the low SNR region.

which finally yields

$$P(\mathbf{C} \mapsto \mathbf{E}|\mathbf{R}_I) \leq (\frac{P_k}{4\sigma^2})^{-s(LN_R - r(\mathbf{R}_I))} \prod_{i=0}^{s-1} \lambda_i^{-(LN_R - r(\mathbf{R}_I))}(\mathbf{C}, \mathbf{E}). \tag{5.92}$$

Note that the expression above is conditioned on the matrix $\mathbf{R}_I$. However, from the calculations above it can be seen that in the asymptotic case of large SNR the eigenvalues and rank of the matrix $(\frac{\mathbf{R}_I}{\sigma^2} + \mathbf{I})^{-1}$ are independent of the particular realization of the matrix $\mathbf{R}_I$ and therefore it can be written that

$$P(\mathbf{C} \mapsto \mathbf{E}) \leq (\frac{P_k}{4\sigma^2})^{-s(LN_R - r(\mathbf{R}_I))} \prod_{i=0}^{s-1} \lambda_i^{-(LN_R - r(\mathbf{R}_I))}(\mathbf{C}, \mathbf{E}). \tag{5.93}$$

It can be concluded from (5.93) that comparing to the ideal case of perfect feedback and no UCCI, when the fully achievable diversity gain is sLN_R, in the presence of UCCI the achievable diversity and coding gains are decreased by the rank $r(\mathbf{R}_I)$ of the interference covariance matrix. The performance of a receiver for different interference conditions is presented in Fig. 5.21.

5.4 Summary and conclusions

The subject of this chapter was iterative receivers for joint multiuser detection, equalization, channel estimation and unknown interference suppression in SDMA. An SC-MMSE based generic iterative receiver was derived for convolutional and STTr codes. We capitalized on the knowledge of [29], [218], [241] and [223] to derive a generalization of the iterative SC-MMSE receiver for both convolutional and STTr codes in frequency selective channels. It was shown that in the absence of UCCI the proposed receiver is capable of achieving the corresponding single-user bound both in convolutionally and STTr coded systems. These results are summarized in Figs. 5.4, 5.6 and 5.7. Thereby, the number of required receive antennas is *lower* or *equal* to the number of users and not to the total number of transmit antennas, as opposed to the result obtained in [241] for flat fading channel. Moreover, it was shown that in an STTr coded system the performance of the multiuser receiver becomes closer to the ML bound as the number of users and number of receive antennas simultaneously increase. This result is consistent to that of [153] where the performance of ML detection in MIMO scenario was considered.

The performance of the SC-MMSE receiver with iterative channel estimation is evaluated in the presence of UCCI. The hard feedback based UCCI suppression method proposed in [224] is extended to the case of soft feedback. From the

result presented in Fig. 5.10 it can be concluded that the receiver that ignores the existence of the UCCI performs remarkably worse than the one that performs interference suppression. Moreover, iterative channel estimation shows only about a 1 dB degradation in performance compared to the perfect CSI case. Finally, soft decision feedback has been shown to perform slightly better than hard feedback.

In the presence of UCCI the performance of a conventional low-complexity SC-MMSE receiver is compared to the hybrid SC-MMSE-MAP receiver and to the ML receiver. It was shown that the hybrid SC-MMSE-MAP iterative receiver can offer better performance than the low complexity SC-MMSE receiver by jointly detecting signals both in space and in time. This trend can be observed from Figs. 5.14–5.20. Note that this is consistent with the results obtained by decoupled schemes [150, 151, 152] and with group ML detection [158]. However, the schemes considered there are *non-iterative* and they do not employ a channel code. Note that the fact that the receivers are iterative allows for MAP instead of pure ML detection, due to the presence of *a priori* information. Moreover, the scheme proposed in this chapter offers more flexibility in the choice of transmit antennas and multipath components to be detected by MAP detection. It should also be noted that the hybrid scheme performs much better than the conventional SC-MMSE scheme for highly spatially correlated transmit antennas, as seen from Fig. 5.19. On the other hand, the two schemes have very similar performance for uncorrelated transmit antennas. We also mention that a similar iterative receiver scheme was proposed independently in [271] for the decoding of a BICM single user system. However, the hybrid scheme is compared only to the low complexity matched filter approximation turbo receiver of [232].

As mentioned above, in channels with low frequency selectivity the ML iterative receiver has a potential of preserving the receiver's DoF in the presence of UCCI. This can be achieved by more accurate modelling of UCCI and estimation of its PDF, since the CSI of the interference is not available. This fact was used in [170, 171] and [216] in CDMA and [168] and [172] for equalization in narrowband systems. A method for non-parametric PDF estimation proposed in [172] is extended in this thesis for use with space-time turbo equalization and multiuser detection. It was shown in Figs. 5.11–5.13 that the ML receiver outperforms the low complexity SC-MMSE receiver if the channel does not suffer from severe frequency selectivity, and if the number of interferers is not significantly large. This is due to the preserved diversity order of the ML receiver.

By establishing a correspondence with the work of [237] we show by asymptotic performance analysis of the iterative receiver in an STTr-coded system that the impact of the UCCI on the performance is similar to that of the spatial correlation at the receiver side. That is, the diversity and coding gains achievable in the UCCI-free scenario are decreased by a factor that depends on the rank of the interference covariance matrix. This result is summarized in Fig. 5.21.

6 Practical considerations

In this chapter issues related to receiver complexity and performance sensitivity related to non-ideal receiver operation and propagation environment changes are considered. For that purpose a realistic channel model obtained through multidimensional channel measurement campaigns is considered. How the measurement data can be used is described in Section 6.1. In reality, path energy is likely to be concentrated in a certain period of the channel delay profile, and this part makes the primary contributions to the performance. Therefore, the rest of the delay profile may be cancelled by estimating the corresponding covariance matrix, by which significant complexity reduction can be expected. A reduced complexity receiver based on these assumptions is derived in Section 6.2. The performance dependency of this receiver on imperfect timing estimation is studied in Section 6.3. Finally, the performance dependency on spatial antenna correlation is considered in Section 6.4. Section 6.5 concludes this chapter.

6.1 Performance evaluation using field measurement data

Understanding receiver behavior and evaluating its performance in realistic situations is of great importance. The receiver performance obtained using different channel models [38, 272] is one possible way of evaluating receiver performance. The drawback of these methods, however, is that it results in the average performance over a set of channel realizations conditioned on the fixed parameters of the model. Moreover, an inaccurate model results in a performance estimate that does not reflect performance in a realistic environment. Another possibility is to evaluate the performance using a realistic channel impulse response obtained directly through measurement campaigns. The advantage of this approach compared to the one based on models is that the results actually reflect a practical situation. Therefore, the need for prototyping is set back to the only stage of implementation where a system's operability has to be verified in real field tests. The drawback of this method, however, is that the performance result is specific only for a considered measurement scenario and propagation environment.

Table 6.1. Parameters of the measurement campaign for Section 6.

Measurement frequency	5GHz
Transmitter	uniform circular array, 16 antennas, spacing of 0.5λ
Receiver	uniform linear array, 8 antennas, spacing of 0.4λ
Transmitter height	2.1 m
Receiver height	1.67 m
Measurement bandwidth	120MHz
Transmit and receive filter	root Nyquist raised cosine, roll-off factor 0.25
Data rate	20 Msymb/sec
Number of multipath components after receive filtering	$L = 24$

In this thesis field measurement data is used to evaluate receiver performance dependency on practical channel impairments. The channel impulse response data is obtained by using a multidimensional channel sounder, described in detail in [273, 258] and Table 6.1.

The measurement campaign that was considered in this thesis took place at a courtyard of the Ilmenau University of Technology, Germany. The measurement route and positions of the transmitter and receiver are illustrated in Fig. 6.1. The receiver was stationary during measurement, while the transmitter was moving at a walking speed. Three different regions can be identified along the route. First, the static non-line-of-sight (S-NLOS) region, where the transmitter was stationary and the line-of-sight (LOS) was obstructed by a metal container. Second, the dynamic NLOS (D-NLOS) region, where the transmitter was moving but LOS was still obstructed. Third, the LOS region, where LOS between the transmitter and receiver exists. Details about spatio-temporal structure of the channel in the given measurement area can be found in [258].

The signal having a certain data rate to be transmitted was upsampled and filtered using a transmitter filter to form a signal whose bandwidth is adjusted to the measurement equipment bandwidth. The upsampled and filtered signal was then convoluted with the measured channel impulse responses to produce the received signal samples. The received signal was again convoluted with the receiver filter and finally downsampled to the original data rate. Thereby, the equivalent

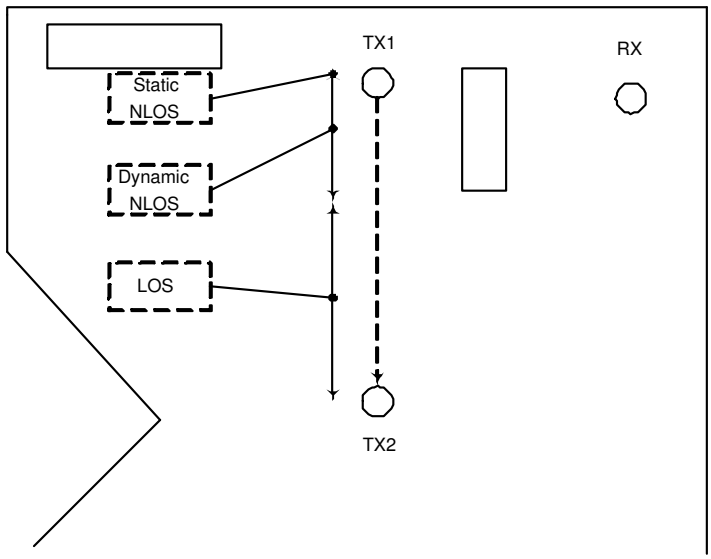

Fig. 6.1. **Map of the measurement area: transmitter (UCA) is moving along the route, receiver (ULA) is fixed. In the first part of the measurement route the LOS is obstructed by the metal container. Total number of measurement snapshots is** 108**. Snapshots** $1-16$ **correspond to S-NLOS,** $17-51$ **to D-NLOS and** $52-108$ **to LOS.**

symbol-spaced channel impulse response coefficients are obtained as a convolution of the transmit filter, measured channel impulse response and the receive filter. The obtained symbol-spaced channel impulse response was then used to form channel matrix $\mathbf{H}$, defined in Section 5.1.

6.2 Reduced complexity turbo receiver based on dominant components of the CIR

In this section, a low complexity receiver that takes into account only a part of the channel impulse response will be derived. The justification for this approach lies in the fact that in many practical situations only a part of the channel impulse response carries most of the signal energy. For simplicity of notation, only a single user system will be considered, resulting in $K = 1$ and $K_I = 0$, and dependency on the user index will be omitted. We will assume that L_{eff} out of L multipath components are taken into account while detecting the signals, and the choice of these components is made *a priori*. Note that in general for different transmit-

receive antenna pairs multipath components at different delays may be selected. Let us rewrite (5.1) so as to take into account only a part of the channel impulse response of length L_{eff}

$$\mathbf{y}_{eff}(i) \quad = \quad \mathbf{H}_{eff}\mathbf{u}(i) + \mathbf{n}_{eff}(i), \tag{6.1}$$

where $\mathbf{y}_{eff} \in \mathbb{C}^{(LN_R)_{eff}\times 1}$, $\mathbf{H}_{eff} \in \mathbb{C}^{(LN_R)_{eff}\times N_T(2L-1)}$ and $\mathbf{n}_{eff} \in \mathbb{C}^{(LN_R)_{eff}\times 1}$ are defined as follows:

- $\mathbf{H}_{eff}$ is obtained by taking only those rows of the matrix $\mathbf{H}$ for which at least one of the column elements indexed from $N_T(L-1)$ to $N_T(L-1)+n_0-1$ belongs to the set of significant multipath components. Note that in general the number of selected rows $(LN_R)_{eff}$ will vary between L_{eff} and $\min\{LN_R, n_0 L_{eff}\}$
- $\mathbf{y}_{eff}(i)$ and $\mathbf{n}_{eff}(i)$ are obtained by taking only those elements of the vectors $\mathbf{y}(i)$ and $\mathbf{n}(i)$, respectively, which correspond to the selected rows of the matrix $\mathbf{H}$.

Eq. (6.1) can now be rewritten as

$$\mathbf{y}_{eff}(i) \quad = \quad \underbrace{\mathbf{H}_d\mathbf{u}(i)}_{\text{desired}} + \underbrace{\mathbf{H}_u\mathbf{u}(i)}_{\text{interference}} + \mathbf{n}_{eff}(i), \tag{6.2}$$

where $\mathbf{H}_d \in \mathbb{C}^{(LN_R)_{eff}\times N_T(2L-1)}$ denotes a matrix in which non-significant multipath components are equal to zero, and $\mathbf{H}_u \in \mathbb{C}^{(LN_R)_{eff}\times N_T(2L-1)}$ is the matrix of interference, defined by

$$\mathbf{H}_u = \mathbf{H}_{eff} - \mathbf{H}_d. \tag{6.3}$$

In a special case which will be considered in numerical results, the L_{eff} consecutive multipath components will be regarded as significant, and their timing will be assumed to be the same for all transmit-receive antenna pairs. Then $\mathbf{H}_d \in \mathbb{C}^{L_{eff}N_R\times N_T(2L-1)}$ and $\mathbf{H}_I \in \mathbb{C}^{L_{eff}N_R\times N_T(2L-1)}$ become

$$\mathbf{H}_d = \begin{bmatrix} \mathbf{0} & \dots & \mathbf{0} & \mathbf{H}(P) & \dots & \mathbf{H}(L-E+1) & \dots & \mathbf{0} & \mathbf{0} & \dots & \mathbf{0} \\ \vdots & & & \vdots & \ddots & & \ddots & \vdots & & & \vdots \\ \mathbf{0} & \dots & \mathbf{0} & \mathbf{0} & \dots & \mathbf{H}(P) & \dots & \mathbf{H}(L-E+1) & \mathbf{0} & \dots & \mathbf{0} \end{bmatrix}$$

and

$$\mathbf{H}_u = \begin{bmatrix} \mathbf{H}(0)\dots\mathbf{H}(P-1) & \mathbf{0} & \dots & \mathbf{0}\mathbf{H}(L-E)\dots\mathbf{H}(L-1) & \dots & \mathbf{0} \\ \vdots & & \vdots & \ddots & \ddots & \vdots & & \vdots \\ \mathbf{0} & \dots & \mathbf{H}(0) & \dots\mathbf{H}(P-1)\mathbf{0} & \dots & \mathbf{0}\,\mathbf{H}(L-E)\dots\mathbf{H}(L-1) \end{bmatrix}$$

with the first P and last E paths not being taken into account, L_{eff} paths taken into account and $L = P + L_{eff} + E$.

The hybrid SC-MMSE-MAP receiver from Section 5.3.1 will be derived under the assumptions above and for the special case of joint detection only in space for

which $l_0 = 1$. Without loss of generality, derivation is shown for the first set of transmit antennas. For simplicity of notation dependency on the user index k is omitted.

Soft cancellation. Let us denote by $\tilde{\mathbf{u}}(i)$ the vectors that are obtained by replacing the elements of $\mathbf{u}(i)$ by their soft estimates. The soft estimates are, in general, obtained groupwise. For example the soft estimates corresponding to the first antenna set are defined as

$$\tilde{\boldsymbol{\beta}}^{<1>}(i) = \sum_{\boldsymbol{\alpha}_q^{<1>} \in \mathcal{Q}^{n_0}} \boldsymbol{\alpha}_q^{<1>} P_2^{ext}(\boldsymbol{\beta}^{<1>}(i) = \boldsymbol{\alpha}_q^{<1>}), \tag{6.4}$$

where $\boldsymbol{\beta}^{<1>}(i) \in \mathbb{C}^{n_0 \times 1}$ is defined by

$$\boldsymbol{\beta}^{<1>}(i) = [b^{(1)}(i), ..., b^{(n_0)}(i)]^T. \tag{6.5}$$

As before, $P_2^{ext}(\boldsymbol{\beta}^{<1>}(i) = \boldsymbol{\alpha}_q)$ denotes the extrinsic information obtained after SfISfO decoding.

Let us denote with $\mathbf{u}^{<1>}(i)$ the vector which contains soft estimates of the signals that correspond to the n_0 transmit antennas of the first antenna set. The vector $\mathbf{u}^{<1>}(i)$ can be represented by

$$\mathbf{u}^{<1>}(i) = \tilde{\mathbf{u}}(i) - \tilde{\mathbf{u}}(i) \odot \mathbf{e}^{<1>}, \tag{6.6}$$

where

$$\mathbf{e}^{<1>} = [\underbrace{0, ..., 0}_{(L-1)N_T}, \underbrace{1, ..., 1}_{n_0} \underbrace{0, ..., 0}_{LN_T - n_0}]^T. \tag{6.7}$$

After performing soft cancellation one obtains

$$\mathbf{y}^{<1>}(i) = \mathbf{y}_{eff}(i) - \hat{\mathbf{H}}_d \mathbf{u}^{<1>}(i), i = T+1, ..., B+T, \tag{6.8}$$

where $\hat{\mathbf{H}}_d$ denotes the channel estimate obtained using either only pilot sequence $\mathbf{u}(i), i = 1, ..., T$ or both the pilot and soft estimates (see Appendix 3).

MMSE filtering to suppress UCCI and residual interference. The signals contained in $\boldsymbol{\beta}^{<1>}(i)$, are jointly detected by filtering the signal $\mathbf{y}^{<1>}(i)$ using a linear MMSE filter whose weighting matrix $\mathbf{W}^{<1>}(i)$ satisfies the following criterion

$$[\mathbf{W}^{<1>}(i), \mathbf{A}^{<1>}(i)] = \arg \min_{\substack{\mathbf{W} \in \mathbb{C}^{L_{eff} N_R \times n_0}, \\ \mathbf{A} \in \mathbb{C}^{n_0 \times n_0}}} ||\mathbf{W}^H \mathbf{y}^{<1>}(i) - \mathbf{A}^H \boldsymbol{\beta}^{<1>}(i)||^2. \tag{6.9}$$

Under the first constraint described in Appendix 4 the vector $\mathbf{W}^{<1>}(i)$ becomes equal to

$$\mathbf{W}^{<1>}(i) = \left[\frac{\mathbf{M}^{<1>}(i)^{-1} \mathbf{h}^{(1)}}{1 + \mathbf{h}^{(1)^H} \mathbf{M}^{<1>}(i)^{-1} \mathbf{h}^{(1)}} ... \frac{\mathbf{M}^{<1>}(i)^{-1} \mathbf{h}^{(n_0)}}{1 + \mathbf{h}^{(n_0)^H} \mathbf{M}^{<1>}(i)^{-1} \mathbf{h}^{(n_0)}} \right], \tag{6.10}$$

where

$$\mathbf{M}^{<1>}(i) = \underbrace{\hat{\mathbf{H}}_d \boldsymbol{\Lambda}^{<1>}(i) \hat{\mathbf{H}}_d^H + \hat{\mathbf{R}}}_{\mathbf{R}_{cov}} - \sum_{n=1}^{n_0} \mathbf{h}^{(n)} \mathbf{h}^{(n)^H}, \tag{6.11}$$

and $\mathbf{h}^{(n)}$ is the $[(L-1)N_T+n]$th column of matrix $\hat{\mathbf{H}}_d$. Matrix $\hat{\mathbf{R}}$ denotes an estimate of the covariance matrix of the interference-plus-noise defined as

$$\begin{aligned}\mathbf{R} &= E\{\mathbf{H}_d(\mathbf{u}_{eff}(i)-\mathbf{u}^{<1>}(i))\mathbf{u}_{eff}^H(i)\mathbf{H}_u^H \\ &+ \mathbf{H}_u\mathbf{u}_{eff}(i)(\mathbf{u}_{eff}(i)-\mathbf{u}^{<1>}(i))^H\mathbf{H}_d^H \\ &+ \mathbf{H}_u\mathbf{u}_{eff}(i)\mathbf{u}_{eff}^H(i)\mathbf{H}_u^H+\mathbf{n}_{eff}(i)\mathbf{n}_{eff}^H(i)\} \\ &= \mathbf{H}_d\mathbf{\Lambda}^{<1>}(i)\mathbf{H}_u^H+\mathbf{H}_u\mathbf{\Lambda}^{<1>}(i)\mathbf{H}_d^H+\mathbf{H}_u\mathbf{H}_u^H+\sigma^2\mathbf{I}.\end{aligned} \tag{6.12}$$

The matrix $\mathbf{\Lambda}_k^{<1>}(i)$ is defined as

$$\begin{aligned}\mathbf{\Lambda}^{<1>}(i) &= E\{[\mathbf{u}_{eff}(i)-\mathbf{u}^{<1>}(i)][\mathbf{u}_{eff}(i)-\mathbf{u}^{<1>}(i)]^H\} \\ &= E\{\mathbf{u}_{eff}(i){\mathbf{u}_{eff}}^H(i)\}-E\{\mathbf{u}^{<1>}(i)\mathbf{u}^{<1>}(i)\} \\ &= \mathrm{diag}\{\mathbf{\Delta}^{<1>}(i+L-1),...,\mathbf{\Delta}^{<N_T/n_0>}(i+L-1), \\ &... \ \mathbf{\Delta}^{<1>}(i-L+1),...,\mathbf{\Delta}^{<N_T/n_0>}(i-L+1)\} \\ &= E\{[\mathbf{u}_{eff}(i)-\mathbf{u}^{<1>}(i)]\mathbf{u}_{eff}^H(i)\} \\ &= E\{\mathbf{u}_{eff}(i)[\mathbf{u}_{eff}(i)-\mathbf{u}^{<1>}(i)]^H\},\end{aligned} \tag{6.13}$$

where

$$\mathbf{\Delta}^{<1>}(i-l)=E\{\boldsymbol{\beta}^{<1>}(i-l)\boldsymbol{\beta}^{<1>}(i-l)^H\}-\tilde{\boldsymbol{\beta}}^{<1>}(i-l)\tilde{\boldsymbol{\beta}}^{<1>}(i-l)^H, \tag{6.14}$$

with

$$E\{\beta^{<1>}(i-l)\beta^{<1>}(i-l)^H\}=\sum_{\boldsymbol{\alpha}_q^{<1>}\in\mathcal{Q}^{n_0}}\boldsymbol{\alpha}_q^{<1>}\boldsymbol{\alpha}_q^{<1>H}P_2^{ext}(\beta^{<1>}(i-l)=\boldsymbol{\alpha}_q^{<1>}) \tag{6.15}$$

for $l\neq 0$ and

$$\mathbf{\Delta}^{<1>}(i-l)=E\{\boldsymbol{\beta}^{<1>}(i-l)\boldsymbol{\beta}^{<1>}(i-l)^H\}, \tag{6.16}$$

with

$$E\{\beta^{<1>}(i)\beta^{<1>}(i)^H\}=\sum_{\boldsymbol{\alpha}_q^{<1>}\in\mathcal{Q}^{n_0}}\boldsymbol{\alpha}_q^{<1>}\boldsymbol{\alpha}_q^{<1>H}, \tag{6.17}$$

for $l=0$.

Estimation of the covariance matrix of the UCCI plus noise. In order to exactly calculate the covariance matrix $\mathbf{R}$, the matrix $\mathbf{H}_I$ (or its estimate) is needed. In this thesis, instead for practical reasons, we use the time-average approximation of the matrix, as follows

$$\hat{\mathbf{R}}=\frac{1}{T}\sum_{i=1}^{T}(\mathbf{y}_{eff}(i)-\hat{\mathbf{H}}_d\mathbf{u}(i))(\mathbf{y}_{eff}(i)-\hat{\mathbf{H}}_d\mathbf{u}(i))^H. \tag{6.18}$$

In second and subsequent iterations soft feedback can be used for estimation together with the training sequence, as follows

$$\begin{aligned}\hat{\mathbf{R}} &= \frac{1}{T}\sum_{i=1}^{T}(\mathbf{y}_{eff}(i)-\hat{\mathbf{H}}_d\mathbf{u}(i))(\mathbf{y}_{eff}(i)-\hat{\mathbf{H}}_d\mathbf{u}(i))^H \\ &+ \frac{1}{B}\sum_{i=T+1}^{T+B}(\mathbf{y}_{eff}(i)-\hat{\mathbf{H}}_d\overline{\mathbf{u}}(i))(\mathbf{y}_{eff}(i)-\hat{\mathbf{H}}_d\overline{\mathbf{u}}(i))^H,\end{aligned} \tag{6.19}$$

where $\overline{\mathbf{u}}(i)$ denotes the soft feedback vector. Its elements are obtained by replacing the corresponding elements of $\mathbf{u}(i)$ by their soft estimates, which in general are obtained groupwise. More precisely, the soft estimates corresponding to the first group and time instant i are defined as

$$\tilde{\boldsymbol{\beta}}_k^{<1>}(i) = \sum_{\boldsymbol{\alpha}_q^{<1>}\in\mathcal{Q}^{n_0}} \boldsymbol{\alpha}_q^{<1>} P_2^{app}(\boldsymbol{\beta}_k^{<1>}(i)=\boldsymbol{\alpha}_q^{<1>}), \tag{6.20}$$

where P_2^{app} denotes *a posteriori* information obtained after SfISfO decoding.

Derivation of the equivalent Gaussian channel. Assuming that the MMSE filter output $\mathbf{z}^{<1>}(i)\in\mathbb{C}^{n_0\times 1}$ can be viewed as the output of the equivalent Gaussian channel [265] we can write

$$\begin{aligned}\mathbf{z}^{<1>}(i) &= \mathbf{W}^{<1>H}(i)\mathbf{y}^{<1>}(i) \\ &= \boldsymbol{\Omega}^{<1>}(i)\boldsymbol{\beta}^{<1>}(i)+\boldsymbol{\Psi}^{<1>}(i),\end{aligned} \tag{6.21}$$

where matrix $\boldsymbol{\Omega}^{<1>}(i)\in\mathbb{C}^{n_0\times n_0}$ contains the gains of the equivalent channel defined as

$$\boldsymbol{\Omega}^{<1>}(i) = E\{\mathbf{z}^{<1>}(i)\boldsymbol{\beta}^{<1>H}(i-l)\} = \mathbf{W}^{<1>H}(i)\boldsymbol{\Pi}^{<1>}, \tag{6.22}$$

with $\boldsymbol{\Pi}^{<1>}=[\mathbf{h}^{(1)}\dots\mathbf{h}^{(n_0)}]$. The vector $\boldsymbol{\Psi}^{<1>}(i)\in\mathbb{C}^{n_0\times 1}$ is the equivalent additive Gaussian noise with covariance matrix

$$\begin{aligned}\boldsymbol{\Theta}^{<1>}(i) &= E\{\boldsymbol{\Psi}^{<1>}(i)\boldsymbol{\Psi}^{<1>H}(i)\} \\ &= \mathbf{W}^{<1>H}(i)\mathbf{R}_{cov}\mathbf{W}^{<1>}(i).\end{aligned} \tag{6.23}$$

The same procedure is repeated for all N_T/n_0 sets of transmit antennas that are jointly detected. The outputs of the equivalent channels $\mathbf{z}^{<\gamma>}(i)$ and their parameters $\boldsymbol{\Omega}^{<\gamma>}(i)$ and $\boldsymbol{\Theta}^{<\gamma>}(i)$ for $\gamma=1,...,N_T/n_0$ are passed to the MAP block that produces extrinsic information necessary for SfISfO decoding. The MAP block and symbol level SfISfO decoder are described in more detail in Sections 5.3.1 and 5.2.4.

6.3 Interference suppression to reduce sensitivity to timing offset

One very important issue in broadband wireless access using single carrier communications is to determine the correct symbol timing and correspondingly correct

equalizer coverage. In this section the sensitivity of the receivers proposed in Section 6.2 to timing offset will be studied. For that purpose a single measurement snapshot is selected from the measurement data set. Figs. 6.2 (a) and (b) present the channel impulse responses from the transmit antenna elements #1 and #8 to each of the receive antenna elements #1, #4 and #7 for snapshot #50. This scenario results in $(N_T, N_R) = (2, 3)$. It is assumed that each transmit-receive antenna pair is subject to power control so that the total received power per each link is equal and normalized so that

$$P^{(n)} \sum_{l=0}^{L-1} ||h_m^{(n)}(l)||^2 = 1, n = 1, ..., N_T, m = 1, ..., N_R. \tag{6.24}$$

Fig. 6.3 presents the receiver's BER performance vs. E_s/N_0, with the number of significant multipath components $L_{eff} = 3$, while equalizer window starting position P is a parameter. Thereby, the received signal power totalled over all $L = 24$ paths was used when defining E_s/N_0. Simulations were performed until 100 frame errors are collected. The receiver with $n_0 = 1$ (antenna by antenna detection) is denoted as rec. #1 and the receiver with $n_0 = 2$ (joint antenna detection with antenna separation using MAP block) is denoted as rec. #2. For comparison, the performance of a receiver that ignores the existence of non-significant multipath components is presented as well, and is referred to as rec. #3. This receiver makes an assumption that the covariance matrix $\mathbf{R}$ of the interference-plus-noise reduces to the covariance matrix of noise only, i.e., $\sigma^2\mathbf{I}$.

As can be seen from Fig. 6.3 the minimum BER value is obtained with the parameter $P = 3$. It is also found in Fig. 6.3 that receivers #1 and #2 perform very similarly, due to the fact that snapshot #50 belongs to the D-NLOS region, where the spatial spread at the transmitter is relatively large. If the synchronism is maintained perfectly (P= 3) the performance of rec. #1 and #2 is almost the same as that of rec. #3, since most of the received signal power is concentrated in the significant portion of the channel impulse response, and the energy from the significant portion falls into the equalizer coverage. However, in cases where $P = 2$ or $P = 4$ rec. #3's performance is significantly degraded and it plateaus at a certain BER level. However, the receivers which estimate the covariance matrix (rec. #1 and rec. #2) can significantly reduce the remaining interference components and they can achieve relatively low BER values for sufficiently large E_s/N_0. Thereby, the performance sensitivity to the timing offset is significantly reduced.

6.4 Joint detection to reduce receiver sensitivity to spatial correlation

The basic assumption made in SDMA is that the channels of different transmit antenna elements are sufficiently different from each other. This, in turn, enables the MMSE-based receivers defined in Section 5.3.1 and 6.2 to separate signals coming from different transmit antennas of the SOI and suppress interference coming from

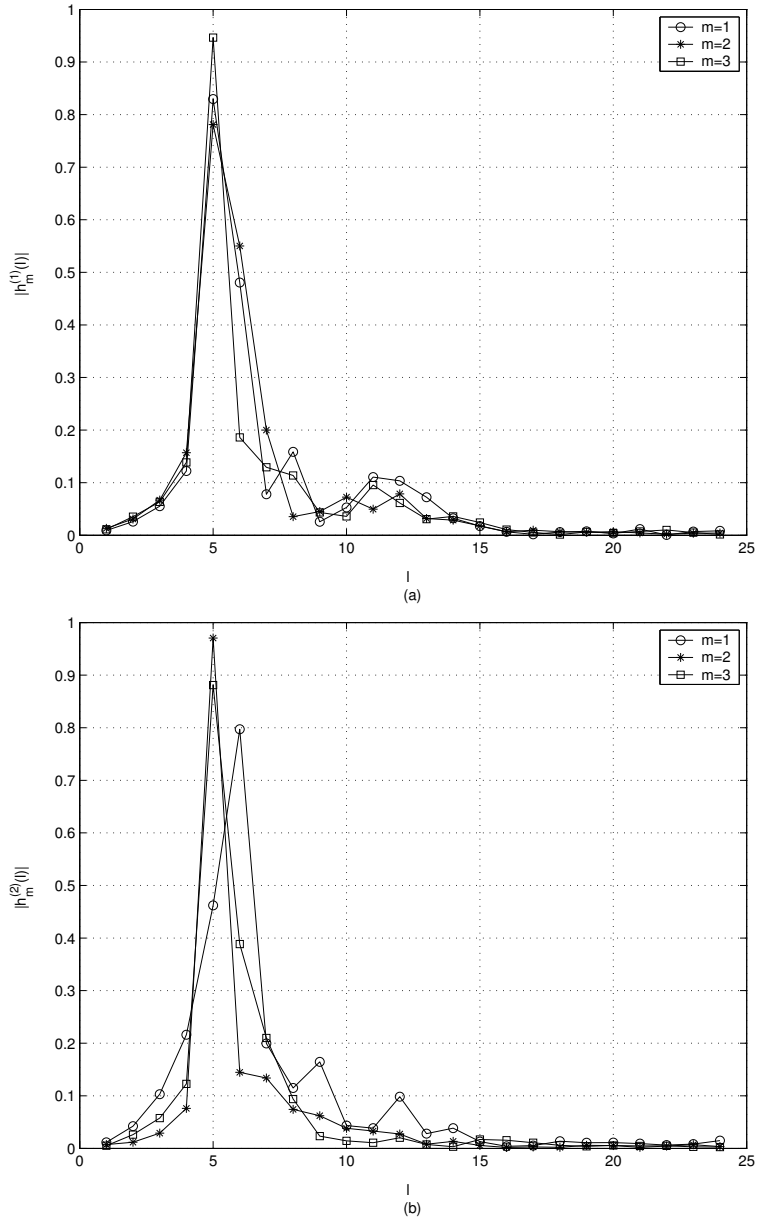

Fig. 6.2. **Symbol-spaced channel impulse responses observed after the receive filter and downsampling, snapshot #50, normalized so as to satisfy (6.24): (a) from transmit antenna #1 to the receive antennas #1, #4 and #7, (b) from transmit antenna #2 to the receive antennas #1, #4 and #7.**

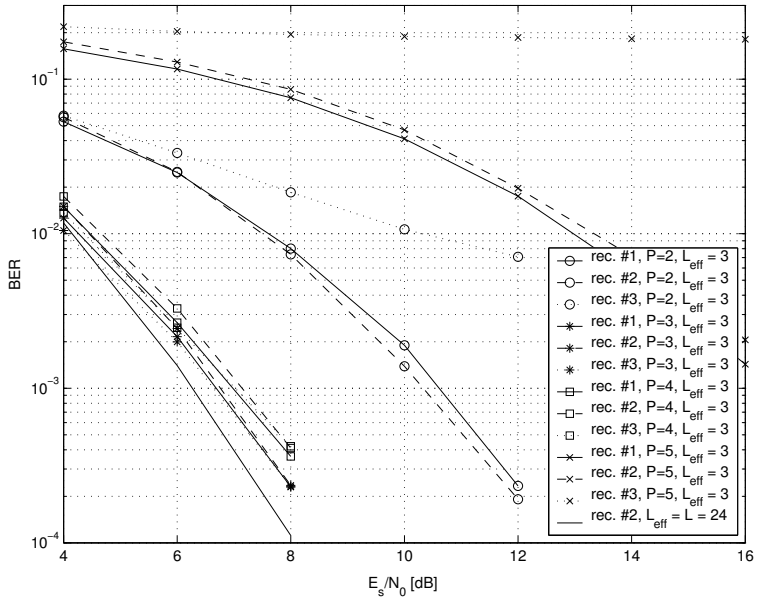

Fig. 6.3. **BER vs.** E_s/N_0**, comparison of receivers with and without covariance matrix estimation, rec.** $\#1$ **and rec.** $\#2$ **are with R estimation, rec.** $\#3$ **is without R estimation,** $(N_T, N_R) = (2, 3)$**,** $L_{eff} = 3$ **and** 24**,** $Q_{ext} = 0.5$**.**

the unwanted users. The difference between the channels of different transmit antennas depends on many factors describing the propagation environment. Some of them are antenna separation, carrier frequency, number and positions of scatterers in the vicinity of the transmitter and receiver, angles of departure, arrival of radio waves etc. In order to assess the performance of receivers in realistic environments different channel models can be used. While the common purpose of all the models is to describe different propagation conditions with a finite set of parameters, the fundamental difference between them is whether they are deterministic [274] or stochastic [272] in nature. As mentioned above, the receiver's performance in this section is evaluated directly using measurement data. The measurement data is also used to determine a spatial correlation at the transmitter, which is then used as a parameter describing different propagation environments. Note that a special correlation is specific for stochastic models. However, in this section the spatial correlation is defined in a way that best suites the receiver structure, and it is slightly different from the commonly adopted stochastic channel models based on correlation [272].

Let us denote with $\mathbf{\Pi}$ a matrix containing channel impulse responses from every transmit antenna to all receive antennas

$$\mathbf{\Pi} = [\mathbf{h}^{(1)}, ..., \mathbf{h}^{(N_T)}] \in \mathbb{C}^{LN_R \times N_T}. \tag{6.25}$$

We define correlation matrix R_{MIMO} as follows

$$\mathbf{R}_{MIMO} = \begin{bmatrix} \rho^{(1,1)} & \dots & \rho^{(1,N_T)} \\ \vdots & & \vdots \\ \rho^{(N_T,1)} & \dots & \rho^{(N_T,N_T)} \end{bmatrix} \in \mathbb{C}^{N_T \times N_T},$$

where

$$\rho^{(n_1,n_2)} = \frac{E\{\mathbf{h}^{(n_1)^H}\mathbf{h}^{(n_2)}\}}{E\{||\mathbf{h}^{(n_1)}||^2\}E\{||\mathbf{h}^{(n_2)}||^2\}} \tag{6.26}$$

denotes correlation between the vectors $\mathbf{h}^{(n_1)}$ and $\mathbf{h}^{(n_2)}$. An estimate of $\rho^{(n1,n2)}$ is obtained by using measurement data as follows

$$\rho^{(n1,n2)} = \frac{1}{S}\sum_{s=1}^{S} \frac{\mathbf{h}_s^{(n_1)^H}\mathbf{h}_s^{(n_2)}}{||\mathbf{h}_s^{(n_1)}||^2||\mathbf{h}_s^{(n_2)}||^2}, \tag{6.27}$$

where $\mathbf{h}_s^{(n_1)}$ and $\mathbf{h}_s^{(n_2)}$ denote the sth measurement snapshot which corresponds to the vectors $\mathbf{h}^{(n_1)}$ and $\mathbf{h}^{(n_2)}$, with S being the number of available snapshots corresponding to a certain propagation environment.

In Fig. 6.4 the estimate of the matrix $\mathbf{R}_{MIMO}$, obtained by replacing its elements given by (6.26) with their estimates defined by (6.27), is presented for three regions along the measurement route. The measurement route is described in Section 6. It can be concluded that the correlations between different transmit antenna elements are much higher in the LOS than in the D-NLOS and S-NLOS regions. This can be explained by the fact that in the LOS region the angular

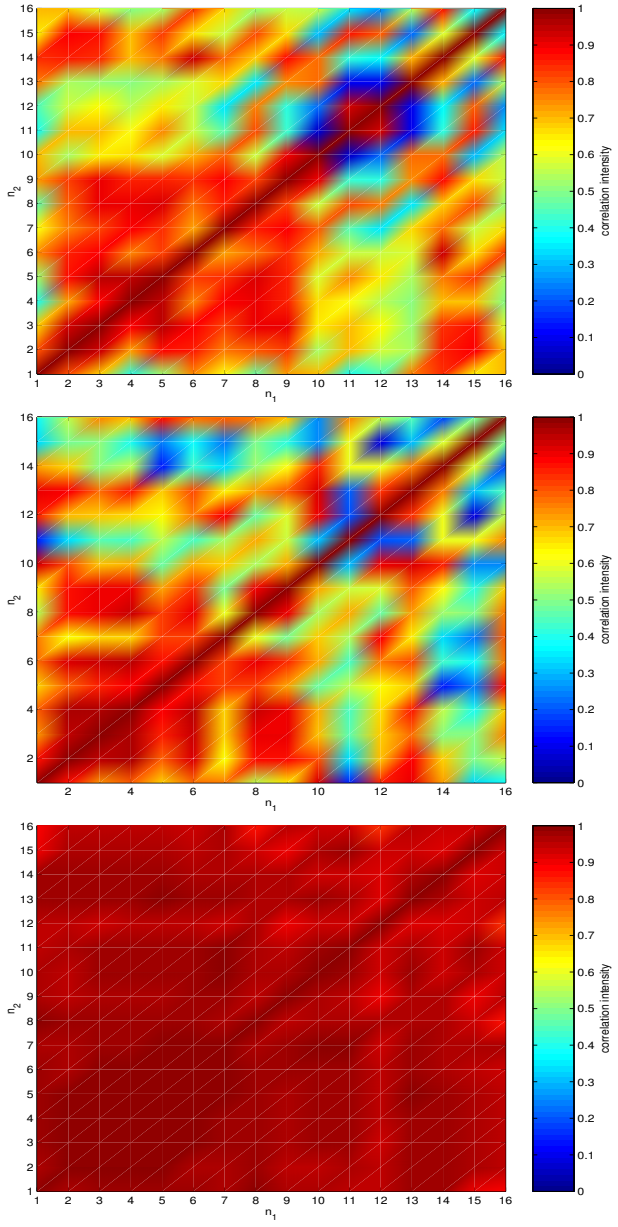

Fig. 6.4. **Absolute values of an estimate of the 16×16 matrix $\mathbf{R}_{MIMO}$ for the 16 transmit antennas and 1st receive antenna, obtained by (6.27), linear interpolation applied between adjacent values of $\mathbf{R}_{MIMO}$ values for convenience of presentation, (a) averaged over snapshots $1-15$ which correspond to the S-NLOS, (b) averaged over snapshots $22-36$ which correspond to the D-NLOS, (c) averaged over snapshots $62-76$ which correspond to LOS.**

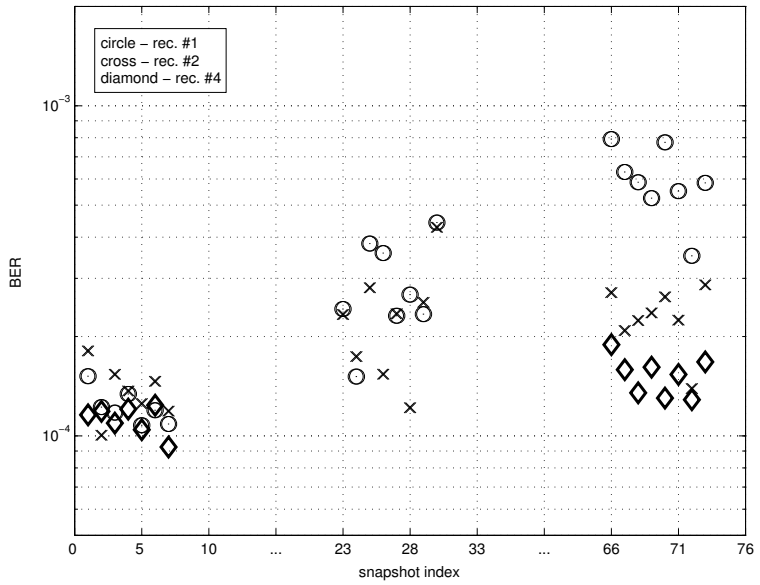

Fig. 6.5. **BER vs. snapshot index,** $(N_T, N_R) = (2, 1)$**,** $E_s/N_0 = 12dB$**,** $Q_{ext} = 0.5$**,** $L_{eff} = 11$**, transmit antennas** $\#1$ **and** $\#8$ **used, receive antenna** $\#1$ **used,** $\rho^{(1,8)} = 0.48$ **in the S-NLOS region,** $\rho^{(1,8)} = 0.56$ **in the S-NLOS region,** $\rho^{(1,8)} = 0.98$ **in the S-NLOS region (from Fig. 6.4).**

spread at the transmitter is much lower than in the D-NLOS and S-NLOS regions, which is known to have a direct impact on the antenna correlation [268].

Fig. 6.5 presents bit error rate performance vs. the measurement snapshot index. The effective number L_{eff} of multipath components is kept constant for all snapshots and chosen to be 11. The optimal timing P was determined for each snapshot separately by sliding the timing window along the channel impulse response vector and timing optimality $P = P_{opt}$ was defined such that the total received power contained in a window of length L_{eff} is maximized, as

$$P_{opt} = \arg\max_{P} \sum_{l=P}^{P+Leff-1} \sum_{m=1}^{N_R} \sum_{n=1}^{N_T} ||h_m^{(n)}(l)||^2. \tag{6.28}$$

The signal power is then controlled so that the total received power for each transmit-receive antenna pair is equal to unity for each snapshot. The antenna elements #1 and #8 of the transmit uniform circular array (UCA) and element #1 of the receive uniform linear array (ULA) were used at the transmitter and receiver sides, respectively, resulting in the radio network topology $(N_T, N_R) = (2, 1)$. Simulations for each snapshot were performed until 100 frame errors took place.

It is found in Fig. 6.5 that the performance of rec. #1 is far better in the NLOS region than in the LOS region. On the contrary, rec. #2's performance is almost constant regardless of the propagation condition. This is due to the larger spatial spread at the transmitter side in the NLOS region resulting in lower spatial correlation among the transmit antenna elements. Since receiver #1 performs spatial separation of transmit antenna elements' streams using MMSE filtering, its performance is better in the NLOS case. The superiority of receiver #2 is due to the joint detection of signals transmitted using two transmit antenna elements. Thereby, the separation of two transmit antennas' signals is performed in the MAP block itself instead of in the MMSE receiver. The improvement achieved by rec. #2 over rec. #1 is larger in the LOS region. Therefore, preserving the degrees of freedom of the MMSE receiver by joint detection is more beneficial in LOS than in NLOS regions. Note that a similar effect was observed in the multiuser scenario described in Fig. 5.19 of Section 5.3.3, where the antennas of a single user were assumed to be either totally uncorrelated or fully correlated.

For comparison the performance of the receiver defined in Section 6.2 which uses a MAP block in the same way as in Section 5.2.2 is also shown in Fig. 6.5. The receiver is denoted as rec. #4. It is shown that receiver #4 outperforms both of the previously mentioned receivers, showing very robust behavior regardless of the environment. This is due to the fact that receiver #4 separates different transmit antennas in the SfISfO decoder itself, and not in the MMSE or MAP block. The STTr code, in turn is known to be rather robust against spatial correlation.

6.5 Summary and conclusions

The performance sensitivity of the turbo equalizer for an STTr-coded system to channel impairments and receiver imperfections was studied in this chapter. First,

sensitivity to spatial correlation at the transmitter side was studied. Second, sensitivity to imperfect timing estimation was considered.

It was shown that the receiver that relies on antenna separation using MMSE criterion performs relatively well in a rich scattering environment, as can be seen from Fig. 6.5. However, in cases with relatively high antenna correlation it suffers from performance degradation. This behavior is inherent for MMSE processing which performs the separation of transmit antennas' signals by linear combining [161]. On the other hand, the receiver that performs joint antenna detection performs almost equally well in both environments and at least as good as the antenna-by-antenna based receiver. The reason for this behavior is twofold. First, ML detection is known to be robust to spatial correlation, which causes only SNR loss but not diversity loss [275]. Second, the STTr code itself is known to be robust against spatial correlation [239].

Low complexity turbo receivers that exploit only the significant portions of the channel impulse response were proposed. They are shown to perform reasonably well even with a very small portion of the CIR taken into account in the detection process. In cases of imperfect timing the receivers that take into account the interference originating from the remaining multipath components are shown to be much less sensitive to the timing offset than the receiver that simply ignores the existence of the interference. By suppressing interference the receiver can perform reasonably well in the presence of a timing offset equal to even several symbol durations, as can be seen from Fig. 6.3. This comes at the expense of an increased SNR requirement, which can be handled by appropriate power control. On the other hand, the receiver that ignores the existence of the interference becomes useless even with a slight timing offset.

7 Conclusions and future work

7.1 Summary and conclusions

Iterative (turbo) receivers for interference suppression and cancellation in channel coded CDMA and SDMA systems were studied in this thesis. The literature on non-iterative and iterative interference suppression and cancellation algorithms was reviewed in Chapter 2. A unified system model for both CDMA and SDMA was given in Chapter 3.

Chapter 4 focused on *unknown* interference suppression and cancellation algorithms in CDMA overlay systems. In the first part of Chapter 4, a linear interpolation-based iterative receiver for NBI and WBI interference cancellation in overlay situations was proposed and analyzed. A self-reconfigurable scheme for NBI and WBI cancellation is adjusted for use in an iterative (turbo) receiver with turbo codes. Interference was assumed to be a digitally modulated tone, that may have come from the same or a competing communication system. The worst case scenario of the interference bandwidth being the same as that of the SOI was considered. A single user scenario was used.

A simple theoretical performance analysis showed that the scheme has a great potential for performance improvement over the non-iterative receiver. However, it was shown that this improvement becomes significant only in large SINR regions. Since the operating SINR point in an CDMA overlay situation is usually low, the iteration gain is not significant. Moreover, a channel code's operating point usually lies in a low SINR region. Another important observation is that the iteration gain is more significant if the processing gain is smaller.

In the second part of Chapter 4 the interference is assumed to come from many interfering sources transmitting in an uncoordinated fashion. In this case a statistical model of the interference is more appropriate than the deterministic one. Therefore, Middleton's class A model was used. Worst case[1] of interference being independent between different diversity branches is considered. A problem of interference mitigation becomes equal to that of the estimation of the PDF of the interference. A new detection-decoding scheme, based on type-based detection

[1] In terms of performance.

and LogMap decoding, is proposed, which requires neither knowledge of the noise distribution nor SNR estimation prior to decoding.

A comparative simulation study of a type-based detector and optimal receivers was conducted in a turbo-coded DS-SS system with AWGN, and Middleton's class A interference. Close-to-optimal performance of the type-based detector was obtained in all kinds of interference scenarios both in static and i.i.d Rayleigh fading channels. The performance loss compared to the optimal case is within the span of 0.5 dB in a static channel and 2 dB in a Rayleigh fading channel.

The iterative receiver that uses decoder outputs to improve the interference PDF estimation was shown to outperform the non-iterative one, especially for short training sequences, thereby improving the bandwidth efficiency of the system. An important observation is that the type-based receiver was shown to be relatively robust to the number of interference sources and to their distances from the receiver.

The focus of Chapter 5 was on iterative receivers for joint multiuser detection, equalization and unknown interference suppression in SDMA. In the first part of Chapter 5 the iterative cancellation of known interference was studied, where the term 'known' denotes multiple access interference (or co-channel interference) and inter-symbol interference. An SC-MMSE-based generic iterative receiver was derived for convolutional and STTr codes. In the second part of Chapter 5 the suppression of unknown interference was considered in more detail. The term "unknown" was used to describe digitally modulated interference coming either from the neighboring cell or from the undetected users of the same cell.

It was shown that in the absence of UCCI the receivers are capable of achieving the corresponding single-user bounds both in convolutionally and STTr-coded systems. Thereby, the number of required receive antennas is equal to the number of *users* and not to the total number of *transmit antennas*. The iterative SC-MMSE receiver with STTr codes was shown to be capable of handling overloaded situations where the number of users exceeds the number of receive antennas. This result complements the results from the literature where similar findings were shown for convolutional codes.

In the presence of UCCI the performance of a conventional low-complexity SC-MMSE receiver was compared to the hybrid SC-MMSE-MAP receiver and to the SC/ML receiver. It was shown that the hybrid SC-MMSE-MAP iterative receiver can offer better performance than the low complexity SC-MMSE receiver. This can be achieved by the joint detection of signals in space and time. In channels with low frequency selectivity the SC/ML iterative receiver has a potential of preserving the receiver's DoF in the presence of UCCI. This can be achieved by more accurate modelling of UCCI and estimation of its PDF. A method for non-parametric PDF estimation was presented. It was shown that the SC/ML receiver outperforms the low complexity SC-MMSE receiver if the channel does not suffer from too severe frequency selectivity, and if the number of interferers is not too large.

Asymptotic performance analysis of the iterative receiver in an STTr-coded system shows that the impact of the UCCI on the performance is similar to that of the spatial correlation at the receiver side. That is, the diversity and coding gains achievable in a UCCI-free scenario are decreased by a factor that depends

on the rank of the interference covariance matrix.

In Chapter 6, a low complexity hybrid SC-MMSE-MAP receiver that takes into account only the most dominant components of the CIR was proposed. The performance sensitivity of a low complexity hybrid SC-MMSE-MAP turbo equalizer for an STTr-coded system to receiver imperfections and propagation environment changes was studied. In order to assess the receiver performance in a real field test, channel measurement data was used. First, sensitivity to spatial correlation at the transmitter side was studied. Second, sensitivity to imperfect timing estimation was considered.

It was shown that the conventional iterative receiver that relies on antenna separation using SC and MMSE filtering performs relatively well in a rich scattering environment. However, in cases with relatively high antenna correlation it suffers from performance degradation. On the other hand, the hybrid SC-MMSE-MAP receiver that performs joint antenna detection performs almost equally well in both environments and at least as good as the conventional SC-MMSE receiver.

The low complexity hybrid receiver was shown to perform reasonably well even with a rather small portion of the CIR taken into account in the detection process. In cases of imperfect timing the receiver that suppresses the interference originating from the remaining multipath components was shown to be much less sensitive to the timing offset than the receiver that simply ignores the existence of the interference. By suppressing interference the receiver can perform reasonably well with a timing offset equal to even several symbol durations. This comes at the expense of increased required SNR, which can be handled by appropriate power control. On the other hand, the receiver that ignores existence of the interference becomes useless even with a slight timing offset.

7.2 Future research directions

In the second part of Chapter 4, the interference model assumed independent noise observations between different diversity branches (multipaths and receive antennas). This assumption gives the worst performance in the error rate sense, and non-linear receivers which can exploit spatio-temporal dependency are of great interest. A type detection-based receiver might be capable of exploiting this additional information, but the number of training samples needed might be prohibitively large. This is due to the fact that the *joint* PDF of all interference components has to be estimated. On the other hand, kernel-smoothing techniques might offer a reasonable tradeoff between performance and complexity. The fact that the PDF-estimation based receivers are robust to the number of interference sources and their distances from the receiver can be used to handle different collision situations in WLANs, thereby reducing the need for carrier sensing. This topic deserves more study.

Further improvements of the hybrid SC-MMSE-MAP receiver would be possible based on appropriate selection algorithms, which would select significant portions of the channel impulse response in space and time based on certain optimization

criteria. That would enable us to maximize error rate performance or to maximize capacity with the available computational complexity. Another important issue to be considered is the estimation of the amount of UCCI in order to be able to predict the complexity increase due to the signal processing needed to mitigate the estimated UCCI while keeping the performance at a certain level.

A further reduction of complexity in turbo receivers can be achieved by use of adaptive filtering or FDE and it will certainly gain considerable attention in the future. Hybrid receivers with FDE and joint MAP detection in space would be an interesting future topic as well. Recent advances in the complexity reduction of ML receivers in terms of sphere decoding or minimum error rate linear receivers could be used to reduce complexity of the MAP part of the hybrid receiver and make it even more attractive for practical applications. Similarly, complexity reduction of the kernel-smoothing method presented in Chapter 5 would be possible by taking only those samples that are in the vicinity of the point for which the PDF is calculated.

Recent developments in the area of space-time coding may be used to achieve more accurate soft cancellation, which would in turn result in a less complex receiver. Iterative receiver convergence properties with different channel coding and decoding schemes as well as different channel realizations would give an important insight into the receiver requirements in order to achieve the required level of robustness. Performance evaluation of the proposed receivers in a cellular scenario is also required to determine their practical applicability. The proposed hybrid receiver offers a significant design flexibility in terms of complexity and robustness against both intra-cell and inter-cell interference. Performance evaluation in a real field test and in a multi-cell environment would be a significant step forward towards the long desired goal - a frequency reuse factor of one.

References

[1] Kay SM (1998) Fundamentals of Statistical Signal Processing: Detection Theory. Prentice-Hall, Englewood Cliffs, NJ, USA.

[2] Cover TM & Thomas JA (1991) Elements of Information Theory. John Wiley, New York, USA.

[3] Proakis JG (1995) Digital Communications. McGraw-Hill, Inc., New York, USA third edn.

[4] Middleton D (1977) Statistical-physical models of electromagnetic interference. IEEE Transactions on Electromagnetic Compatibility 19(3): p 106–127.

[5] Blackard K, Rappaport T & Bostian C (1993) Measurements and models of radio frequency impulsive noise for indoor wireless communications. IEEE Journal on Selected Areas in Communications 11(7): p 991–1001.

[6] Parsons JD (2001) The Mobile Radio Propagation Channel. John Wiley & Sons second edn.

[7] Verdu S (1998) Multiuser Detection. Cambridge University Press, Cambridge, UK.

[8] Forney GD (1972) Maximum-likelihood sequence estimation of digital sequences in the presence of intersymbol interference. IEEE Transactions on Information Theory 18(3).

[9] Forney GD (1973) The Viterbi algorithm. Proceedings of the IEEE 61(3): p 268–278.

[10] Haykin S (1989) An Introduction to Analog and Digital Communications. John Wiley and Sons, New York, USA.

[11] Talwar S, Viberg M & Paulraj A (1996) Blind separation of synchronous co-channel digital signals using an antenna array: I. Algorithms. IEEE Transactions on Signal Processing 44(5): p 1184–1197.

[12] Benveniste A & Goursat M (1984) Blind equalizers. IEEE Transactions on Communications 32(8): p 871–883.

[13] Honig M (1994) Blind adaptive interference suppression for near-far resistant CDMA. Proc. IEEE Global Telecommunications Conference (GLOBECOM), San Francisco, CA, USA, vol.1, p 379–384

[14] Wang X & Poor HV (1998) Blind equalization and multiuser detection in dispersive CDMA channels. IEEE Transactions on Communications 46(1): p 91–103.

[15] Spaulding AD & Middleton D (1977) Optimum reception in an impulsive interference environment–Part I: Coherent detection. IEEE Transactions on Communications 25: p 910–923.

[16] Wang X & Poor HV (1997) Joint channel estimation and symbol detection in rayleigh flat-fading channels with impulsive noise. IEEE Communications Letters 1(1): p 19–21.

[17] Buzzi S, Conte E, Maio AD & Lops M (2001) Optimum diversity detection over fading dispersive channels with non-Gaussian noise. IEEE Transactions on Signal Processing 49(4): p 767–775.

[18] Blum RS, Kozick RJ & Sadler BM (1999) An adaptive spatial diversity receiver for non-Gaussian interference and noise. IEEE Transactions on Signal Processing 47(8): p 2100–2111.

[19] Milstein LB (1988) Interference rejection techniques in spread spectrum communications. Proceedings of the IEEE 76(6): p 657–671.

[20] Poor HV (2001) Active interference suppression in CDMA overlay systems. IEEE Transactions on Communications 19(1): p 4–20.

[21] Gardner WA (1993) Cyclic Wiener filtering: Theory and method. IEEE Transactions on Communications 41(1): p 151–163.

[22] Winters JH (1984) Optimum combining in digital mobile radio with cochannel interference. IEEE Journal on Selected Areas in Communications 2(4): p 528–539.

[23] Paulraj A & Papadias C (1997) Space–time processing for wireless communications. IEEE Signal Processing Magazine 14(6): p 49–83.

[24] Glisic SG & et al. (1999) Performance enhancement of DSSS systems: Two-dimensional interference suppression. IEEE Transactions on Communications 47(10): p 1549–1560.

[25] Rush LA & Poor HV (1995) Multiuser detection techniques for narrowband interference suppression in spread spectrum communications. IEEE Transactions on Communications 43(2/3): p 1725–1737.

[26] Glisic S, Nikolic Z & Dimitrijevic B (1999) Adaptive self-reconfigurable interference suppression schemes for CDMA wireless networks. IEEE Transactions on Communications 47(4): p 598–607.

[27] Giallorenzi TR & Wilson SG (1996) Multiuser ML sequence estimator for convolutionally coded asynchronous DS-CDMA systems. IEEE Transactions on Communications 44(8): p 997–1007.

[28] Berrou C & Glavieux A (1996) Near optimum error correcting coding and decoding: Turbo codes. IEEE Transactions on Communications 44(10): p 1261–1271.

[29] Wang X & Poor HV (1999) Iterative (turbo) soft interference cancellation and decoding for coded CDMA. IEEE Transactions on Communications 47(7): p 1046–1061.

[30] Douillard C, Jezequel CM, Berrou C, Picart A, Didier P & Glavieux A (1995) Iterative correction of intersymbol interference: Turbo-equalisation. European Transactions on Telecommunications 6(5): p 507–511.

[31] Grant A (2000) Joint decoding and channel estimation for space-time codes. Proc. IEEE Vehicular Technology Conference (VTC), Tokyo, Japan, p 416–420.

[32] Davis LM, Collings IB & Hoeher P (2001) Joint MAP equalization and channel estimation for frequency-selective and frequency-flat fast-fading channels. IEEE Transactions on Communications 49(12): p 2106–2114.

[33] Nefedov N, Pukkila M, Visoz R & Berthet AO (2003) Iterative data detection and channel estimation for advanced TDMA Systems. IEEE Transactions on Communications 51(2): p 141–144.

[34] Loeliger HA (2004) An introduction to factor graphs. IEEE Signal Processing Magazine 21(1): p 28–41.

[35] Lee WCY (1991) Overview of cellular CDMA. IEEE Transactions on Vehicular Technology 40(2): p 291–302.

[36] Bingham JAC (1990) Multicarrier modulation for data transmission: an idea whose time has come. IEEE Communications Magazine 28(5): p 5–14 Telebit Corporation, USA.

[37] Winters JH (1998) Smart antennas for wireless systems. IEEEACM Personal Communications The Magazine of Nomadic Communications and Computing 5(1): p 23–27.

[38] Gesbert D, Bolcskei H, Gore DA & Paulraj AJ (2002) Outdoor MIMO wireless channels: models and performance prediction. IEEE Transactions on Communications 50(12): p 1926–1934.

[39] Falconer D, Ariyavisitakul S, Benyamin-Seeyar A & Eidson B (2002) Frequency domain equalization for single-carrier broadband wireless systems. IEEE Communications Magazine 40(4): p 58–66.

[40] Milstein LB & Das P (1977) Spread spectrum receiver using acoustic surface wave technology. IEEE Transactions on Communications 25(8): p 841–847.

[41] Milstein LB & Das PK (1980) An analysis of a real-time transform domain filtering digital communication system–part I: Narrowband interference rejection. IEEE Transactions on Communications 28(6): p 816–824.

[42] Milstein LB, Das PK & Gevargiz J (1982) Processing gain advantage of transform domain filtering DS spread spectrum systems. Proc. IEEE Military Communications Conference (MILCOM), p 21.2.1–21.2.4.

[43] Saulnier GI, Das P & Milstein LB (1984) Suppression of narrow-band interference in a PN spread-spectrum receiver using a CTD-based adaptive filter. IEEE Transactions on Communications 32(11): p 1227–1232.

[44] Davidovici S & Kanterakis EG (1989) Narrow-band interference rejection using real-time Fourier transforms. IEEE Transactions on Communications 37(7): p 713–722.

[45] Gevargiz J, Das PK & Milstein LB (1989) Adaptive narrow-band interference rejection in a DS spread-spectrum intercept receiver using transform domain signal-processing techniques. IEEE Transactions on Communications 37(12): p 1359–1366.

[46] Hsu FM & Giordano AA (1978) Digital whitening techniques for improving spread-spectrum communications performance in the presence of narrow-band jamming and interference. IEEE Transactions on Communications 26(2): p 209–216.

[47] Ketchum JW & Proakis JG (1982) Adaptive algorithm for estimating and suppressing narrowband interference in PN spread spectrum systems. IEEE Transactions on Communications 30(5): p 913–924.

[48] Li L & Milstein LB (1982) Rejection of narrow band interference in PN spread spectrum signals using transversal filters. IEEE Transactions on Communications COM-30(5): p 925–928.

[49] Li L & Milstein LB (1983) Rejection of pulsed CW interference in PN spread spectrum signals using complex adaptive filters. IEEE Transactions on Communications COM-31(1): p 10–20.

[50] Li L & Milstein LB (1983) Rejection of CW interference in QPSK systems using decision-feedback filters. IEEE Transactions on Communications 31(4): p 473–483.

[51] Iltis RA & Milstein LB (1984) Performance analysis of narrow-band interference rejection techniques in a DS spread-spectrum systems. IEEE Transactions on Communications 32(11): p 1169–1177.

[52] Masry E (1984) Closed form analytical results for the rejection of narrow band interference in PN spread spectrum systems–part I: Linear prediction filters. IEEE Transactions on Communications 32(8): p 888–896.

[53] Masry E (1985) Closed form analytical results for the rejection of narrow band interference in PN spread spectrum systems–part II: Linear interpolator filters. IEEE Transactions on Communications 33(1): p 10–19.

[54] Iltis RA & Milstein LB (1985) An approximate statistical analysis of the Widrow LMS algorithm with application to narrow-band interference rejection. IEEE Transactions on Communications 33(2): p 121–130.

[55] Masry E & Milstein LB (1986) Performance of DS spread-spectrum receiver employing interference-suppression filters under a worst-case jamming condition. IEEE Transactions on Communications 34(1): p 13–21.

[56] Bershad NJ (1988) Error probabilities of DS spread-spectrum systems using an ALE for narrow-band interference rejection. IEEE Transactions on Communications 36(5): p 587–595.

[57] Laster JD & Reed JH (1997) Interference rejection in digital wireless communications. IEEE Signal Processing Magazine 14(3): p 37–62.

[58] Theodosidis S & et al. (1989) Interference rejection in PN spread-spectrum systems with LS linear-phase FIR filters. IEEE Transactions on Communications 37(9): p 991–994.

[59] Kalidis P & Prabhu KMM (1995) Improved LMS adaptive algorithm for narrowband interference suppression in direct-sequence spread-spectrum. IEEE Transactions on Aerospace and Electronic Systems 31: p 1198–1201.

[60] Ansari I & Viswanathan R (1994) Performance study of maximum likelihood receivers and transversal filters for the detection of direct-sequence spread-spectrum signal in narrowband interference. IEEE Transactions on Communications 42(2/3/4): p 1939–1946.

[61] Ansari A & Viswanathan R (1995) On SNR as a measure of performance for narrowband interference rejection in direct sequence spread spectrum. IEEE Transactions on Communications 43(2/3/4): p 1318–1322.

[62] Soderstrand MA & et al. (1997) Suppression of multiple narrow-band interference using real-time adaptive notch filters. IEEE Transactions on Circuits and Systems Part II Analog and Digital Signal Processing 44: p 217–225.

[63] Amin MG, Wang CS & Lindsey AR (1999) Optimum interference excision in spread spectrum communications using open-loop adaptive filters. IEEE Transactions on Signal Processing 47: p 1966–1976.

[64] Nagaraj S & et al. (2000) Adaptive interference suppression for CDMA systems with a worst-case error criterion. IEEE Transactions on Signal Processing 48: p 284–289.

[65] Kosminchuk BW & Sheikh AUH (1995) A Kalman filter-based architecture for interference excision. IEEE Transactions on Communications 43(2/3/4): p 574–580.

[66] Vijayan R & Poor HV (1990) Nonlinear techniques for interference suppression in spread-sprectrum systems. IEEE Transactions on Communications 37: p 1060–1065.

[67] Garth L & Poor HV (1992) Narrowband interference suppression in impulsive channels. IEEE Transactions on Aerospace and Electronic Systems 28(1): p 15–34.

[68] Dukic ML, Stojanovic ZD & Stojanovic IS (1990) Performance of direct-sequence spread-spectrum receiver using decision feedback and transversal filters for combating narrow-band interference. IEEE Journal on Selected Areas in Communications 8: p 907–914.

[69] Bijjani R & Das PK (1990) Rejection of narrowband interference in PN spread-spectrum systems using neural networks. Proc. IEEE Global Telecommunications Conference (GLOBECOM), San Diego, CA, USA, vol.2, p 1037–1041.

[70] Hasan MA, Lee JC & Bhargava VK (1994) A narrowband interference canceller with adjustable center weight. IEEE Transactions on Communications 42(2/3/4): p 877–880.

[71] Poor HV & Wang X (1997) Code-aided interference suppression for DS/CDMA communications - part I: Interference suppression capability. IEEE Transactions on Communications 45(9).

[72] Buzzi S, Lops M & Tulino AM (2001) A new family of MMSE multiuser receivers for interference suppression in DS/CDMA systems employing BPSK modulation. IEEE Transactions on Communications 49(1): p 154–167.

[73] Gerstacker H, Schober R & Lampe A (2003) Receivers with widely linear processing for frequency-selective channels. IEEE Transactions on Communications 51(9): p 1512–1523.

[74] Gelli G, Paura L & Tulino AM (1998) Cyclostationarity-based filtering for narrowband interference suppression in direct-sequence spread-spectrum systems. IEEE Journal on Selected Areas in Communications 16: p 1747–1755.

[75] Lops M, Ricci G & Tulino AM (1998) Narrow-band-interference suppression in multiuser CDMA systems. IEEE Transactions on Communications 46(9): p 1163–1175.

[76] Verdú S (1989) Computational complexity of optimum multiuser detection. Algorithmica 4(3): p 303–312.

[77] Rusch LA & Poor HV (1994) Narrowband interference suppression in CDMA spread spectrum communications. IEEE Transactions on Communications 42(2/3/4): p 1769–1779.

[78] Poor HV & Rusch LA (1994) A promising multiplexing technology for cellular telecommunications: Narrowband interference suppression in spread spectrum CDMA. IEEEACM Personal Communications The Magazine of Nomadic Communications and Computing 1(3): p 14.

[79] Lupas R & Verdú S (1990) Near-far resistance of multiuser detectors in asynchronous channels. IEEE Transactions on Communications 38(4): p 496–508.

[80] Juntti M (1997) Multiuser Demodulation for DS-CDMA Systems in Fading Channels. vol C106 of Acta Universitatis Ouluensis, Doctoral thesis University of Oulu Press, Oulu, Finland.

[81] Latva-aho M (1998) Advanced Receivers for Wideband CDMA Systems. vol C125 of Acta Universitatis Ouluensis, Doctoral thesis University of Oulu Press, Oulu, Finland.

[82] Hasegawa F, Luo J, Pattipati KR, Willett P & Pham D (2004) Speed and accuracy comparison of techniques for multiuser detection in synchronous CDMA. IEEE Transactions on Communications 52(4): p 540–545.

[83] Juntti MJ, Schlösser T & Lilleberg JO (1997) Genetic algorithms for multiuser detection in synchronous CDMA. Proc. IEEE International Symposium on Information Theory (ISIT), Ulm, Germany, p 492.

[84] Ergün C & Hacioglu K (2000) Multiuser detection using a genetic algorithm in CDMA communications systems. IEEE Transactions on Communications 48(8): p 1374–1383.

[85] Abedi S & Tafazolli R (2002) Genetically modified multiuser detection for code division multiple access systems. IEEE Journal on Selected Areas in Communications 20: p 463–473.

[86] Punskaya E, Andrieu C, Doucet A & Fitzgerald WJ (2001) Particle filtering for multiuser detection in fading CDMA channels. Proc. Signal Processing Workshop on Statistical Signal Processing (SPWSSP), Singapore, p 38–41.

[87] Djuric PM, Kotecha JH, Jianqui Z, Yufei H, Ghirmai T, Bugallo M & Miguez J (2003) Particle filtering. IEEE Signal Processing Magazine 20(5): p 19–38.

[88] Luo J, Pattipati KR, Willett PK & Hasegawa F (2001) Near-optimal multiuser detection in synchronous CDMA using probabilistic data association. IEEE Communications Letters 5(9): p 361–363.

[89] Pham D, Pattipati KR, Willett PK & Luo J (2004) A generalized probabilistic data association detector for multiple antenna systems. IEEE Communications Letters 8(4): p 205–207.

[90] Wijting CS, Ojanperä T, Juntti MJ, Kansanen K & Prasad R (1999) Groupwise serial multiuser detectors for multirate DS-CDMA. Proc. IEEE Vehicular Technology Conference (VTC), Houston, TX, vol.1, p 836–840.

[91] Varanasi MK & Aazhang B (1990) Multistage detection in asynchronous code-division multiple-access communications. IEEE Transactions on Communications 38(4): p 509–519.

[92] Duel-Hallen A (1992) Equalizers for multiple input/multiple output channels and PAM systems with cyclostationary input sequences. IEEE Journal on Selected Areas in Communications 10(3).

[93] Nelson LB & Poor HV (1994) Soft-decision interference cancellation for AWGN multi-user channels. Proc. IEEE International Symposium on Information Theory, Trondheim, Norway, p 134.

[94] Glisic SG, Nikolic ZB, Dimitrijevic B & Woodward GK (2000) Multilayer LMS interference suppression algorithms for CDMA wireless networks. IEEE Transactions on Communications 48(8): p 1413–1422.

[95] Henttu P (2003) Blind Interference Suppression in FH/DS Communication System. Acta Universitatis Ouluensis, Licentiate thesis University of Oulu, Oulu, Finland.

[96] Rifkin A (1991) Narrow-band interference rejection using real-time Fourier transforms - comment. IEEE Transactions on Communications 39(9): p 1292–1294.

[97] Saulnier GJ (1992) Suppression of narrowband jammers in a spread-spectrum receiver using transform-domain adaptive filtering. IEEE Journal on Selected Areas in Communications 10: p 742–749.

[98] Sandberg SD (1995) Adapted demodulation for spread-spectrum receivers which employ transform-domain interference rejection. IEEE Transactions on Communications 43(9): p 2502–2510.

[99] Medley M, Saulnier G & Das P (1994) Applications of the wavelet transform in spread spectrum communications systems. Proc. SPIE International Symposium on Optics, Imaging and Instrumentation (ISOII), Princeton, NJ, vol.2242, Wavelet Applications, p 54–68.

[100] Yang WM & Bi GG (1997) Adaptive wavelet packet transform-based narrowband interference canceller in DSSS systems. IEE Electronics Letters 33(14): p 1189–1190.

[101] Medley MJ, Saulnier GJ & Das PK (1997) Narrow-band interference excision in spread spectrum systems using lapped transforms. IEEE Transactions on Communications 45(11): p 1444–1455.

[102] Sandberg SD & et al. (1995) Some alternatives in transform-domain suppression of narrow-band interference for signal detection and demodulation. IEEE Transactions on Communications 43(12): p 3025–3036.

[103] Li CN, Hu GR & Liu MJ (2000) Narrow-band interference excision in spread-spectrum systems using self-orthogonalizing transform-domain adaptive filters. IEEE Journal on Selected Areas in Communications 18: p 403–406.

[104] Narayanan KR & Doherty JF (1997) A convex projections method for improved narrow-band interference rejection in direct-sequence spread-spectrum systems. IEEE Transactions on Communications 45(7): p 772–774.

[105] Schlegel C, Roy S, Alexander PD & Xiang ZJ (1996) Multiuser projection receivers. IEEE Journal on Selected Areas in Communications 14(8): p 1610–1618.

[106] Wang X & Poor HV (1998) Blind multiuser detection: A subspace approach. IEEE Transactions on Information Theory 44(2): p 677–690.

[107] Buzzi S & Poor HV (2002) A single-antenna blind receiver for multiuser detection in unknown correlated noise. IEEE Transactions on Vehicular Technology 51(1): p 209–215.

[108] Lops M & Tulino A (1999) Automatic suppression of narrow-band interference in direct-sequence spread-spectrum systems. IEEE Transactions on Communications 47(8): p 1133–1136.

[109] Fathallah H & Rusch LA (1997) A subspace approach to adaptive narrow-band interference suppression in DSSS. IEEE Transactions on Communications 45(12): p 1575–1585.

[110] Ranheim A (1995) Narrowband interference rejection in direct-sequence spread-spectrum system using time-frequency decomposition. IEE Proceedings 142: p 393–400.

[111] Krishnamurthy V & Logothetis A (1999) Adaptive nonlinear filters for narrow-band interference suppression in spread-spectrum CDMA systems. IEEE Transactions on Communications 47(5): p 742–753.

[112] Carlemalm C, Poor HV & Logothetis A (2000) Suppression of multiple narrowband interferers in a spread-spectrum communication system. IEEE Journal on Selected Areas in Communications 18(8): p 1365–1374.

[113] Nelson LB & Poor HV (1995) Iterative multi-user detection in the synchronous CDMA channel: An EM-based approach. IEEE Transactions on Communications 44(12): p 1700–1710.

[114] Monzingo RA & Miller TW (1980) Introduction to Adaptive Arrays. John Wiley & Sons.

[115] Telatar IE (1995) Capacity of multi-antenna Gaussian channels. Tech. rep. Bell Laboratories Internal Tech.Memo, pp. 1–28.

[116] Telatar E (1999) Capacity of multi-antenna Gaussian channels. European Transactions on Telecommunications 10(6): p 585–595.

[117] Winters JH, Salz J & Gitlin RD (1994) The impact of antenna diversity on the capacity of wireless communication systems. IEEE Transactions on Communications 42(2/3/4).

[118] Foschini G (1996) Layered space–time architecture for wireless communication in a fading environment when using multi-element antennas. Bell Labs Technical Journal 1: p 41–59.

[119] Tarokh V, Seshadri N & Calderbank AR (1998) Space-time codes for high data rate wireless communication: Performance criterion and code construction. IEEE Transactions on Information Theory 44(2): p 744–765.

[120] Alamouti SM (1998) A simple transmit diversity technique for wireless communications. IEEE Journal on Selected Areas in Communications 16(8): p 1451–1458.

[121] Haimovich AM & Shah A (1997) On spatial and temporal processing for CDMA overlay situations. Proc. IEEE Workshop on Signal Processing Advances in Wireless Communications (SPAWC), Paris, France, p 365–368.

[122] Shah A & Haimovich AM (1997) Performance of space-time receiver architecture for CDMA overlay of narrowband waveforms for personal communication systems. Proc. IEEE International Conference on Communications (ICC), Montreal, Canada, p 314–318.

[123] Klang G, Astely D & Ottersten B (1999) Structured spatio-temporal interference rejection with antenna arrays. Proc. IEEE Vehicular Technology Conference (VTC), Houston, TX, USA, vol.1, p 841–845.

[124] Astely D & Ottersten B (1999) Constrained complexity spatio-temporal interference rejection combining. Proc. IEEE Workshop on Signal Processing Advances in Wireless Communications (SPAWC), Annapolis, MD, USA, p 110–113.

[125] Astely D & Artamo A (2001) Uplink spatio-temporal interference rejection combining for WCDMA. Proc. IEEE Workshop on Signal Processing Advances in Wireless Communications (SPAWC), Taoyuan, Taiwan, vol.1, p 326–329.

[126] Chang R & Hancock J (1966) On receiver structures for channels having memory. IEEE Transactions on Information Theory 12(4): p 463–468.

[127] Abend K & Fritchman BD (1970) Statistical detection for communications channels with intersymbol interference. Proceedings of the IEEE p 779–785.

[128] Bahl LR, Cocke J, Jelinek F & Raviv J (1974) Optimal decoding of linear codes for minimizing symbol error rate. IEEE Transactions on Information Theory 20(2): p 284–287.

[129] Lucky RW (1965) Automatic equalization for digital communications. Bell Systems Technical Journal 45: p 255–286.

[130] Monsen P (1984) MMSE equalization of interference on fading diversity channels. IEEE Transactions on Communications 32(1): p 5–12.

[131] George D, Bowen R & Storey J (1971) An adaptive decision feedback equalizer. IEEE Transactions on Communications 19(3): p 281–293.

[132] Salz J (1973) Optimum mean-square decision feedback equalization. Bell Systems Technical Journal 52: p 1341–1373.

[133] Qureshi S (1985) Adaptive equalization. Proceedings of the IEEE 73(9): p 1349–1387.

[134] Hooli K (2003) Equalization in WCDMA Terminals. vol C192 of Acta Universitatis Ouluensis, Doctoral thesis University of Oulu Press, Oulu, Finland.

[135] Clark M (1998) Adaptive frequency-domain equalization and diversity combining for broadband wireless communications. IEEE Journal on Selected Areas in Communications 16(8): p 1385–1395.

[136] Dhahir NA (2001) Single-carrier frequency-domain equalization for space-time-coded transmissions over broadband wireless channels. Proc. IEEE International Symposium on Personal, Indoor and Mobile Radio Communications (PIMRC), p 143–146.

[137] Falconer D & Ariyavisitakul SL (2002) Broadband wireless using single carrier and frequency domain equalization. Proc. International Symposium on Wireless Personal and Multimedia Communications (ISWPMC), Honolulu, Hawaii, vol.1, p 27–36.

[138] Klein A, Kaleh GK & Baier PW (1996) Zero forcing and minimum mean-square-error equalization for multiuser detection in code-division multiple access channels. IEEE Transactions on Vehicular Technology 45(2): p 276–287.

[139] Petersen BR & Falconer DD (1991) Minimum mean square equalization in cyclostationary and stationary interference - analysis and subscriber line calculations. IEEE Journal on Selected Areas in Communications 9(6): p 931–940.

[140] Petersen BR & Falconer DD (1994) Suppression of adjacent-channel, cochannel, and intersymbol interference by equalizers and linear combiners. IEEE Transactions on Communications 42(12): p 3109–3118.

[141] Lo NWK, Falconer DD & Sheikh AUH (1995) Adaptive equalization for co-channel interference in a multipath fading environment. IEEE Transactions on Communications 43(2/3/4): p 1441–1453.

[142] Ginesi A, Vitetta GM & Falconer DD (1999) Block channel equalization in the presence of a cochannel interferent signal. IEEE Journal on Selected Areas in Communications 17(11): p 1853–1862.

[143] Balaban P & Salz J (1991) Dual diversity combining and equalization in digital cellular mobile radio. IEEE Transactions on Vehicular Technology 40(2): p 342–354.

[144] Balaban P & Salz J (1992) Optimum diversity combining and equalization in digital data transmission with applications to cellular mobile radio–Part I: Theoretical considerations. IEEE Transactions on Communications 40(5).

[145] Balaban P & Salz J (1992) Optimum diversity combining and equalization in digital data transmission with applications to cellular mobile radio–Part II: Numerical results. IEEE Transactions on Communications 40(5).

[146] Tseng SH (1995) Optimum diversity combining and equalization over interference-limited cellular radio channel. IEEE Transactions on Vehicular Technology 47(1): p 103–118.

[147] Thomas TA & Zoltowski MD (1997) Nonparametric interference cancellation and equalization for narrowband TDMA communications via space-time processing. Proc. IEEE Workshop on Signal Processing Advances in Wireless Communications (SPAWC), Paris, France, p 185–188.

[148] Ariyavisitakul SL, Winters JH & Lee I (1999) Optimum space-time processors with dispersive interference: Unified analysis and required filter span. IEEE Transactions on Communications 47(7): p 1073–1083.

[149] Ariyavisitakul SL, Winters JH & Sollenberger NR (2000) Joint equalization and interference suppression for high data rate wireless systems. IEEE Journal on Selected Areas in Communications 18(7): p 1214–1220.

[150] Liang JW, Chen JT & Paulraj AJ (1997) A two-stage hybrid approach for CCI/ISI reduction with space-time processing. IEEE Communications Letters 1(6): p 163–165.

[151] Leou ML, Yeh CC & Li HJ (2000) A novel hybrid of adaptive array and equalizer for mobile communications. IEEE Transactions on Vehicular Technology 49(1): p 1–10.

[152] Lagunas MA, Vidal J & Neira AI (2000) Joint array combining and MLSE for single-user receivers in multipath Gaussian multiuser channels. IEEE Journal on Selected Areas in Communications 18(11): p 2252–2259.

[153] Grant SJ & Cavers JK (2000) Further analytical results on the joint detection of cochannel signals using diversity arrays. IEEE Transactions on Communications 48(11): p 1788–1792.

[154] Zelst AV, Nee RV & Awater G (2000) Space division multiplexing (SDM) for OFDM systems. Proc. IEEE Vehicular Technology Conference (VTC), Tokio, Japan vol.2, p 1070–1074.

[155] Nee RV, Zelst AV & Awater G (2000) Maximum likelihood decoding in a space division multiplexing system. Proc. IEEE Vehicular Technology Conference (VTC), Tokyo, Japan, p 6–10.

[156] Speth M, Senst A & Meyr H (1999) Low complexity space-frequency MLSE for multi-user COFDM. Proc. IEEE Global Telecommunications Conference (GLOBECOM), Rio de Janeiro, Brazil, vol.1, p 2395–2399.

[157] Zhu X & Murch RD (2002) Performance analysis of maximum likelihood detection in a MIMO antenna system. IEEE Transactions on Communications 50(2): p 187–191.

[158] Li X, Huang H, Lozano A & Foshini GJ (2000) Reduced-complexity detection algorithms for systems using multi-element arays. Proc. IEEE Global Telecommunications Conference (GLOBECOM), San Francisco, USA, p 1072–1076.

[159] de Lamare RC & Sampaio-Neto R (2003) Adaptive MBER decision feedback multiuser receivers in frequency selective fading channels. IEEE Communications Letters 7(2): p 73–75.

[160] Yeh CC & Barry JR (2000) Adaptive minimum bit-error rate equalization for binary signalling. IEEE Transactions on Communications 48(7): p 1226–1235.

[161] Gesbert D (2003) Robust linear MIMO receivers: A minimum error-rate approach. IEEE Transactions on Signal Processing 51(11): p 2863–2871.

[162] Mulgrew B & Chen S (2001) Adaptive minimum-BER decision feedback equalizers for binary signalling. EURASIP Journal on Applied Signal Processing 81(7): p 1479–1489.

[163] Siu S, Gibson GJ & Cowan CFN (1990) Decision feedback equalisation using neural network structures and performance comparison with standard architecture. IEE Proceedings 137(4): p 221–225.

[164] Chen S, Gibson G & Cowan C (1990) Adaptive channel equalisation using a polynomial-perceptron structure. IEE Proceedings 137(5): p 257–264.

[165] Chen S, Mulgrew B & McLaughlin S (1993) Adaptive Bayesian equalizer with decision feedback. IEEE Transactions on Signal Processing 41(9): p 2918–2927.

[166] Chen S, Mulgrew B & Grant PM (1993) A clustering technique for digital communications channel equalization using radial basis function networks. IEEE Transactions on Neural Networks 4(4): p 570–590.

[167] Mulgrew B (1996) Applying radial basis functions. IEEE Signal Processing Magazine 13(2): p 50–65.

[168] Chen S, McLaughlin S, Mulgrew B & Grant PM (1996) Bayesian decision-feedback equalizer for overcoming co-channel interference. IEE Proceedings 143(4): p 219–225.

[169] Sebald DJ & Bucklew JA (2000) Support vector machine techniques for nonlinear equalization. IEEE Transactions on Signal Processing 148(11): p 3217–3226.

[170] Robler JF & Huber JB (2003) Matched-filter based iterative soft decision interference cancellation employing the distribution of interference. Proc. IEEE Vehicular Technology Conference (VTC), vol.3, p 1619–1623.

[171] Robler JF & Huber JB (2003) Matched filter for transmission over channels with ISI employing the distribution of interference. Proc. IEEE Vehicular Technology Conference (VTC), vol.4, p 2648–2652.

[172] Luschi C & Mulgrew B (2003) Nonparametric trellis equalization in the presence of non-Gaussian interference. IEEE Transactions on Communications 51(2): p 229–239.

[173] Middleton D (1967) A statistical theory of reverberation and similar first-order scattered fields - Part I: Waveforms and the general process. IEEE Transactions on Information Theory IT-13: p 372–392.

[174] Middleton D (1967) A statistical theory of reverberation and similar first-order scattered fields - Part II: Moments, spectra, and special distributions. IEEE Transactions on Information Theory IT-13: p 393–413.

[175] Middleton D (1987) Second order non-Gaussian probability distributions and their applications to 'classical' nonlinear processing problems in communication theory. Proc. Conference on Information Sciences and Systems (CISS), Baltimore, MD, p 393–400.

[176] McDonald KF & Blum RS (2000) A statistical and physical mechanisms-based interference and noise model for array observations. IEEE Transactions on Signal Processing 48(7): p 2044–2056.

[177] Delaney PA (1995) Signal detection in multivariate class-A interference. IEEE Transactions on Communications 43(2/3/4): p 365–373.

[178] Spaulding AD & Middleton D (1977) Optimum reception in an impulsive interference environment. IEEE Transactions on Communications 25(9): p 910–923.

[179] Vastola K (1984) Treshold detection in narrowband non-Gaussian noise. IEEE Transactions on Communications 32(2).

[180] Kassam S (1988) Signal Detection in Non-Gaussian Noise. Springer-Verlag, New York.

[181] Poor HV (1988) An Introduction to Signal Detection and Estimation. Springer-Verlag, New York.

[182] Aazhang B & Poor HV (1987) Performance of DS/SSMA communications in impulsive channels–Part I: Linear correlation receivers. IEEE Transactions on Communications 35(11): p 1179–1188.

[183] Aazhang B & Poor HV (1988) Performance of DS/SSMA communications in impulsive channels–Part II: Hard limiting correlation receivers. IEEE Transactions on Communications 36(1): p 88–97.

[184] Zhang Y & Blum R (2000) An adaptive receiver with an antenna array for channels with correlated non-Gaussian interference and noise using the SAGE algorithm. IEEE Transactions on Signal Processing 48(4): p 2172–2175.

[185] Dempster AP, Laird NM & Rubin DB (1977) Maximum likelihood from incomplete data via the EM algorithm. Journal of Royal Statistical Society 39(1): p 1–38.

[186] Fessler J & Hero A (1994) Space-alternating generalized expectation-maximization algorithm. IEEE Transactions on Signal Processing 42(10): p 2664–2677.

[187] Wang X & Poor HV (1998) Robust adaptive array for wireless communications. IEEE Transactions on Communications 16: p 1352–1366.

[188] Nikias CL & Shao M (1995) Signal Processing with Alpha-Stable Distributions and Applications. John Wiley & Sons.

[189] Swami A & Sadler B (1998) Parameter estimation for linear alpha-stable processes. IEEE Signal Processing Letters 5(2): p 48–50.

[190] Conte E, Bisceglie MD, Longo M & Lops M (1995) Canonical detection in spherically invariant noise. IEEE Transactions on Communications 43(2/3/4): p 347–353.

[191] Gutman M (1989) Asymptotically optimal classification for multiple tests with empirically observed statistics. IEEE Transactions on Information Theory 35(2): p 401–408.

[192] Johnson DH, Lee YK, Kelly OE & Pistole JL (1996) Type-based detection for unknown channels. Proc. IEEE International Conference on Acoustics, Speech, and Signal Processing (ICASSP), Atlanta, GA, vol.5, p 2475–2478.

[193] Yue L & Johnson DH (1998) Universal classification for CDMA communications : Single-user receivers and multi-user receivers. Proc. IEEE International Conference on Communications (ICC), Atlanta, USA, vol.2, p 748–752.

[194] Yue L & Johnson DH (1998) Signal detection on wireless CDMA downlink. Proc. IEEE Vehicular Technology Conference (VTC), Ontario, Canada vol.2, p 2522–2526.

[195] Stolpman VJ & Orsak GC (1999) Type-based receiver for wideband CDMA. Proc. IEEE Wireless Communications and Networking Conference (WCNC), New Orleans, US vol.3, p 1470–1474.

[196] Silverman BW (1986) Density Estimation for Statistics and Data Analysis. Chapman and Hall, New York, USA.

[197] Hwang JN, Lay SR & Lippman A (1994) Nonparametric multivariate density estimation: A comparative study. IEEE Transactions on Signal Processing 42(10): p 2795–2810.

[198] Hagenauer J (1996) Forward error correcting for CDMA systems. Proc. IEEE International Symposium on Spread Spectrum Techniques and Applications (ISSSTA), Mainz, Germany, vol.2, p 566–569.

[199] Benedetto S, Divsalar D, Montorsi G & Pollara F (1998) Serial concatenation of interleaved codes: Performance analysis, design, and iterative decoding. IEEE Transactions on Information Theory 44: p 909–926.

[200] Reed MC & Alexander PD (1999) Iterative multiuser detection using antenna arrays and FEC on multipath channels. IEEE Journal on Selected Areas in Communications 17(12): p 2082–2089.

[201] Wong CH, Yeap BL & Hanzo L (2000) Wideband burst-by-burst modulation with turbo equalization and iterative channel estimation. Proc. IEEE Vehicular Technology Conference (VTC), Tokyo, Japan.

[202] Thomas J & Geraniotis E (1999) Narrowband jammer suppression in coded DS/CDMA channels. Proc. IEEE Military Communications Conference (MILCOM), Atlantic City, NJ, USA, vol.2, p 831–835.

[203] Wang J & Geraniotis E (2000) Narrow-band interference suppression in spread spectrum communication with iterative decoding. Proc. IEEE International Symposium on Spread Spectrum Techniques and Applications (ISSSTA), New Jersey, USA vol.1, p 98–101.

[204] Narayanan KR & Stber GL (1999) A serial concatenation approach to iterative demodulation and decoding. IEEE Transactions on Communications 47(7): p 956–961.

[205] Tulino AM, Biglieri EM & Glisic S (2000) Iterative interference suppression and decoding in DS/FH spread-spectrum systems. IEICE Transactions on Communications E83-B(8): p 1591–1601.

[206] Jordan MA & Nichols RA (1998) The effects of channel characteristics on turbo code performance. Proc. IEEE Military Communications Conference (MILCOM), Boston, MA, USA, vol.1, p 17–21.

[207] Summers TA & Wilson SG (1998) SNR mismatch and online estimation in turbo decoding. IEEE Transactions on Communications 46(4): p 421–423.

[208] Valenti MC & Woerner BD (1998) Performance of turbo codes in interleaved flat fading channels with estimated channel state information. Proc. IEEE Vehicular Technology Conference (VTC), Ottawa, Canada vol.1, p 66–70.

[209] Frenger P (1999) Turbo decoding on Rayleigh fading channels with noisy channel estimates. Proc. IEEE Vehicular Technology Conference (VTC), Houston, TX USA vol.2, p 884–888.

[210] Reed MC & Asenstorfer J (1997) A novel variance estimator for turbo-code decoding. Proc. International Conferenece on Telecommunications (ICT), Melbourne, Australia, p 173–178.

[211] Worm A, Hoeher P & Wehn N (2000) Turbo-decoding without SNR estimation. IEEE Communications Letters 4(6): p 193–195.

[212] Summers TA & Wilson SG (1998) Turbo code performance in heavy-tailed noise. Proc. Conference on Information Sciences and Systems (CISS), Princeton, NJ, USA vol.1, p 495–500.

[213] Huang X & Phamdo N (1998) Turbo decoders that adapt to noise distribution mismatch. IEEE Communications Letters 2(12): p 321–323.

[214] Wei L, Li Z, James MR & Petersen IR (2000) A minimax robust decoding algorithm. IEEE Transactions on Information Theory 46(4): p 1158–1167.

[215] Faber T, Scholand T & Jung P (2003) Turbo decoding in impulsive noise environments. IEE Electronics Letters 39(14): p 1069–1071.

[216] Li Y & Li KH (2000) Iterative PDF estimation and decoding for CDMA systems with non-Gaussian characterisation. IEE Electronics Letters 36(8): p 730–731.

[217] Reed MC, Schelegel CB, Alexander PD & Asenstorfer JA (1998) Iterative multiuser detection for CDMA with FEC: Near-single-user performance. IEEE Transactions on Communications 46(12): p 1693–1699.

[218] Reynolds D & Wang X (2000) Low-complexity turbo-equalization for diversity channels. Signal Processing Elsevier Science Publishers 81(5): p 989–995.

[219] Tuchler M, Koetter R & Singer A (2000) Iterative correction of ISI via equalization and decoding with priors. Proc. IEEE International Symposium on Information Theory (ISIT), Sorento, Italy, p 100.

[220] Tüchler M & Hagenauer J (2001) Linear time and frequency domain turbo equalisation. Proc. IEEE Vehicular Technology Conference (VTC), Rhodes,Greece, vol.4, p 2773–2777.

[221] Tüchler M, Koetter R & Singer AC (2002) Turbo equalisation: Principles and new results. IEEE Transactions on Communications 50(5): p 754–767.

[222] Tüchler M, Singer AC & Koetter R (2002) Minimum mean squared error equalisation using a priori information. IEEE Transactions on Signal Processing 50(3): p 673–683.

[223] Abe T & Matsumoto T (2003) Space-time turbo equalization in frequency-selective MIMO channels. IEEE Transactions on Vehicular Technology 52(3): p 469–475.

[224] Abe T, Tomisato S & Matsumoto T (2003) A MIMO turbo equaliser for frequency selective channels with unknown interference. IEEE Transactions on Vehicular Technology 52(3): p 476–482.

[225] Abe T & Matsumoto T (2001) Space-time turbo detection in frequency selective MIMO channels with unknown interference. Proc. IEEE International Symposium on Wireless Personal Mobile Communications (ISWPMC), Aalborg, Denmark.

[226] Reynolds D & Wang X (2002) Turbo multiuser detection with unknown interferers. IEEE Transactions on Communications 50(4): p 616–622.

[227] Vook FW & Baum KL (1998) Adaptive antennas for OFDM. Proc. IEEE Vehicular Technology Conference (VTC), vol.1, p 606–610.

[228] Li Y & Sollenberger NR (1999) Adaptive antenna arrays for OFDM systems with cochannel interference. IEEE Transactions on Communications 47(2): p 217–229.

[229] Dejonghe A & Vandendorpe L (2002) Turbo-equalisation for multilevel modulation: an efficient low-complexity scheme. Proc. IEEE International Conference on Communications (ICC), New York, USA, vol.3, p 1863–1867.

[230] Bauch G (2000) Iterative equalization and decoding with channel shortening filters for space-time coded modulation. Proc. IEEE Vehicular Technology Conference (VTC), Tokyo, Japan, p 1575–1582.

[231] Bauch G & Al-Dhahir N (2002) Reduced-complexity space-time turbo equalization for frequency selective MIMO channels. IEEE Transactions on Wireless Communications 1(4): p 819–828.

[232] Oomori H, Asai T & Matsumoto T (2001) A matched filter approximation for SC/MMSE turbo equalisers. IEEE Communications Letters 5(7): p 310–312.

[233] Kansanen K & Matsumoto T (2003) A computationally efficient MIMO turbo-equaliser. Proc. IEEE Vehicular Technology Conference (VTC), Jeju, Korea, vol.1.

[234] Yee MS, Yeap BL & Hanzo L (2003) Radial basis function-assisted turbo equalization. IEEE Transactions on Communications 51(4): p 664–675.

[235] Tarokh V, Naguib A, Seshadri N & Calderbank AR (1999) Space-time codes for high data rate wireless communication: Performance criteria in the presence of channel estimation errors, mobility and multiple paths. IEEE Transactions on Communications 47(2): p 199–207.

[236] Gong Y & Letaief KB (2000) Performance evaluation and analysis of space-time coding in unequalized multipath fading links. IEEE Transactions on Communications 48(11): p 1778–1782.

[237] Boelcskei H & Paulraj AJ (2000) Performance of space-time codes in the presence of spatial fading correlation. Proc. Annual Asilomar Conference on Signals, Systems and Computers (ASILOMAR), Pacific Grove, USA.

[238] Uysal M & Georghiades CN (2001) Effect of spatial fading correlation on performance of space-time codes. IEE Electronics Letters 37(3): p 181–183.

[239] Uysal M & Georghiades CN (2004) On the error performance analysis of space-time trellis codes. IEEE Transactions on Wireless Communications 3(4): p 1118–1123.

[240] Hanzo L, Liew T & Yeap B (2002) Turbo Coding, Turbo Equalisation and Space-Time Coding for Transmission over Fading Channels. John Wiley & Sons, Chichester, UK.

[241] Lu B & Wang X (2000) Iterative receivers for multiuser space-time coding systems. IEEE Journal on Selected Areas in Communications 18(11): p 2322–2335.

[242] Yang H, Yuan J & Vucetic B (2003) Interference suppression schemes for space-time Trellis coded CDMA systems. Proc. IEEE Vehicular Technology Conference (VTC), vol.1, p 717–721.

[243] Ariyavisitakul SL (2000) Turbo space-time processing to improve wireless channel capacity. IEEE Transactions on Communications 48(8): p 1347–1359.

[244] Shen J & Burr AG (2002) Iterative multi-user-antenna detector for MIMO CDMA employing space-time turbo codes. Proc. IEEE Global Telecommunications Conference (GLOBECOM), vol.1, p 419–423.

[245] Shen J & Burr AG (2003) Turbo multiuser receiver for space-time turbo coded downlink CDMA. Proc. IEEE Vehicular Technology Conference (VTC), vol.2, p 1099–1103.

[246] Shen J, Mai H & Burr AG (2004) Turbo joint multiuser detection and channel estimation for space-time turbo coded TDMA systems. Proc. IEEE Vehicular Technology Conference (VTC), Milan, Italy.

[247] Dai H, Molisch AF & Poor HV (2004) Downlink capacity of interference-limited MIMO systems with joint detection. IEEE Transactions on Wireless Communications 3(2): p 442–453.

[248] Middleton D (1999) Non-Gaussian noise models in signal processing for telecommunications: New methods and results for class A and class B noise models. IEEE Transactions on Information Theory 45(4): p 1129–1149.

[249] Yue L & Johnson DH (1997) Type-based detection in macro-diversity reception for mobile radio channels. Proc. IEEE International Conference on Acoustics, Speech and Signal Processing (ICASSP), Munich, Germany, vol.5, p 4013–4016.

[250] Berry LA (1981) Understanding Middleton's canonical formula for class A noise. IEEE Transactions on Electromagnetic Compatibility 23(4): p 337–344.

[251] Czylwik A (1997) Comparison between adaptive ofdm and single carrier modulation with frequency domain equalization. Proc. IEEE Vehicular Technology Conference (VTC), vol.2, p 865–869.

[252] Tubbax L, Come B, van der Perre L, Deneire L, Donnay S & Engels M (2001) OFDM versus single carrier with cyclic prefix: a system-based comparison. Proc. IEEE Vehicular Technology Conference (VTC), Atlantic City, NJ, USA vol.2, p 1115–1119.

[253] Wang Z, Ma X & Giannakis GB (2004) OFDM or single-carrier block transmissions. IEEE Transactions on Communications 52(3): p 380–394.

[254] Fischer RFH, Stierstorfer C & Huber JB (2004) Point-to-point transmission over MIMO channels with intersymbol interference: Comparison of single- and multi-carrier modulation. Proc. International OFDM Workshop (IOW), Dresden, p 1–5.

[255] Abe T & Matsumoto T (2001) Space-time turbo equalization and symbol detection in frequency selective MIMO channels. Proc. IEEE Vehicular Technology Conference, Atlantic City, NJ, USA, vol.2, p 1230–1234.

[256] Spencer QH, Swindlehurst AL & Haardt M (2004) Zero-forcing methods for downlink spatial multiplexing in multiuser MIMO channels. IEEE Transactions on Signal Processing 52(2): p 461–471.

[257] Ng BK & Sousa ES (2002) On bandwidth-efficient multiuser-space-time signal design and detection. IEEE Journal on Selected Areas in Communications 20(2): p 320–329.

[258] Schneider C, Trautwein U, Matsumoto T & Thomä R (2003) Dependency of turbo MIMO equalizer performances on spatial and temporal multipath channel structure - a measurement based evaluation. Proc. IEEE Vehicular Technology Conference (VTC), Jeju, Korea, vol.1.

[259] Haykin S (1996) Adaptive Filter Theory. Prentice Hall, Upper Saddle River, NJ, USA third edn.

[260] Poor H (2001) Turbo multiuser detection: A primer. Journal of Communications and Networks AIEI Korean Institute of Communication Sciences KICS 3(3): p 196–201.

[261] Milstein LB, Schilling DL, Pickholtz RL, Erceg V, Kullback M, Kanterakis EG, Fishman DS, Biederman WH & Salermo ED (1992) On the feasibility of a CDMA overlay for personal communication networks. IEEE Journal on Selected Areas in Communications p 655–667.

[262] Pahlavan K & Levesque A (1995) Wireless Information Networks. John Wiley and Sons, New York, USA.

[263] Verdú S (1985) Minimum probability of error for asynchronous multiple access commumnication systems. Coordinated Science Laboratory Technical Report University of Illinois Urbana-Champaign, IL.

[264] Benedetto S, Montorsi G, Divsalar D & Pollara F (1997) Soft-in-soft-output APP module for iterative decoding of concatenated codes. IEEE Communications Letters 1(1): p 22–24.

[265] Poor HV & Verdú S (1997) Probability of error in MMSE multiuser detection. IEEE Transactions on Information Theory 43(3): p 858–871.

[266] Benedetto S, Divsalar D, Montorsi G & Pollara F (1997) A soft-input soft-output maximum APP module for iterative decoding of concatenated codes. IEEE Communications Letters 1(1): p 22–24.

[267] Lu B & Wang X (2000) Space-time code design in OFDM systems. Proc. IEEE Global Telecommunications Conference (GLOBECOM), San Francisco, CA, USA vol.2, p 1000–1004.

[268] Naguib AF (1996) Adaptive antennas for CDMA wireless networks. Ph.D. thesis Standford University Standford.

[269] Vucetic B & Yuan J (2000) Turbo Codes: Principles and Applications. Kluwer Academic Publishers, Sydney, Australia.

[270] Loncar M, Muller R, Wehinger J & Abe T (2002) Iterative joint detection, decoding and channel estimation for dual antenna arrays in frequency selective fading. Proc. IEEE International Symposium on Wireless Personal Mobile Communications (ISWPMC), Honolulu, Hawai, vol.1, p 125–129.

[271] Chtourou S, Visoz R & Berthet AO (2004) A class of low complexity iterative equalizers for space-time BICM over MIMO block fading multipath AWGN channel. Proc. IEEE International Conference on Communications (ICC), Paris, France, p 618–624.

[272] Kermoal JP, Schumacher L, Pedersen K, Mogensen PE & Frederiksen F (2002) A stochastic MIMO radio channel model with experimental validation. IEEE Journal on Selected Areas in Communications 20(6): p 1211–1226.

[273] Thomä R, Hampicke D, Landmann M, Richter A & Sommerkorn G (2002) MIMO channel sounding and double-directional modeling. XXVIIth URSI General Assembly Maastricht, Netherlands.

[274] Braun WR & Dersch U (1991) A physical mobile radio channel model. IEEE Transactions on Vehicular Technology 40(2): p 472–482.

[275] Gritsch G, Weinrichter H & Rupp M (2004) A union bound on the bit error ratio for data transmission over correlated wireless MIMO channels. Proc. IEEE International Conference on Acoustics, Speech and Signal Processing (ICASSP), Vienna, Austria, p 405–408.

[276] Kay SM (1993) Fundamentals of Statistical Signal Processing: Estimation Theory. Prentice-Hall, Englewood Cliffs, NJ, USA.

[277] Golub GH & Loan CFV (1989) Matrix Computations, 2nd edn. The Johns Hopkins University Press, Baltimore.

Appendices

Derivation of likelihoods for the type-based iterative receiver

From the definition of $\hat{P}_{\alpha_q,\mathbf{y}_\Xi(i)}$ and for constant G it can easily be concluded that

$$\lim_{TG\to\infty} \hat{P}_{\alpha_q\mathbf{y}_\Xi(i)}(\mathbf{q}) = \hat{P}_{\alpha_q\mathbf{n}_c}(\mathbf{q}), \tag{A1.1}$$

from where it can be concluded that

$$\lim_{TG\to\infty} D(\hat{P}_{\mathbf{y}_\Xi(i)}||\hat{P}_{\alpha_q\mathbf{y}_\Xi(i)}) = D(\hat{P}_{\mathbf{y}_\Xi(i)}||\hat{P}_{\alpha_q\mathbf{n}_d}). \tag{A1.2}$$

Due to the noise independence it holds that

$$\log \hat{P}_{\alpha_q\mathbf{n}_d}(\mathbf{y}_\Xi(i)) = \sum_{j=0}^{G-1} \log \hat{P}_{\alpha_q\mathbf{n}_d}(\mathbf{x}_j(i)) = \tag{A1.3}$$

$$\sum_{\mathbf{q}\in\Xi^{L_cN_R}} \hat{P}_{\mathbf{y}_\Xi(i)}(\mathbf{q}) \log \hat{P}_{\alpha_q\mathbf{n}_d}(\mathbf{q}),$$

that after elementary calculations becomes

$$\log \hat{P}_{\alpha_q\mathbf{n}_d}(\mathbf{y}_\Xi(i)) = G(H(\hat{P}_{\mathbf{y}_\Xi(i)}) - D(\hat{P}_{\mathbf{y}_\Xi(i)}||\hat{P}_{\alpha_q\mathbf{n}_d}(\mathbf{y}_\Xi(i)))), \tag{A1.4}$$

where H denotes entropy.

Now we prove that the second part on the right hand side of (A1.4) diminishes for large T. According to the definition of the Kullback-Leibler distance, after substituting the expression for $\hat{P}_{\alpha_q\mathbf{y}_\Xi(i)}$ and simple calculations we have

$$\lim_{T\to\infty} TD(\hat{P}_{\alpha_q}||\hat{P}_{\alpha_q\mathbf{y}_\Xi(i)}) =$$

$$\lim_{T\to\infty} \sum_{\mathbf{q}\in\Xi^{L_cN_R}} \hat{P}_{\alpha_q}(\mathbf{q}) T \log \frac{\hat{P}_{\alpha_q}(\mathbf{q})}{\frac{T}{T+1}(\hat{P}_{\alpha_q}(\mathbf{q}) + \frac{1}{T}\hat{P}_{\mathbf{y}_\Xi(i)}(\mathbf{q}))}. \tag{A1.5}$$

Applying l'Hopital's rule to the expression above and assuming that for large T there holds $\frac{d\hat{P}_{\alpha_q}}{dT} = 0$, it is easy to obtain

$$\lim_{T\to\infty} TD(\hat{P}_{\alpha_q}||\hat{P}_{\alpha_q\mathbf{y}_\Xi(i)}) = 0. \tag{A1.6}$$

Finally, for $T \to \infty$ and $G = const$ we can write

$$\log \hat{P}_{\alpha_q \mathbf{n}_d}(\mathbf{y}_\Xi(i)) = G(H(\hat{P}_{\mathbf{y}_\Xi(i)}) - S_{\alpha_q}(i)). \tag{A1.7}$$

In the special case of i.i.d noise between different diversity branches the estimate of the $\log \hat{P}_{\alpha_q \mathbf{n}_d}(\mathbf{y}_\Xi(i))$ can be obtained as

$$\log \hat{P}_{\alpha_q \mathbf{n}_d}(\mathbf{y}_\Xi(i)) = \sum_{j=1}^{LN_R} G(H(\hat{P}_{\mathbf{y}_\Xi^{(j)}(i)}) - S_{\alpha_q}^{(j)}(i)), \tag{A1.8}$$

where $\hat{P}_{\mathbf{y}_\Xi^{(j)}(i)}$ and $S_{\alpha_q}^{(j)}(i)$ are one dimensional types and decision variables, respectively. They are obtained by repeating exactly the same procedure as described above $L_c N_R$ times for the special case of $L_c N_R = 1$.

Iterative channel estimation

For the purpose of channel estimation we will introduce a different system model notation than in the main body of the paper, following [270] for convenience of notation. Starting from (5.1) we collect the received signal samples at the mth receive antenna into the vector $\mathbf{q}_m \in \mathbb{C}^{(T+\Delta+L-1)\times 1}$ given by

$$\begin{aligned}
\mathbf{q}_m &= [r_m(1), \ldots, r_m(T+\Delta+L-1)]^T && \text{(A2.1)}\\
&= \overline{\mathbf{B}}\mathbf{g}_m + \overline{\mathbf{B}}_I \mathbf{g}_{m,I} + \nu_m,\\
\overline{\mathbf{B}} &= [\overline{\mathbf{B}}_1, \ldots, \overline{\mathbf{B}}_N],\\
\overline{\mathbf{B}}_I &= [\overline{\mathbf{B}}_{N+1}, \ldots, \overline{\mathbf{B}}_{N+N_I}], && \text{(A2.2)}\\
\mathbf{g}_m &= [\mathbf{g}_{m,1}^T, \ldots, \mathbf{g}_{m,N}^T]^T, && \text{(A2.3)}\\
\mathbf{g}_{m,I} &= [\mathbf{g}_{m,N+1}^T, \ldots, \mathbf{g}_{m,N+N_I}^T]^T. && \text{(A2.4)}
\end{aligned}$$

In the first iteration $\Delta = 0$ (no soft feedback is available), in the subsequent iterations $\Delta = B$, and

$$\overline{\mathbf{B}}_n = \begin{bmatrix} \mathbf{s}_n & 0 & \ldots & 0 \\ 0 & \mathbf{s}_n & \ldots & 0 \\ 0 & 0 & \ldots & 0 \\ \vdots & \vdots & \ddots & \vdots \\ 0 & 0 & \ldots & \mathbf{s}_n \end{bmatrix} \in \mathbb{C}^{(T+\Delta+L-1)\times L},$$

$$\mathbf{s}_n = [b_n(1), \ldots, b_n(T), \overline{b}_n(T+1), \ldots, \overline{b}_n(T+\Delta)]^T \in \mathbb{C}^{(T+\Delta)\times 1}, \qquad \text{(A2.5)}$$

and $\mathbf{g}_{m,n} \in \mathbb{C}^{L\times 1}$ and $\nu_m \in \mathbb{C}^{(T+\Delta+L-1)\times 1}$ are defined as

$$\begin{aligned}
\mathbf{g}_{m,n} &= [h_{m,n}(0), \ldots, h_{m,n}(L-1)]^T && \text{(A2.6)}\\
\nu_m &= [v_m(1), \ldots, v_m(T+\Delta+L-1)]^T. && \text{(A2.7)}
\end{aligned}$$

The channel estimate for the mth receive antenna is obtained using the least-squares (LS) criterion, expressed by

$$\hat{\mathbf{g}}_m = \arg\min_{\mathbf{g}_m} ||\mathbf{q}_m - \overline{\mathbf{B}}\mathbf{g}_m||^2, \qquad \text{(A2.8)}$$

resulting in [276]

$$\hat{\mathbf{g}}_m = (\overline{\mathbf{B}}^H \overline{\mathbf{B}})^{-1} \overline{\mathbf{B}}^H \mathbf{q}_m. \tag{A2.9}$$

If the knowledge about the second order statistics of the UCCI and noise $\overline{\mathbf{B}}_I^H \overline{\mathbf{B}}_I + \sigma^2 \mathbf{I}$ is available, the MMSE channel estimation would result in the following estimate [276]

$$\hat{\mathbf{g}}_m = (\overline{\mathbf{B}}^H \overline{\mathbf{B}} + \overline{\mathbf{B}}_I^H \overline{\mathbf{B}}_I + \sigma^2 \mathbf{I})^{-1} \overline{\mathbf{B}}^H \mathbf{q}_m. \tag{A2.10}$$

The elements of vectors $\hat{\mathbf{g}}_m$ are used to form the matrix $\hat{\mathbf{H}}$.

Derivation of the upper bound on the optimal kernel-smoothing factor for PDF estimation based interference suppression

A reasonable approximation of (5.74) can be done by using its Taylor series expansion [196], with which

$$\mathrm{MISE}(\hat{p}_{\hat{\mathbf{x}}}) \approx \frac{\sigma_0^4 \alpha^2 \Gamma(p_{\hat{\mathbf{x}}})}{4} + \frac{\int_{\mathbb{R}^{2LM}} K_1^2(\mathbf{a}) d\mathbf{a}}{T \sigma_0^{2LM}}, \tag{A3.1}$$

where $\alpha = \int_{\mathbb{R}^{2LM}} (\mathrm{Re}a_1)^2 K_1(\mathbf{a}) d\mathbf{a} = 1$ and

$$\Gamma(p_{\hat{\mathbf{x}}}) = \int_{\mathbb{R}^{2LM}} \left[\sum_{i=1}^{LM} \left(\frac{\partial^2 p_{\hat{\mathbf{x}}}(\mathbf{a})}{\partial (\mathrm{Re}a_i)^2} + \frac{\partial^2 p_{\hat{\mathbf{x}}}(\mathbf{a})}{\partial (\mathrm{Im}a_i)^2} \right) \right]^2 d\mathbf{a}. \tag{A3.2}$$

From (A3.1) the optimal smoothing parameter $\sigma_{0,opt}$ is found to be

$$\sigma_{0,opt} = \left(\frac{2LM \int_{\mathbb{R}^{2LM}} K_1^2(\mathbf{a}) d\mathbf{a}}{(T+B)\Gamma(p_{\hat{\mathbf{x}}})} \right)^{\frac{1}{2LM+4}}. \tag{A3.3}$$

with

$$\int_{\mathbb{R}^{2LM}} K_1^2(\mathbf{a}) d\mathbf{a} = \frac{1}{(2\pi)^{LM}} \int_{\mathbb{R}^{2LM}} e^{\frac{-\mathbf{a}^H \mathbf{a}}{2}} d\mathbf{a} = \frac{1}{(4\pi)^{LM}} \tag{A3.4}$$

In general, the function $\Gamma(p_{\hat{\mathbf{x}}})$ is dependent on D and $\mathbf{t}_i$, $i = 1, ..., D$. However, it is shown in [172] for the univariate case that the upper bound on $\Gamma(p_{\hat{\mathbf{x}}})$ obtained using Cauchy's inequality is dependent neither on $\mathbf{t}_i$ nor on D. Adopting the same approach in the sequel, we generalize the upper bound derivation to the multivariate case. Let us denote

$$p_G(\mathbf{a}) = \frac{1}{(\sigma^2 2\pi)^{LM}} e^{-\frac{\mathbf{a}^H \mathbf{a}}{2\sigma^2}}. \tag{A3.5}$$

Eq. (5.70) denoting the exact PDF of the UCCI-plus-noise can be rewritten as

$$p_{\hat{\mathbf{x}}}(\mathbf{x}(k)) = \frac{1}{2^D} \sum_{i=0}^{2^D-1} p_G(\mathbf{x}(k) - \mathbf{t}_i). \tag{A3.6}$$

With (A3.5) the expression for $\Gamma(p_{\hat{\mathbf{x}}})$ can be rewritten as

$$\Gamma(p_{\hat{\mathbf{x}}}) = \int_{\mathbb{R}^{2LM}} \left[\frac{1}{2^D} \sum_{k=0}^{2^D-1} \Upsilon_k(p_G) \right]^2 d\mathbf{a}, \tag{A3.7}$$

where

$$\Upsilon_k(p_G) = \sum_{i=1}^{LM} \left(\frac{\partial^2 p_G(\mathbf{a} - \mathbf{t}_k)}{\partial(\mathrm{Re}a_i)^2} + \frac{\partial^2 p_G(\mathbf{a} - \mathbf{t}_k)}{\partial(\mathrm{Im}a_i)^2} \right). \tag{A3.8}$$

Applying Cauchy's inequality

$$\left[\sum v_1 v_2 \right]^2 \leq \sum v_1^2 \sum v_2^2 \tag{A3.9}$$

to Eq. (A3.7) with $v_1 = 1$ and $v_2 = \Upsilon_k(p_G)$ we obtain

$$\Gamma(p_{\hat{\mathbf{x}}}) \leq \frac{1}{2^D} \sum_{k=0}^{2^D-1} \Gamma_k(p_G), \tag{A3.10}$$

where

$$\Gamma_k(p_G) = \int_{\mathbb{R}^{2LM}} [\Upsilon_k(p_G)]^2 \, d\mathbf{a}. \tag{A3.11}$$

It can be shown that

$$\begin{aligned} &\Gamma_k(p_G) = \qquad\qquad\qquad\qquad\qquad\qquad\qquad\qquad\qquad\qquad\qquad\qquad (A3.12) \\ = \quad &\frac{1}{\sigma^4} \int_{\mathbb{R}^{2LM}} \left[\sum_{i=1}^{LM} \left[\frac{(\mathrm{Re}a_i)^2}{\sigma^2} + \frac{(\mathrm{Im}a_i)^2}{\sigma^2} \right] - 2LM \right]^2 p_G^2(\mathbf{a}) d\mathbf{a}, \end{aligned}$$

which is *independent* of k. Furthermore it can be shown that

$$\Gamma(p_G) = I_1 + I_2 + I_3 + I_4, \tag{A3.13}$$

where

$$\begin{aligned} I_1 &= \frac{1}{\sigma^4} \int_{-\infty}^{\infty} \sum_{i=1}^{LM} \left[\frac{(\mathrm{Re}a_i)^4}{\sigma^2} + \frac{(\mathrm{Im}a_i)^4}{\sigma^2} \right] p_G^2(\mathbf{a}) d\mathbf{a} \qquad (A3.14) \\ &= \frac{3LM}{4\sqrt{\pi}\sigma^5} \left(\frac{1}{2\sigma\sqrt{\pi}} \right)^{2LM-1}, \end{aligned}$$

$$I_2 = \frac{4(LM)^2}{\sigma^4}\int_{-\infty}^{\infty} p_G^2(\mathbf{a})d\mathbf{a} = \frac{4(LM)^2}{\sigma^4}\left(\frac{1}{2\sigma\sqrt{\pi}}\right)^{2LM}, \tag{A3.15}$$

$$I_3 = -\frac{2LM}{\sigma^4}\int_{-\infty}^{\infty}\sum_{i=1}^{LM}\left[\frac{(\mathrm{Re}a_i)^2}{\sigma^2}+\frac{(\mathrm{Im}a_i)^2}{\sigma^2}\right]p_G^2(\mathbf{a})d\mathbf{a} = -\frac{(LM)^2}{\sigma^5\sqrt{\pi}}\left(\frac{1}{2\sigma\sqrt{\pi}}\right)^{2LM-1}, \tag{A3.16}$$

$$I_4 = \frac{1}{\sigma^4}\int_{-\infty}^{\infty}\sum_{q_i,q_j\in\mathbb{A}}\frac{q_i^2q_j^2}{\sigma^2}p_G^2(\mathbf{a})d\mathbf{a} = \frac{2LM(2LM-1)}{16\sigma^6\sqrt{\pi}}\left(\frac{1}{2\sigma\sqrt{\pi}}\right)^{2LM-2}, \tag{A3.17}$$

$$\mathbb{A} = \{\mathrm{Re}a_i, \mathrm{Re}a_j, \mathrm{Im}a_i, \mathrm{Im}a_j | i\neq j; i,j=1,\ldots,LM\}.$$

From (A3.13)-(A3.17) it follows that

$$\Gamma_k(p_G) = \frac{LM(LM+1)}{(4\pi)^{LM}\sigma^{2LM+4}}. \tag{A3.18}$$

Finally, by replacing (A3.18) in (A3.10) and (A3.10) in (A3.3) the lower bound of (5.75) directly follows.

Derivation of the MMSE filter output for space-time transmission

Without loss of generality, derivation of the optimal pair $[\mathbf{W}_k^{<1>}(i), \mathbf{A}_k^{<1>}(i)]$ of matrices is presented only for the first group of n_0 jointly detected antennas and l_0 jointly detected multipath components. The derivation is similar for the other groups, with difference only in indexing. Let us denote the nth columns of the matrices $\mathbf{W}_k^{<1>}(i)$ and $\mathbf{A}_k^{<1>}(i)$ as $\mathbf{w}^{(n)}$ and $\mathbf{a}^{(n)}$, respectively. For simplicity of notation we omit the dependence of $\mathbf{w}^{(n)}$ and $\mathbf{a}^{(n)}$ on user index k, antenna group index γ and time instant i. The cost function in (5.40) that is to be minimized can be written as

$$\mathcal{J}(\mathbf{W}_k^{<1>}(i), \mathbf{A}_k^{<1>}(i)) = E\left\{\sum_{n=1}^{n_0} |\mathbf{m}^{(n)H}\mathbf{g}|^2\right\}, \tag{A4.1}$$

where

$$\mathbf{m}^{(n)} = [\mathbf{w}^{(n)H}, -\mathbf{a}^{(n)H}]^H \tag{A4.2}$$

with

$$\mathbf{g} = [\mathbf{y}_k^{<1>}(i)^H, \mathbf{B}_k^{<1>}(i)^H]^H. \tag{A4.3}$$

This is equivalent to minimizing each of the component cost functions defined as

$$\mathcal{J}^{(n)}(\mathbf{m}^{(n)}) = E\left\{|\mathbf{m}^{(n)H}\mathbf{g}|^2\right\}. \tag{A4.4}$$

To avoid the trivial solution $\mathbf{m}^{(n)} = \mathbf{0}$ different constraints can be imposed. We will derive the MMSE for two different constraints in the sequel.

(1) *Path constraint*. A constraint on $\mathbf{a}^{(n)}$ is imposed so that $a_{nl_0}^{(n)}$ is set to be equal to 1. Introducing the Lagrange multiplier λ, the equivalent cost function to be minimized becomes

$$\mathcal{J}_{eq}^{(n)}(\mathbf{m}^{(n)}) = E\left\{|\mathbf{m}^{(n)H}\mathbf{g}|^2\right\} - \lambda(\mathbf{m}^{(n)H}\mathbf{j}^{(n)} = 1), \tag{A4.5}$$

where

$$\mathbf{j}^{(n)} = [\mathbf{0}_{1\times(n-1)l_0}\ 1\ \mathbf{0}_{1\times(n_0-n)l_0}]^T. \tag{A4.6}$$

Differentiating Eq. (A4.5) with respect to $\mathbf{m}^{(n)}$ gives

$$\frac{\partial \mathcal{J}_{eq}^{(n)}(\mathbf{m}^{(n)})}{\partial \mathbf{m}^{(n)}} = \mathbf{R_{gg}}\mathbf{m}^{(n)} - \lambda \mathbf{j}^{(n)}, \tag{A4.7}$$

where

$$\mathbf{R_{gg}} = \begin{bmatrix} \mathbf{R}_{cov}^{<1>} & \mathbf{\Pi}_k^{<1>} \\ \mathbf{\Pi}_k^{<1>H} & \mathbf{I} \end{bmatrix} \in \mathbb{C}^{LN_R+n_0l_0 \times LN_R+n_0l_0}.$$

From Eq. (A4.7) the optimal value of $\mathbf{m}^{(n)}$ can be found as

$$\mathbf{m}^{(n)} = \frac{\mathbf{R}_{\mathbf{gg}}^{-1}\mathbf{j}^n}{\mathbf{j}^{(n)^H}\mathbf{R}_{\mathbf{gg}}^{-1}\mathbf{j}^{(n)}}. \tag{A4.8}$$

Applying the property of the inverse of the block-matrix [277]

$$\begin{bmatrix} \mathbf{A} & \mathbf{B} \\ \mathbf{C} & \mathbf{D} \end{bmatrix}^{-1} = \begin{bmatrix} \mathbf{Q}^{-1} & -\mathbf{Q}^{-1}\mathbf{B}\mathbf{D}^{-1} \\ -\mathbf{D}^{-1}\mathbf{C}\mathbf{Q}^{-1} & \mathbf{D}^{-1}(\mathbf{I}+\mathbf{C}\mathbf{Q}^{-1}\mathbf{B}\mathbf{D}^{-1}) \end{bmatrix},$$

to the inverse of the matrix $\mathbf{R_{gg}}$, where $\mathbf{Q} = \mathbf{A} - \mathbf{BD}^{-1}\mathbf{C}$, we obtain

$$\mathbf{m}^{(n)} = \begin{bmatrix} \frac{\mathbf{M}_k^{<1>}(i)^{-1}\mathbf{h}_k^{(n)}}{1+\mathbf{h}_k^{(n)H}\mathbf{M}_k^{<1>}(i)^{-1}\mathbf{h}_k^{(n)}} \\ \frac{\mathbf{h}_k^{(n)}(0)^H\mathbf{M}_k^{<1>}(i)^{-1}\mathbf{h}_k^{(1)}(0)}{1+\mathbf{h}_k^{(n)H}\mathbf{M}_k^{<1>}(i)^{-1}\mathbf{h}_k^{(n)}} \\ \vdots \\ \frac{\mathbf{h}_k^{(n)}(0)^H\mathbf{M}_k^{<1>}(i)^{-1}\mathbf{h}_k^{(1)}(l_0-1)}{1+\mathbf{h}_k^{(n)H}\mathbf{M}_k^{<1>}(i)^{-1}\mathbf{h}_k^{(n)}} \\ \vdots \\ \frac{\mathbf{h}_k^{(n)}(0)^H\mathbf{M}_k^{<1>}(i)^{-1}\mathbf{h}_k^{(n-1)}(0)}{1+\mathbf{h}_k^{(n)H}\mathbf{M}_k^{<1>}(i)^{-1}\mathbf{h}_k^{(n)}} \\ \vdots \\ \frac{\mathbf{h}_k^{(n)}(0)^H\mathbf{M}_k^{<1>}(i)^{-1}\mathbf{h}_k^{(n-1)}(l_0-1)}{1+\mathbf{h}_k^{(n)H}\mathbf{M}_k^{<1>}(i)^{-1}\mathbf{h}_k^{(n)}} \\ 1 \\ \vdots \\ \frac{\mathbf{h}_k^{(n)}(0)^H\mathbf{M}_k^{<1>}(i)^{-1}\mathbf{h}_k^{(n)}(l_0-1)}{1+\mathbf{h}_k^{(n)H}\mathbf{M}_k^{<1>}(i)^{-1}\mathbf{h}_k^{(n)}} \\ \frac{\mathbf{h}_k^{(n)}(0)^H\mathbf{M}_k^{<1>}(i)^{-1}\mathbf{h}_k^{(n+1)}(0)}{1+\mathbf{h}_k^{(n)H}\mathbf{M}_k^{<1>}(i)^{-1}\mathbf{h}_k^{(n)}} \\ \vdots \\ \frac{\mathbf{h}_k^{(n)}(0)^H\mathbf{M}_k^{<1>}(i)^{-1}\mathbf{h}_k^{(n+1)}(l_0-1)}{1+\mathbf{h}_k^{(n)H}\mathbf{M}_k^{<1>}(i)^{-1}\mathbf{h}_k^{(n)}} \\ \vdots \\ \frac{\mathbf{h}_k^{(n)}(0)^H\mathbf{M}_k^{<1>}(i)^{-1}\mathbf{h}_k^{(n_0)}(0)}{1+\mathbf{h}_k^{(n)H}\mathbf{M}_k^{<1>}(i)^{-1}\mathbf{h}_k^{(n)}} \\ \vdots \\ \frac{\mathbf{h}_k^{(n)}(0)^H\mathbf{M}_k^{<1>}(i)^{-1}\mathbf{h}_k^{(n_0)}(l_0-1)}{1+\mathbf{h}_k^{(n)H}\mathbf{M}_k^{<1>}(i)^{-1}\mathbf{h}_k^{(n)}} \end{bmatrix},$$

from which it follows that

$$\mathbf{w}^{(n)} = \frac{\mathbf{M}_k^{<1>}(i)^{-1}\mathbf{h}_k^{(n)}}{1+\mathbf{h}_k^{(n)H}\mathbf{M}_k^{<1>}(i)^{-1}\mathbf{h}_k^{(n)}} \tag{A4.9}$$

and

$$\mathbf{a}^{(n)} = \begin{bmatrix} \frac{\mathbf{h}_k^{(n)}(0)^H \mathbf{M}_k^{<1>}(i)^{-1} \mathbf{h}_k^{(1)}(0)}{1+\mathbf{h}_k^{(n)H} \mathbf{M}_k^{<1>}(i)^{-1} \mathbf{h}_k^{(n)}} \\ \vdots \\ \frac{\mathbf{h}_k^{(n)}(0)^H \mathbf{M}_k^{<1>}(i)^{-1} \mathbf{h}_k^{(1)}(l_0-1)}{1+\mathbf{h}_k^{(n)H} \mathbf{M}_k^{<1>}(i)^{-1} \mathbf{h}_k^{(n)}} \\ \vdots \\ \frac{\mathbf{h}_k^{(n)}(0)^H \mathbf{M}_k^{<1>}(i)^{-1} \mathbf{h}_k^{(n-1)}(0)}{1+\mathbf{h}_k^{(n)H} \mathbf{M}_k^{<1>}(i)^{-1} \mathbf{h}_k^{(n)}} \\ \vdots \\ \frac{\mathbf{h}_k^{(n)}(0)^H \mathbf{M}_k^{<1>}(i)^{-1} \mathbf{h}_k^{(n-1)}(l_0-1)}{1+\mathbf{h}_k^{(n)H} \mathbf{M}_k^{<1>}(i)^{-1} \mathbf{h}_k^{(n)}} \\ 1 \\ \vdots \\ \frac{\mathbf{h}_k^{(n)}(0)^H \mathbf{M}_k^{<1>}(i)^{-1} \mathbf{h}_k^{(n)}(l_0-1)}{1+\mathbf{h}_k^{(n)H} \mathbf{M}_k^{<1>}(i)^{-1} \mathbf{h}_k^{(n)}} \\ \frac{\mathbf{h}_k^{(n)}(0)^H \mathbf{M}_k^{<1>}(i)^{-1} \mathbf{h}_k^{(n+1)}(0)}{1+\mathbf{h}_k^{(n)H} \mathbf{M}_k^{<1>}(i)^{-1} \mathbf{h}_k^{(n)}} \\ \vdots \\ \frac{\mathbf{h}_k^{(n)}(0)^H \mathbf{M}_k^{<1>}(i)^{-1} \mathbf{h}_k^{(n+1)}(l_0-1)}{1+\mathbf{h}_k^{(n)H} \mathbf{M}_k^{<1>}(i)^{-1} \mathbf{h}_k^{(n)}} \\ \vdots \\ \frac{\mathbf{h}_k^{(n)}(0)^H \mathbf{M}_k^{<1>}(i)^{-1} \mathbf{h}_k^{(n_0)}(0)}{1+\mathbf{h}_k^{(n)H} \mathbf{M}_k^{<1>}(i)^{-1} \mathbf{h}_k^{(n)}} \\ \vdots \\ \frac{\mathbf{h}_k^{(n)}(0)^H \mathbf{M}_k^{<1>}(i)^{-1} \mathbf{h}_k^{(n_0)}(l_0-1)}{1+\mathbf{h}_k^{(n)H} \mathbf{M}_k^{<1>}(i)^{-1} \mathbf{h}_k^{(n)}} \end{bmatrix}.$$

After repeating a similar procedure for all the n_0 transmit antennas from the 1st group of the kth user, the optimal pair of matrices $[\mathbf{W}_k^{<1>}(i), \mathbf{A}_k^{<1>}(i)]$ is obtained as

$$\mathbf{W}_k^{<1>}(i) = [\mathbf{w}^{(1)}, ..., \mathbf{w}^{(n_0)}] \quad \text{and} \quad \mathbf{A}_k^{<1>}(i) = [\mathbf{a}^{(1)}, ..., \mathbf{a}^{(n_0)}]. \quad \text{(A4.10)}$$

(2) *Norm constraint*. A family of constraints is imposed on the vector $\mathbf{g}$ so that $\mathbf{m}^{(n)H} \mathbf{\Gamma}^{(n)} \mathbf{m}^{(n)} = 1$. Introducing the Lagrange multiplier λ, the equivalent cost function to be minimized becomes

$$\mathcal{J}_{eq}^{(n)}(\mathbf{m}^{(n)}) = E\left\{ |\mathbf{m}^{(n)H} \mathbf{g}|^2 \right\} - \lambda(\mathbf{m}^{(n)H} \mathbf{\Gamma}^{(n)} \mathbf{m}^{(n)H} = 1). \quad \text{(A4.11)}$$

Differentiating Eq. (A4.11) with respect to $\mathbf{m}^{(n)}$ gives

$$\frac{\partial \mathcal{J}_{eq}^{(n)}(\mathbf{m}^{(n)})}{\partial \mathbf{m}^{(n)}} = \mathbf{R}_{\mathbf{gg}} \mathbf{m}^{(n)} - \lambda \mathbf{\Gamma}^{(n)} \mathbf{m}^{(n)}, \quad \text{(A4.12)}$$

where

$$\mathbf{R}_{gg} = \begin{bmatrix} \hat{\mathbf{H}}\boldsymbol{\Lambda}_k^{<1>}(i)\hat{\mathbf{H}}^H + \hat{\mathbf{R}} & \boldsymbol{\Pi}_k^{<1>} \\ \boldsymbol{\Pi}_k^{<1>H} & \sigma^2\mathbf{I} \end{bmatrix} \in \mathbb{C}^{(LN_R+l_0)\times(LN_R+l_0)}.$$

From (A4.12) the optimal value of $\mathbf{m}^{(n)}$ can be found as a solution to the eigenvalue problem

$$\mathbf{R}_{\mathbf{gg}}^{-1}\boldsymbol{\Gamma}^{(n)}\mathbf{m}^{(n)} = \lambda^{-1}\mathbf{m}^{(n)}. \tag{A4.13}$$

Applying the property of the inverse of the block-matrix [277]

$$\begin{bmatrix} \mathbf{A} & \mathbf{B} \\ \mathbf{C} & \mathbf{D} \end{bmatrix}^{-1} = \begin{bmatrix} \mathbf{Q}^{-1} & -\mathbf{Q}^{-1}\mathbf{B}\mathbf{D}^{-1} \\ -\mathbf{D}^{-1}\mathbf{C}\mathbf{Q}^{-1} & \mathbf{D}^{-1}(\mathbf{I}+\mathbf{C}\mathbf{Q}^{-1}\mathbf{B}\mathbf{D}^{-1}) \end{bmatrix},$$

to the inverse of the matrix $\mathbf{R}_{\mathbf{gg}}$, where $\mathbf{Q} = \mathbf{A} - \mathbf{B}\mathbf{D}^{-1}\mathbf{C}$, we obtain that the vector $\mathbf{m}^{(n)}$ is equal to the eigenvector of the matrix $\mathbf{R}_{\mathbf{gg}}^{-1}\boldsymbol{\Gamma}^{(n)}$ that corresponds to its minimum eigenvalue.